Online Condition Monitoring of Electric Powertrains using Machine Learning and Data Fusion

Jagath Sri Lal Senanayaka

UiA University of Agder

Doctoral Dissertations at the University of Agder 270

Jagath Sri Lal Senanayaka

Online Condition Monitoring of Electric Powertrains using Machine Learning and Data Fusion

Doctoral Dissertation for the Degree *Philosophiae Doctor (PhD)* at
the Faculty of Engineering and Science, Specialisation in Mechatronics

University of Agder
Faculty of Engineering and Science
2020

Doctoral dissertations at the University of Agder 270
ISSN: 1504-9272
ISBN: 978-82-7117-971-7

Printed by Media 07
Kristiansand

Acknowledgements

This dissertation is based on research activities carried out at the University of Agder during the period February 2016 to December 2019. This PhD project is funded by the Ministry of Education in Norway. I want to express my gratitude to all who supported my PhD studies.

Foremost, I would like to express my sincere gratitude to my supervisors Prof. Kjell G. Robbersmyr and Prof. Van Khang Huynh. Their guidance helped me in all the time of research and writing of this dissertation. My sincere thanks to the main supervisor Prof. Kjell for providing research directions, facilities, motivation and guidance to complete the research. I'm extremely grateful to co-supervisor Prof. Khang for his great support, motivation and guidance for improving technical content and publications of the research by allocating plentiful time from his schedule. I was fortunate to have two supervisors, each specialised in mechanical engineering and electrical engineering for improving my knowledge in Mechatronics. Besides my supervisors, I would like to thank Prof. Mohan Lal Kolhe and Prof. Hamid Reza Karimi for providing the foundation to my research career.

I am thankful to the Head of the Department Prof. Geir Grasmo and PhD coordinator Emma E. Horneman for providing me the necessary facilities and pleasant working environment for research activities. Special thanks for my friends Surya, Witold, Andreas, Martin, Rafael, Saeed, Gulshan and Dipendra for their support and motivation during my PhD studies.

I would like to thank Dr. Keerthi Gunawikrama and Dr. Chandana Perera from the University of Ruhuna, for providing guidance and support for enrolling my master studies at University of Agder through the Norwegian quota scheme in 2012. A special mention to my Sri Lankan friends in Norway; Indika, Buddhika, Dimuthu, Thilina, Pabasara, Ranga, Samangi, Madhawa, Kalpani, Harsha, Sasanka, Konara and Dharshana: Thank you all for your support.

I would like to thank my parents K. Senanayaka and D.K. Dayawathi for their continued love and understanding. Last, but not the least, I want to thank my wife Sudeepika for her love, sharing my life, and caring of our daughter Vidushi.

Jagath Sri Lal Senanayaka
December 2019
Grimstad, Norway

Abstract

Safe and reliable operations of industrial machines are highly prioritized in industry. Typical industrial machines are complex systems, including electric motors, gearboxes and loads. A fault in critical industrial machines may lead to catastrophic failures, service interruptions and productivity losses, thus condition monitoring systems are necessary in such machines. The conventional condition monitoring or fault diagnosis systems using signal processing, time and frequency domain analysis of vibration or current signals are widely used in industry, requiring expensive and professional fault analysis team. Further, the traditional diagnosis methods mainly focus on single components in steady-state operations. Under dynamic operating conditions, the measured quantities are non-stationary, thus those methods cannot provide reliable diagnosis results for complex gearbox based powertrains, especially in multiple fault contexts.

In this dissertation, four main research topics or problems in condition monitoring of gearboxes and powertrains have been identified, and novel solutions are provided based on data-driven approach. The first research problem focuses on bearing fault diagnosis at early stages and dynamic working conditions. The second problem is to increase the robustness of gearbox mixed fault diagnosis under noise conditions. Mixed fault diagnosis in variable speeds and loads has been considered as third problem. Finally, the limitation of labelled training or historical failure data in industry is identified as the main challenge for implementing data-driven algorithms. To address mentioned problems, this study aims to propose data-driven fault diagnosis schemes based on order tracking, unsupervised and supervised machine learning, and data fusion. All the proposed fault diagnosis schemes are tested with experimental data, and key features of the proposed solutions are highlighted with comparative studies.

List of Publications

The following listed papers are based on research activities conducted by the author and have been published or submitted for publications in peer-reviewed journals and conference proceedings.

Paper A J. S. L. Senanayaka, S. T. Kandukuri, H. V. Khang and K. G. Robbersmyr, "Early Detection and Classification of Bearing Faults using Support Vector Machine Algorithm", *IEEE Workshop on Electrical Machines Design, Control and Diagnosis (WEMDCD)*, Nottingham, pp. 250-255, 2017.

Paper B J.S.L Senanayaka H.V. Khang, K.G. Robbersmyr, "Fault Detection and Classification of Permanent Magnet Synchronous Motors in Variable Load and Speed Conditions using Order Tracking and Machine Learning", *Journal of Physics: Conference Series*, vol. 1037, no. 3, 2018

Paper C J. S. L. Senanayaka, H. V. Khang and K. G. Robbersmyr, "Multiple Classifiers and Data Fusion for Robust Diagnosis of Gearbox Mixed Faults", in *IEEE Transactions on Industrial Informatics*, vol. 15, no. 8, pp. 4569-4579, Aug. 2019.

Paper D: J. S. L. Senanayaka, H. V. Khang and K. G. Robbersmyr, "Multiple Fault Diagnosis of Electric Powertrains under Variable Speeds using Convolutional Neural Networks", *XXIII International Conference on Electrical Machines (ICEM)*, Alexandroupoli, pp. 1900-1905, 2018.

Paper E: J. S. L. Senanayaka, H. V. Khang and K. G. Robbersmyr, "Online Fault Diagnosis System for Electric Powertrains Using Advanced Signal Processing and Machine Learning", *XXIII International Conference on Electrical Machines (ICEM),* Alexandroupoli, pp. 1932-1938, 2018.

Paper F: J. S. L. Senanayaka, H. V. Khang and K. G. Robbersmyr, "Towards Self-Supervised Feature Learning for Online Diagnosis of Multiple Faults in Electric Powertrains", Under review at *IEEE Transactions on Industrial Informatics.*

The following publications are within the framework of this dissertation and published during the time of this project, but are not included in the dissertation.

Paper G: J.S.L. Senanayaka, H.V. Khang, K.G. Robbersmyr, "A robust method for detection and classification of permanent magnet synchronous motor faults: Deep autoencoders and data fusion approach", *Journal of Physics: Conference Series*, vol. 1037, no. 3, 2018.

Paper H: S. T Kandukuri, J. S .L. Senanayaka, H. V. Khang, K. G. Robbersmyr, "Current Signature-based Fault Diagnosis of Field-oriented and Direct Torque Controlled Induction Motor Drives", *Proceedings of the Institution of Mechanical Engineers. Part I Journal of Systems and Control Engineering*, vol. 231, no. 10, pp. 849-866, 2017

Paper I: S. T. Kandukuri, J. S. L. Senanyaka, V. K. Huynh and K. G. Robbersmyr, "A Two-Stage Fault Detection and Classification Scheme for Electrical Pitch Drives in Offshore Wind Farms Using Support Vector Machine", in *IEEE Transactions on Industry Applications*, vol. 55, no. 5, pp. 5109-5118, Sept.-Oct. 2019.

Paper J: J. S. L. Senanayaka, H. V. Khang and K. G. Robbersmyr, "Towards Online Bearing Fault Detection using Envelope Analysis of Vibration Signal and Decision Tree Classification Algorithm", *20th International Conference on Electrical Machines and Systems (ICEMS)*, Sydney, pp. 1-6, 2017.

Paper K: J.S.L. Senanayaka, H. V. Khang, and Kjell G. Robbersmyr. "Autoencoders and Data Fusion Based Hybrid Health Indicator for Detecting Bearing and Stator Winding Faults in Electric Motors." *2018 21st International Conference on Electrical Machines and Systems (ICEMS)*, Jeju, pp. 531-536, 2018.

Paper L: J. S. L. Senanayaka, H. V. Khang and K. G. Robbersmyr, "Autoencoders and Recurrent Neural Networks Based Algorithm for Prognosis of Bearing Life", *21st International Conference on Electrical Machines and Systems (ICEMS)*, Jeju, pp. 537-542, 2018.

Contents

List of Figures

List of Tables

List of Abbreviations

AE	autoencoder
AI	artificial intelligence
BF	bearing fault
BPFI	ball pass frequency inner race
BPFO	ball pass frequency outer race
BSF	ball spin frequency
CBM	condition-based maintenance
CI	condition indicator
CM	condition monitoring
CNN	convolutional neural networks
CWT	continuous wavelet transformation
DAI-DAO	data in data out
DAI-FEO	data in features out
DEI-DEO	decision in decision out
DF	domain features
DL	deep learning
EDM	electric discharge machining
FDD	fault detection and diagnosis
FEI-DEO	features in decision out
FEI-FEO	feature in feature out
FNR	false negative rates
FT	fault type

GB	gearbox
GF	gear fault
GMF	gear meshing frequency
GPU	graphics processing unit
HI	health indicator
IM	induction motor
ISO	international standard organization
k-NN	k nearest neighbour
ML	machine learning
MLP	multi-layer perceptron
NB	naïve Bayes
PHM	prognostics and health management
PMSG	permanent magnet synchronous generator
PMSM	permanent magnet synchronous motor
RCM	reliability centred maintenance
RMS	root mean square
RNN	recurrent neural networks
RUL	remaining useful life
SF	stator winding fault
SNR	signal-to-noise ratio
STFT	short-time Fourier transformation
SVM	support vector machine
TBM	time-based maintenance
TPR	true positve rates

Chapter 1

Introduction

1.1 Background

Safe and reliable operations of industrial machines, such as electric motors and gearboxes, are important in industry. A failure of a critical machine may end up with huge financial losses, not only because of the failed machine, but also the loss of production. Therefore, appropriate maintenance practices are required to increase the availability of machines. The main objective of a maintenance operation is to improve system reliability and safety while reducing the cost of maintenance manpower, monitoring equipment, parts inventories, etc. In addition, early diagnosis of potential catastrophic failures and estimating remaining useful life (RUL) of components are also important for proper maintenance planning and scheduling.

Electric powertrains are widely used in manufacturing, wind energy and transportation sectors. The industrial applications of powertrains can be found in various mechanical systems such as pumps, fans, conveyor belts, robotics and wind turbines. An electric powertrain typically consists of an electric motor, a gearbox and a control system to drive the motor.

The reliability and failure modes of motors used in various industrial applications are presented in [1-6]. These studies conclude that 40-50 % induction motor faults occur in bearings, and faults on stator winding, being the second most common fault, contribute 15-30 % faults in the machines while the rest is a combination of other mechanical and electrical faults. Therefore, this research

mainly deals with bearing faults and inter-turn stator winding faults of electric motors. Further, bearing and gear faults of gearboxes are also of interest in this study.

Figure 1.1: Gearbox based motors in an electric powertrain

This dissertation aims to propose and develop data-driven fault diagnostic algorithms for online condition monitoring (CM) of electric motors and gearboxes. A laboratory test setup is built to collect required data for training and validating the developed algorithms. Figure 1.1 shows some gearbox based motors used in an in-house test setup. An industrial motor drive is used as the control unit, and a permanent magnet synchronous generator (PMSG) connected to a variable resistor bank is used as the load. Vibration and current sensors are connected for data collection. Further, public datasets provided by reputed research organisations are also used for validating the proposed diagnostics schemes.

1.2 Motivation and research problem

Early detection of faults in critical components of electric powertrains, e.g bearings or stator windings, is significant in industrial applications because it gives an additional time for planning maintenance [7, 8]. Existing fault diagnosis methods mainly analyse stationary signals in steady state. Unlike industrial productions, electric powertrains for wind turbine and electric vehicles dynamically operate based on drive commands or wind conditions, rendering additional difficulties for a fault diagnosis. New fault diagnostic schemes are required to deal with non-stationary signals and dynamic operations.

The robustness and accuracy of CM and fault diagnosis systems are highly important in industry because the false diagnosis can result in unnecessarily forced system shutdowns, and the inaccurate diagnosis may cause unexpected failures. A CM system may work properly for a single fault in an ideal condition. However, background or sensor noise is present in a complex system like gearboxes [9, 10], fault diagnosis is a challenging task. Hence, finding novel methods to improve the robustness and accuracy of fault diagnosis algorithms are of importance for both academia and industry.

Dynamic operating conditions such as variable loads and speeds are common in industrial applications such as wind turbines and robotics. Further, concurrent faults in a system might cause missing alarms. Traditional diagnosis techniques focusing on single faults at steady state may not work for those applications [9]. CM and diagnostic of multiple faults under variable speeds and loads are very challenging, requiring new advanced diagnostic schemes.

Online CM systems aim to improve the effectiveness of systems and reduce the maintenance cost [11, 12]. The new wireless sensors, cloud data storage and modern artificial intelligent (AI) algorithms are the driving forces to make smart CM systems. Machine learning (ML), deep learning (DL) algorithms, and its applications in CM and diagnostics are necessary for industry 4.0 [13-15]. In ML and DL based CM, fault diagnosis algorithms require a lot of historical data for training and validation, but the training data is difficult to obtain in reality, or the available datasets are unbalanced or unlabeled. For example, data from a healthy machine is usually available in industry, but historical data for faults is limited or not available due to regular maintenance [18-19]. Maximizing the use of healthy machine data is important for developing novel diagnostic schemes.

1.3 Contributions of the dissertation

The scientific contributions of this dissertation are withdrawn from six research papers published or submitted to international journals and conference proceedings.

Paper A: Early Detection and Classification of Bearing Faults using Support Vector Machine Algorithm

Summary: In paper A, an algorithm is proposed for early detection and classification of bearing faults. Time-domain and frequency-domain features are extracted using envelop analysis and the energies of signal at characteristic frequency bands for early fault detection. A support vector machine (SVM) algorithm is used for fault classification and severity detection. The algorithm can detect and classify bearing fault at the early stage. The use of envelope analysis allows for capturing the features for early fault diagnosis, and the SVM algorithm ensures the classification of different fault severities in the multi-dimensional feature space. The proposed algorithm is validated using a well-known run-to-failure test dataset.

Contributions: A data-driven diagnosis method is proposed for detecting bearing faults in early stage using envelope analysis-based feature generation and SVM algorithm.

This paper has been published as:

J. S. L. Senanayaka, S. T. Kandukuri, H. V. Khang and Kjell. G. Robbersmyr, "Early Detection and Classification of Bearing Faults using Support Vector Machine Algorithm", *IEEE Workshop on Electrical Machines Design, Control and Diagnosis (WEMDCD)*, Nottingham, pp. 250-255, 2017.

Paper B: Fault Detection and Classification of Permanent Magnet synchronous Motors in Variable Load and Speed Conditions using Order Tracking and Machine Learning

Summary: Common faults in the permanent magnet machines occur in the bearing and stator winding, being mainly detected in steady-state operating

conditions under constant loads and speeds. However, variable loads and speeds are typical operations of powertrains in wind turbines. Therefore, it is important to detect bearing and stator winding faults in variable speed and load conditions. Paper B proposes an algorithm to diagnose multiple faults in variable speed and load conditions. The proposed algorithm is based on tracking the frequency orders associated with faults from the normalised order spectrum. The normalised order spectrum is generated by resampling the measured vibration signal via estimated motor speeds. The fault features are then generated from the tracking orders in addition to the estimated torque and speed features. Finally, a support vector machine (SVM) algorithm is used to classify the faults. The proposed method is validated using experimental data, and the validated results confirm its usefulness for practical applications.

Contributions: A fault diagnosis scheme based on SVM and order tracking of fault-related characteristic frequencies is proposed for diagnosing bearing and stator winding faults of a permanent magnet synchronous motor at variable loads and speeds.

This paper has been published as:

J.S.L Senanayaka H. V. Khang, Kjell. G. Robbersmyr, "Fault Detection and Classification of Permanent Magnet Synchronous Motors in Variable Load and Speed Conditions using Order Tracking and Machine Learning", *Journal of Physics: Conference Series*, vol. 1037, no. 3, 2018

Paper C: Multiple Classifiers and Data Fusion for Robust Diagnosis of Gearbox Mixed Faults

Summary: Accurate diagnosis of gearbox mixed faults is a challenging task as a faulty gearbox, consisting of several bearings, shafts and gears, generates a complex vibration spectrum. A novel diagnosis scheme is proposed for diagnosing multiple faults in a gearbox. Two parallel classifiers based on convolutional neural networks (CNN) and multilayer perceptrons (MLP) are used in the proposed scheme. Continuous wavelet transformation (CWT) is used to generate a time-frequency representation of vibration measured at two locations of the gearbox, being fed to CNN for feature learning, feature fusion and classification. The features for MLP are generated using time and frequency domain signals, and the

energies associated with faults at characteristic frequencies. Furthermore, the naïve Bayes (NB) combiner is used for decision level data fusion to improve the accuracy and robustness of the proposed algorithm under noises. This algorithm demonstrates that both feature level and decision level data fusion could improve the accuracy and robustness of a fault diagnosis system under noise.

Contributions: A novel fault diagnosis scheme based on MLP, CNN and NB combiner is proposed for a robust diagnosis of gearbox mixed faults.

This paper has been published as:

J. S. L. Senanayaka, H. V. Khang and Kjell. G. Robbersmyr, "Multiple Classifiers and Data Fusion for Robust Diagnosis of Gearbox Mixed Faults," in *IEEE Transactions on Industrial Informatics*, vol. 15, no. 8, pp. 4569-4579, 2019.

Paper D: Multiple Fault Diagnosis of Electric Powertrains under Variable Speeds using Convolutional Neural Networks

Summary: In this paper, a new fault diagnosis system is proposed to diagnose multiple faults (bearing, gear and inter-turn short circuit stator winding faults) for electric powertrains at variable load and speed conditions. The order tracking method is used to generate order normalised short-time Fourier transform (STFT) based spectrograms from current and vibration signals of the powertrain. This method helps to deal with variable speed conditions, and CNN algorithm is used as a classification algorithm. The combined vibration and current STFT spectrograms fed to CNN for feature level fusion can deal with load variations. Further, the algorithm requires only training data for single faults, but the algorithm can detect multiple faults, reducing the training data requirements. The experimental results show that the algorithm can detect multiple faults at variable load and speed conditions.

Contributions: A new algorithm is proposed for diagnosing electric powertrain multiple faults at variable load and speeds. The proposed method can reduce the required training data as it can be trained by using only data from single faults, but the algorithm can detect multiple faults.

This paper has been published as:

J. S. L. Senanayaka, H. V. Khang and Kjell. G. Robbersmyr, "Multiple Fault Diagnosis of Electric Powertrains under Variable Speeds using Convolutional Neural Networks", *XXIII International Conference on Electrical Machines (ICEM), Alexandroupoli*, pp. 1900-1905, 2018.

Paper E: Online Fault Diagnosis System for Electric Powertrains using Advanced Signal Processing and Machine Learning

Summary: The online implementation of the algorithm proposed in paper D is considered in paper E. The fault diagnosis algorithm proposed in paper D is improved by adding online data acquisition, diagnostics, decision-making and visualisation components. Online data acquisition, decision making, and visualisation aspects were tested using experimental data.

Contributions: An online fault diagnosis algorithm is proposed for accurate decision making in electric powertrains by utilising historical diagnosis results.

This paper has been published as:

J. S. L. Senanayaka, H. V. Khang and Kjell. G. Robbersmyr, "Online Fault Diagnosis System for Electric Powertrains using Advanced Signal Processing and Machine Learning", *XXIII International Conference on Electrical Machines (ICEM), Alexandroupoli*, pp. 1932-1938, 2018.

Paper F: Towards Self-Supervised Feature Learning for Online Diagnosis of Multiple Faults in Electric Powertrains

Summary: This paper proposes a novel online fault diagnosis scheme for industrial powertrains while addressing the challenges of limited labelled training data. The proposed method combines one-class SVM anomaly detection and supervised CNN algorithm. The one-class SVM aims to derive a score for detecting faults, and the detected fault results are used as the training data for the CNN classifier. Within the framework, an online diagnosis scheme is developed with two stages, utilizing the two algorithms in self-supervised feature learning passion. The proposed online diagnosis scheme can detect multiple faults at

variable loads and speeds in powertrains. The proposed diagnosis scheme is validated using experimental data from an in-house test setup.

Contributions: A new online fault diagnosis system is proposed to learn the features for fault diagnosis in self-supervised online passion using limited historical data, while minimizing expertise demand.

This paper has been submitted as:

J. S. L. Senanayaka, H. V. Khang and Kjell. G. Robbersmyr, "Towards Self-Supervised Feature Learning for Online Diagnosis of Multiple Faults in Electric Powertrains", *Submitted to IEEE Transactions on Industrial Informatics (*Under review*).*

1.4 Structure of this dissertation

This dissertation consists of seven chapters. The introduction chapter gives an overview of the dissertation. The remaining chapters of this dissertation are organized as follows. In the second chapter, the state-of-the-art of CM, fault diagnostics and prognostics methods are presented, and the research direction is identified. The experimental works and the datasets used for validating the perused algorithms are summarized in Chapter 3. Chapter 4 covers the algorithms proposed for bearings fault diagnosis at early stages and dynamic working conditions through papers A and B. Chapter 5 provides a summary of the fault diagnostics schemes proposed for gearbox and electric powertrain applications through papers C, D and E, respectively. A self-supervised online CM system is given in Chapter 6, which summarizing the online fault diagnosis scheme proposed in paper F. The conclusions of the dissertation and future improvements are presented in Chapter 7. The contents of each chapter are summarised in Figure 1.2.

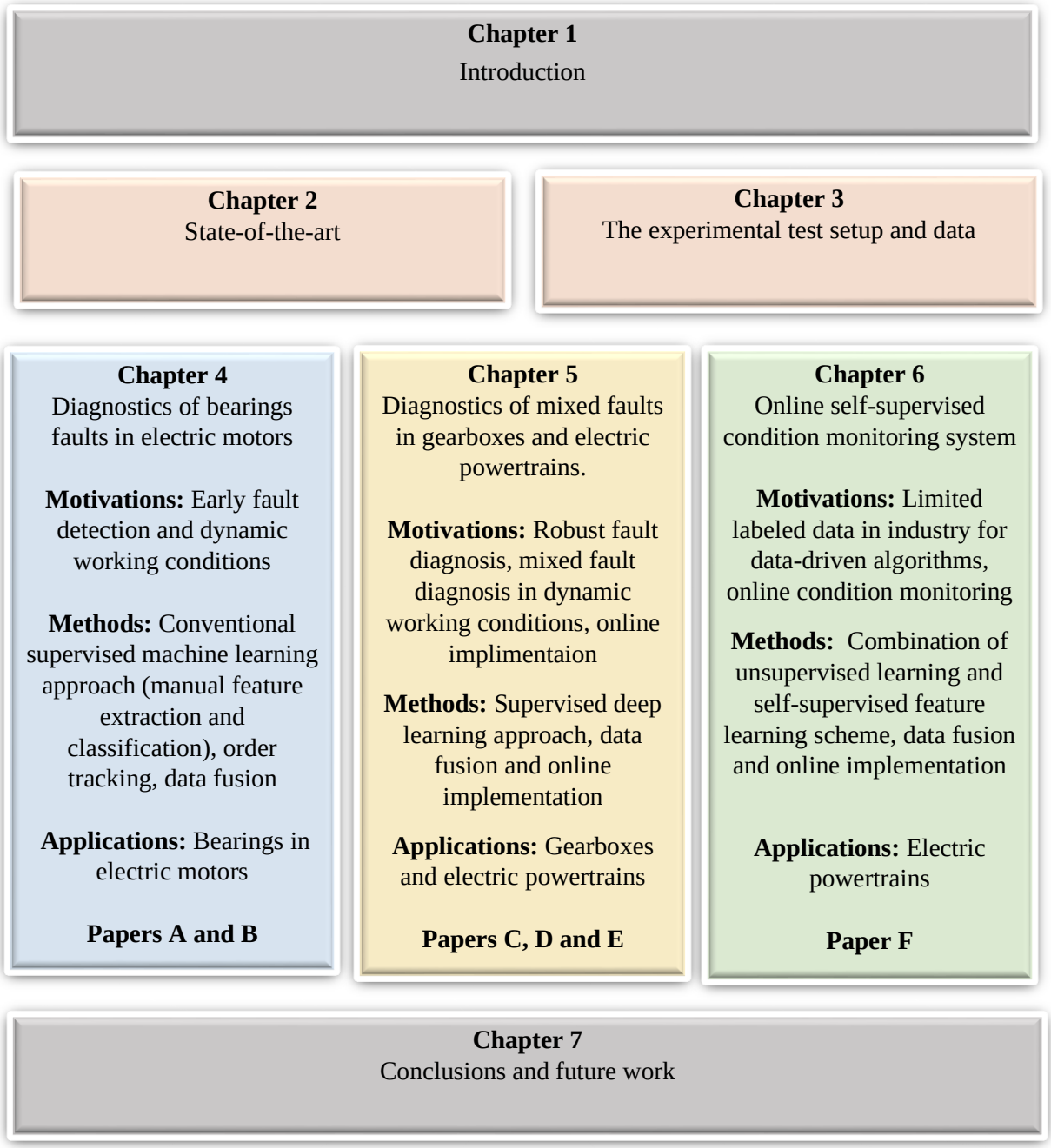

Figure 1.2: Summary of chapter contents

Chapter 2

State-of-the-art

The state-of-the-art condition monitoring, fault diagnostics, prognostics and data fusion methods for gearboxes, electric motors and bearings are discussed in this chapter. This is important to define the baseline and identify the research direction for this dissertation.

2.1 Maintenance strategies

Depending on applications, various types of maintenance, namely reactive, preventive, predictive and proactive maintenance, are used in industry [16, 17]. In the reactive maintenance, the maintenance tasks are conducted to fix a machine when it breaks. The main issue of reactive maintenance is the cost of unexpected failures. In critical machines, the loss of production hours may lead to huge financial costs. Therefore, reactive maintenance is generally used for non-critical machines. Preventive maintenance can be adopted to reduce unexpected breakdowns in critical machines, where maintenance is conducted in regular time intervals and sometimes known as time-based maintenance (TBM) [17]. This method reduces the unexpected breakdown cost, but the maintenance cost can be higher than the reactive maintenance, because of the increased cost of the spare parts, tools and maintenance manpower. Preventive maintenance sometimes can lead to unnecessary costly component replacements. Since the failures of components are based on the operating condition, failures can happen at any time,

depending on the condition of the machine. Enhancing maintenance is required to reduce the cost.

To minimise unexpected failures, more efficient predictive maintenance can be used [18]. In the predictive maintenance, the condition of a machine or component is continuously monitored by condition indicators (vibration, temperature, etc.) in order to identify a significant change, which is indicative of a developing fault. The fault diagnostic and prognostic functions can be performed using the results of CM. The International Standard Organization (ISO) -13374 - condition monitoring and diagnostics of machines, defines the functionality in a condition monitoring system in eight blocks [19]. Each subunit has a defined function and interrelation with other subunits. Anyone who develops CM and diagnostics systems shall follow this standard. Furthermore, the ISO-18436-2:2014 specifies the necessities for the training, relevant experience, and examination of personnel performing condition monitoring and diagnostics of machines using vibration analysis [20]. Various terms used in condition monitoring and diagnostics of machines are defined in ISO-13372 [21].

Condition-based maintenance (CBM) is a predictive maintenance strategy that uses CM, fault diagnosis and prognosis to determine the health of machines and schedule the maintenance accordingly. Generally, CM is performed on working machines, and CBM can reduce the cost of unexpected failures and the downtime, and improve the system reliability and safety [18]. However, the maintenance cost can be further increased in CBM due to the cost of condition monitoring technologies, sensors and expert manpower for analyzing the data generated from CM. Timely and reliable monitoring and maintenance decisions can reduce the unexpected breakdown cost, and increasing the system availability. In this way, the increased maintenance cost can be compensated with an overall cost benefit. The predictive maintenance is suitable for critical machines, requiring high reliability and availability. For general applications, it may not be cost-effective. In a proactive maintenance, CM and failure-root-cause analysis are utilised for additional maintenance activities such as ensuring proper lubrication, alignment and balancing of rotating components in order to eliminate possible future failures.

Different maintenance methods, rather than being applied independently, can be combined to maximize their corresponding strengths in order to optimize the facility and equipment efficiency while minimizing life-cycle costs. The reliability centred maintenance (RCM) is an advanced control strategy, that can be

implemented to optimize the maintenance program of a company or facility [16]. An optimal mix of reactive, preventive, predictive and proactive maintenance practices is adopted in RCM. When implementing RCM, first, the criticality level of the machine should be analysed. Then depending on the critical level of the machine, proper maintenance strategy should be selected for relevant components. For non-critical components, reactive or preventive maintenance may be sufficient, but critical components may require predictive or proactive maintenance. In RCM, a systematic methodology is used to identify the maintenance tasks that are necessary to realise the essential reliability of components at the lowest possible cost.

Another emerging maintenance discipline is prognostics and health management (PHM). The key duties of the PHM technology are to detect emerging component or system fault, performing failure diagnostics and health management [22]. The concept of prognostics is to diagnose and predict remaining useful life (RUL) of an item (e.g. device, component, or system). Systems with a prognostic capability will be able to identify potential failures in advance and provide information on the system health. This information could be used to reduce an unscheduled maintenance or to extend scheduled maintenance intervals. PHM can be considered as an evolution of the CBM and RCM.

CBM, RCM and PHM methods focus on different aspects of industrial maintenance strategies and asset management. However, the CM, fault diagnostics and prognostics are the key functions of any advance maintenance program. Thus, it is important to have reliable and accurate CM, fault diagnosis and prognosis schemes for industrial applications.

2.2 Data-driven fault diagnostics

Fault diagnostics includes fault detection, isolation and severity quantification. The fault diagnostic systems can be established through model-based, data-driven or hybrid algorithms [23-26]. The model-based diagnosis requires a detailed physical model of the system and accurate parameters. In a model-based diagnosis, the model output variables and actual output variables are compared, and a residual of the comparison is used for fault diagnosis. In electric powertrains, components, such as bearings and gearboxes, are difficult to build their precise mathematical models. The data-driven method using statistical or machine

learning algorithms does not need such a physical model [27], and it is attractive for an automatic CM and diagnosis system of bearings and gearboxes.

In a data-driven machinery fault diagnosis, the machine condition is monitored using various sensors, and collected signals are fed to a data-driven fault diagnosis system. The measured data could be temperature, thermography images, chemical and wear monitoring information (e.g. lubricant oil contamination), vibration signals, acoustic emission signals, shock pulses, motor current signals, etc. [28, 29]. The operating temperature is a primary indicator of machine health, and the temperature or infrared image analysis is one of the easiest methods to monitor the machine condition. Lubricant oil analysis is often used for detecting bearing and gearbox faults. Vibration analysis is the most common technique for analysing mechanical faults, such as bearing and gear faults. The electrical signature analysis can be used to detect the mechanical and electrical faults in electrical machines. In CM of electric powertrains, the vibration and the current signals are the common choice in industry as they are easy to be implemented and integrated into the systems.

A basic fault detection system can be built by measuring the root mean square (RMS) vibration of the machine and defining a threshold for normal vibration level. A deviation of the measured RMS vibration from the threshold can be an indicator for a variation from a normal operating status, but it is not sufficient to isolate a fault as the increased vibration may be generated from other sources such as unbalance, misalignment, etc. Therefore, fault isolation or classification and severity quantification are necessary despite requiring additional features from signal processing, statistics or machine learning methods.

As shown in Figure 2.1, a data-driven fault diagnostics system typically consists of several subunits, namely data acquisition, data processing and feature extraction, fault diagnosis and maintenance decision.

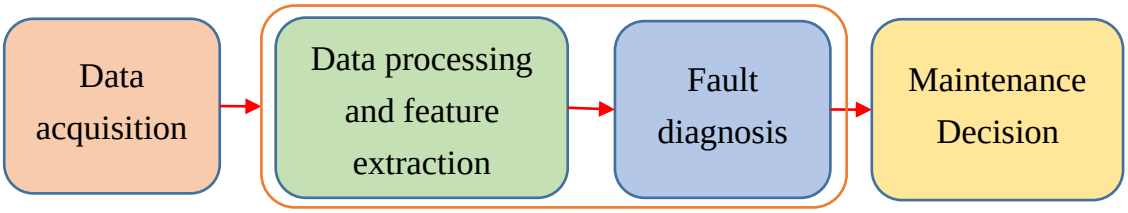

Figure 2.1: A simplified block diagram of a data-driven fault diagnosis system.

Data acquisition is to collect signals from sensors such as vibration, current or acoustic emission. The collected signals can be processed to identify the most useful abstract information for fault diagnosis. If using deep learning algorithms, both feature learning and classification are combined into one algorithm. In a machine learning or deep learning algorithm, the feature learning and fault diagnosis can be achieved in a supervised, unsupervised or semi-supervised way. The fault diagnosis includes fault detection, fault isolation and fault severity quantification [30]. The fault diagnosis results will be used for making a maintenance decision.

2.2.1 Feature extraction using signal processing and statistical methods

To monitor rotating machinery health, the machine vibration, acoustic emission or motor current are measured and analyzed for finding fault-related features in time (e.g. RMS of signal), frequency (e.g. Fourier transformation and signal energies at characteristic frequencies) or time-frequency analysis (e.g. short-time Fourier transformation, wavelet transformation). In addition, statistical features of signals, e.g. mean, standard deviation or kurtosis, may be appropriate features [30, 31]. Fixed or statistical thresholds (e.g. ISO vibration thresholds, multivariate statistical methods) can be used for a fault diagnosis [18].

The above mentioned methods are suitable for a componenet level single-fault diagnosis. Strong features can be manually produced by expert knowledge. For example, if the characteristic frequencies are easy to be identified, the high-quality features can be produced with signal processing skills. However, in a complex fault context with multiple faults under variable load and speed conditions, the feature generation is time-consuming and expensive, and may result in missing or false alarms [32]. Therefore, enhanced methods for feature generation are required to be developed for accurate fault diagnostics.

2.2.2 Fault diagnosis based on supervised machine learning and deep learning

To address problems in fixed or statistical thresholds based fault diagnosis, supervised machine learning methods can be used. The first step of the machine

learning algorithm is the feature generation. The signal processing and statistical methods discussed in Section 2.2.1 can be used to manually generate features for machine learning algorithms. Several classification algorithms, such as SVM [33], k-nearest neighbour (k-NN) [34], decision tree (DT) and numerous neural network architectures [35], can be applied to find complex relations on the feature space via the time-frequency features extracted by the domain knowledge [36] or statistical methods. Thus, machine learning methods are appropriate for both single and multiple fault diagnostics.

Performance of supervised machine learning highly depends on the feature generation and selection. In early fault detections and noisy conditions, additional signal processing methods are required for capturing hidden features from original signals. To obtain the better results from a machine learning algorithm, features have to be relevant and strong. Irrelevant and redundant features will result in a high-dimensional feature space or complex machine learning model, requiring more data for training [37, 38]. Additional statistical or optimization methods, e.g. principal component analysis, particle swarm optimization and independent component analysis, are thus useful to find the best features for classification algorithms.

A deep learning algorithm can be used to address challenges on feature generation, selections and extra optimizations by extracting and transforming features via nonlinear processing layers, and learn itself the best features by detecting patterns from the training data of a signal or an image to differentiate faults [34]. Thus, deep learning provides one advanced step towards smart fault diagnosis systems. For example, a CNN based supervised deep learning algorithm can combine feature generation and classification [39]. The algorithm can learn the features from data, and the fault diagnosis problem is solved as a pattern recognition problem using automatically detected features [15, 40, 41].

Deep learning methods are widely used in fault diagnosis due to their merit of analyzing complex or big data while the improved technologies of sensors, cost-effective processors, graphics processing units (GPUs) and their parallel processing capabilities allow for collecting and processing big data effectively [13-15]. The deep learning algorithms are completely based on the information gathered from training data to identify patterns and relations within the data. In other words, the deep learning algorithms are advanced pattern recognizers without using domain knowledge. Therefore, expert knowledge is not required as characteristic frequencies are not considered separately, being suitable for a

complex fault diagnosis of multiple faults under variable load and speed conditions. Supervised deep learning methods can reduce the difficulty of feature generation and selection, but labelled training data or historical faulty data is required for fault diagnosis.

2.2.3 Unsupervised and semi-supervised learning methods

Even though supervised deep learning methods have many merits over traditional machine learning and statistical methods, the practical implications of these algorithms require labelled training data, which is difficult to obtain or is limited in reality. Feature learning and fault diagnosis are combined in a supervised CNN deep learning algorithm [39]. There are other classes of deep learning algorithms, where the feature extraction and fault diagnosis are separated, without using labelled training data or requiring considerably smaller training data than the supervised CNN.

Most widely used deep learning-based feature extraction methods are unsupervised autoencoders (AEs) [42], or semi-supervised feature learning using transfer learning methods [43]. AEs are neural networks designed to learn features from unlabeled input data. Unlabelled healthy and faulty status data can be fed into an AE to learn features without labels. AE feature learning is suitable for applications, where healthy and faulty data is offered without being labelled to differentiate the healthy and faulty data. In transfer learning, features can be extracted using a pre-trained CNN network or AlexNet [41], which is designed for image classifications. The internal layers of pre-train CNN represent a set of filters to identify different patterns of input images. Since the fault diagnosis problem is solved as a pattern recognition problem using spectrograms of fault signals, the extracted filters can be fine-tuned using less healthy and faulty data. The transfer learning is able to extract features, and implements fault diagnosis systems using less amount of labelled training data.

Data for healthy conditions is much more than faulty conditions in industry. Unsupervised fault detection algorithms, such as one-class SVM [44-46], can be used in such situations. The one-class SVM algorithm requires features from healthy status and faulty status features are not mandatory for training. Once trained, one-class SVM can calculate a hyper distance in the feature space for new data, thus a threshold can be defined to differentiate the healthy and faulty classes

Combination of AE feature learning and one-class SVM fault detection might be a promising solution to deal with unlabeled training data.

2.2.4 Data fusion for fault diagnosis

The data fusion algorithms can be integrated to improve the accuracy and robustness of a fault diagnosis system [27]. Various data fusion algorithms can be found in statistical estimation, pattern recognition, and artificial intelligence disciplines. The widely used definition of data fusion is defined by Joint Directors of Laboratory (JDL) as "a multi-level process dealing with the association, correlation, combination of data and information from single and multiple sources to achieve refined position, identify estimate and complete and timely assessment of the situation, threats and their significance" [47]. By considering the relationship among the data sources, three types of data fusion methods have been proposed by Durrant-Whyte [48], namely complementary, redundant and cooperative fusion. Based on the abstraction level, data fusion algorithms are categorised into four levels in [49], namely; low-level fusion (signal level), medium level (feature level), high level (decision level) and multiple level fusion (data from the signal, feature or decision level). Another widely used classification of data fusion algorithms is proposed by Dasarathy [50], namely, data in data out (DAI-DAO), data in features out (DAI-FEO), feature in feature out (FEI-FEO), features in decision out (FEI-DEO), and decision in decision out (DEI-DEO).

Depending on the applications, proper data fusion methods can be adopted. In complementary fusion, the data is generated from different sources, and the fusion is applied to get broad evidence by combining the complementary information. For example, using both vibration and current signals for a fault diagnosis is a complementary data fusion because the vibration and current signals give different viewpoints of the fault information. In the redundant fusion, two or more information are fused to increase the confidence of data fusion. For example, signals from two accelerometers in each side of the motor are used in the redundant fusion to enhance the confidence and accuracy of vibration information. In a cooperative fusion, the information from sources is fused to get new, and more complex information, representing a better reality. Further, the selection of a proper abstract level is important in CM and fault diagnosis applications.

2.3 Prognostics

Prognostics is the process of estimating the remaining useful life (RUL) of a system or a component, after which the system or component will not perform its intended function. The RUL estimation is usually based on model-based or data-driven methods, and their combination [51]. The physical degradation models, e.g. crack propagation via fatigue, corrosion or wear, are required for model-based prognostics. In the data-driven approach, data of the health condition of a component is collected by various sensors, such as vibration, acoustic emission, temperature, etc. Then the collected data is used to model the component degradation process via data-driven models, namely, statistical or machine learning [52]. An accurate RUL estimation requires a reliable health indicator (HI), which should be sufficiently sensitive to capture defects in early degradation stages and consistent over an entire degradation process. Various RUL estimation methods are reported in literature [53, 54]. Due to the randomness of RUL, there is no universal approach for identifying a HI and estimating RUL [55]. Most existing bearing and gearbox prognosis algorithms are based on vibration signals, and their features are extracted in time, frequency and time-frequency domains. These features are evaluated to identify the best features, being applied to statistical or machine learning methods to track the degradation process and predict the remaining useful life [56, 57]. Recurrent neural networks (RNNs) are another supervised deep learning algorithm, which can be used for time-series predictions and suitable in prognostic applications. The availability of low-cost sensors, data storages, data processing, deep learning, and data fusion algorithms unveils the capabilities of data-driven prognostics. When more data is available, the data-driven algorithms can capture more features to identify more failure modes and improve the accuracy of prognostic results.

2.4 Condition monitoring of electric powertrains: The research directions

As highlighted in Section 2.1, CM is the key function of CBM, RCM or PHM maintenance strategies. Implementing a CM system faces certain challenges, e.g. cost or expertise demand. A CM system requires various sensors and large

databases to store data. These equipment costs can be reduced through the innovation and improvement of sensors, data acquisition, data transmission and storage systems. Further, diagnostics, prognostics and decision-making process are mostly done by the expert personal, increasing the maintenance cost. CM and diagnostics of powertrains, including gearboxes and bearings, face challenges due to the following factors.

- Detecting faults in the early stages in dynamic operating conditions is challenging since the fault indicator is very small or difficult to capture in such contexts.
- Various background noises available in the working environment can reduce the accuracy and robustness of CM systems of gearboxes and powertrains, especially in multiple fault conditions. Finding novel methods to deal with background noises is important to improve the accuracy and robustness of the CM systems.
- Variable load and speed operations of industrial machines cause measured quantities non-stationary, thus a mixed fault diagnosis under such conditions is difficult if using conventional signal processing techniques.
- Labelled training data is required for supervised data-driven algorithms, but labelled training data is limited or restricted in industry and academia. Therefore, developing new algorithms to deal with limited training data is very important.

This research focuses on proposing data-driven methods for online CM and fault diagnostic schemes while addressing above challenges, reducing the manpower of CM and making it feasible for a wide range of industrial applications.

Chapter 3

The experimental test setup and data

Proper experimental data is required to validate the proposed CM, fault diagnosis schemes. Real industrial machine failure data is generally difficult to obtain due to confidentiality and limited availability. Therefore, the proposed algorithms are validated using in-house experimental data and published external datasets. This chapter presents experimental works carried out during the research and other datasets used in the dissertation.

3.1 Types of experiments

Two types of datasets are used to verify the proposed algorithms. Some algorithms are tested using seeded faults. This type of data is relatively easy to produce in laboratory conditions. Noise can be added to data to make the data more practical. Other types of data are from the run-to-failure test datasets. In such a test, additional forces, speed or temperature are added to the components, and run until they completely fail. This type of data is more suitable for prognosis applications, as the data is for a complete life cycle of the component. A description of the experiments and datasets used in this dissertation is given in Table 3.1.

Table 3.1: Description of experiments and datasets used in this dissertation.

Section	Experiment	Focus	Papers
3.2	Seeded faults with different severities for electric powertrain faults	Mixed Fault diagnosis at variable speeds and loads, unsupervised fault detection and online implementation	Paper D, -E, and -F.
3.3	Seeded faults for PMSM	Fault diagnosis at variable speeds and loads	B
3.4.1	Bearing run-to-failure tests	CM and early fault diagnosis	A
3.4.2	Seeded faults of a gearbox	Robust fault diagnosis at mixed fault conditions	C

PMSM: permanent magnet synchronous motor

3.2 The developed in-house test bench

A schematic of the experimental test bench used for electric powertrain fault diagnosis is shown in Figure 3.1, and the details of actual test bench components are given in Figure 3.2. The powertrain includes a 1.1 kW, 1450 rpm induction motor (IM) coupled to the 2-stages parallel shaft gearbox (GB) with 1:8.01 gear reduction.

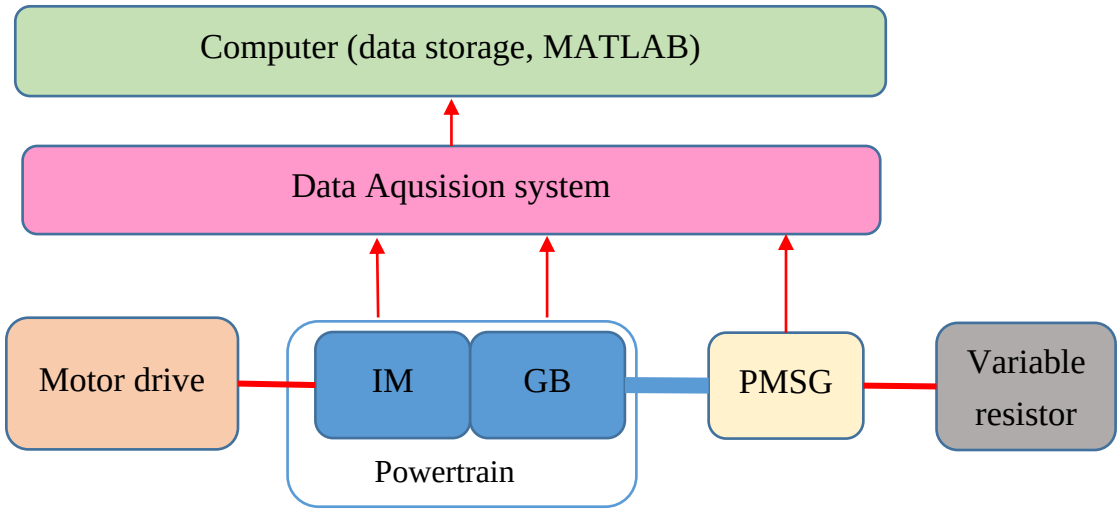

Figure 3.1: Schematics of the test bench.

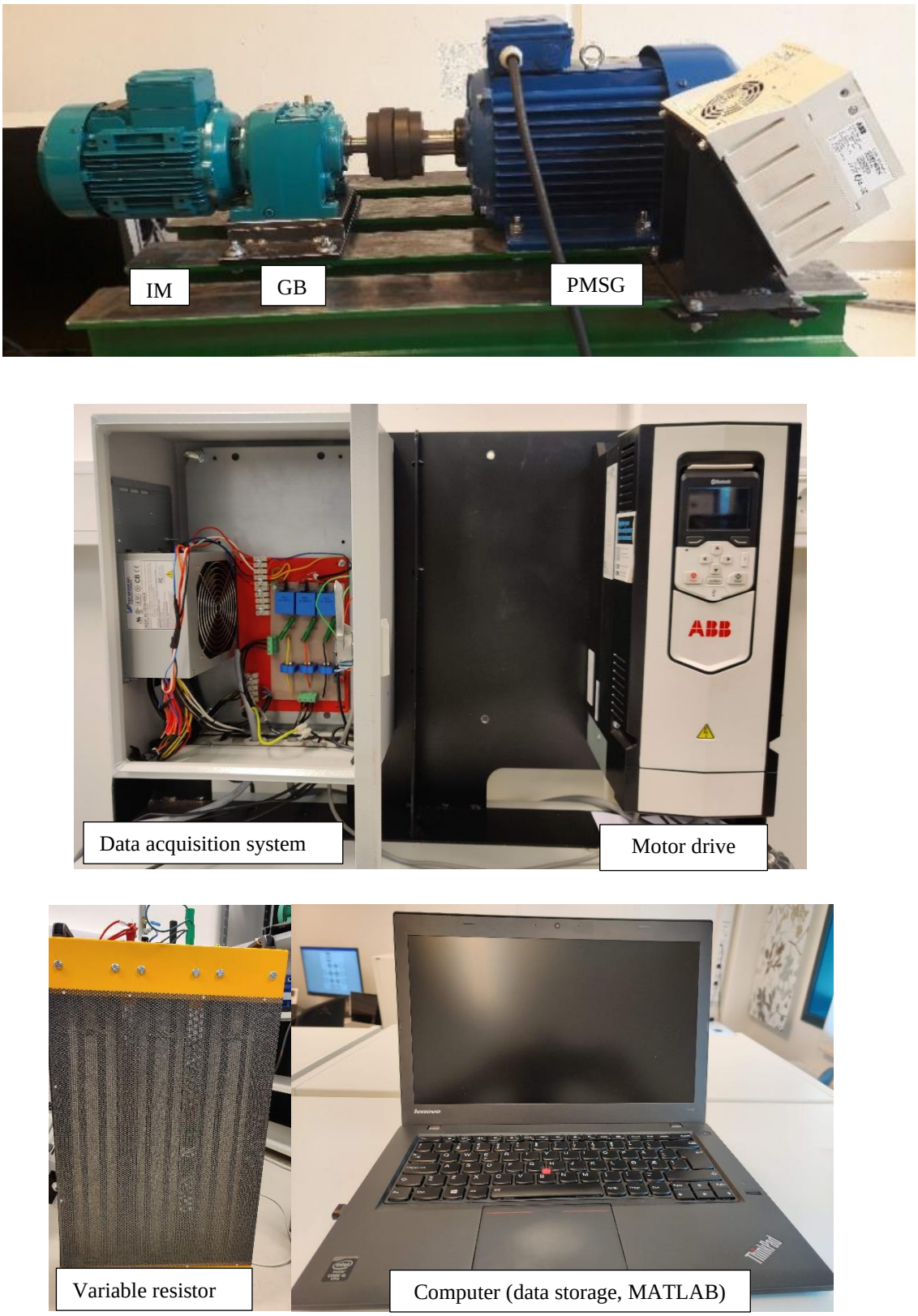

Figure 3.2: Components of the experimental test bench.

The internal components of the complete powertrain are shown in Figure 3.3, including 8 bearings, 4 gears and 3 shafts. The gearbox output shaft is coupled to a permanent magnet synchronous generator (PMSG), and the generator output is connected to a variable resistive load. When the resistance of the load is fixed, the powertrain load is proportional quadratically to the rotational speed. The output currents of the PMSG are measured and used to estimate the rotational speed of the electric powertrain. However, in real applications, an encoder is required to measure the speed. An acceleration sensor is placed on top of the gearbox, and the accelerometer data and motor input currents are collected. Depending on the test type, the induction motor can be operated at constant speeds or variable speed profiles. More details of operating profiles can be found in the published papers. Data files at the sampling rate of 20 kHz and 120 seconds duration are collected by the data acquisition system. Several repeated tests were conducted to collect more data and improve the performances of data-driven algorithms.

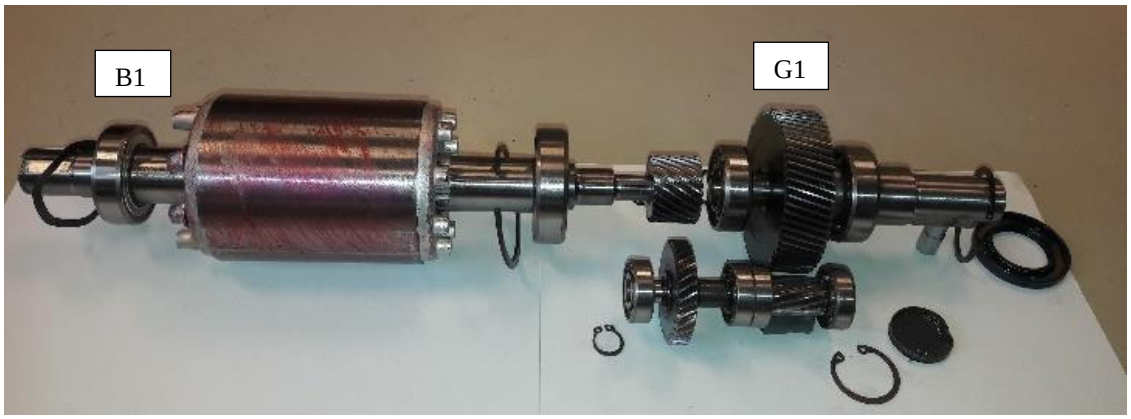

Figure 3.3: The internal components of the electric powertrain.

Electric discharge machining (EDM) is used to produce seeded faults in bearings and gears. Figure 3.4 shows the EDM equipment used for making the seeded faults in a controlled way. An outer-race defect on the induction motor bearing is made as shown in Figure 3.5 (a). As shown in Figure 3.5 (b), a small-scale damage is produced in the large gear using EDM. There were identical 5-units of the powertrain. Different fault severities are produced for bearings and gears of each powertrain. The details of fault severities can be found in the published papers. For stator winding faults, 10% inter-turn short circuit is seeded to one phase of the stator winding as shown in Figure 3.5 (c).

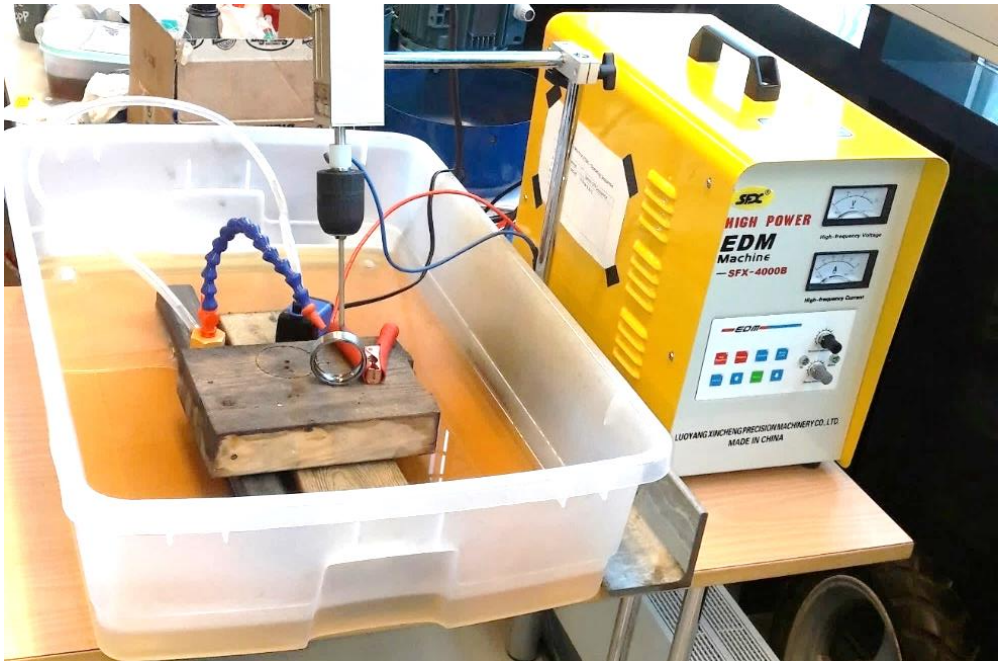

Figure 3.4: The electric discharge machining equipment.

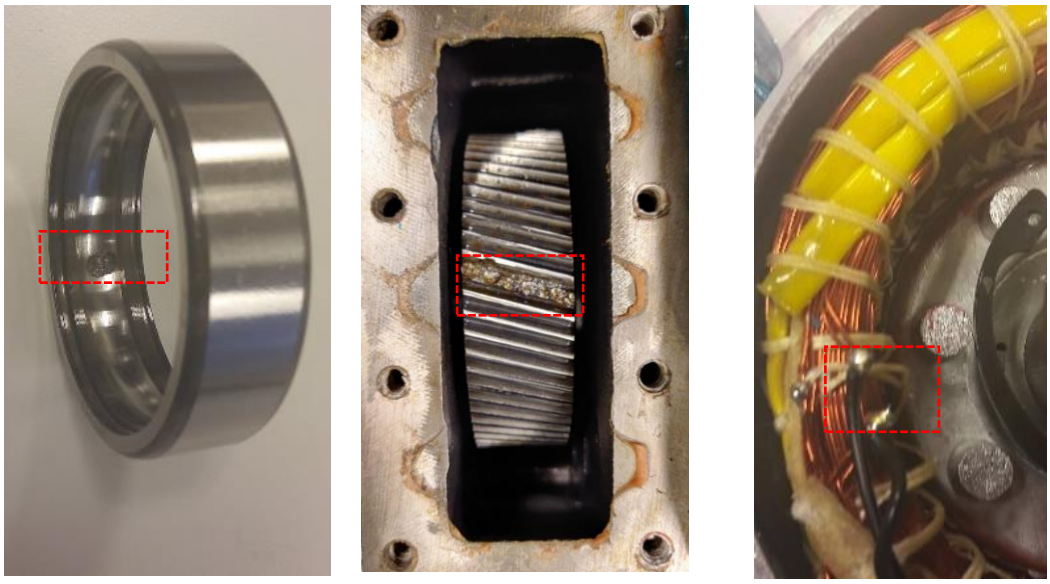

(a) (b) (c)

Figure 3.5: The faulty components of electric powertrain.
(a) outer-race damaged bearing (b) damaged gear (c) 10% inter-turn short circuit fault in the stator.

3.3 The modified in-house test bench

The in-house test bench is modified to collect the data for the proposed fault diagnosis scheme in paper B. As shown in Figure 3.6, the electric powertrain used in Section 3.2 test bench is replaced by a PMSM motor while the data acquisition system remain same. A vibration sensor is attached to the PMSM for collecting vibration signal, and a current sensor is used for collecting motor current signal. A seeded fault with 2 mm surface damage of the outer race is applied to a bearing in the PMSM using EDM, and 10% inter-turn short circuit fault is applied to one phase of the stator winding.

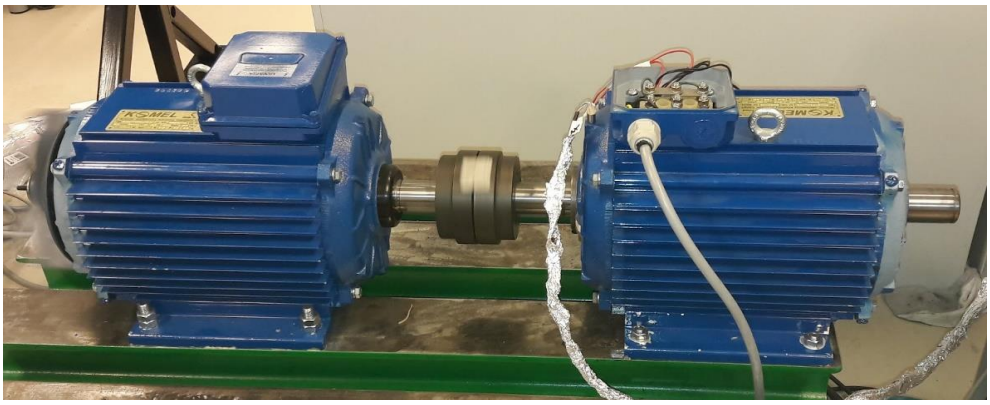

Figure 3.6: The experimental setup used for PMSM fault data

3.4 External datasets

3.4.1 Bearing run-to-failure tests by University of Cincinnati

A run-to-failure test conducted by Intelligent Maintenance Systems, University of Cincinnati, USA [58, 59] is used in paper A. In this experiment, four bearings were connected to a shaft rotating at 2000 rpm. A 2700 kg radial load was applied to the shaft. Four accelerometers were used to collect vibration signals at 20 kHz sampling frequency. One-second samples were recorded every 10 minutes. Inner-race, outer-race and rolling element faults have been observed at the end of the test. Early fault detection and classification of outer-race and inner-race bearing faults are considered in paper A.

3.4.2 PHM challenge dataset for gearbox fault diagnosis

An experimental data provided by PHM society data challenge in [60] is used to validate the algorithm proposed in paper C. A two-stage parallel shaft gearbox is used for collecting the vibration data. It consists of four gears, three shafts and six bearings. The gears are removable, and two types of gears, namely spur and helical, are used. Eight fault cases of the spur gearbox and six fault cases for the helical gearbox have been tested. Each fault case includes multiple faults from gears, bearings or shafts. Two accelerometers and one tachometer are used to collect the vibration data and input-shaft speed. The accelerometers are placed on the input and output shafts of the gearbox. The data of each channel is sampled at 200 kHz. Each fault class was tested at five different speeds (30 Hz, 35 Hz, 40 Hz, 45 Hz, and 50 Hz) and two different load conditions (high and low), and repeated, thus 20 data files were collected. The data is used to train and validate the proposed robust fault diagnosis system for diagnosing the gearbox mixed faults.

Chapter 4

Diagnostics of bearings faults in electric motors

Bearings are the most critical elements in rotating machinery systems, and bearing faults are the main reasons for failures in electrical motors [1, 2, 5]. Therefore, early bearing fault detection is very important to prevent critical system failures. With the proposed diagnostic method in Section 4.1, the bearing faults can be detected at early stages, and the machine operators will have time to take preventive action before a large-scale failure. More details of the proposed diagnosis algorithm are given in Paper A. The bearing fault diagnosis in electric motors at variable speeds and loads is proposed in paper B. In addition to single bearing fault diagnosis, a mixed bearing and inter-turn stator winding fault is given in Section 4.2. The summary of the chapter is presented in Section 4.3.

4.1 Early detection and classification of bearing faults

Numerous bearing fault diagnosis schemes can be found in literature [8, 14, 33, 35, 37, 54, 58, 61], but the focus on early-stage fault diagnosis is limited. Some patented high-frequency techniques, such as PeakVue^{TM} , Shock Pulse^{TM} Method (SPM) and Spike Energy^{TM} [62-64], have been used in industry for early fault detections, but those methods are expensive or applicable in certain applications. Combination of suitable signal processing and machine learning methods can be

an useful approach for early fault detection at a reasonable cost. Envelop analysis provides more information about bearing characteristic frequencies than the original vibration signal [65]. Using the strong features allows a SVM algorithm to detect bearing faults in early stages in the multidimensional feature space, which is the main content of paper A.

4.1.1 The proposed algorithm

The proposed fault diagnosis algorithm consists of two main sections. First, the vibration signals are processed to collect relevant time and frequency domain features. Then the SVM algorithm given in Figure 4.1 is used to train a classifier for fault detection and classification.

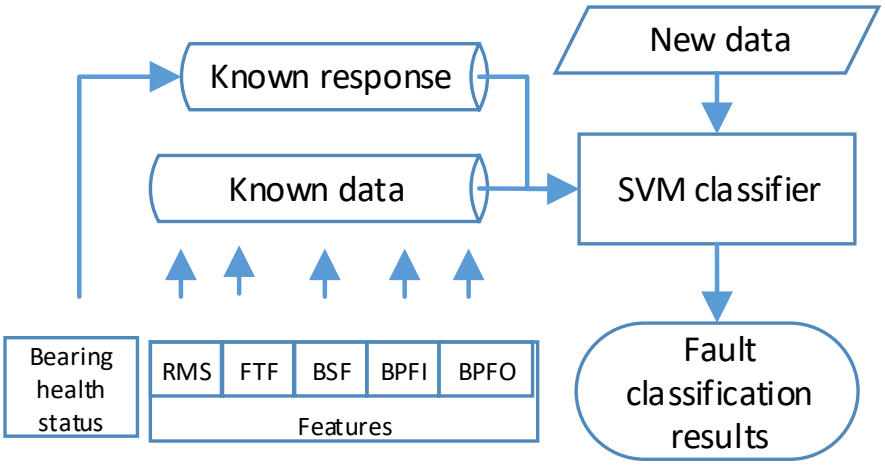

Figure 4.1: Block diagram of the SVM classifier.

Feature extraction is the first step for building the data-driven SVM algorithm. Time and frequency domain features are extracted from the vibration signals. Root mean square (RMS) of vibration signal is selected as the time domain feature. For frequency-domain features, envelop analysis is applied to get the envelope signal from the time domain signal, and fast Fourier transformation is used to convert the envelope signal into the frequency domain. Then, fault characteristics frequencies located in the frequency spectrum and energy associated with frequency bands are extracted. The characteristic frequency bands of the bearing consist of fundamental train frequency (FTF), ball spinning

frequency (BSF), ball pass frequency inner race (BPFI), and ball pass frequency outer race (BPFO) [66, 67]. Five fault cases were considered: healthy, inner race degradation (IR_D), inner race failure (IR_F), outer race degradation (OR_D), and outer race failure (OR_F). The SVM classification algorithm is used to classify the faults.

In SVM classification, the objective is to make a multidimensional hyperspace using the available features, and then draw an optimum hyperplane to separate fault classes. 80% of the available data is used for training the algorithm, and the remaining 20% data is used for validating the algorithm. The trained classifier is applied to detect and classify the faults in early stages from new data.

4.1.2 The experimental results and discussion

A run-to-failure dataset explained in Section 3.4.1 is used to validate the algorithm. Figure 4.2 shows the RMS of vibration signal for a complete life of an inner-race faulty bearing.

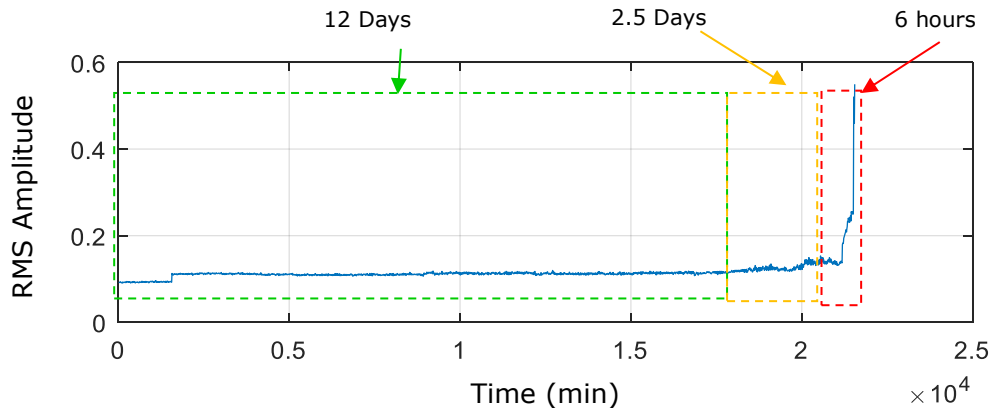

Figure 4.2: RMS of the vibration signal for a complete life in case of an inner-race faulty bearing.

The green dotted area is related to healthy duration, and the yellow dotted area is related to IR_D. The IR_F region is given in red dotted lines. Similarly, the RMS of vibration signal for outer race fault is given in Figure 4.3, in which the green, yellow and red dotted areas show the healthy, OR_D, and OR_F of the bearing, respectively.

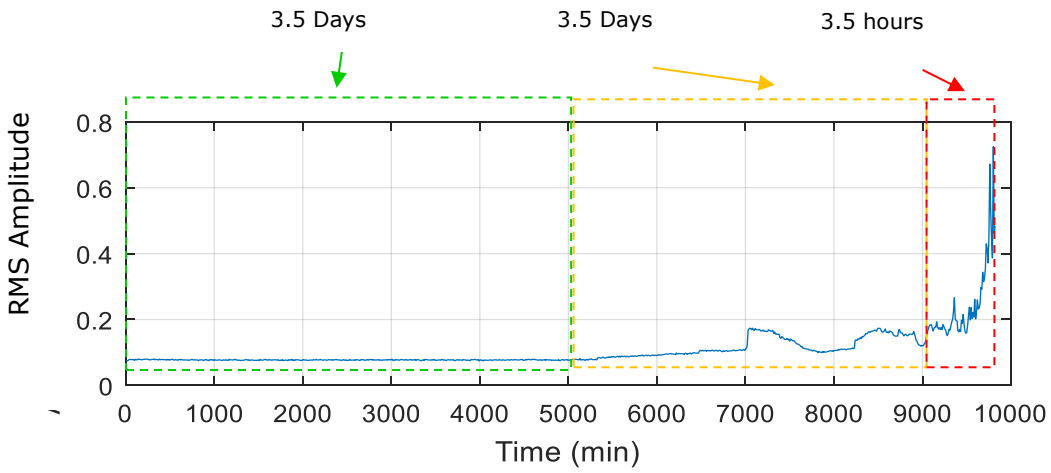

Figure 4.3: RMS of vibration signal for complete life of outer-race faulty bearing.

Figure 4.4 shows the frequency spectrum of vibration signals for the inner race fault and healthy cases. The expected frequency for the inner race fault is 300.6 Hz and 1X (shaft rotating frequency = 33.75 Hz) sidebands. The observed frequencies are 301.3 Hz and 1X sidebands. For the healthy case, the fault-related frequency components are not present in the vibration spectrum. Therefore, the inner race faults can be clearly seen from the vibration spectrum.

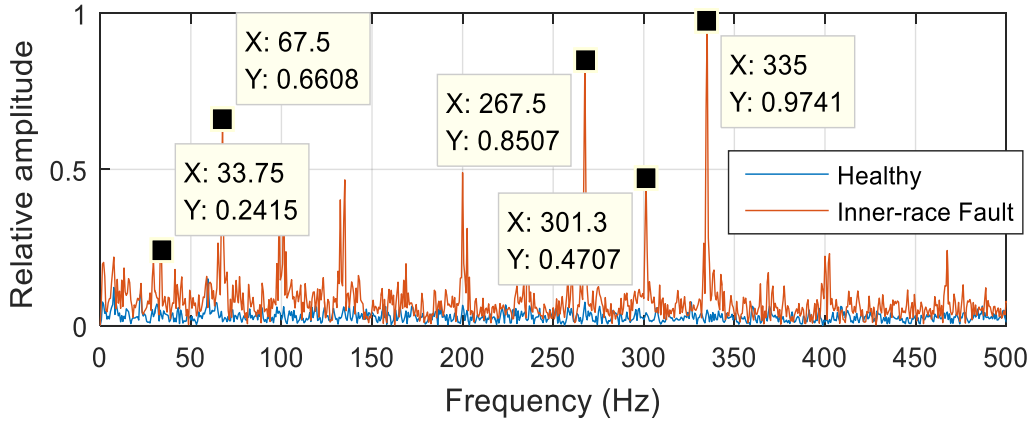

Figure 4.4: The frequency spectrum of a vibration signal for inner race fault.

As shown in Figure 4.5, the expected frequency associated with an outer race fault is also present in the frequency spectrum. The expected frequency is 239.3 Hz, and the observed frequency is 236.3 Hz. The deviation is small, and this small frequency variation is normal in detecting bearing faults since the right value of

contact angles is unknown. In the healthy case, fault-related frequency components are not visible, being closer to zero.

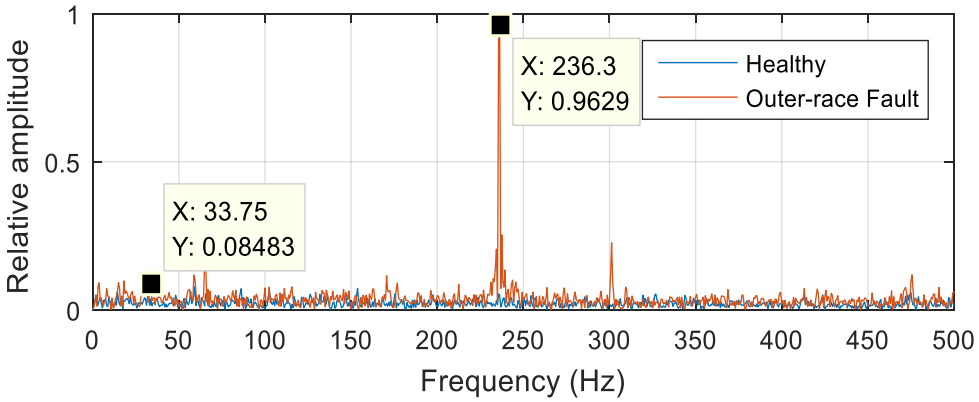

Figure 4.5: The frequency spectrum of the vibration signal for an outer race fault.

Two types of SVM kernels are used for a comparison of the SVM algorithm, and the results are summarised in Table 4.1. The accuracies of fault classification are about 86% in the IR_D class, and 96% in the OR_D class. Both linear SVM and quadratic SVM classifiers are able to detect faults in early stages, and the accuracy of classification is reliable since a bearing fault can be detected 2.5-3.5 days ahead in the run-to-failure test. The proposed method can be extendable to an online fault diagnosis system.

Table 4.1: Performance summary of the proposed algorithms.

Fault Class	Classification accuracies : True positve rates (TPR) / False negative rates (FNR)			
	Linear SVM classifier		Quadratic SVM classifier	
	TPR	FNR	TPR	FNR
H	99.4%	0.6%	99.3%	0.7%
IR_D	87.0%	13.0%	86.2%	13.8%
IR_F	90.2%	9.8%	87.8%	12.2%
OR_D	96.0%	4.0%	97.7%	2.3%
OR_F	78.9%	21.1%	84.2%	15.8%

4.2 Fault diagnostics of electric motors under variable load and speed conditions

The bearing and stator winding faults are common faults in electrical machines, and conventionally detected in steady states, e.g. constant speeds and loads. However, variable loads and speeds are typical operations in wind turbines and powertrains. Therefore, it is important to detect bearing and stator winding faults in variable speed and load conditions. This section provide a summary of the proposed fault diagnosis scheme used to address above challenges. More details of the proposed method are given in paper B.

4.2.1 The proposed algorithm

A block diagram of proposed algorithm is given in Figure 4.6, and the algorithm focuses on tracking the frequency orders associated with faults from the normalised order spectrum. The normalised order spectrum can be generated by resampling the measured vibration signal via estimated motor speeds [68, 69].

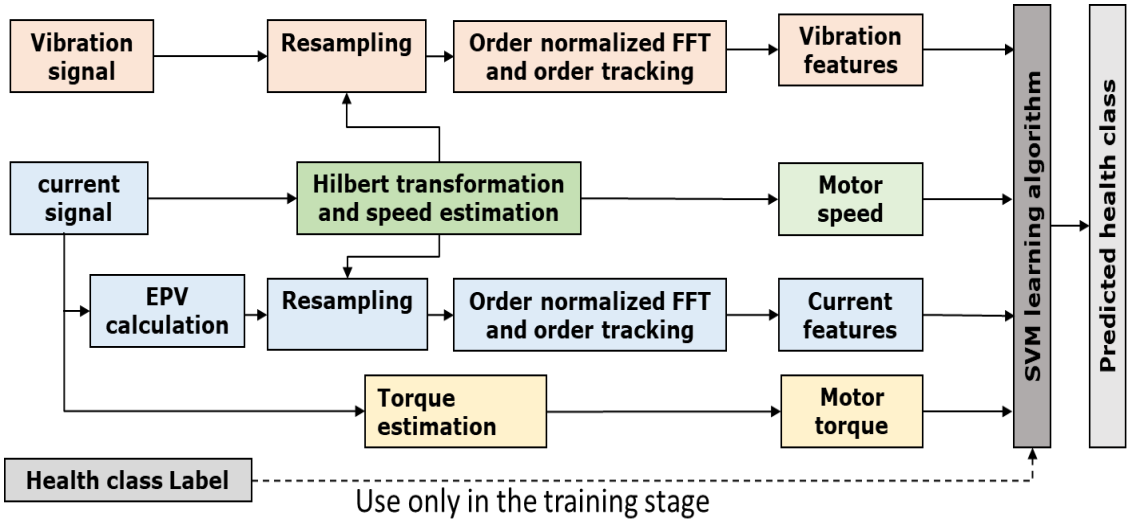

Figure 4.6: Block diagram of the proposed fault diagnosis and classification algorithm.

The fault features are then derived from the RMS of tracked charasteristic frequency orders, estimated torque and speed of the motor. The details of the features used in the algorithm is given in Table 4.2. Finally, a SVM algorithm is used to classify the faults.

Table 4.2: The features used in the SVM classification algorithm.

Signal source	Feature name	Description
Current	Speed	Represent the motor speed
	Torque	Represent the motor torque
	$2f_s$	Characteristic frequency of inter-turn winding fault from the extended Park's vector (EPV) [70] current i_p
	Torque Variance	Moving variance of 10 consecutive values of the torque signal
Vibration	3.05X order	Characteristic frequency of outer-race bearing fault = 3.05 × Motor rotating speed/frequency
	1X	Motor rotating speed
	8X order	Motor rotating speed × No. of motor pole pairs
	16X order	Motor rotating speed × 2 × No. of motor pole pairs (2nd harmonics)

4.2.2 The experimental results and discussion

The experimental test setup explained in Section 3.3 is used to collect the data. Manually seeded faults are applied to the bearing and stator winding. The single and mixed faults are tested at constant speeds (150, 250 and 350 rpm), and 2 types of variable speed profiles. A speed profile used in the study is given in Figure 4.7.

In the speed profiles, 10 repeated tests have been conducted, and 50 samples of 2 minute data are recorded. The sampling rate was 20 kHz. After the order normalisation, the number of samples per 2 minute signal is approximately 360. This value is selected by compensating for both order and time resolutions. Finally, a table of 18000 sample rows and 9 columns (8 features and the health class labels)

have been produced. Then 75% of available data is used to train the SVM algorithm, and 25% data is applied for validating the algorithm.

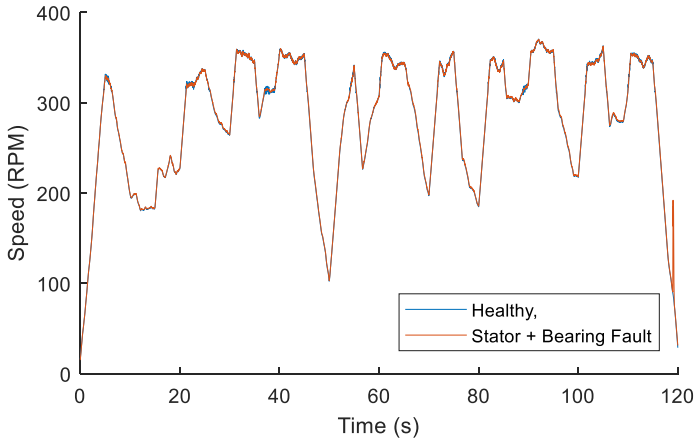

Figure 4.7: A variable speed profile used in experiments.

The average order spectrum of i_p is given in Figure 4.8. The 2nd order (peak at 1.989) is the strongest feature for stator winding fault. The 2nd order of i_p is tracked over time, and the tacked signal for healthy and faulty cases are given in Figure 4.9. The amplitude of signal variation according to the dynamic operating conditions, but, the amplitude is greater than healthy case.

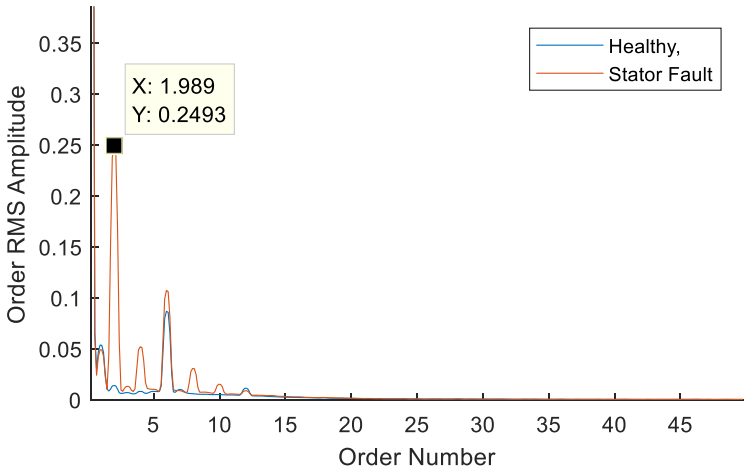

Figure 4.8: Average i_p order spectrum for stator winding fault.

Similarly, as given in Figure 4.10, the 3.05X order of the vibration signal is tracked for the outer race bearing fault. A mixed fault condition is also established. The RMS amplitude of 3.05X order vibration signal fluctuates over dynamic

operation, and a fixed threshold cannot be defined to detect bearing faults in single or mixed fault conditions. Therefore, a statistical threshold or classification rule using machine learning is mandatory, and a SVM algorithm with additional features is used in the proposed diagnosis scheme.

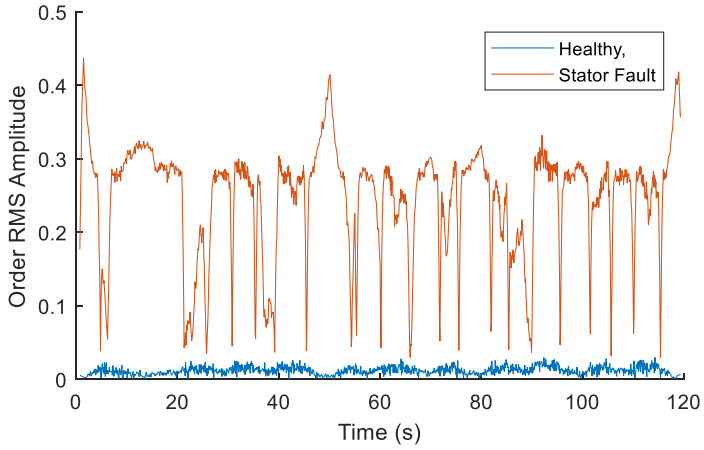

Figure 4.9: Tracked 2nd order of i_p order spectrum for stator winding fault.

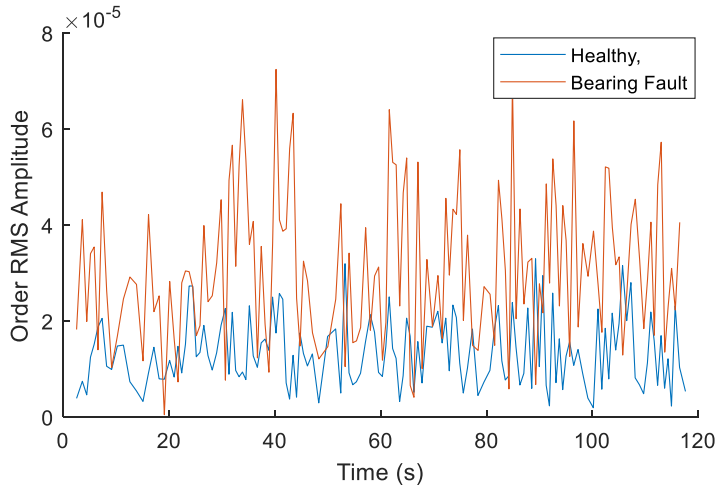

Figure 4.10: Tracked 3.05X order of vibration signal for a bearing fault.

The confusion matrix for validating dataset is given in Figure 4.11. The overall accuracy of the SVM classifier is about 92.9%. For all the fault classes, more than 90% classification accuracy is obtained, and the maximum classification accuracy is 94%. These results are highly acceptable, proving that the SVM can detect and classify the two faults in variable speed and load conditions.

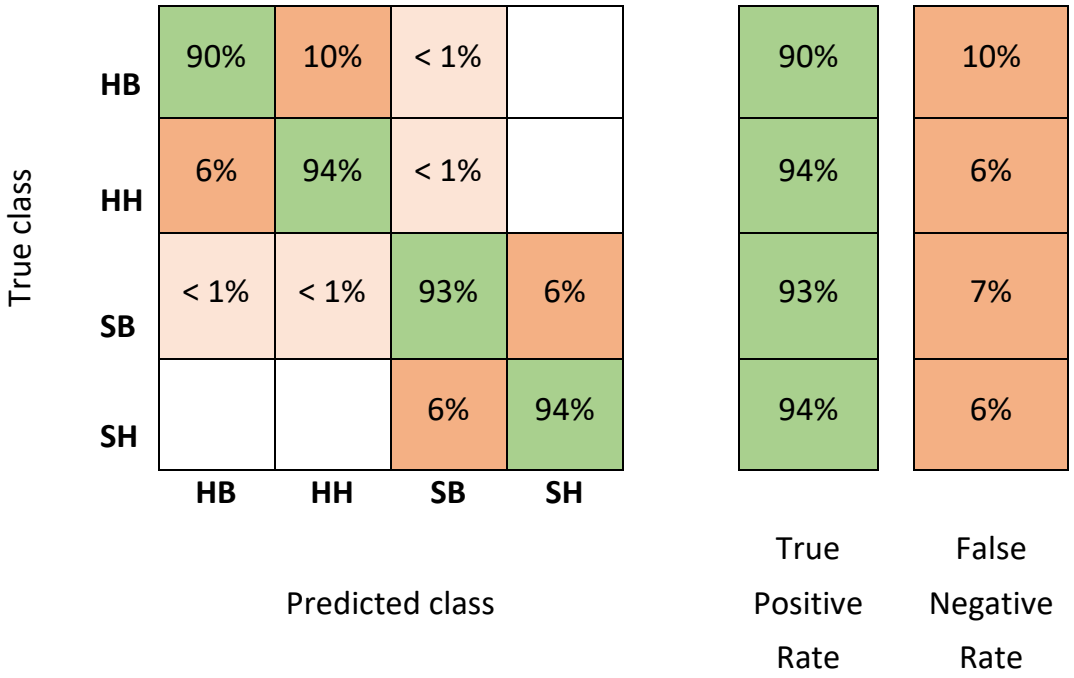

HB (Stator winding healthy and bearing fault)
HH (both stator winding and bearing are healthy)
SB (both stator winding and bearing are defective)
SH (stator winding is faulty and bearing is healthy).

Figure 4.11: The confusion matrix for the test dataset.

4.3 Summary

This chapter focuses on condition monitoring of bearings in electric motors, presenting two schemes for fault diagnosis. The algorithm presented in Section 4.1 is applied for early fault diagnosis at constant speed and load conditions. The diagnosis scheme introduced in Section 4.2 is suitable for fault diagnosis at variable speeds and loads. The mixed fault diagnosis performances is also tested, and promising results have been obtained for both cases. The fault diagnosis algorithms proposed in this chapter, are based on traditional machine learning procedure, in which the features are manually derived by signal processing and collected energies at fault-related characteristic frequency bands. In Section 4.1, the envelope analysis of vibration signal is used to produce strong features for detecting bearing faults in early developing stages. An order tracking algorithm is used to detect bearing faults related characteristics frequency orders at variable speed conditions in Section 4.2. These algorithms work well for considered two

fault cases. However, in practice, the fault types might be unknown, thus the manual feature generation is a challenging task. For detecting faults in complex gearboxes and powertrains, the traditional machine learning process is time-consuming, requiring automatic feature generation methods.

Chapter 5

Diagnostics of mixed faults in gearboxes and electric powertrains

As discussed in the state-of-the-art, new algorithms and diagnosis schemes are required for dealing with mixed faults under dynamic operations. This chapter provides solutions for such contexts via two application studies in Papers C, D and E. In paper C, being summarized in Section 5.1, the machine learning and data fusion methods are used to improve the accuracy and robustness of a gearbox fault diagnosis system under noises and steady-state operations. The performance of the proposed algorithms are compared with those without using data fusion. Being summarized in Section 5.2, as a summary of papers D and E, briefly presents an electric powertrain fault diagnosis scheme for diagnosing mixed faults at variable loads and speeds, and gives a short introduction of the online implementation the proposed diagnosis system. The conclusion of the chapter is given in Section 5.3.

5.1 Robust fault diagnosis system for gearbox mixed faults

A gearbox has a complex structure with many bearings, shafts, and gears. Under a mixed fault context, using traditional signal processing to the vibration spectrum is difficult, requiring the details of gearbox internal structure. In [71], a review of gear fault diagnosis using various vibration signal condition indicators (CI) and features, such as RMS, crest factors, kurtosis, and spectral kurtosis, is presented, and performances of the different CIs are compared in the work. However, most existing methods focus on single fault diagnosis of gearbox faults. A gearbox

multi-fault diagnosis scheme is proposed in [72], but the robustness of the system under noises is not considered. Other studies also deal with either single or multi-fault diagnosis, but the details of robustness analysis under noises are very limited or missing [9, 10, 30, 73-75]. Increasing performance of the detection system might be more important than looking for a highly reliable feature since the machine cannot be completely healthy due to the absence of clear characteristic frequencies as argued in [73]. AI algorithms and data fusion might be a solution for increasing the accuracies and robustness of a fault diagnosis system [34].

The main objective of paper C is to implement a robust fault diagnosis system, which can give accurate results at various noise conditions. The experimental dataset provided by PHM society data challenge is used to validate the proposed algorithm.. Figure 5.1 shows the structure of the gearbox used in the experiments. More details of experiments and data can be found in paper C.

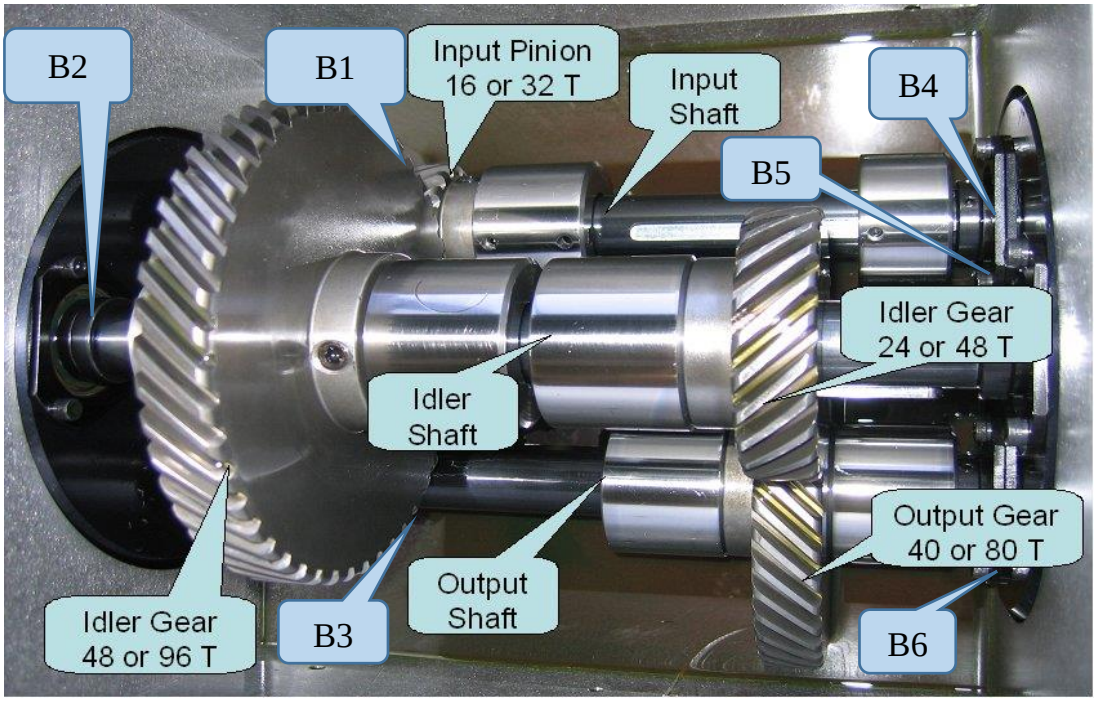

Figure 5.1: The structure of the gearbox [60].

In the given experiments, a two-stage parallel shaft gearbox is used for collecting the vibration data at the sampling rate of 200 kHz. The gearbox consists of four gears, three shafts and six bearings (B1,2,…6) as described in Chapter 3. There are 8 different fault classes for spur gearbox and 6 fault classes for helical gearbox. A summary of fault classes are given in Table 5.1. Each fault class represents a combination of faults in gears, bearings and shafts of respective

gearbox arrangements. Each fault class is tested at five constant speeds (30 Hz, 35 Hz, 40 Hz, 45 Hz, and 50 Hz), two load levels (high and low) and two repeated tests, making 20 test conditions for each fault class

Table 5.1: Fault classes of the gearbox [60]

	Gear				Bearing ID						Shaft	
Fault Class	32T	96T	48T	80T	B1	B2	B3	B4	B5	B6	Input	Output
Spur 1	Good	Good	Good	Good	Good	Good	Good	Good	Good	Good	Good	Good
Spur 2	Chipped	Good	Eccentric	Good	Good	Good	Good	Good	Good	Good	Good	Good
Spur 3	Good	Good	Eccentric	Good	Good	Good	Good	Good	Good	Good	Good	Good
Spur 4	Good	Good	Eccentric	Broken	Ball	Good	Good	Good	Good	Good	Good	Good
Spur 5	Chipped	Good	Eccentric	Broken	Inner	Ball	Outer	Good	Good	Good	Good	Good
Spur 6	Good	Good	Good	Broken	Inner	Ball	Outer	Good	Good	Good	Imbalance	Good
Spur 7	Good	Good	Good	Good	Inner	Good	Good	Good	Good	Good	Good	Keyw ay Sheared
Spur 8	Good	Good	Good	Good	Good	Ball	Outer	Good	Good	Good	Imbalance	Good
Fault Class	16T	48T	24T	40T	B1	B2	B3	B4	B5	B6	Input	Output
Helical 1	Good	Good	Good	Good	Good	Good	Good	Good	Good	Good	Good	Good
Helical 2	Good	Good	Chipped	Good	Good	Good	Good	Good	Good	Good	Good	Good
Helical 3	Good	Good	Broken	Good	Good	Good	Good	Combination	Inner	Good	Bent Shaft	Good
Helical 4	Good	Good	Good	Good	Good	Good	Good	Combination	ball	Good	Imbalnce	Good
Helical 5	Good	Good	Broken	Good	Good	Good	Good	Good	Inner	Good	Good	Good
Helical 6	Good	Good	Good	Good	Good	Good	Good	Good	Good	Good	Bent Shaft	Good

5.1.1 The proposed hybrid algorithm

A block diagram of the proposed hybrid fault diagnosis algorithm is shown in Figure 5.2. Two vibration sensors are connected at two different places of the gearbox (input shaft and output shaft sides) to collect the vibration data of gearbox from two different viewpoints. A redundancy data fusion scheme is implemented to enhance the accuracy and robustness of the diagnosis, which includes both feature level and decision level data fusion.

Two types of features, namely domain knowledge features and time-frequency pattern features, are extracted. The domain knowledge features (20 features) are extracted using time-domain signal and a bank of filters where centre frequencies are defined by the frequencies of the gearbox shafts and gear meshing frequencies.

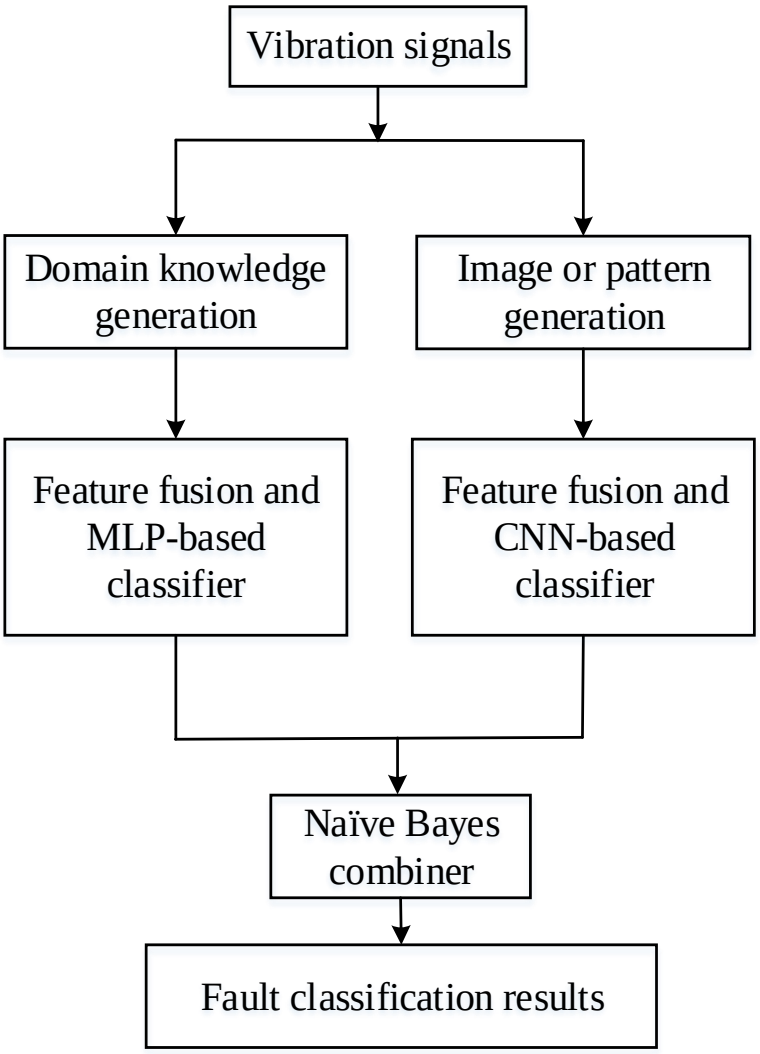

Figure 5.2: Block diagram of the proposed hybrid fault diagnosis for the gearbox.

The time-frequency pattern features are extracted using the continuous wavelet transformation (CWT) from the collected vibration signal. For each sample, two CWT images are produced from each vibration signals and merged into one image. In addition, STFT based images were also produced for a comparative study to find the best images or pattern generation for this application. Figure 5.3 shows 2-D representation of a vibration signal for a gearbox fault class.

Classifiers based on MLP and CNN are used for feature level fusion and to increase the confidence of fault classification. In addition to the feature level data fusion, decision level fusion is used for increasing the robustness of classification in noisy conditions. More details of this feature extraction and fusion algorithms can be found in paper C.

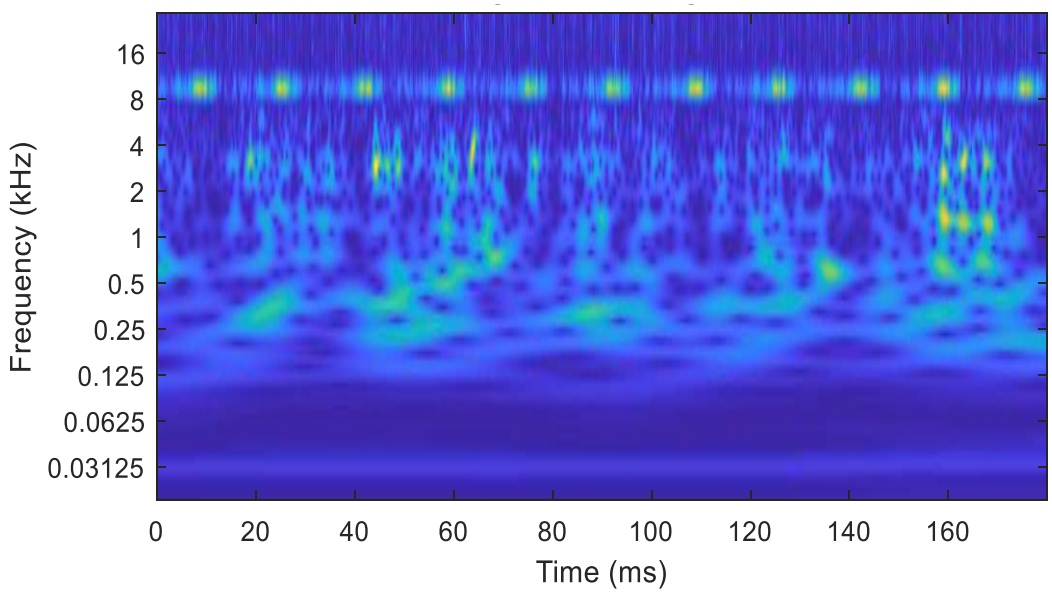

Figure 5.3: The 2-D representation of the signal using wavelet transform.

5.1.2 The experimental results and discussions

There are 280 files for 14 different fault classes or 20 files for each class in the original dataset. More data samples are required to enhance the effectiveness of the proposed algorithm. A complete time-frequency representation of a vibration signal requires the data of one complete cycle of rotation. Based on this rule, one data file is subdivided into 20 samples, so 400 samples are created for each fault class. Therefore, 5600 samples for 14 fault classes are used for training and testing of the algorithm, in which 75% of the data is used for training.

Accuracy and robustness of individual classification algorithms

First, the classification accuracies of each individual MLP and CNN algorithms are tested (without naïve Bayes combiner) using nine test cases as given in Table 5.2. Then, the performance of the proposed feature level fusion scheme is evaluated and compared with that of the baseline without using data fusion. The test cases 1, 2 and 3 represent the individual MLP algorithm performances, where vibration data from a single sensor is used in cases 1 and 2. In case 3, vibration data from both sensors are used for feature level data fusion.

The test cases 4 to 9 represent the performance of CNN classifier, where STFT images are used as input for CNN in test cases 4, 5 and 6. CWT-based

images are used in test cases 7,8 and 9. The results in Table 5.2 show that the feature level fusion can increase the classification accuracies (by 0.5% to 21.8% depending on test case) of the individual MLP and CNN algorithms. Furthermore, in case of CNN, the CWT images give best results for both helical and spur gearbox tests. According to the results in Table 5.2, the CWT based CNN, and domain feature-based MLP with feature level fusion can be selected as the best classifier in this application.

Table 5.2: Overall performances of individual MLP and CNN classifiers.

Test case	Algorithm	Signal	Spectrogram images	Feature fusion	Accuracy and difference compared to feature level fusion (%)			
					Spur		Helical	
1		Input	-	No	94.1	- 4.2	81.8	- 16.2
2	MLP	output	-	No	97.0	- 1.3	86.2	- 11.8
3		**both**	**-**	**Yes**	**98.3**		**98.0**	
4		input	STFT	No	94.0	- 3.5	59.5	- 21.8
5		output	STFT	No	90.3	- 7.2	80.8	- 0.5
6	CNN	**both**	**STFT**	**Yes**	**97.5**		**81.3**	
7		input	CWT	No	92.0	- 6.0	87.8	- 8.4
8		output	CWT	No	90.6	- 7.4	90.8	- 5.4
9		**both**	**CWT**	**Yes**	**98.0**		**96.2**	

Two types of noises are added to the original signals to test the robustness of the proposed individual algorithms. The noise type-1 signals are generated by adding white Gaussian noises to the signals with a signal to noise ratio (SNR) of 14 dB. Noise type-2 signals are generated by mixing each signal to another signal. This scenario demonstrates a practical beating situation in a gearbox, where the original vibration signal (R_{su}) being measured is mixed with a fraction (f %) of another vibration source (R_e). The helical fault class 2 is selected as R_e in case of helical gearbox. The mixing weight (f %) is selected at 0.5, and the helical fault class 2 is added as noise to all other helical fault classes. In spur gear faults, a similar rule is applied, and the spur fault class 2 is used as a noise (R_e) for other spur fault classes.

To further compare the accuracy and robustness of the proposed individual MLP and CNN algorithms, other classification algorithms are also used. The comparison results are given in Figure 5.4.

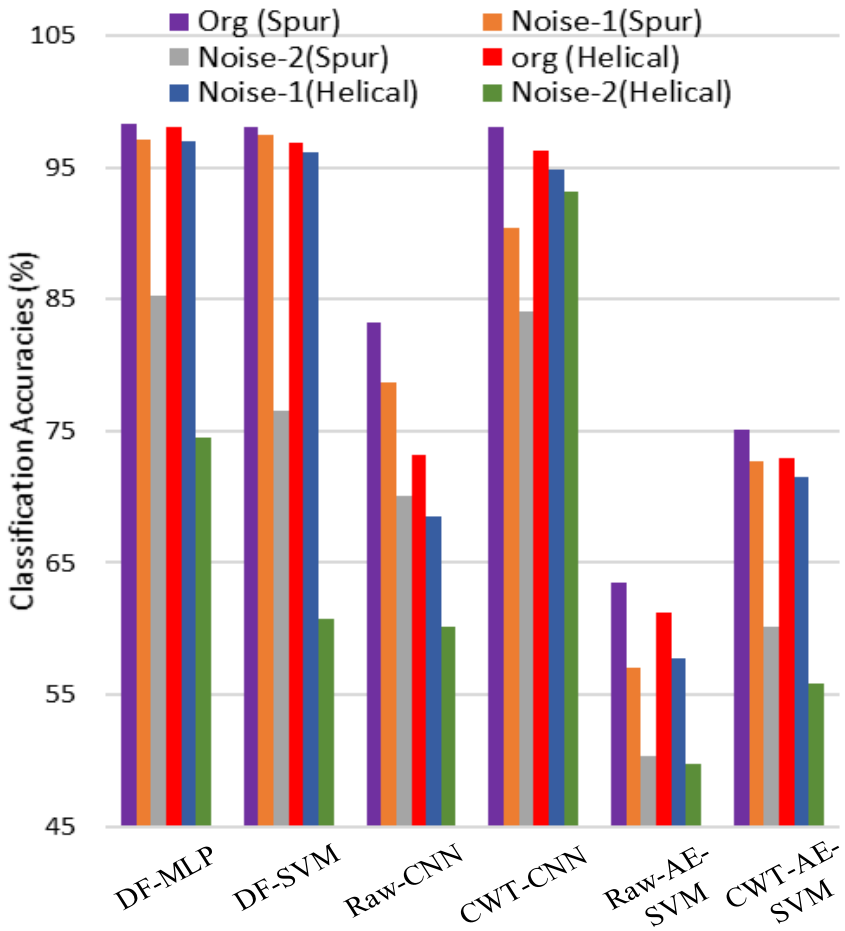

Figure 5.4: Accuracy and robustness comparison of individual algorithms.

The DF-MLP represents the proposed domain features (DF) and MLP algorithm combination, while DF-SVM represents a DF with a SVM algorithm. When comparing the DF-MLP and DF-SVM, both algorithms can produce relatively high accuracies for noiseless case (Org) and the noise type-1 case. However, compared to DF-MLP, the classification accuracies of DF-SVM are significantly lower for noise type-2, showing that the DF-MLP algorithm is more robust than the DF-SVM algorithm. Similarly, the performance of the proposed CWT-CNN algorithm is compared with that of three different algorithms. In raw-CNN, the raw vibration signal is fed to CNN without generating CWT images.

Other two algorithms use, autoencoder based feature learning and SVM classification. The raw vibration signal is used for feature generation in Raw-SVM while CWT images are used in CWT-SVM. The comparative study results show that the CWT-CNN is more accurate and robust under the considered noises.

Accuracy and robustness of the multiple-fault classification using the hybrid neural networks and decision level fusion

The comparison study in Figure 5.4 shows that both DF-MLP and CWT-CNN are the best classifiers for the considered diagnosis application. Next, a decision level fusion based on naïve Bayes algorithm is applied to the output of each individual classifiers, and the accuracies and robustness of the algorithm are further increased. Table 5.3 summarises the performance of the proposed decision level fusion.

Table 5.3: Overall performances of MLP and CNN classifiers with noise.

Test case	Algorithm	Noise type	Decision level fusion	Accuracy and difference compared to decision level fusion (%)			
				Spur		Helical	
1	MLP		No	98.3	- 0.1	98.0	- 0.2
2	CNN	-	No	98.0	- 0.4	96.2	- 2.0
3	**MLP + CNN**		**Yes**	**98.4**		**98.2**	
4	MLP		No	97.1	- 0.4	97.0	- 0.7
5	CNN	Noise 1	No	90.4	- 7.1	94.8	- 2.9
6	**MLP + CNN**		**Yes**	**97.5**		**97.7**	
7	MLP		No	85.3	- 5.8	74.5	- 19.0
8	CNN	Noise 2	No	84.1	- 7.0	93.2	- 0.3
9	**MLP + CNN**		**Yes**	**91.1**		**93.5**	

The test case 3 shows the performance of decision level fusion without noise, and the test cases 6 and 7 show the performance of decision level fusion for noise type-1 and type-2, respectively. Other test cases represent individual algorithm performances without decision level fusion. For the noiseless case, there is no much improvement of classification accuracies (from 0.1 to 2.0%

improvement). For the noise type-1 case, the classification accuracy improvement of the proposed decision level fusion is in between 0.4 and 7.1%, being considerable. In the case of noise type-2, the improvement is in between 0.3 and 19%, which is a significant improvement.

The mean and standard deviation of classification accuracy improvement in individual algorithms and the proposed decision level fusion are shown in Figure 5.5. For example, the mean and deviation of the MLP algorithm are 91.7% and 8.92% using the six classification accuracies (98.3%, 98.0%, 97.1%, 97.0%, 85.3% and 74.5%) given in test cases 1, 4 and 7 in Table 5.3. This means that the MLP classifier has the mean accuracy of 91.7%, but it is not robust under noises due to the big variation. As seen from Figure 5.5, the mean accuracy is maximized, and the deviation is minimized if using decision fusion of the CNN and MLP results.

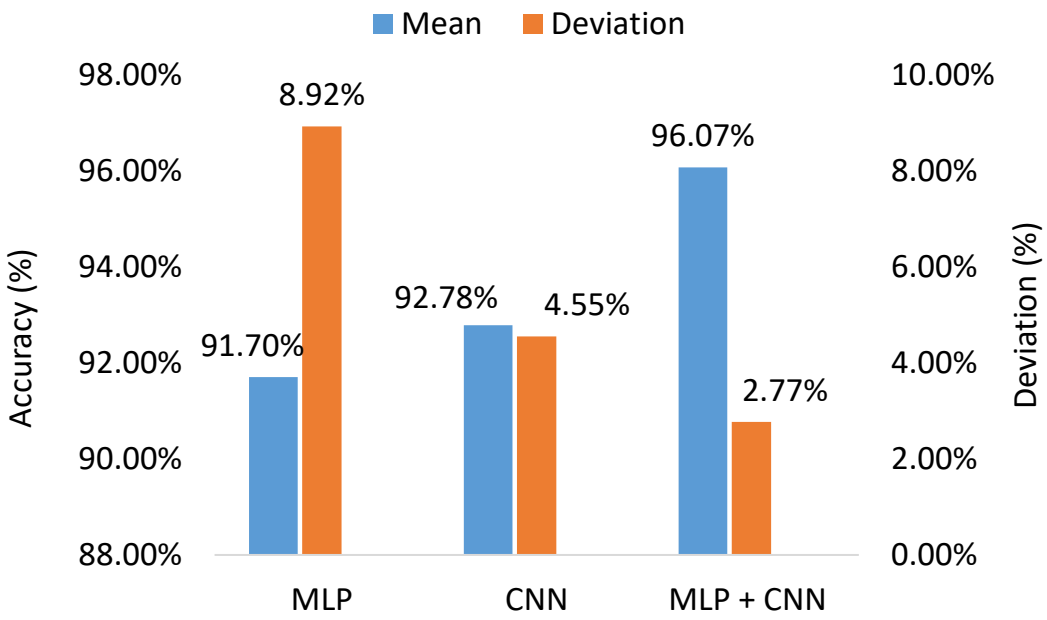

Figure 5.5: Mean and deviation in different test cases.

5.2 Fault diagnosis system for an electric powertrain

Reliable diagnosis for defects in the critical components of electric powertrains such as bearings, gears and stator windings, is important to prevent failures and enhance the system reliability. Most existing fault diagnosis methods are based on measuring specific characteristic frequencies to single faults at constant speed operations. As mentioned, the measured quantities are non-stationary under variable loads and speeds, thus multiple fault diagnosis of gearboxes or electric powertrains under such contexts are challenging. Once multiple faults occur in the system, the existing methods may not detect the faults effectively and may give false alarms. In [76], a machine learning method is proposed for fault diagnosis of electric motors, but this study focuses only on single faults under fixed speeds. Although various bearing faults and gear faults are analysed in a gearbox multi-fault diagnosis system in [72], the test conditions were at single faults with fixed loads and speeds. Most recent studies consider either multiple fault diagnosis at constant speeds, or single fault diagnosis at constant or variable loads and speeds. It is difficult to find a study dealing with both multiple faults and variable load and speed levels in literature. Further, research on multiple fault dignosis under variable loads and speeds using limited data is missing in both academia and industry.

In this section, a deep learning based fault diagnosis method is proposed to detect common faults in the electric powertrains. The proposed method is based on pattern recognition using a convolutional neural network to detect effectively not only single faults at constant speed but also multiple faults in variable speed operations. In addition, the algorithm is trained only using single faults, but the trained algorithm can detect multiple faults. This allows to reduce the training data requirements. The developed in-house test bench discussed in Section 3.2 is used for data collection. The internal components of the complete powertrain are disassembled as shown in Figure 3.3. They include 8 bearings, 4 gears and 3 shafts. Small-scale damage is artificially produced in the large gear G1 and an outer-race defect on the induction motor bearing B1 using an EDM. For stator winding faults, 10% inter-turn short circuit is seeded to one phase of the stator winding. Eight fault cases are conducted with individual and multiple faults. The gearbox is coupled to a PMSG, and the generator output is connected to a fixed resistive load. Therefore, the powertrain load is proportional quadratically to the rotational speed. The output

currents of the PMSG are measured and used to estimate the rotational speed of the electric powertrain.

5.2.1 The proposed algorithm

A block diagram of the proposed fault diagnosis system for electric powertrains is shown in Figure 5.6. Motor currents and the vibration sensors are used to diagnose faults. An order tracking algorithm is applied for collecting currents and vibration signals to deal with the variable speeds. Then spectrograms of both currents and vibration signals are generated and combined into large images. This combination provides an enlargement in the feature space. Based on the generated spectrograms, CNN can fuse the current and vibration spectrograms and implement a fault classification.

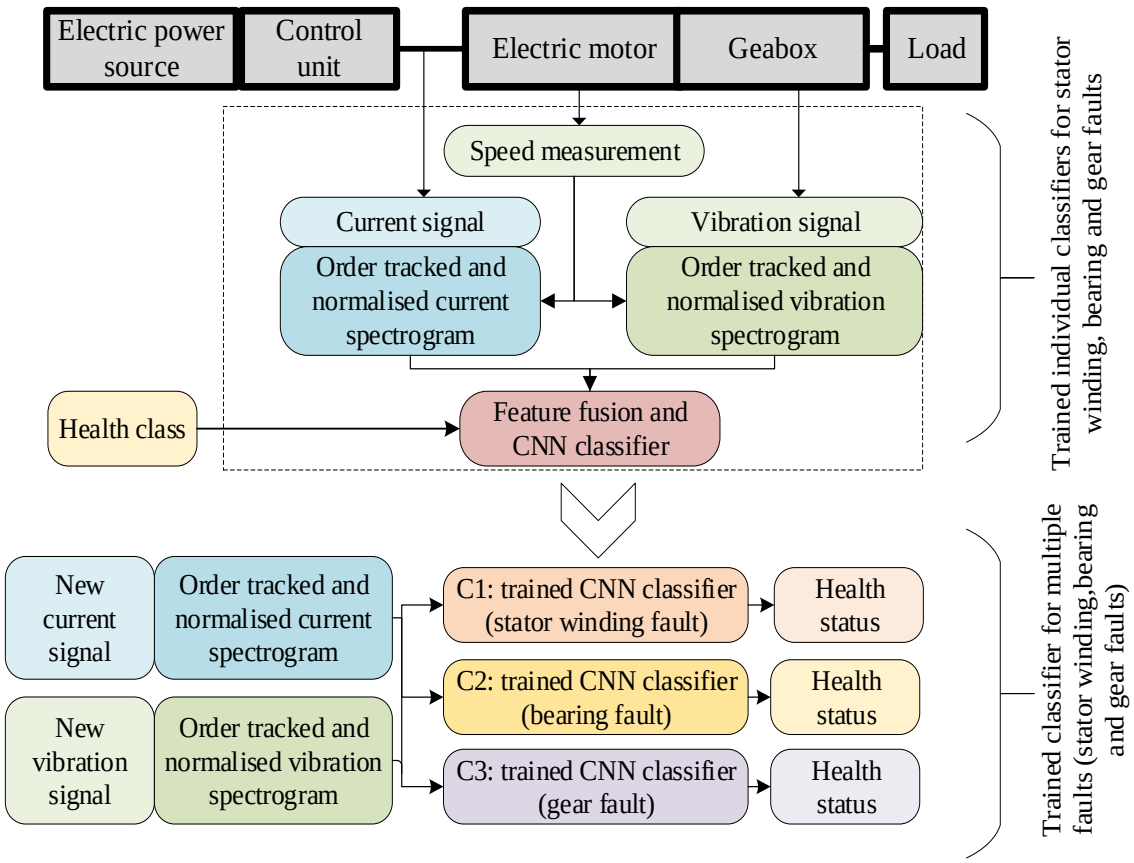

Figure 5.6: A block diagram of training and testing of the fault diagnosis system.

Although CNN is widely used in many applications of image classification, a CNN based fault diagnosis needs to be carefully implemented on spectrograms. The information of faults is hidden in the collected signals, thus proper signal processing methods are required to extract the hidden information from the signals and convert into spectrograms. For this purpose, the order normalization for vibration signals and the Park's vector of currents are used together with CNN.

In the training phase, three classifiers, namely C1, C2 and C3, as shown in Figure 5.6, are individually trained to detect stator winding faults, bearing faults, and gear faults, respectively. After the training process, the trained classifiers are employed to detect multiple fault cases. More details of this system are given in Paper D. The extension of this algorithm for online implementation is given in Paper E.

5.2.2 The experimental results and discussion

The classification accuracies for individual classifiers are summarized in Table 5.4. The C1 classifier is trained to detect stator winding faults, giving an accuracy of 100 %. The classification accuracy of C2 bearing outer-race fault classifier is 98.8 %, and the classification accuracy of C3 gear fault classifier is 99.8%. In other words, all three classifiers work very effectively for detecting single faults.

Table 5.4: Performance summary of individual classifiers.

Case ID	Classifier ID	Component			Fault class	Test Accuracy (%)
		SW	B1	G1		
1	-	H	H	H	HHH	-
2	C1	F	H	H	SHH	100
3	C2	H	F	H	HBH	98.8
4	C3	H	H	F	HHG	99.6

SW: stator winding, B1: bearing 1, G1: gear 1, H: healthy, F: faulty.
HHH: all components are healthy.
SHH: faulty stator, healthy bearing and healthy gear.
HBH: healthy stator, faulty bearing and healthy gear.
HHG: healthy stator, healthy bearing and faulty gear.

The classification accuracies for multiple fault cases are summarized in Table 5.5. The C1 classifier works well for detecting stator winding faults at any multiple fault cases considered in the study, and classification accuracies are greater than 98.8% in all the cases. The C3 classifier also effectively detects the damaged teeth gear fault in multiple fault conditions with a minimum accuracy of 87.8%. The weakest classifier in this study is the C2 classifier, which performs well in some multiple faults (Case 5 and Case 8), but not well for the outer-race bearing faults in Cases 6 and 7, with the accuracies of 76.2% and 71.5%, respectively.

Table 5.5: Performance of multiple fault diagnosis.

Case	Component			Fault class	Test Accuracy (%)		
ID	Sw	B1	G1		C1	C2	C3
5	F	F	H	SBH	**100**	**86.8**	**87.8**
6	H	F	F	HBG	**99.8**	76.2	**98.6**
7	F	H	F	SHG	**100**	71.5	**100**
8	F	F	F	SBG	**98.4**	**90.2**	**99.4**

SW: stator winding, B1: bearing 1, G1: gear 1, H: healthy, F: faulty.
SBH: faulty stator, faulty bearing, and healthy gear.
HBG: healthy stator, faulty bearing and faulty gear.
SHG: faulty stator, healthy bearing and faulty gear.
SBG: faulty stator, faulty bearing and faulty gear.

The classifiers for the stator and gear fault diagnosis have an excellent performance for fault classification under individual and multiple fault conditions. The experimental results confirm that the proposed algorithm can detect single and multiple faults under variable speed conditions. Although the classifier for the bearing fault detection works well for single fault conditions, it has a limited capacity for classifying some multiple fault conditions. Three types of localized faults in the stator winding, bearing and gearbox have been studied in this study, but the concept can be extended to other types of faults such as shaft unbalance, shaft misalignments, bearing inner race faults, gear misalignments, and broken gear tooth.

5.2.3 Online implementation of the powertrain fault diagnosis system

Online fault diagnosis systems are important in industry to monitor the machine condition over a period of time, and automatically get the decisions about the machine health. The online implementation details of an electric powertrain fault diagnosis system are discussed in this section, being detailed in papers D and E. The procedure used for development of the online fault diagnosis system is given in Figure 5.7.

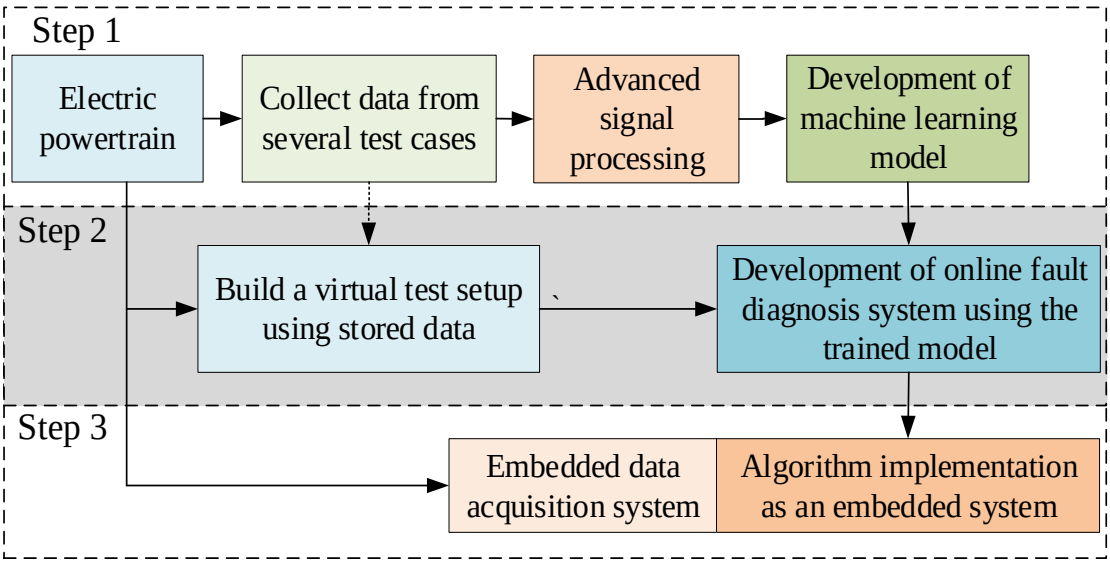

Figure 5.7: The procedure used for development of the online fault diagnosis system

In the first step, the required machine learning algorithm is developed as summarised in Section 5.2.1. Next, the online fault diagnosis system is developed by considering the collected experimental data as a virtual system. The latest step considers aspects of an embedded system development, which is out of scope of this dissertation.

A block diagram of the developed online fault diagnosis system is shown in Figure 5.8, including two subunits, namely health class predictor and decision-maker. In the first subunit, the health classes of the collected signals are predicted using the trained machine learning and data fusion algorithm. Several consecutive prediction results are collected and analyzed in the second subunit for the final decision.

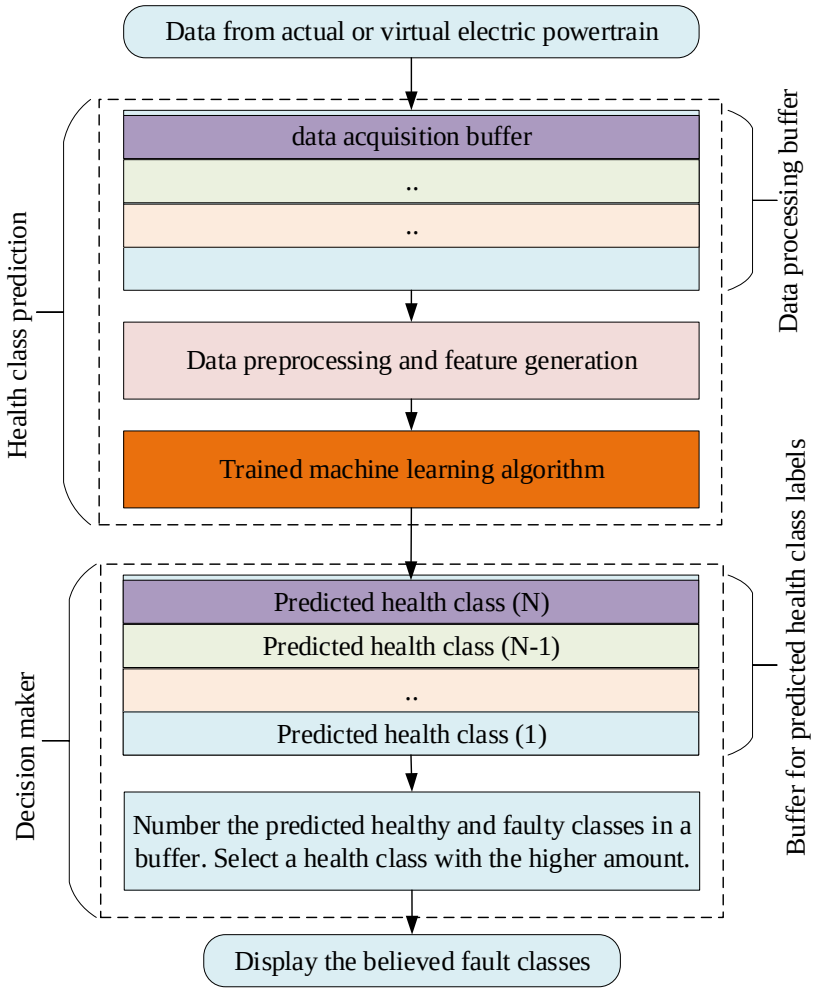

Figure 5.8: The algorithm used in the online fault diagnosis system in the step 2.

The online operation of the algorithm uses two buffers. In the data acquisition buffer, the data inflow is controlled. A large data processing buffer is used in case the length of the dataset is not sufficient for data processing. Further, this dataset is sent for data preprocessing and feature generation. The trained CNN classifier bank is applied on these processed spectrograms to classify the faults.

Confusion matrixes and Receiver Operating Characteristic (ROC) are commonly used to analyse the performance of a trained machine learning model. In online fault diagnosis applications, these measures cannot be obtained because the prior information of the faults is unknown. Therefore, a new decision criterion is proposed. Each classifier has three parallel buffers to store the predictions. In each buffer, the health class label with the maximum count is selected as the final decision. This method can compensate for false predictions from unexpected noises or interferences. The interface of the developed online fault diagnosis system is given in Figure 5.9.

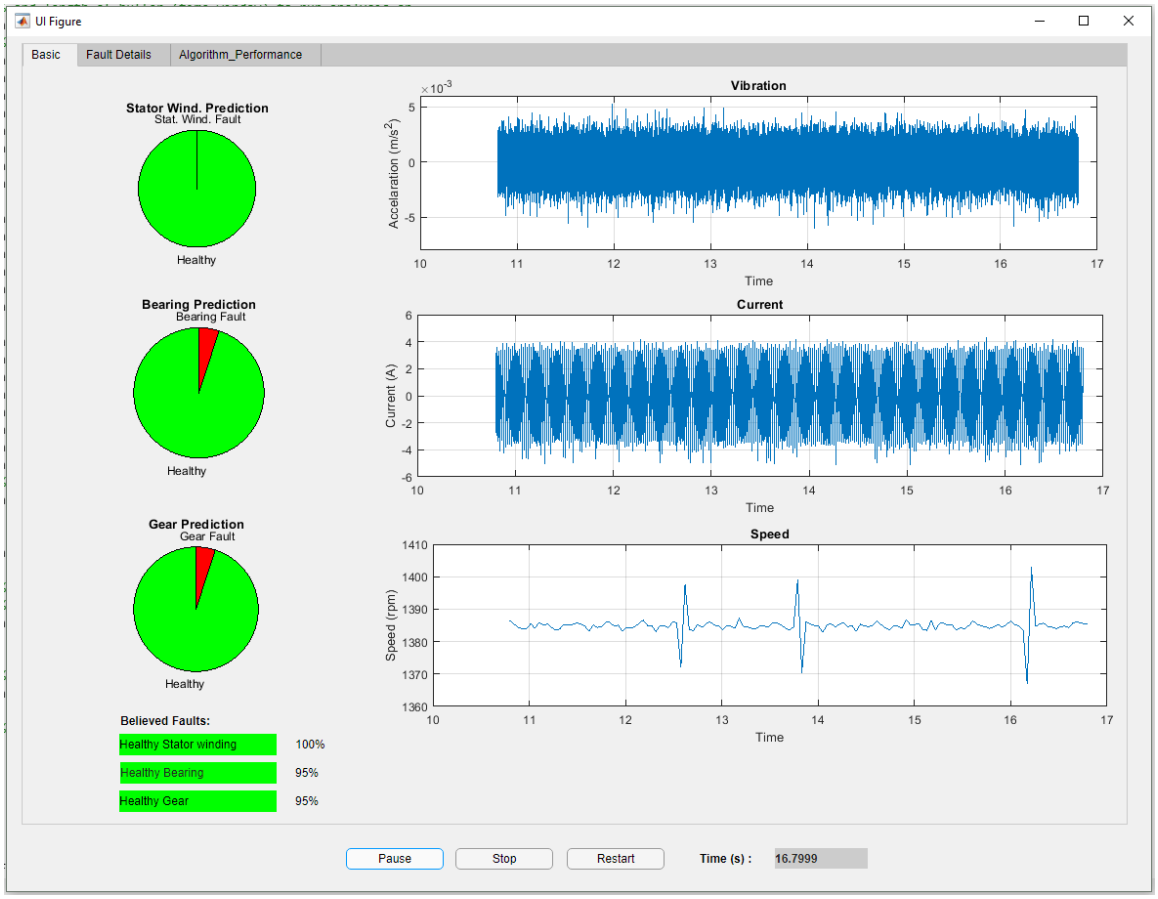

Figure 5.9: The interface of the developed online fault diagnosis system for the electric powertrain.

The performance of the online fault diagnosis system for three fault cases is given in Figure 5.10. Each pie chart shows the percentage of the predicted class labels in each classifier for 20 consecutive predictions. The prediction label with the highest count is selected as the believed fault type.

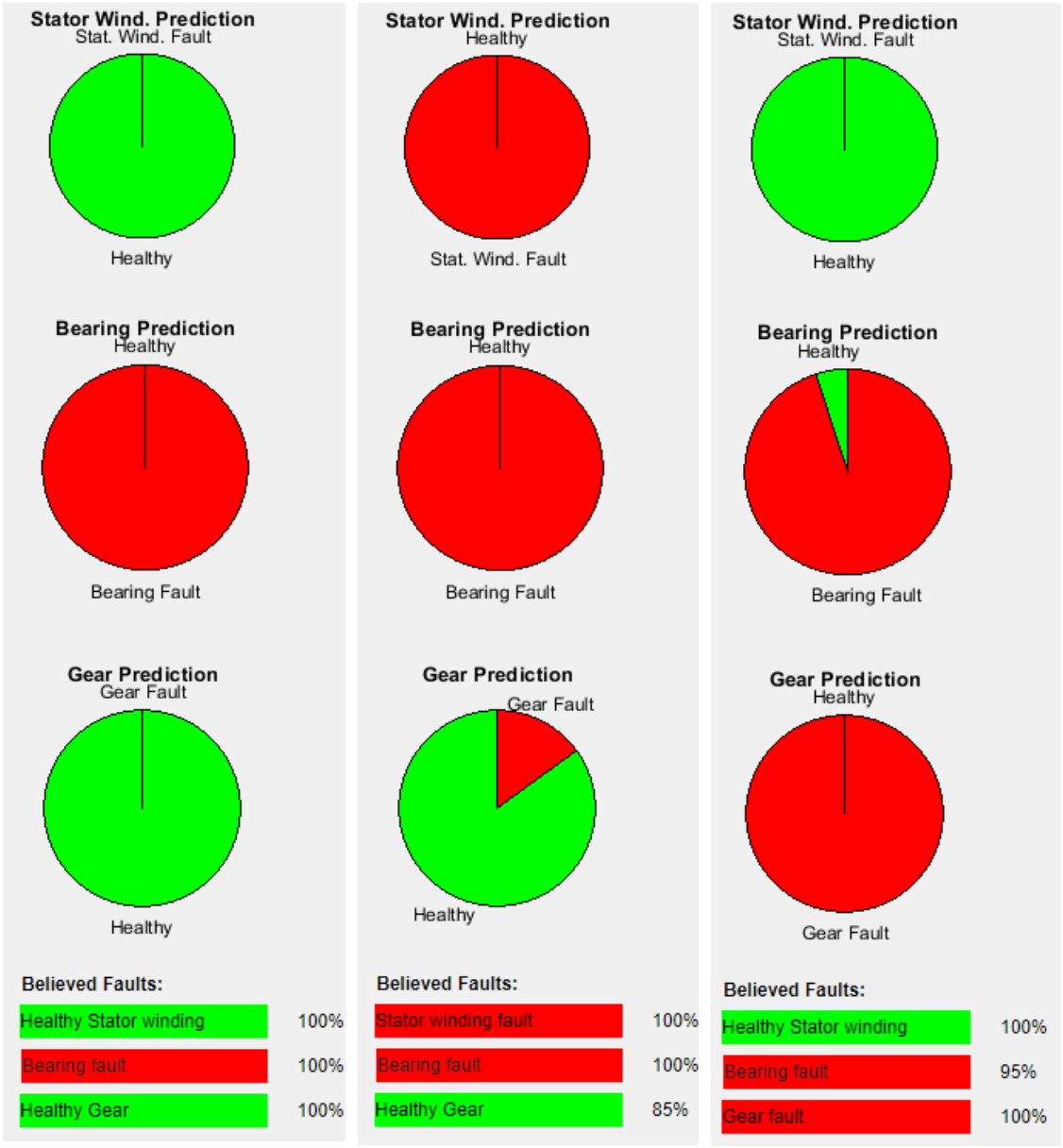

(a) (b) (c)

Figure 5.10: A snapshot of online fault diagnosis system performance:
(a) bearing fault (b) stator winding and bearing faults (c) bearing and gear faults

5.3 Summary

In this chapter, two novel fault diagnostics schemes are proposed for mixed fault diagnosis of gearboxes and electric powertrains at challenging working conditions, e.g. presence of noise, variable speeds and loads. The foundation for proposed solutions is based on CWT and STFT based time-frequency representation of input

signals, deep learning and data fusion. The proposed algorithms are validated using experimental data, and following remarks are drawn from the experimental results.

- Due to the complexity of feature generation, the traditional machine learning process used in Chapter 4 is time-consuming for fault diagnosis of complex gearboxes and powertrains. Alternatively, time-frequency spectrograms and a CNN deep learning algorithm are suitable to combine feature learning and classification within a unified supervised training scheme. The CNN algorithm can learn complex features for mixed fault diagnosis, which is difficult to do manually.
- Feature-level data fusion can significantly improve the accuracy of a fault diagnosis irrespective of the type of machine learning algorithms.
- If an individual fault classifier is not robust under noisy conditions, using an additional classifier and decision fusion can enhance its robustness.
- Accuracy of the CNN-based classification depends on the quality of input data, image or patterns. Using the spectrograms as input data for CNN gives a higher classification accuracy than the raw vibration signals.
- Fusion of order normalised vibration and current spectrograms at feature level using a CNN algorithm allows for detecting multiple faults at variable speeds and loads of an electric powertrains.
- The online implementation of such algorithms as decision support systems would reduce the workload of maintenance personnel and downtime, and increase the productivity.

Chapter 6

Online self-supervised condition monitoring system

6.1 Introduction

Various data-driven supervised machine learning, and data fusion based fault diagnosis schemes are proposed in Chapters 4 and 5, confirming that the proposed algorithms can work well in challenging working conditions, namely, variable speeds and loads, and noisy conditions. However, those proposed schemes require labelled training data or historical data at faults. Labelled training data is limited in reality, rendering a challenge for any data-driven algorithm. To address the challenge of limited data, unsupervised and supervised learning methods can be combined, and a proper combination of different techniques can give an overall improvement of performance by compensating the weaknesses of each method.

Online implementation of data-driven algorithms is important to obtain an autonomous diagnostics, and reduce the manpower requirement for fault diagnosis. Commercial online condition monitoring systems are available in the market [11, 12], but they are expensive and require high expertise of the system operators. On the other hand, most published research works focus on proposing new condition monitoring algorithms [9, 10, 30, 71-75], but details on their online implementation are limited. As stated in [12], online implementation based on artificial intelligence, and wireless multi-sensor data fusion is a possible direction to achieve an intelligent CM system.

In this research, a novel online condition monitoring system is proposed to deal with limited data. The proposed solution in this chapter is suitable for fault diagnosis of new powertrains without prior data of faulty cases. The proposed diagnosis scheme is summarized in Section 6.2 while Section 6.3 briefly presents the developed online diagnosis system and its performance. Paper F details information in this chapter.

6.2 The proposed fault diagnosis scheme

A block diagram of the proposed fault diagnosis scheme comprised of two stages is given in Figure 6.1.

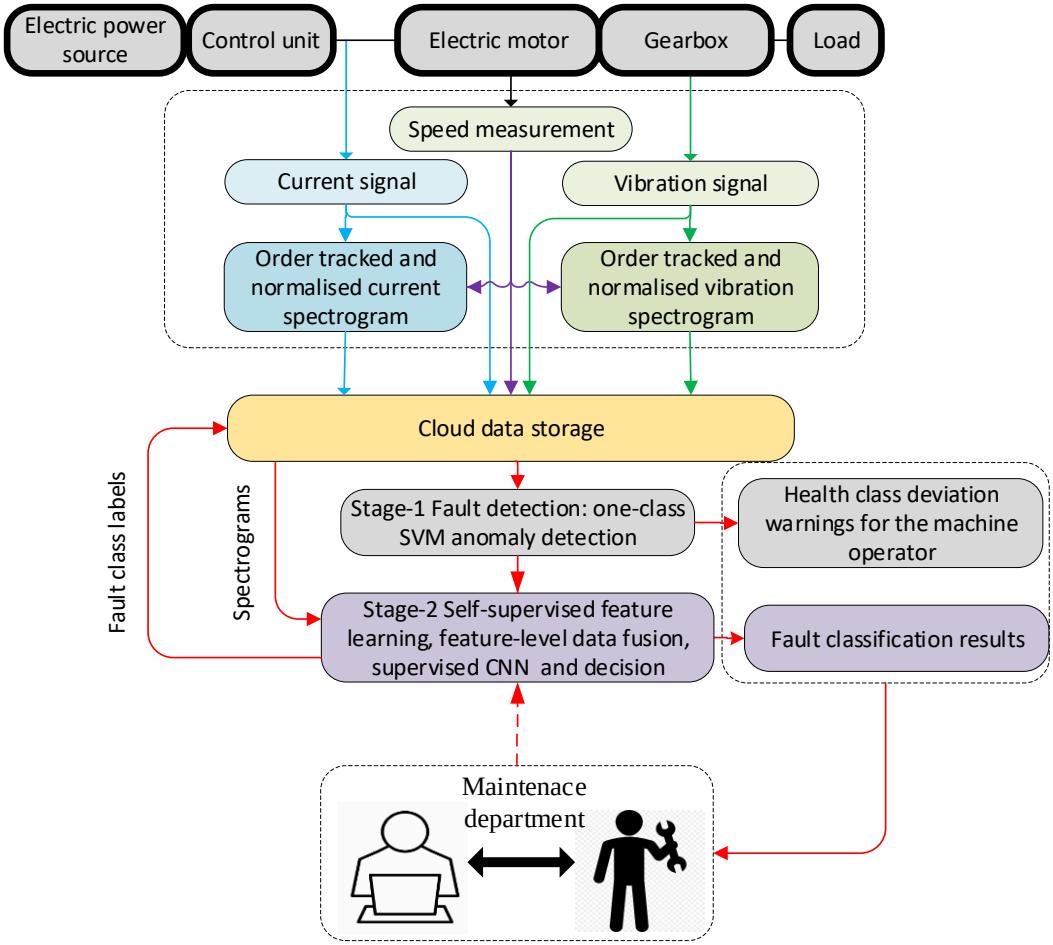

Figure 6.1: A block diagram of the proposed fault diagnosis scheme for electric powertrain.

The first stage is fault detection, and the second stage is fault isolation. A combination of one-class SVM anomaly detection and supervised CNN algorithms have been used for fault detection and isolation. The powertrain vibration, speed and input current signals are measured in online passion and stored in the cloud storage for stage-1. The order normalised spectrograms are generated using measured speeds and stored for the stage-2 algorithm. The detailed flowchart of the operation of the proposed fault diagnostics scheme is given in Figure 6.2.

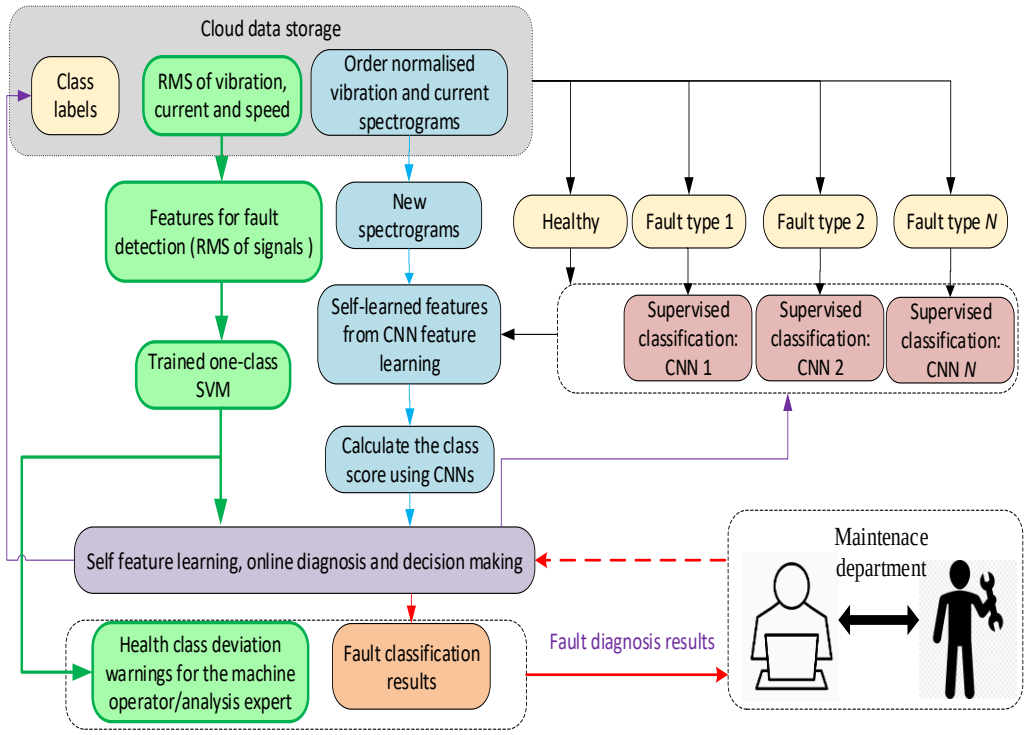

Note: The green colour boxes and lines represent the stage-1 algorithm, and the remaining boxes and lines represent the stage 2 algorithm

Figure 6.2: Detailed flowchart of stages-1 and -2 of the proposed diagnosis scheme.

There are three main steps in the fault detection algorithm in stage 1;

1) Train the boundaries for healthy class data using features (RMS of the vibration signal, RMS of IM current signal and IM speed) and one-class SVM.
2) Calculate the score from the trained one-class SVM for incoming data in a dynamic manner and take the average of the latest samples.
3) Compare the average score and make the decision. If the score is greater than zero, the machine is assumed to be healthy and otherwise faulty.

The fault detection results in generating the training data for CNN classifiers in stage 2. Once a fault is detected in stage 1, a temporary class label (e.g. Fault type 1 (FT-1)) is assigned. In the stage 2, the supervised CNN algorithm is trained using healthy data and the FT-1 data. In this self-supervised feature learning method, the algorithm can learn features related to multiple faults (FT-1, 2, …). The algorithm keeps a bank of feature types learned from the cloud data storage. For new data, the learned feature set is applied to generate a score, which represents the similarity of new data respective to the corresponding feature type. The final decision is taken based on a defined decision criteria. When the powertrain is repaired, the actual label is available, and maintenance department can update the FT-1 with a correct label.

6.3 The experimental results and discussion

The laboratory test setup explained in Section 3.2 is used to generate data for single and multiple faults with different fault severities. As given in Figure 6.3, the powertrain operates at variable speeds and loads, making a realistic diagnosis scenario.

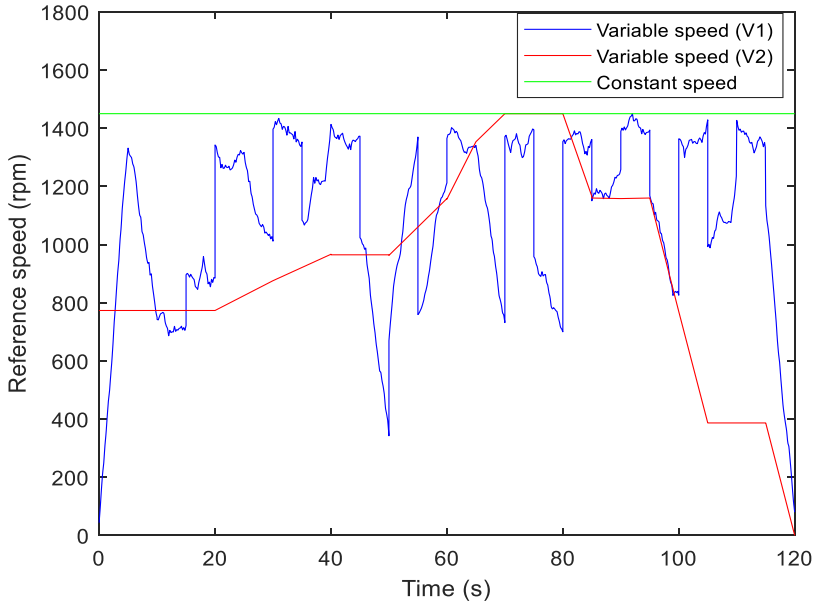

Figure 6.3: The constant and variable speeds of each fault class.

Three levels of gear damage scenario are tested (GF1, GF2 and GF3), where GF1 is a small gear tooth damage, and GF2 has a further damaged gear tooth. The GF3

is a complete broken tooth gear. Three severity levels of outer-race defects on the induction motor bearing (BF1, BF2 and BF3) were tested. For stator winding faults, 6% (SF1) and 10% (SF2) inter-turn short circuit faults are applied in one phase. The sampling rate of the data was 20 kHz for the vibration, motor current and speed measurements. After preprocessing, there are 3820 samples for each fault class. More details of experimental data and data preprocessing can be found in Paper F.

6.3.1 Stage-1 - unsupervised fault detection

As discussed in Section 6.2, the one-class SVM is trained, using healthy system data, and the trained algorithm is used to generate scores for fault class data. The scores greater than zero is considered as data from healthy powertrain, and the scores less than zero is considered as faulty. Table 6.2 shows the summary of one-class SVM performances for the first 9 fault classes. The high detection accuracies of Table 6.1 confirm that proposed one-class SVM algorithm can detect fault reliably in variable speed and loads conditions. However, the stage-1 is to find whether a component is healthy or faulty, but in this stage the fault type or severity is unknown.

Table 6.1: One-class SVM performances for fault detection.

Fault class ID	Fault class	Detection score (%)	Detection criteria	Powertrain Status
1	H	99.9	Score > 0	Healthy
2	GF1	98.6	Score < 0	Faulty
3	GF2	95.9	Score < 0	Faulty
4	GF3	92.0	Score < 0	Faulty
5	BF1	100.0	Score < 0	Faulty
6	BF2	99.9	Score < 0	Faulty
7	BF3	100.0	Score < 0	Faulty
8	SF1	100.0	Score < 0	Faulty
9	SF2	99.9	Score < 0	Faulty

6.3.2 Stage-2 - supervised CNN fault diagnosis algorithm

The proposed stage-2 algorithm is implemented as explained in Section 6.2, and the classification accuracies for 11 fault classes are tested. To compare the performance of stage-2 CNN algorithm, a comparison study is designed using domain features, binary SVM and MLP algorithms. The average order spectrums of time-domain signals (vibration and current) are derived, and the amplitude of fault-related characteristics frequency orders are extracted as features. In this study, nine features are generated as domain features. The details of fault-related characteristics frequency orders used for domain feature generation can be found in paper F. In the comparison study, nine classifiers are trained using the data from lowest severity fault classes (GF1, BF1 and SF1), and the classification accuracies are tested for 11 fault classes as shown in Table 6.2. All gear fault algorithms (GF1-SVM, GF1-MLP and GF1-CNN) classify the healthy class with accuracies over 97.1%.

Table 6.2: The classification accuracies of different classifiers.

Fault Class ID	Fault Class	Classification accuracies (%)								
		GF1-SVM	GF1-MLP	GF1-CNN	BF1-SVM	BF1-MLP	BF1-CNN	SF1-SVM	SF1-MLP	SF1-CNN
1	H	97.1	97.8	98.6	94.8	93.7	99.6	100.0	100.0	99.8
2	GF1	97.4	97.6	94.2	67.5	65.1	99.6	95.4	97.0	100.0
3	GF2	68.4	91.6	98.6	55.0	67.0	99.5	43.4	98.0	100.0
4	GF3	71.4	81.3	99.1	53.0	57.1	99.6	60.0	100.0	100.0
5	BF1	81.1	75.3	94.9	94.7	94.0	90.0	99.0	100.0	100.0
6	BF2	54.1	82.7	96.2	79.0	80.5	99.0	90.0	100.0	100.0
7	BF3	51.0	77.0	82.5	99.0	99.0	99.0	63.0	100.0	100.0
8	SF1	76.0	94.0	80.1	60.0	99.0	99.0	100.0	100.0	99.7
9	SF2	71.0	95.0	82.7	61.0	98.0	99.0	100.0	100.0	99.7
10	GF2_BF2	88.0	80.0	93.4	86.0	89.0	67.4	60.0	100.0	99.6
11	GF2_BF2_SF1	97.0	84.0	97.1	96.0	70.0	72.1	98.0	75.0	98.1
	Average	77.5	86.9	92.5	76.9	82.9	93.1	82.6	97.3	99.7
	Minimum	51.0	75.3	80.1	53.0	57.1	67.4	43.4	75.0	98.1
	Maximum	97.4	97.8	99.1	99.0	99.0	99.6	100.0	100.0	100.0

The GF1-SVM has the lowest performance with minimum and average accuracies of 51.0% and 77.5%, respectively, while those minimum and average accuracies of the GF1-MLP are 75.3% and 86.9%. The proposed GF1-CNN classifier has the best performance with the minimum and average accuracies of 80.1% and 92.5%, respectively. The GF1-SVM classifier has the lowest average performances, but still, the classification accuracy of its original trained class (GF1) is 97.4% while having moderate accuracies for other fault classifications.

Domain feature-based classifiers (binary SVM and MLP) have some lower accuracies due to the limitations of DF, and the amplitudes of characteristic frequency bands are calculated from average order spectrum, which contains approximations for the dynamic load and speed operations. However, the CNN feature learning covers the local regions in the spectrograms for dynamic operations, resulting in a better feature learning. The CNN-based classifier can compensate for spatial deviation of fault-related frequency bands in the spectrograms produced in the order normalization algorithm during sudden speed changes. This cannot be achieved in DF-SVM and DF-MLP. Therefore, the performances of CNN classifiers are better than other two methods.

6.3.3 Online implementation

The proposed fault diagnosis system is implemented as an online system. The interface in Figure 6.4 shows the result of one-class SVM score in stage-1 for a healthy powertrain at variable speeds. The score is online calculated, and the average score from historical scores is used for fault detection decision. After detecting a fault, a temporary label is assigned to new data (e.g. FT1), and a CNN is trained using data from healthy and fault (FT1). The learned CNN feature dataset can be used for generating a score (from 0 to 1) to define the similarity level of new spectrogram data with respect to the learned fault type. A bank of CNN classifiers are trained for other fault types, and the CNN scores are calculated for new spectrogram data. The scores of five CNNs for a gear fault case are given in Figure 6.5. The score for GF1-CNN classifier is very high, and the scores of other CNN classifiers are low. This clearly indicates a gear fault. The historical score of each CNN classifier is given in Figure 6.6, and the maintenance personnel can have more confidence on the final decision based on historical scores.

Figure 6.4: One-class SVM fault detection interface.

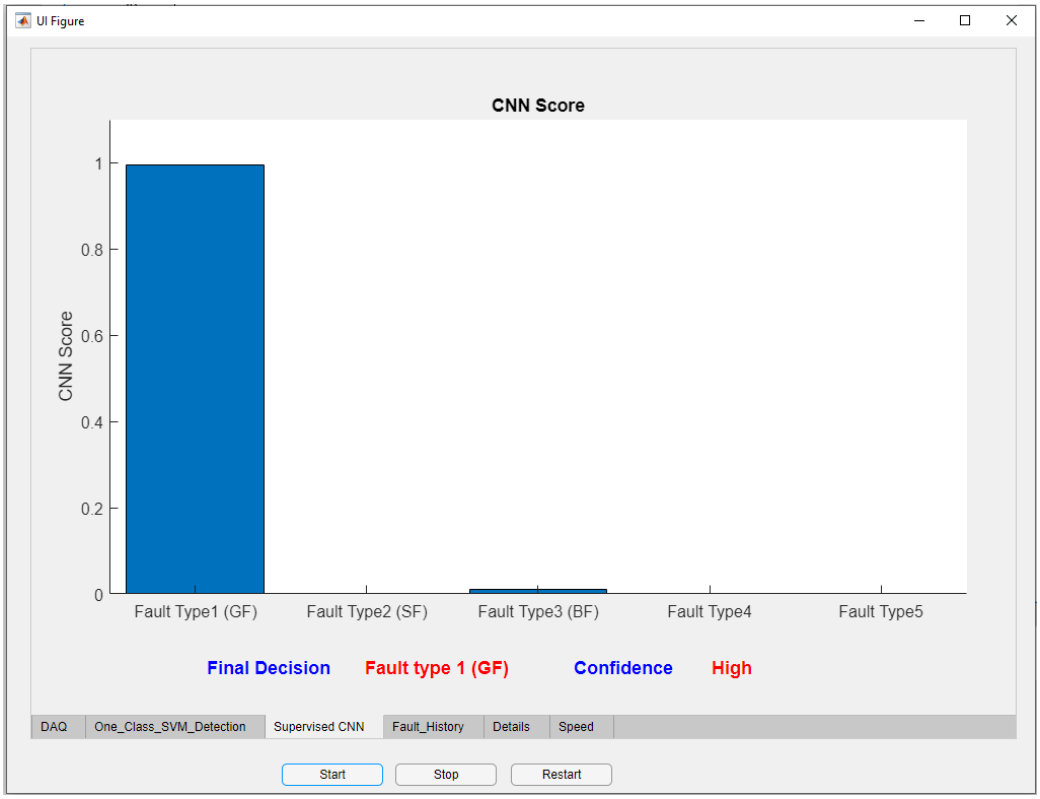

Figure 6.5: CNN fault score and decision-making interface.

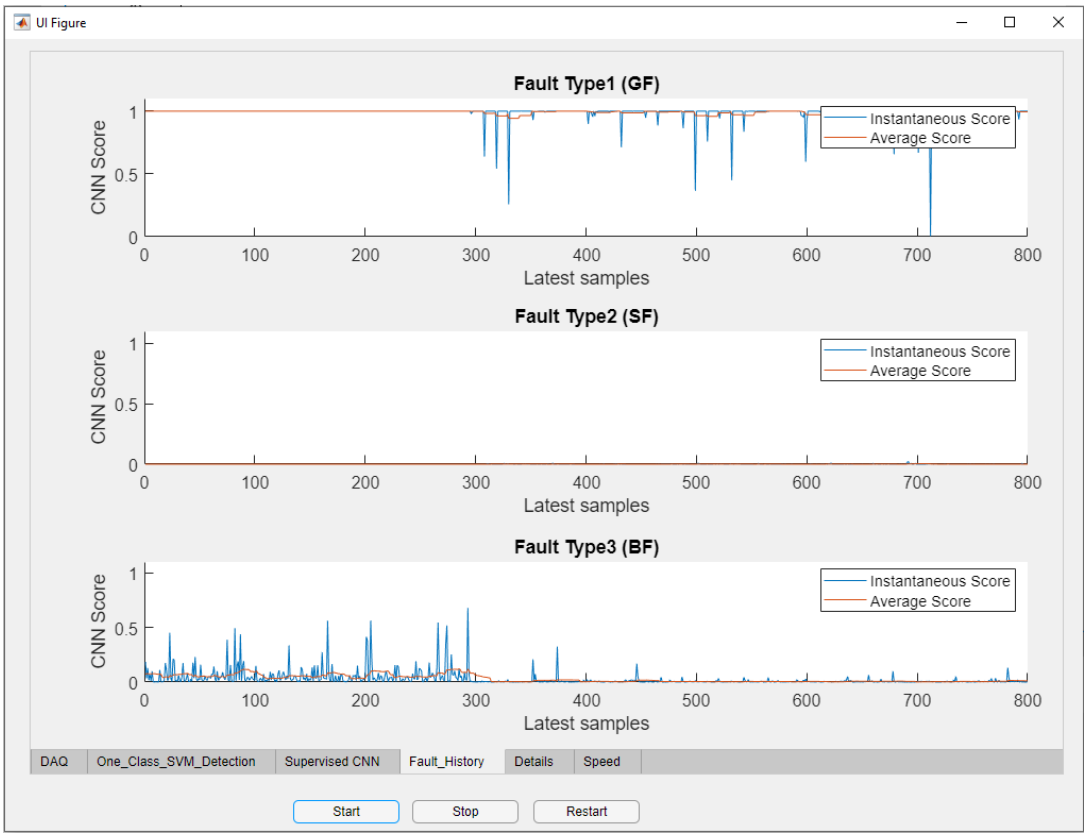

Figure 6.6: CNN fault score history interface.

6.4 Summary

This chapter introduces an outline for an online fault diagnosis system consisting of self-supervised feature learning. The rationale for using such a concept is to eliminate the requirement of historical fault data for data-driven algorithms. In the proposed method, the data from single faults and temporary labels are used for initial self-supervised feature learning process. Then, the learned features are used for detecting future single and multiple faults. The proposed algorithm is validated using data from signals and multiple faults under variable speeds and loads, obtaining promising results. A basic similarity score calculation and decision rule are introduced, working well in the considered fault scenario. More experimental data is required for improving the decision rule. The generalisability of the proposed CNN feature learning is tested. The features learnt from initial fault severity levels are used for detecting faults at higher severity levels, which are not used in the training process.

The proposed algorithm has some limitations. In the case of initial multiple faults, the proposed method cannot learn single fault features separately, requiring further improvements. An insight for improvements can be obtained from self-supervised image segmentation applications, where the individual objects in the images are assigned for each object in self-supervised manner. A similar concept can be applied for initial multiple fault diagnostics using spectrograms and CNN, where the local fault features related to individual faults might be detected in the local context of spectrograms. Therefore, the proposed algorithm, together with wireless sensors and cloud data storages, might be a possible future direction for realizing intelligent and online condition monitoring systems for industrial machines.

Chapter 7

Conclusions and future work

7.1 Conclusions

This research focuses on online condition monitoring of gearboxes and electric powertrains. Existing research and industrial products aimed at component level fault diagnosis for single faults at steady-state operating conditions. Condition monitoring of complex gearboxes and electric powertrains under dynamic conditions is limited in literature. Within the framework, four major research topics or problems were identified within condition monitoring of gearbox-based electric powertrains, and novel diagnosis schemes based on data-driven approach were presented to solve the problems.

First research problem focuses on bearing fault detection at early stage and dynamic operating conditions. Bearing failures modes may depend on its operating conditions, and it is difficult to detect bearing faults in early-stage. Therefore, an early-fault diagnosis scheme based on envelop analysis, domain feature generation and SVM, is proposed via paper A. The envelope analysis generates strong features for SVM classifier and the trained SVM can detect faults in a multidimensional hyperspace. The bearing fault diagnosis at variable speeds and loads are solved by tracking the fault related characteristics frequencies and generating additional strong features manually for a SVM. The results of Paper B show that the proposed method is useful for fault diagnosis in wind turbines and powertrain applications.

The second research problem identified in this work is improving the robustness of gearbox mixed faults diagnosis. A robust fault diagnosis scheme consisting of CNN, MLP and data fusion is proposed through paper C, and a comparative study is used to highlight performance of the proposed method using experimental data. The results of the gearbox fault diagnosis study show that the feature level and decision level data fusion can improve the robustness of gearbox mixed fault diagnosis under noise conditions.

The third research problem focuses on multiple fault diagnosis in variable speed and load conditions. A new fault diagnosis scheme based on CNN is proposed via paper D. The spectrograms generated from vibration and motor current signals are fed in CNN algorithm for feature level fusion to diagnose the fault at variable speeds and loads. The order tracking process can generate order normalised spectrograms for CNN algorithm. The CNN can compensate the frequency overlappings at order normalisation process by compensating the variations of frequencies in the spectrograms. Based on the proposed algorithm, an online fault diagnosis scheme is implemented for autonomous fault classification at dynamic operating conditions in paper E.

This work proposes new data-driven diagnosis methods. The main challenge of any data-driven approach is requirement of training data. Therefore, the fourth research topic focuses on finding methods to reduce the training data requirements of data-driven algorithms. A self-supervised feature learning algorithm is proposed for online diagnosis of powertrain mixed faults under dynamic operating conditions. The proposed solution in paper F is based on two stages. In the first stage, fault are detected, and temporary labels are assigned. The results of stage-1 algorithm were used for training CNN algorithms. The order normalisation process allows for detecting faults at variable speeds, and the proposed CNN scores and decision criteria have the capability to isolate single and multiple faults.

The existing diagnosis methods based on signal processing, statistical or domain feature generation and machine learning have limitations for complex machines at dynamic operating conditions. The domain feature generation may generate strong features for single fault diagnosis at steady-state operating conditions, but it is time-consuming and may generate weak features for multiple fault diagnosis at dynamic operations. The results of this research confirm that the pattern features from time-frequency spectrograms using CNN learning and data

fusion algorithms can be used to diagnose multiple faults at variable speeds and loads. In addition, the usage of many sensors (e.g. vibration and current) allow for detecting the physical fault information in different domains or viewpoints, thus data fusion results in more robust diagnosis decisions. The proposed self-supervised online condition monitoring system can work without historical data for faults, and the algorithm can learn features for online fault detection and give automatic decisions to the machine operator.

7.2 Limitations and future works

The deep learning algorithms used in this research are pattern recognisers, which can detect the difference of patterns for healthy and faulty data. However, to detect fault patterns, proper spectrogram images should be fed into algorithms. For example, the quality of input images affects performance of fault detection. The input spectrogram image quality is constrained by several factors such as sensitivity of sensors used for data collection, the sampling rate and number of samples, and the signal processing methods used for image generation. For example, CWT based images are better than STFT based images. Further, order tracking at variable speeds has limitations, where the frequency resolution and time resolution cannot increase at same time to adjust image quality. In this research, reasonable size spectrograms (maximum dimension :113×226×3) are generated from each vibration and current signal to represent the time-frequency patterns. A detailed study is required to find the tradeoff between the size of input data, classification accuracies, complexity of machine learning algorithms and computational burden. High-resolution large spectrogram images may capture large portion of time-frequency patterns from the signals. However, this increases the complexity and computational burden of the algorithm.

The selection of proper sensors, location and number of sensors is important in fault diagnosis. For example, the vibration sensor data is more useful for mechanical faults than current sensor data. In the proposed gearbox fault diagnosis scheme, two vibration signals are used. In the powertrain application, one vibration sensor is used, and the vibration sensor is placed on top of the gearbox in the powertrain for measuring the gearbox vibration. However, using more than one

vibration sensor and data fusion may give a better result in powertrain applications. Future study should investigate this issue further.

In this work, the spectrograms of IM currents are mainly used for detecting electrical faults, and mechanical fault detection using current signatures was not focused. The deep learning approach with pattern recognition may be relevant for this task. However, when generating spectrograms, the time and frequency resolution and frequency ranges are the main parameters to consider. The mechanical fault signatures in stator current signal can be hidden, weak and present in diferent frequecy ranges. High resolution spectrograms with large frequency range may results in high computational burden. Therefore, instead of using one large spectrograms, many spectrograms can be used with different range (e.g. 0-1000 Hz covered by one spectrogram, 1kHz to 10 kHz covered by another and more than 10 kHz by another spectrogram). In this way, complete time-frequency patterns can be identified using CNN and data fusion.

In this study, the early fault detection of electric powertrain components are focused and the RUL estimation problem was not studied. Intergration of RUL estimation capability to proposed online solution is a suitable direction for future studies. In addition, there is high potential to improve the proposed online self-supervised feature learning fault diagnosis scheme. The diagnosis scheme should be tested with further experimental data using various operating conditions, and the decision criteria should be improved. The local time-frequency patterns learning and detection capabilities of CNN for single and multiple fault features should be improved. In this research, three types of faults (gear, bearing and inter-turn stator winding) are considered. However the proposed concept can be extended for detecting other types of faults such as misalignment, unbalance, etc. Proper combinations of wireless sensors, cloud data storage and deep learning algorithms will be attractive topics for condition monitoring of complex machineries under dynamic operations. The online implimentaion of such diagnostic schemes will help to reduce the overall maintenance cost, and ensure safe and reliable operations.

References

[1] "Report of Large Motor Reliability Survey of Industrial and Commercial Installations," *IEEE Transactions on Industry Applications,* vol. IA-21, no. 4, I, 1985.

[2] P. Albrecht et al., "Assessment of the Reliability of Motors in Utility Applications – Updated," *IEEE Transactions on Energy Conversion,* vol. EC-1, no. 1, pp. 39-46, 1986.

[3] "Report of Large Motor Reliability Survey of Industrial and Commercial Installations," *IEEE Transactions on Industry Applications,* vol. IA-23, no. 1, III, 1987.

[4] P. Albrecht et al., "Assessment of the Reliability of Motors in Utility Applications," *IEEE Transactions on Energy Conversion,* vol. EC-2, no. 3, pp. 396-406, 1987.

[5] O. Thorsen and M. Dalva, "A Survey of Faults on Induction Motors in Offshore Oil Industry, Petrochemical Industry, Gas Terminals, and Oil Refineries," *IEEE Transactions on Industry Applications,* vol. 31, no. 5, 1995.

[6] A. H. Bonnett, "Root cause failure analysis for AC Induction Motors in the petroleum and chemical industry," in *2010 Record of Conference Papers Industry Applications Society 57th Annual Petroleum and Chemical Industry Conference (PCIC)*, San Antonio, TX, 2010, pp. 1-13.

[7] J. Chen *et al.*, "Wavelet transform based on inner product in fault diagnosis of rotating machinery: a review," *Mechanical systems and signal processing*, vol. 70, pp. 1–35, 2016.

[8] Z. Huo, Y. Zhang, P. Francq, L. Shu, and J. Huang, "Incipient Fault Diagnosis of Roller Bearing Using Optimized Wavelet Transform Based Multi-Speed Vibration Signatures," *IEEE Access,* vol. 5, pp. 19442-19456, 2017.

[9] T. Wang, M. Liang, J. Li, W. Cheng, and C. Li, "Bearing fault diagnosis under unknown variable speed via gear noise cancellation and rotational order sideband identification," *Mechanical Systems and Signal Processing*, vol. 62–63, pp. 30-53, 2015.

[10] Chuan Li, René-Vinicio Sanchez, Grover Zurita, Mariela Cerrada, Diego Cabrera, and Rafael E. Vásquez, "Gearbox fault diagnosis based on deep random forest fusion of acoustic and vibratory signals," *Mechanical Systems and Signal Processing*, vol. 76–77, pp. 283-293, 2016.

[11] "ABB Ability™ Condition Monitoring for powertrains." ABB. https://new.abb.com/drives/digital-powertrain-monitoring (accessed August, 2019).

[12] H. Pütz and T. Lantermann. "Digitalization and brownfield facilities – can these fit together." Mitsubishi Electric. https://eu3a.mitsubishielectric.com/fa/en/news/file/3544/Mitsubishi_Digitalization_and_Brownfield_facilities_can_these_fit_together_ENGLISH.pdf (accessed August, 2019).

[13] F. Lv, C. Wen, Z. Bao, and M. Liu, "Fault diagnosis based on deep learning," presented at the 2016 American Control Conference (ACC), Boston, 2016.

[14] M. He and D. He, "Deep Learning Based Approach for Bearing Fault Diagnosis," *IEEE Transactions on Industry Applications*, vol. 53, no. 3, pp. 3057-3065, 2017.

[15] R. Liu, G. Meng, B. Yang, C. Sun, and X. Chen, "Dislocated Time Series Convolutional Neural Architecture: An Intelligent Fault Diagnosis Approach for Electric Machine," *IEEE Transactions on Industrial Informatics*, vol. 13, no. 3, pp. 1310-1320, 2017.

[16] "Reliability centered maintenance guide for Facilities and collateral equipment." NASA. https://www.hq.nasa.gov/office/codej/codejx/Assets/Docs/RCMGuideMar2000.pdf (accessed August, 2019).

[17] R. Ahmad and S. Kamaruddin, "An overview of time-based and condition-based maintenance in industrial application," *Computers & Industrial Engineering*, vol. 63, no. 1, pp. 135-149, 2012.

[18] Andrew Jardine, Daming Lin, and Dragan Banjevic, "A review on machinery diagnostics and prognostics implementing condition-based maintenance," *Mechanical Systems and Signal Processing*, vol. 20, no. 7, pp. 1483-1510, 2006.

[19] "Condition monitoring and diagnostics of machines -- data processing, communication and presentation -- part 1: general guidelines (ISO 13374-

1:2003)." ISO. https://www.iso.org/obp/ui/#iso:std:iso:13374:-1:ed-1:v1:en (accessed May, 2019).

[20] "Condition monitoring and diagnostics of machines — Requirements for qualification and assessment of personnel — Part 2: Vibration condition monitoring and diagnostics (ISO 18436-2:2014)." ISO. https://www.iso.org/standard/50447.html (accessed May, 2019).

[21] "Condition monitoring and diagnostics of machines -- vocabulary (ISO 13372:2012)." ISO. https://www.iso.org/obp/ui/#iso:std:iso:13372:ed-2:v1:en (accessed may, 2019).

[22] T. Sutharssan, S. Stoyanov, C. Bailey, and C. Yin, "Prognostic and health management for engineering systems: a review of the data-driven approach and algorithms," *The Journal of Engineering,* vol. 2015, no. 7, pp. 215-222, 2015.

[23] D. Jung and C. Sundström, "A Combined Data-Driven and Model-Based Residual Selection Algorithm for Fault Detection and Isolation," *IEEE Transactions on Control Systems Technology*, vol. PP, no. 99, pp. 1-15, 2017.

[24] X. Dai and Z. Gao, "From model, signal to knowledge: A data-driven perspective of fault detection and diagnosis," *IEEE Transactions on Industrial Informatics,* vol. 9, no. 4, pp. 2226-2238, 2013.

[25] Z. Gao, C. Cecati, and S. X. Ding, "A Survey of Fault Diagnosis and Fault-Tolerant Techniques-Part II: Fault Diagnosis with Knowledge-Based and Hybrid/Active Approaches," *IEEE Transactions on industrial electronics,* vol. 62, no. 6, pp. 3768-3774, 2015.

[26] Z. Gao, C. Cecati , and S. X. Ding, "A Survey of Fault Diagnosis and Fault-Tolerant Techniques—Part I: Fault Diagnosis with Model-Based and Signal-Based Approaches," *IEEE Transactions on industrial electronics,* vol. 62, no. 6, pp. 3757-3767, 2015.

[27] G. Niu, *Data-Driven Technology for Engineering Systems Health Management: Design Approach, Feature Construction, Fault Diagnosis, Prognosis, Fusion and Decision*. Springer, 2016.

[28] G. K. Singh and S. A. Saleh Al Kazzaz, "Induction machine drive condition monitoring and diagnostic research-a survey," *Electric Power Systems Research,* vol. 64, no. 2, pp. 145-158, 2003.

[29] P. J. Tavner, "Review of condition monitoring of rotating electrical machines," *IET Electric Power Applications,* vol. 2, no. 4, pp. 215-247, 2008.

[30] N. Baydar, Q. Chen, A. Ball, and U. Kruger, "Detection of incipient tooth defect in helical gears using multivariate statistics," *Mechanical Systems and Signal Processing,* vol. 15, no. 2, pp. 303-321, 2001.

[31] D. Goyal and B.S. Pabla, "Condition based maintenance of machine tools—A review," *CIRP Journal of Manufacturing Science and Technology*, vol. 10, pp. 24-35, 2015.

[32] P. Girdhar and C. Scheffer, *Machinery fault diagnosis using vibration analysis*. Oxford, Newnes, 2004, pp. 89-133.

[33] P. Konar and P. Chattopadhyay, "Bearing fault detection of induction motor using wavelet and support vector machines (SVMs)," *Applied Soft Computing*, vol. 11, no. 6, pp. 4203–4211, 2011.

[34] Ruonan Liu, Boyuan Yang, Enrico Zio, and Xuefeng Chen, "Artificial intelligence for fault diagnosis of rotating machinery: A review," *Mechanical Systems and Signal Processing*, vol. 108, pp. 33-47, 2018.

[35] L. Wu, B. Yao, Z. Peng, and Y. Guan, "Fault Diagnosis of roller bearings based on a wavelet neural network and manifold learning," *Applied Sciences*, vol. 7, no. 158, pp. 1–10, 2017.

[36] G. Susto, A. Schirru, S. Pampuri, S. McLoone, and A. Beghi, "Machine learning for predictive maintenance: A multiple classifier approach," *IEEE Transactions on Industrial Informatics*, vol. 11, no. 3, pp. 812-820, 2015.

[37] M. Van and H. Kang, "Bearing defect classification based on individual wavelet local fisher discriminant analysis with particle swarm optimization," *IEEE Transactions on Industrial Informatics*, vol. 12, no. 1, pp. 124-135, 2016.

[38] B. Xue, M. Zhang, W. N. Browne, and X. Yao, "A Survey on Evolutionary Computation Approaches to Feature Selection," *IEEE Transactions on Evolutionary Computation*, vol. 20, no. 4, pp. 606-626, 2016.

[39] N. Tajbakhsh et al., "Convolutional Neural Networks for Medical Image Analysis: Full Training or Fine Tuning?," *IEEE Transactions on Medical Imaging*, vol. 35, no. 5, pp. 1299-1312, 2016.

[40] W. Sun, R. Zhao, R. Yan, S. Shao, and X. Chen, "Convolutional Discriminative Feature Learning for Induction Motor Fault Diagnosis," *IEEE Transactions on Industrial Informatics*, vol. 13, no. 3, pp. 1350-1359, 2017.

[41] P. Cao, S. Zhang, and J. Tang, "Preprocessing-Free Gear Fault Diagnosis Using Small Datasets With Deep Convolutional Neural Network-Based Transfer Learning," *IEEE Access*, vol. 6, pp. 26241-26253, 2018.

[42] C. Lu, Z. Wang, W. Qin, and J. Ma, "Fault diagnosis of rotary machinery components using a stacked denoising autoencoder-based health state identification," *Signal Processing*, vol. 130, pp. 377-388, 2017.

[43] R. Zhang, H. Tao, L. Wu, and Y. Guan, "Transfer Learning With Neural Networks for Bearing Fault Diagnosis in Changing Working Conditions," *IEEE Access*, vol. 5, pp. 14347-14357, 2017.

[44] Y. Guerbai, Y. Chibani, and B. Hadjadji, "“The effective use of the oneclass SVM classifier for handwritten signature verification based on writer-independent parameters," *Pattern Recognition*, vol. 48, no. 1, pp. 103-113, 2015.

[45] Y. Xiao, H. Wang, W. Xu, and J. Zhou, "Robust one-class SVM for fault detection," *Chemometrics and Intelligent Laboratory Systems*, vol. 151, pp. 15-25, 2016.

[46] A. Theissler, "Detecting known and unknown faults in automotive systems using ensemble-based anomaly detection," *Knowledge-Based Systems*, vol. 123, pp. 163-173, 2017.

[47] H. Waltz, "Data Fusion for C3I: A Tutorial," in *Command, Control, Communications Intelligence (C31) Handbook*. Palo Alto, CA, 1986, pp. 217-226.

[48] H. F. Durrant-Whyte, "Sensor models and multisensor integration," *International Journal of Robotics Research*, vol. 7, no. 6, pp. 97-113, 1988.

[49] F. Castanedo, "A Review of Data Fusion Techniques," *The Scientific World Journal*, vol. 2013, 2013.

[50] B. V. Dasarathy, "Sensor fusion potential exploitation-innovative architectures and illustrative applications," *Proceedings of the IEEE*, vol. 85, no. 1, pp. 24-38, 1997.

[51] K. T.-M. Medjaher, D. A.; Zerhouni, N., "Remaining Useful Life Estimation of Critical Components With Application to Bearings," *IEEE Transactions on Reliability*, vol. 61, no. 2, pp. 292-302, 2012.

[52] A. Heng, A. Tan, J. Mathew, N. Montgomery, D. Banjevic, and A. K. Jardine, "Intelligent condition-based prediction of machinery reliability," *Mechanical Systems and Signal Processing*, vol. 23, no. 5, pp. 1600–1614, 2009.

[53] A. R. Soualhi, H.; Clerc, G.; Doan, D. D., "Prognosis of Bearing Failures Using Hidden Markov Models and the Adaptive Neuro-Fuzzy Inference System," *IEEE Transactions on Industrial Electronics*, vol. 61, no. 6, pp. 2864-2874, 2014.

[54] X. S. Jin, Y; Que, Z.; Wang, Y.; Chow, T. W. S., "Anomaly Detection and Fault Prognosis for Bearings," *IEEE Transactions on Instrumentation and Measurement*, vol. 65, no. 9, pp. 2046-2054, 2016.

[55] X. S. Si, W. Wang, C. H. Hu, and D. H. Zhou, "Remaining useful life estimation – A review on the statistical data driven approaches," *European Journal of Operational Research,* vol. 213, no. 1, pp. 1-14, 2011.

[56] A. K. S. L. Jardine, D.; Banjevic, D., "A review on machinery diagnostics and prognostics implementing condition-based maintenance," *Mechanical Systems and Signal Processing,* vol. 20, no. 7, pp. 1483–1510, 2006.

[57] W. Yan, H. Qiu, and N. Iyer, "Feature extraction for bearing Prognostics and Health Management (PHM)–A survey," presented at the The 62nd Meeting Society Machinery, Virginia Beach, VA, 2008.

[58] J. B. Ali et. el, "Application of empirical mode decomposition and artificial neural network for automatic bearing fault diagnosis based on vibration signals," *Applied Acoustics,* vol. 89, pp. 16-27, 2015.

[59] H. Qiu, J. Lee, J. Lin, and G. Yu, "Wavelet filter-based weak signature detection method and its application on rolling element bearing prognostics," *Journal of Sound and Vibration,* vol. 289, pp. 1066-1090, 2006.

[60] PHM-society. 2009 PHM Challenge Competition Data Set [Online] Available: https://www.phmsociety.org/references/datasets

[61] W. Li, Z. Zhu, F. Jiang, G. Zhou, and G. Chen, "Fault diagnosis of rotating machinery with a novel statistical feature extraction and evaluation method," *Mechanical Systems and Signal Processing,* vol. 50-51, pp. 414-426, 2015.

[62] "PeakVue Analysis for Antifriction Bearing Fault Detection." Emerson Electric Co. https://www.emerson.com/documents/automation/white-paper-peakvue-analysis-for-antifriction-bearing-fault-detection-en-39106.pdf (accessed October, 2018).

[63] "Shock Pulse Monitoring." SPM Instrument AB. https://www.spminstrument.com/Measuring-techniques/Shock-Pulse-Monitoring/ (accessed 2018).

[64] M. Xu. "Spike Energy™ Measurement and Case Histories (Technical Report)." ENTEK IRD International Corporation. https://www.maintenance.org/fileSendAction/fcType/0/fcOid/399590942962664303/filePointer/399590942964788372/fodoid/399590942964788370/MingXu_gSE_Paper.pdf (accessed 2018).

[65] R. B. Randall, *Vibration-based condition monitoring: industrial, aerospace and automotive applications*. John Wiley & Sons, 2011.

[66] I. Howard, "A Review of Rolling Element Bearing Vibration : Detection, Diagnosis and Prognosis," Defence science and technology organization, Australian government department of defence. Accessed: September 2016.

[Online]. Available:
http://dspace.dsto.defence.gov.au/dspace/handle/1947/3347

[67] N. Tandon and A. Choudhury, "A review of vibration and acoustic measurement methods for the detection of defects in rolling element bearings," *Tribology International,* vol. 32, no. 8, pp. 469-480, 1999.

[68] J. Blough, "Improving the analysis of operating data on rotating automotive components PhD Thesis," College of Engineering, University of Cincinnati, USA, 1998.

[69] A. Brandt, *Noise and Vibration Analysis: Signal Analysis and Experimental Procedures*. Chichester UK: John Wiley and Sons, 2011.

[70] A. M. Cardoso, S. Cruz, and D. Fonseca, "Inter-turn stator winding fault diagnosis in three-phase induction motors by Park's vector approach," *IEEE Trans. Energy Conversion,* vol. 14, pp. 595-598, 1999.

[71] V. Sharma and A. Parey, "A Review of Gear Fault Diagnosis Using Various Condition Indicators," *Procedia Engineering*, vol. 144, pp. 253-263, 2016.

[72] Z. Li, X. Yan, Z. Tian, C. Yuan, Z. Peng, and L. Li, "Blind vibration component separation and nonlinear feature extraction applied to the nonstationary vibration signals for the gearbox multi-fault diagnosis," *Measurement,* vol. 46, no. 1, pp. 259-271, 2013.

[73] Z. Du, X. Chen, H. Zhang, and R. Yan, "Sparse feature identification based on union of redundant dictionary for wind turbine gearbox fault diagnosis," *IEEE Transaction on Industrial Electronics*, vol. 62, no. 10, pp. 6594-6605, 2015.

[74] F. Cheng, J. Wang, L. Qu, and W. Qiao, "Rotor Current-Based Fault Diagnosis for DFIG Wind Turbine Drivetrain Gearboxes Using Frequency Analysis and a Deep Classifier," *IEEE Transactions on Industry Applications,* vol. 99, pp. 1-1, 2017.

[75] D. Wang, K. Tsui, and Q. Miao, "Prognostics and Health Management: A Review of Vibration Based Bearing and Gear Health Indicators," *IEEE Access,* vol. 6, pp. 665-676, 2018.

[76] C. Sun, M. Ma, Z. Zhao, and X. Chen, "Sparse Deep Stacking Network for Fault Diagnosis of Motor," *IEEE Transactions on Industrial Informatics,* vol. 14, no. 7, pp. 3261-3270, 2018.

Appended Papers

Paper A

Early Detection and Classification of Bearing Faults using Support Vector Machine Algorithm

Jagath Sri Lal Senanayaka, Surya Teja Kandukuri, Huynh Van Khang, Kjell G. Robbersmyr

This paper has been published as:

J. S. L. Senanayaka, S. T. Kandukuri, Huynh Van Khang and K. G. Robbersmyr, "Early detection and classification of bearing faults using support vector machine algorithm," *2017 IEEE Workshop on Electrical Machines Design, Control and Diagnosis (WEMDCD)*, Nottingham, pp. 250-255, 2017
doi: 10.1109/WEMDCD.2017.7947755

Early Detection and Classification of Bearing Faults using Support Vector Machine Algorithm

Jagath Sri Lal Senanayaka, Surya Teja Kandukuri, Huynh Van Khang, Kjell G. Robbersmyr

Department of Engineering Sciences, University of Agder, 4879 Grimstad, Norway
E-mails: {jagaths; suryak; huynh.khang; kjell.g.robbersmyr }@uia.no

***Abstract*— Bearings are one of the most critical elements in rotating machinery systems. Bearing faults are the main reason for failures in electrical motors and generators. Therefore, early bearing fault detection is very important to prevent critical system failures in the industry. In this paper, the support vector machine algorithm is used for early detection and classification of bearing faults. Both time and frequency domain features are used for training the support vector machine learning algorithm. The trained classier can be employed for real-time bearing fault detection and classification. By using the proposed method, the bearing faults can be detected at early stages, and the machine operators have time to take preventive action before a large-scale failure. The usefulness of the algorithm is validated by using a run-to-failure experimental test data.**

***Index Terms*--** Fault diagnosis, Fault detection, Support vector machines, Ball bearings

A.1 Introduction

Rotating machinery systems are one of the fundamental pillars of modern human society. They can be found in most household appliances, industrial manufacturing processes, electric power generation, wind turbines, automobiles, etc. Early fault detection is necessary for large industrial machines as those faults may lead to catastrophic failures, service interruption and productivity losses. The rotating machines normally fail because of mechanical or electrical stresses which can be either structural or dynamic. The primary mechanical failures of rotating machines can be categorised as static, fatigue and surface failures. Based on the study of EPRI, 41–42 % of induction motor failures are due to bearing faults, and stator faults are followed by 36% [1]. Early detection of bearing faults is significant in industrial applications since the rotating machines are the heart of industrial processes. Proper maintenance practice is required to reduce the impact of failures and increase the service availability of these machines.

The oldest maintenance method was breakdown maintenance where the maintenance tasks were conducted after the failure of the machinery. The breakdown maintenance practice is suitable for non-critical machinery where reliability and availability are not very important. For critical machines, such as electric power plants, manufacturing machines, breakdown maintenance is not an option since unexpected failures can result in service interruptions and massive financial losses.

Consequently, preventive maintenance has been used in industry where the maintenance was conducted at scheduled regular intervals. The major disadvantages of preventive maintenance are needless planned shutdown and high maintenance cost. Later, condition-based maintenance (CBM) practices were slowly adopted by industry. The primary objectives of CBM are reducing the maintenance cost, increasing the machine reliability and service availability, etc. CBM is one of the modern maintenance practices where the conditions of machines are continuously monitored to detect system faults. Based on the observed machine conditions, the maintenance tasks can be arranged. The basis for condition/health monitoring is that machine faults can be diagnosed based on measured quantities of the rotating machines. The measured data could be temperature, thermography images, chemical and wear monitoring (e.g. lubricant oil contamination), vibration signals, acoustic emission signals, shock pulses,

motor current signals, etc. [2-3]. Operating temperature is a primary indicator of the machine health. Temperature or infrared image analysis is one of the easiest methods to monitor the machine condition. Lubricant oil analysis is often used for detecting bearing and gearbox faults. The electrical signature analysis is applied to detect the mechanical and electrical faults in electrical machines. However, vibration analysis is the most common technique for analysing mechanical faults, typically bearing, gearbox, misalignments, etc.

In the broad category, most fault diagnosis approaches can be summarised into model-based or data-driven. In the model-based fault diagnosis approach, a predetermined system/process model is required. The system can be modelled using physical system modelling, system identification techniques or system observers. Based on the system model, the system status can be predicted, and the predictions can be compared with the measured system status. The final step is analysing the residual of the comparison for fault diagnosis and prognosis purpose. The primary challenge of this method is making an accurate system model. However, in the data-driven approach, sensor data is used in statistical or machine learning algorithms to identify and classify the faults of the system. In this method, the predetermined system model is not required. The data- driven approach together with advanced signal processing techniques are very powerful tools for rotating machinery fault diagnosis and prognosis. Therefore, the data-driven approach is selected for this study.

In the most common system of vibration analysis, root mean square (RMS) of vibration signal and/or frequency spectrum is analysed in a monitoring process. Normally the data collection and processing are conducted one a manual inspection basis and have several limitations, for instance, expensive manpower, lack of statistical and machine learning fault detection. To solve the above problems, a system for online classification of bearing faults in electric motors is proposed in this study. For the proposed system, an accelerometer must be placed on the motor, and short-duration (e.g. 1 second) vibration signals should be recorded at predefined time intervals (e.g. in every 60 minutes). During the first time, there may not be sufficient data to train the classifier. If a manufacturing or process plant has a large collection of similar motors, it is economical to make this training data by using few motors, and once the data is available, the classier can be trained. Then the real-time vibration data can be applied to the trained classier for detecting possible faults in early stages. In this paper, A support vector machine algorithm is used for early detection and classification of bearing faults. A data-

driven condition monitoring approach is adopted for the study. The next task after the fault detection is predicting the remaining lifetime of the faulty bearing, and this information can be used to make CBM schedules. The final objective is reducing the downtime and overall maintenance cost of the system.

This paper is organised as follows: in Section A.2, vibration signal-based bearings fault diagnosis method is discussed. Then the details of the fault classification algorithm are presented in section A.3. The experimental results are analysed in section A.4. The conclusion of the work is provided in section A.5.

A.2 Vibration signal-based diagnosis of bearing faults

The main components of rotating machines are bearings, gears and shafts. Vibration signal analysis is the traditional method used for fault diagnosis in above components. The failures can happen in any element of the rolling bearing such as inner race, outer race, rolling elements and cage. Faults in the bearings, gears and shafts are presented in the vibration signal, and such faults can be detected by using time, frequency and time-frequency analysis. The primary task of the signal processing is to extract fault-related features from the raw data. Most common time-domain features are RMS, kurtosis, crest factor, time synchronous average, etc. The essential features in frequency domain include amplitude and power of frequency components, the length of sidebands, natural frequency, harmonics, etc. Various combination of signal processing, statistics and machine learning techniques for the fault diagnosis and prognosis can be found in the literature [4-12].

Signal processing has been used as the enabling technique in many fault diagnosis algorithms. The selection, location and orientation of sensors are very important in detecting the expected faults. Vibration sensors should be selected based on the rotational speed of the machines and placed closer to the bearing or gearbox under consideration. Features or fault characteristics can be derived from different analysis domains. Statistical and machine learning algorithms can be utilised for automatic detection and classification of faults [4-12]. Moura et al. [4] demonstrated a data-driven approach for bearing fault diagnosis. First, the vibration signal of the bearings is recorded, and time domain features were extracted. Then the principle component analysis (PCA) and artificial neural networks (ANN) are used to classify the severities of the bearing faults. An

evaluation of fault recognition efficiency was completed for each combination of signal processing and pattern recognition techniques. It is determined in [4] that all four schemes of classification yielded reasonably good results and were thus shown to be a promising approach for rolling bearing fault diagnosis. Multiresolution analysis (MRA) is used in [5] to extract the features from vibration signals. Afterwards, a supervised neural network (NN) is adopted for classification purposes which can classify four bearing statuses (healthy, inner race fault, outer race fault and ball fault). Subsequently, the algorithm has been extended to extract the features from wavelet packet transformation (WPT) and classify them with ANN [6]. Other studies on feature extraction techniques and classification methods could be found in [7-12]. In this paper, the SVM algorithm is used for early bearing fault detection and classification.

A typical rolling element bearing consists of four elements namely, inner race, outer race, rolling elements and cage. Depending on applications different types of rolling elements are selected. Ball bearings provide the best performance/price ratio and are widely used in industry. Other types of bearings are cylindrical rollers, taper rollers and spherical bearings which are often designated for high load applications. Figure A.1 shows the spherical roller bearing used in this study.

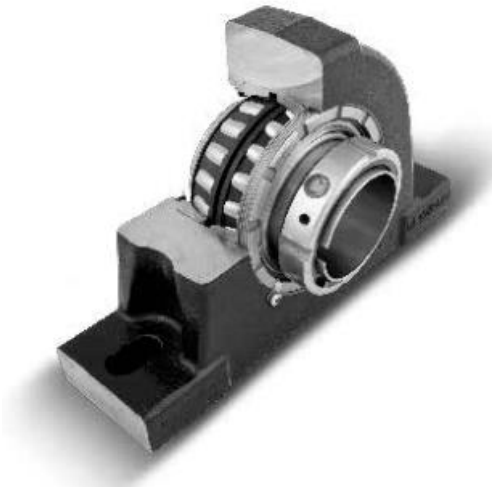

Figure A.1: A typical spherical roller bearing [19].

When a bearing starts its degradation process, very high-frequency (5-40 kHz or level 1) components associated with bearing faults begin appearing in the vibration spectrum. At the second stage, in addition to the high-frequency components, medium frequency (1-5 kHz or level 2) also begin appearing.

However, detecting faults at these levels are difficult. At the next, fault associated frequency components are visible at low-frequency range (< 1 kHz or level 3) in the vibration spectrum [18]. Based on the geometry, dimensions of the bearing and the rotational speed, these characteristic frequencies can be calculated. At the level 4, the bearing drives to a complete failure and vibration spectrum becomes a noisy spectrum. Thus, diagnosis of bearing faults should be focused on the level 3 where the frequencies associated with bearing defects are given in (A.1) -(A.5) [16], [20].

The fundamental train frequency/cage frequency is defined as

$$FTF = \frac{f_s}{2}\left(1 - \frac{D_b}{D_c}\,cos\theta\right) \tag{A.1}$$

The ball/roller spinning frequency (BSF) can be defined as

$$BSF = \frac{D_c}{2D_b}\,f_s\left(1 - \left(\frac{D_b}{D_c}\,cos\theta\right)^2\right) \tag{A.2}$$

The characteristic frequency of an outer race defect is given by

$$BPFO = \frac{N_b}{2}\,f_s\left(1 - \frac{D_b}{D_c}\,cos\theta\right) \tag{A.3}$$

The characteristic frequency of an inner race fault can be calculated as

$$BPFI = \frac{N_b}{2}\,f_s\left(1 + \frac{D_b}{D_c}\,cos\theta\right) \tag{A.4}$$

The characteristic frequency of a rolling element fault is defined as

$$REF = \frac{D_c}{D_b}\,f_s\left(1 - \left(\frac{D_b}{D_c}\,cos\theta\right)^2\right) \tag{A.5}$$

where N_b is the number of rolling elements in the bearing, D_b denotes the diameter of a rolling element, D_c represents the pitch diameter, θ is the contact angle between the outer-race and rolling element, and f_s is the shaft speed.

A.3 Fault diagnosis and classification algorithm

The fault diagnosis and classification algorithm consists of two main sections. First, the vibration signals are processed to collect relevant time and frequency domain features. Then the SVM algorithm is used to train a classifier for fault detection and classification. Experimental data is used to train and validate the algorithm.

A.3.1 Signal processing and feature extraction

The steps of signal processing and the feature extraction process are shown in Figure A.2. First, the time domain signal is collected, and the RMS of the signal is calculated. Then the Hilbert transformation is applied to detect the envelope of the time domain signal. Fast Fourier transformation is used to convert the envelope signal into the frequency domain.

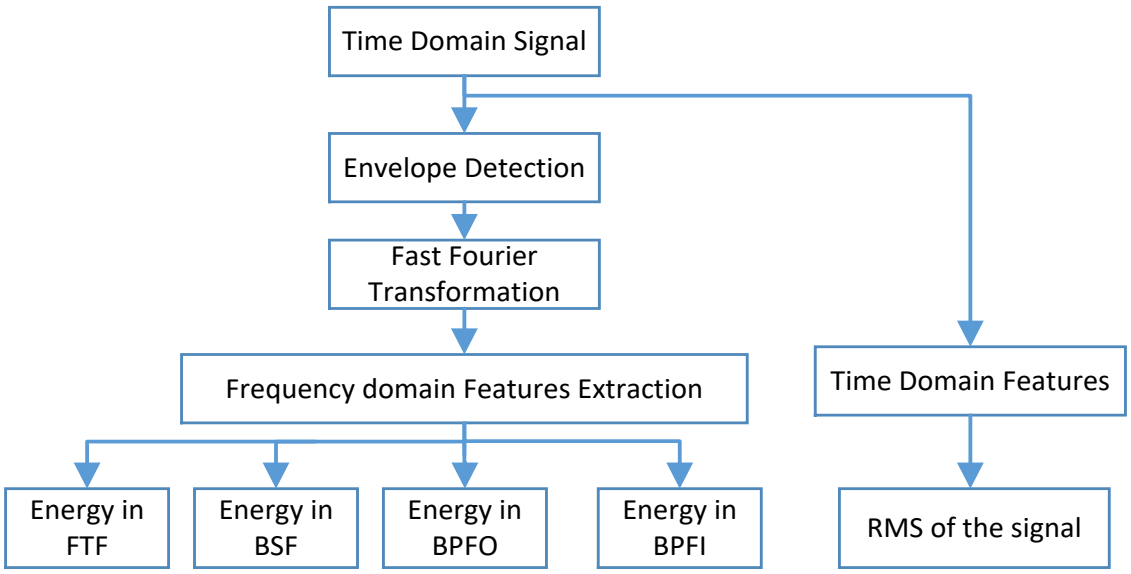

Figure A.2: The steps of signal processing and feature extraction process..

Finally, fault specific frequencies located in the frequency spectrum and energy associated with each frequency bands are extracted. Five fault cases were considered: healthy, inner race degradation (IR_D), inner race failure (IR_F), outer

race degradation (OR_D), and outer race failure (OR_F). SVM classification algorithm is used to classify the faults.

A.3.2 SVM-based Classification algorithm

In the previous section, five features used to predict about bearing faults were selected. Since the status of bearings in each data sample is already known, it is possible to train a SVM classifier using collected data. However, only 80% of the collected data is used to train the classifier, and the remaining 20% of data can be applied to validate the fault detection and classification capability of the system. In real time applications, after the validation process, this classifier can be used to make an online fault detection and classification system. Figure A.3 shows a block diagram of the online fault detection and classification system. When new data is collected, trained classifier can be used to detect and classify the faults in early stages.

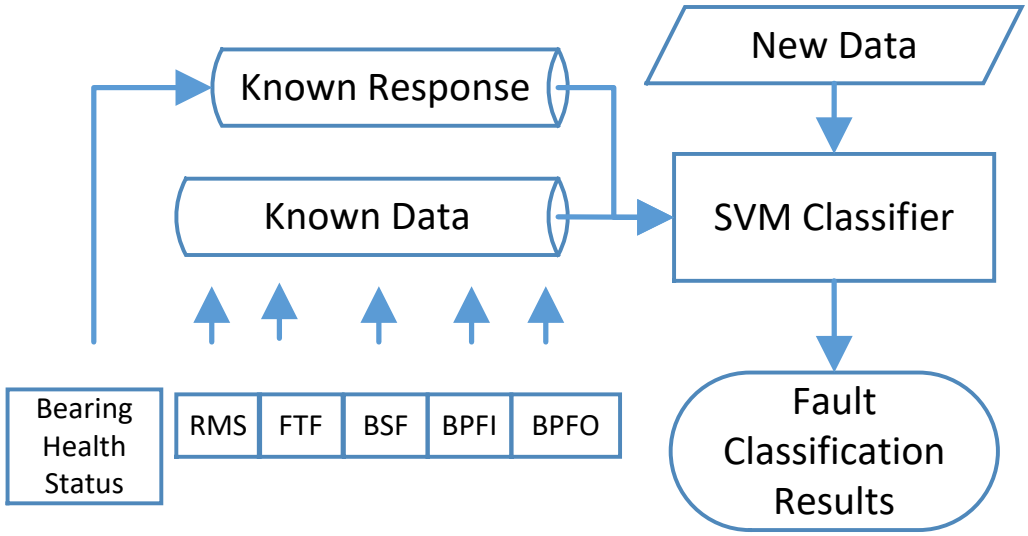

Figure A.3: Block diagram of the SVM classifier.

In the algorithm of SVM classification, the objective is to make a multidimensional hyperspace using the available features and then draw an optimum hyperplane to separate fault classes. Figure A.4 shows an example including two features and two classes.

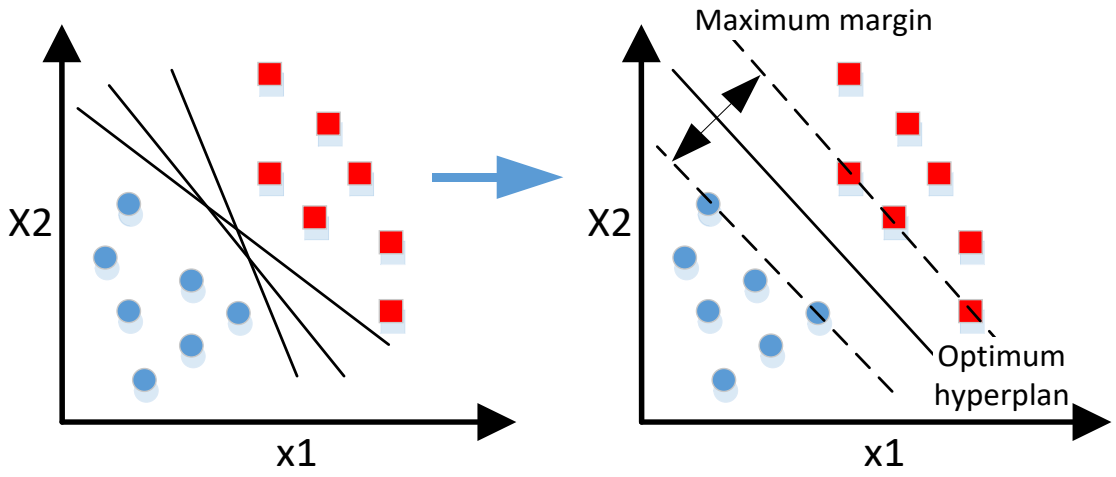

Figure A.4: An example of SVM classification.

Many possible lines can be drawn to separate two classes. However, the objective of SVM is to draw an optimum line to separate two classes with maximum separating margins. This idea can be conceptualised to make an optimisation problem [17].

Consider the training data set in Figure A.4 with inputs $x_i \in R^l$ and outputs $y_i \in \{\pm 1\}$;

$$(x_i, y_i) \in R^l * \{\pm 1\} \ , i = 1, \dots N \tag{A.6}$$

There are two classes, and '+1' represents one class, and '-1' accounts for the other class. After the training, it is expected to get a decision function given by;

$$f_{w,b}(x) = sgn\ (w.x + b) \tag{A.7}$$

Where w is the coefficient vector and b is the bias of the hyperplane. The 'sgn' represents the bipolar sign function. Ideally the, following condition should be satisfied by the hyperplane of the classifier.

$$y_i\ [w.x_i + b] \geq 1\ , i = 1,2, \dots\dots, N \tag{A.8}$$

Among all the separating hyperplanes satisfying (8), the one with the maximum distance to the closest point is considered as the optimum separating hyperplane. Based on structural risk minimization inductive method, the training of an SVM is to minimise the guaranteed risk bound as follows.

$$\min J(w, e, b) = \frac{1}{2} w^T . w + \frac{1}{2}\ C\ \sum_{i=1}^{N} e_i^2 \quad \text{(A.9)}$$

Subject to

$$y_i\ [w . x_i + b] \geq 1 - e_i\ , i = 1,2, \ldots . , N \quad \text{(A.10)}$$

where e_i is a slack variable $e_i > 0$ which allows to manage when the ideal hyperplane in (A.8) is not possible.

The SVM algorithm doesn't consider complete dataset, but the boundary data. SVM can work with both linear and non-linear classification problems. For nonlinear problems, the data can be mapped to another dot product space F via nonlinear map $\emptyset: R^N \rightarrow F$, and then perform the above analysis in F. Two commonly used kernel functions are polynomial kernels and Gaussian RBF kernels [17]. However, it may be tricky to find the kernel function for a non-linear classification.

A.4 Experimental setup and results

The primary objective of this study is to make an algorithm for detecting and classifying the bearing faults. The data for this study was collected from a run-to-failure test conducted by Intelligent Maintenance Systems, University of Cincinnati, USA [14-15]. In this experiment, four bearings were connected to a shaft rotating at 2000 rpm. A 2700 kg radial load was applied to the shaft as shown in Figure A.5. Four accelerometers were used to collect vibration signals at 20 kHz sampling frequency. One second samples were recorded every 10 minutes. As shown in Figure A.6, inner-race, outer-race and rolling element faults have been observed at the end of the test. In this study, the healthy, outer race and inner-race

faults are considered. Dimensions of the bearing are given in Table A.1. Based on the bearing dimensions, characteristic frequencies of the faults are calculated via (A.1)-(A.5) and shown in Table A.2.

Table A.1: Dimensions of a test bearing.

Parameter	**Value**
Number of rolling elements (N_b)	16
Diameter of a rolling element (D_b)	8.4074 mm
Pitch diameter (D_c)	71.501 mm
Contact angle (θ)	0.265 rad
Rotational speed (f_s)	33.75 Hz

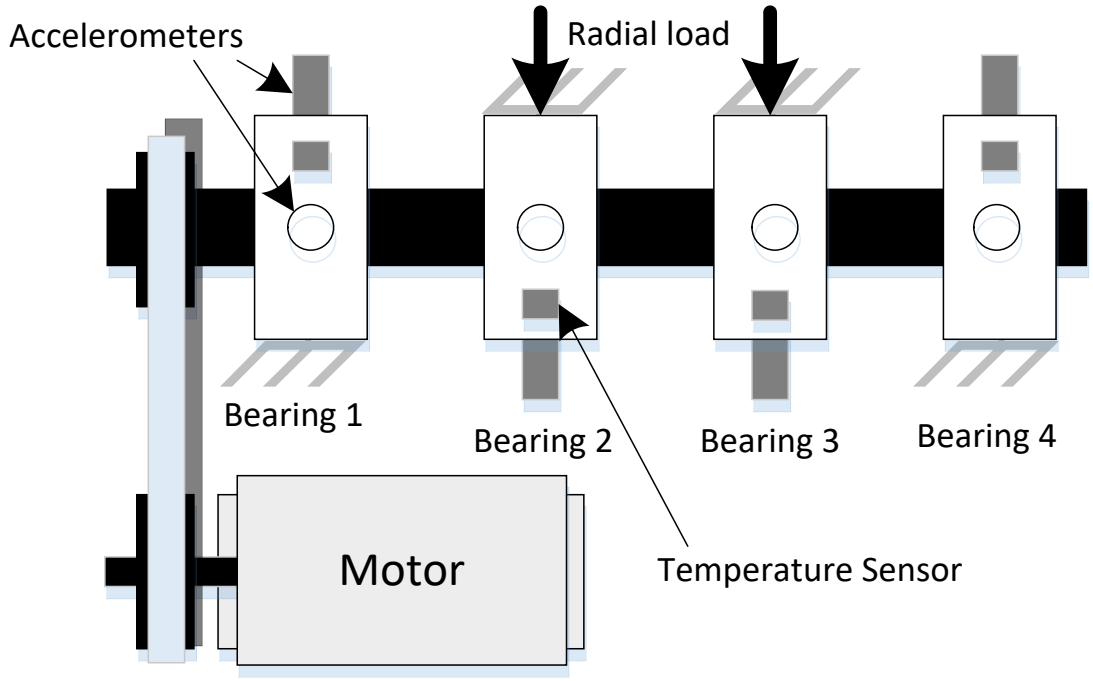

Figure A.5: Experimental setup [13-14].

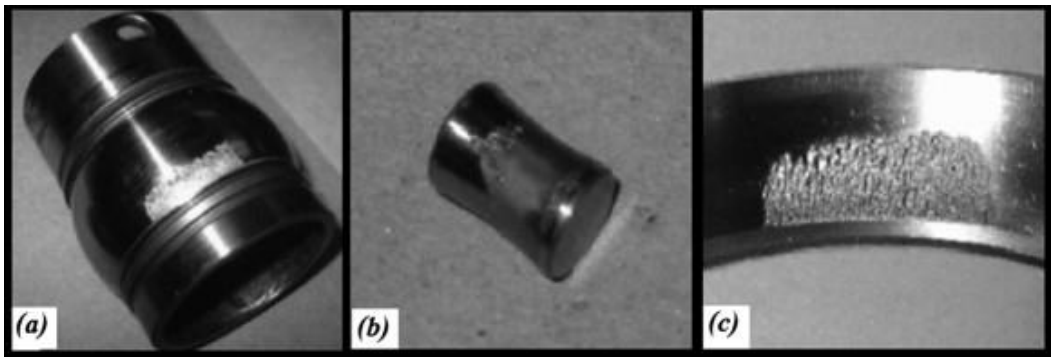

Figure A.6: Failed bearings components after the test.
(a) inner race failure, (b) roller element failure and (c) outer race failure [14-15].

Table A.2: Expected characteristics frequencies.

Frequency component	**Expected frequency**
Fundamental train frequency (FTF)	15 Hz
Shaft Rotational frequency (1X)	33.75 Hz
Ball/roller spinning frequency (BSF)	141.6
Outer-race fault (BPFO)	239.3 Hz
Inner-race fault (BPFI)	300.6 Hz and 1X side bands

Figure A.7 shows the frequency spectrum of vibration signals for the inner race fault and healthy cases. The expected frequency for the inner race fault is 300.6 Hz and 1X sidebands. The observed frequency is 301.3 Hz and 1X sidebands. For healthy case, fault related frequency components are not present in the vibration spectrum. Therefore, the inner race faults can be clearly seen from the vibration spectrum. As shown in Figure A.8, the expected frequency associated with an outer race fault is also present in the frequency spectrum. The expected frequency is 239.3 Hz, and the observed frequency is 236.2 Hz. The deviation is small, and this small frequency variation is normal in detecting bearing faults since the right value of contact angles is unknown. In the healthy case, fault related frequency components are not visible, and it remains closer to zero.

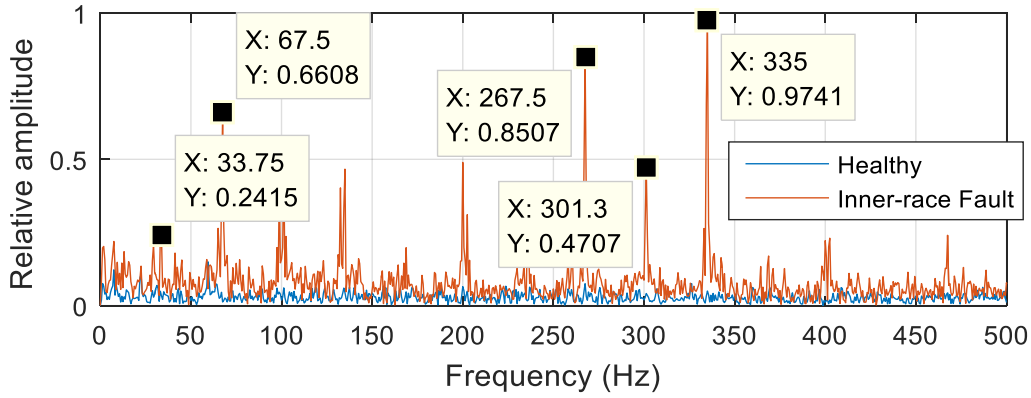

Figure A.7: The frequency spectrum of a vibration signal for inner race fault.

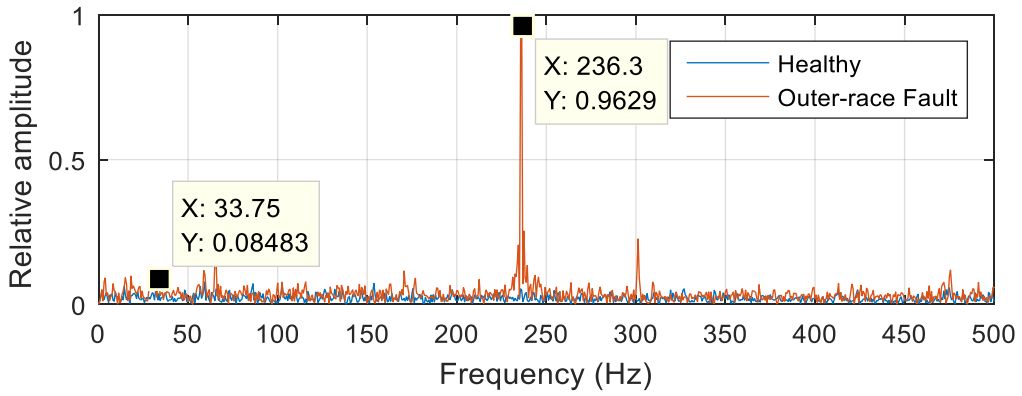

Figure A.8: The frequency spectrum of the vibration signal for an outer race fault.

In the above analyses, only healthy and faulty cases of inner race and outer race faults have been considered. However, in most cases, bearing faults are subjected to a pre-degradation process, and if a proper condition monitoring process is applied, an early fault detection is possible.

The RMS of a vibration signal for the complete life of inner-race fault bearing is shown in Figure A.9. There is a significant increase of vibration after 12 days of continues working. Then degradation process starts, and it gradually increases for 2.5 days until failure. Based on RMS signals, it is possible to detect a fault in the bearing. However, to find the type of the fault, further analysis is required. Other frequency domain features have to be analysed to examine the fault type. Figure A.10 shows the energy content of fault specific frequencies of a

vibration signal for the complete life of the inner-race faulty bearing. There is a significant deviation of energy in inner-race fault related frequencies.

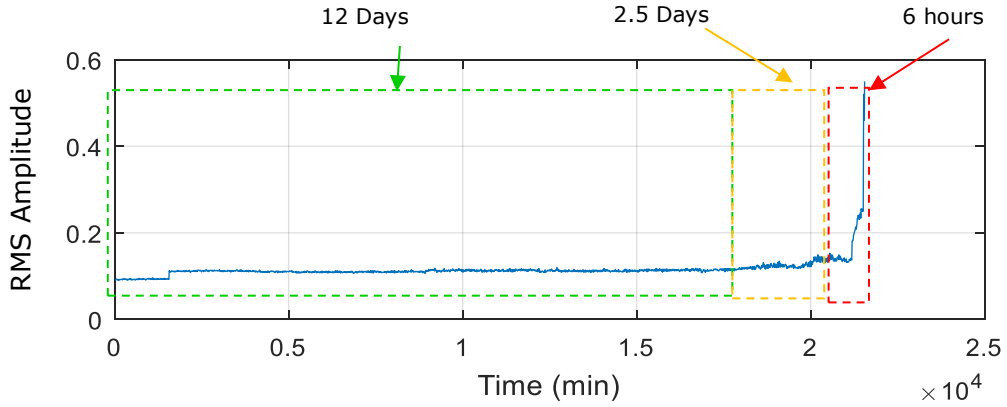

Figure A.9: RMS of the vibration signal for a complete life in case of an inner-race faulty bearing.

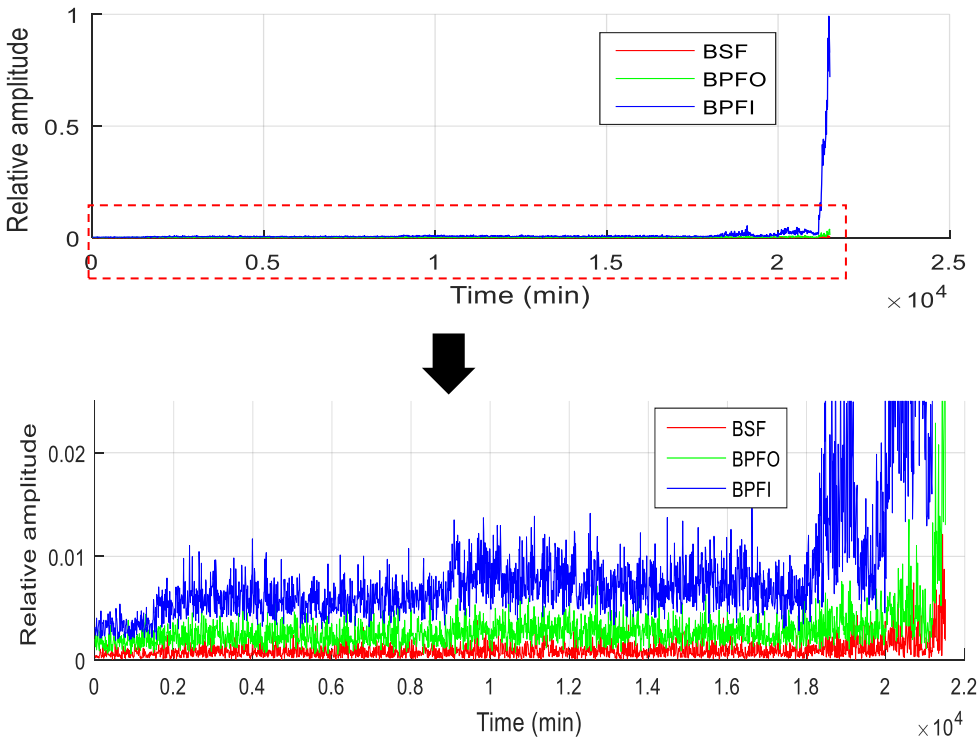

Figure A.10: The energy content of fault specific frequencies of the vibration signal for the complete life of inner race fault bearing.

The RMS of a vibration signal for the complete life of an outer race fault bearing is shown in Figure A.11.

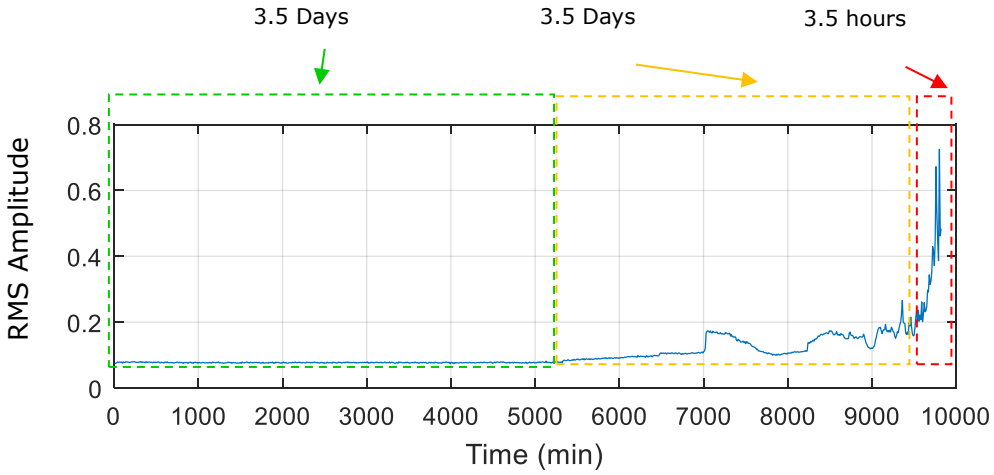

Figure A.11: RMS of vibration signal for complete life of outer race fault bearing.

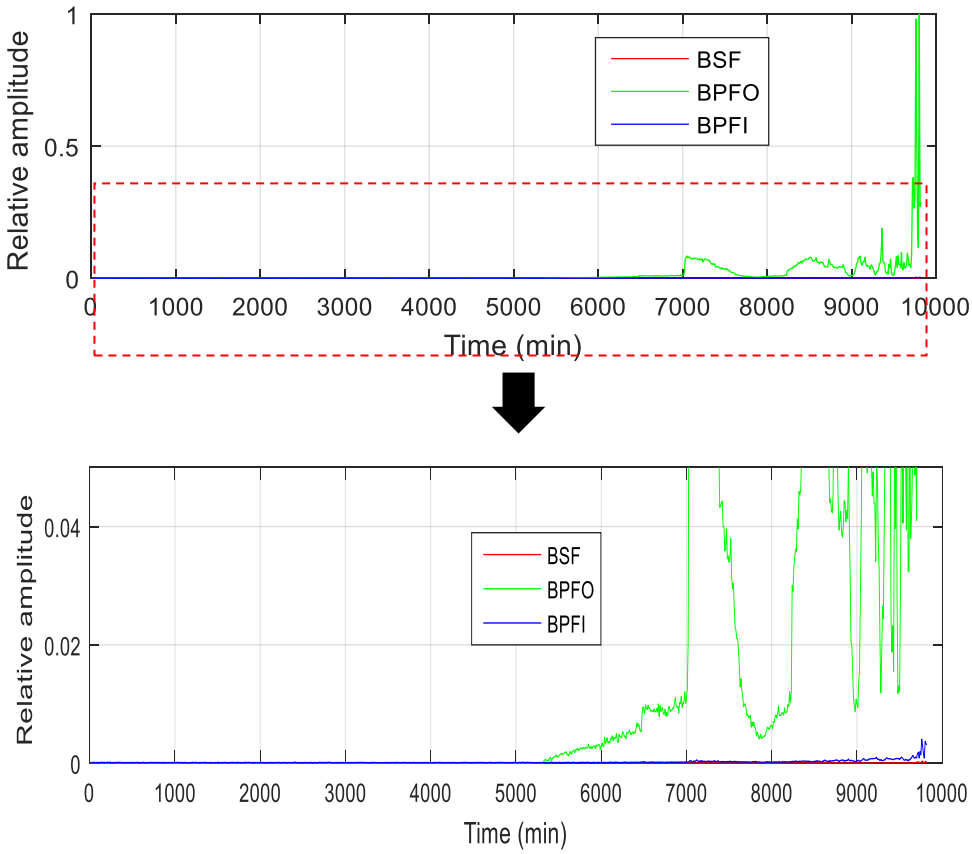

Figure A.12: The energy content of fault specific frequencies of the vibration signal for the complete life of the outer-race faulty bearing.

For 3.5 days, the bearing remains in the healthy stage. Then the bearing starts degrading, and after 3.5 days of degradation process, the bearing completely fails. When analysing other features of the signal, a clear energy increase in outer race fault associated frequencies is visible. Figure A.12 shows the energy content of fault specific frequencies of a vibration signal for the complete life of the outer-race faulty bearing. There is a significant deviation of energy in outer race fault related frequencies.

Based on above analysis and extracted features, two SVM classifiers have been trained. Linear SVM and quadratic SVM algorithms have been applied for a comparison. A portion of available data (80%) has been used to train the classifier and remaining (20%) of the data is used to validate the classifier. The confusion matrix for a decision tree fault classification is given in Figure A.13 and Figure A.14. Y-axis represents the true fault classes which are already known, and x-axis denotes the predicted fault class by the classifier. The diagonal of the matrix gives the accuracy of the prediction of the classifier.

True class							
	H	2281 99.4%	13 0.6%				99.4% 0.6%
	IR_D	46 13%	309 87.0%				87.0% 13.0%
	IR_F		4 9.8%	37 90.2%			90.2% 9.8%
	OR_D	15 3.5%	2 0.5%		413 96.0%		96.0% 4.0%
	OR_F	2 10.5%			2 10.5%	15 78.9%	78.9% 21.1%
		H	IR_D	IR_F	OR_D	OR_F	TPR/FNR
		Predicted class					

Figure A.13: Confusion matrix of linear SVM classifier.

True class	H	2278 99.3%	16 0.7%				99.3% 0.7%
	IR_D	48 13.5%	306 86.2%	1 0.3%			86.2% 13.8%
	IR_F		4 9.8%	36 87.8%		1 2.4%	87.8% 12.2%
	OR_D	9 2.1%			420 97.7%	1 0.2%	97.7% 2.3%
	OR_F			2 10.5	1 5.3%	16 84.2%	84.2% 15.8%
		H	IR_D	IR_F	OR_D	OR_F	TPR/FNR
		Predicted class					

Figure A.14: Confusion matrix of quadratic SVM classifier.

Other boxes represent the prediction errors. There is an accuracy of about 86% in the inner-race degradation (IR_D) class and an accuracy of 96% in the outer-race degradation (OR_D) class. Furthermore, both classifiers show a high accuracy. This means that an early fault detection and classification can be done in both linear SVM and quadratic SVM classifiers, and the accuracy of classification is trustworthy.

A.5 Conclusion

In this study, the possibility of making a real-time bearing fault detection and classification algorithm is examined. The support vector machine algorithm is selected as a classifier. Once experimental data is collected, both time and frequency domain features can be extracted for training the classifiers. The trained classifiers are validated using experimental data and shown reliable results. A Bearing fault can be detected 2.5-3.5 days ahead in the run-to-failure test. Therefore, the proposed method can be extended to make a trustworthy real-time fault diagnosis system.

References

[1] F. Allbrecht, J.C. Appiarius, R.M. McCoy, E.L. Owen, D.K. Sharma, “Assessment of the reliability of motors in utility applications”, *IEEE Trans. Energy Convers*. EC-1 (1) (1986) 39 /46.

[2] P. J. Tavner, "Review of condition monitoring of rotating electrical machines," *in IET Elec. Power App.*, vol. 2, no. 4, pp. 215-247, July 2008.

[3] G.K Singh, S.A.A.S Saleh Al Kazzaz, “Induction machine drive condition monitoring and diagnostic research—a survey”, *Electric Power Systems Research*, vol. 64, pp. 145-158, February 2003.

[4] E.P. de Moura, C.R. Souto, A.A. Silva, M.A.S. Irmão, “Evaluation of principal component analysis and neural network performance for bearing fault diagnosis from vibration signal processed by RS and DF analyses”, *Mecha. Sys. and Sig. Pro.*, vol. 25, pp. 1765-1772, July 2011.

[5] C. Castejón, O. Lara, J.C. García-Prada, “Automated diagnosis of rolling bearings using MRA and neural networks”, *Mecha. Sys. and Sig. Proc.*, vol. 24, Issue 1, pp. 289-299, January 2010.

[6] G. Dalpiaz et al. (eds.), “Advances in Condition Monitoring of Machinery in Non-Stationary Operations”, *Lecture Notes in Mechanical Engineering*, Springer-Verlag Berlin Heidelberg 2014.

[7] J. Zhang, W. Ma, J. Lin, L. Ma, X. Jia, “Fault diagnosis approach for rotating machinery based on dynamic model and computational intelligence”, *Measurement*, vol. 59, pp. 73-87, January 2015.

[8] W. Li, Z. Zhu, F. Jiang, G. Zhou, G. Chen, “Fault diagnosis of rotating machinery with a novel statistical feature extraction and evaluation method”, *Mecha. Sys. and Sig. Proc.*, vol. 50, pp. 414-426, January 2015

[9] X. Chen, J. Zhou, J. Xiao, X. Zhang, H. Xiao, We. Zhu, W. Fu, “Fault diagnosis based on dependent feature vector and probability neural network for rolling element bearings”, *Applied Math. and Computation*, vol. 247, pp. 835-847, 15 November 2014.

[10] B. Li, M. Y. Chow, Y. Tipsuwan and J. C. Hung, "Neural-network-based motor rolling bearing fault diagnosis," *in IEEE Transactions on Industrial Electronics*, vol. 47, no. 5, pp. 1060-1069, Oct 2000.

[11] L. Eren, A. Karahoca and M. J. Devaney, "Neural network based motor bearing fault detection," *Proceedings of the 21st IEEE Instrumentation and Measurement Technology Conference* (IEEE Cat. No.04CH37510), Vol.3, pp. 1657-1660, 2004.

[12] G. Yu and L. Zhang, "An Intelligent Approach for Bearing Fault Diagnosis Based on Bayesian Networks and Alpha-Stable Distribution," *2015 International Conference on Computational Intelligence and Communication Networks (CICN)*, Jabalpur, 2015, pp. 76-78.

[13] J. Lee, H. Qiu, G. Yu, J. Lin, and Rexnord Technical Services (2007). IMS, University of Cincinnati. "Bearing Data Set", *NASA Ames Prognostics Data Repository* (http://ti.arc.nasa.gov/project/prognostic-data-repository), NASA Ames Research Center, Moffett Field, CA,2007.

[14] H. Qiu, J. Lee , J. Lin, G. Yu. "Wavelet filter-based weak signature detection method and its application on rolling element bearing prognostics". *J. Sound Vib.*, vol. 289, pp 1066–90, 2006.

[15] J.B. Ali et. el, "Application of empirical mode decomposition and artificial neural network for automatic bearing fault diagnosis based on vibration signals", *Applied Acoustics*, vol. 89, pp. 16-27, March 2015.

[16] N. Tandon, A. Choudhury, "A review of vibration and acoustic measurement methods for the detection of defects in rolling element bearings", *Tribology International*, vol. 32, Issue 8, pp. 469-480, August 1999.

[17] V. Vapnik, "The nature of Statistical Learning Theory", New York: Wiley, 1998.

[18] Vibration Analysis Definitions, Mobius Institute,[Online] Available: http://www.mobiusinstitute.com/

[19] Spherical Roller Bearing Units Catalog, Rexnord Corporation,[Online] Available: http://www.rexnord.com/ContentItems/TechLibrary/Documents/BR2-001_Rex-and-Link-Belt-Spherical-Roller-Bearing.aspx.

[20] I. Howard, "A Review of Rolling Element Bearing Vibration : Detection, Diagnosis and Prognosis", *Defence science and technology organization*, Australian government department of defence,[Online] Available: http://dspace.dsto.defence.gov.au/dspace/handle/1947/3347

Paper B

Fault Detection and Classification of Permanent Magnet Synchronous Motors in Variable Load and Speed Conditions using Order Tracking and Machine Learning

Jagath Sri Lal Senanayaka, Van Khang Huynh, Kjell G. Robbersmyr

This paper has been published as:

J.S.L Senanayaka H.V. Khang, K.G. Robbersmyr, “Fault Detection and Classification of Permanent Magnet Synchronous Motors in Variable Load and Speed Conditions using Order Tracking and Machine Learning”, *Journal of Physics: Conference Series*, vol. 1037, no. 3, 2018

Fault Detection and Classification of Permanent Magnet Synchronous Motors in Variable Load and Speed Conditions using Order Tracking and Machine Learning

Jagath Sri Lal Senanayaka, Van Khang Huynh, Kjell G. Robbersmyr

Department of Engineering Sciences, University of Agder, 4879 Grimstad, Norway.

E-mail: jagaths @uia.no

Abstract: **Permanent magnet synchronous machines have gained popularity in wind turbines due to their merits of high efficiency, power density, and reliability. The wind turbines normally work in a wide range of operations, and harsh environments, so unexpected faults may occur and result in productivity losses. The common faults in the permanent magnet machines occur in the bearing and stator winding, being mainly detected in steady-state operating conditions under constant loads and speeds. However, variable loads and speeds are typical operations in wind turbines and powertrain applications. Therefore, it is important to detect bearing and stator winding faults in variable speed and load conditions. This paper proposes an algorithm to diagnose multiple faults in variable speed and load conditions. The algorithm is based on tracking the frequency orders associated with faults from the normalised order spectrum. The normalised order spectrum is generated by resampling the measured vibration signal via estimated motor speeds. The fault features are then generated from the tracking orders in addition to the estimated torque and speed features. Finally, support vector machine algorithm is used to classify the faults. The proposed method is validated using experimental data, and the validated results confirm its usefulness for practical applications.**

B.1 Introduction

Condition monitoring (CM) is necessary to guarantee the healthy and safe operation of critical rotating machines. The CM is an important part of condition-based maintenance (CBM) program and based on CM results, the maintenance schedules can be arranged. Moreover, by analysing the CM data with failure mechanisms, the remaining useful life (RUL) of the component can be estimated. This complete process is covered in the Prognostics and Health Management (PHM) of engineering systems.

In wind turbines, vibration and current sensors are widely used for CM. The mechanical faults can be detected by investigating the trends of root mean square (RMS) of measured vibration signal. but, the overall RMS of vibration signal can be only used to detect faults, and the classification of multiple faults is not possible. Mechanical faults produce forcing frequencies associated with the faults which can be differentiated by searching those forcing frequencies in the vibration spectrum. Therefore, Faults can be classified by further analysing the frequency spectrum of the vibration signal [1]. Signal processing and statistical detection methods are useful for the analysis due to the noise and stochasticity of vibration signals and machine behaviour. With spectrum analysis, good performances can be expected for individual fault classification tasks, but multiple faults classification can be difficult. Understanding complex spectrum regions is required for the classification of multiple faults. Statistical and machine learning methods have been used in the multiple-fault classifications. Fault-related features can be derived using the statistical methods, or domain knowledge of forcing frequencies, and those features can be used in statistical and machine learning algorithms to classify the faults. A review on different signal processing, statistical and machine learning algorithms can be found in [2]. Decision tree algorithm [3] and support vector machine (SVM) algorithm [11] are used for bearing fault detection under a constant load and speed or in the steady-state. Most of the existing fault diagnosis algorithms are mainly implemented at such conditions, which are not the case for wind turbine applications. This work focuses on fault classification for a permanent magnet synchronous motor (PMSM) working in variable load and speed conditions. The rest of this paper is organised as follows. The details of proposed fault diagnosis Algorithm are discussed in Section B.2. The experimental results are presented in Section B.3. Finally, the conclusion is given in Section B.4.

B.2 Proposed fault diagnosis algorithm

A block diagram of the proposed algorithm is shown in Figure B.1, in which the rotational speed and torque of PMSM are estimated using the current measurements. For the fault classification, features of the variable speed and load torque are required. The speed can be estimated from the Hilbert transformation, and the torque is calculated from the measured currents [4-5]. Since the mechanical rotational speed of a PMSM is directly proportional to the AC supply frequency, it is possible to estimate the rotational speed by estimating the frequency of the current waveform. First, the complex-valued analytic signal of the current signal is extracted using the Hilbert transformation, and the phase angle of the current signal is derived. Next, the rotational speed is calculated by taking the first order derivation of the cumulative angle of the current waveform and multiplying with the number of pole pairs. The collected vibration signal is resampled based on the estimated rotational frequency, and the order normalized frequency spectrum is calculated from the resampled signal.

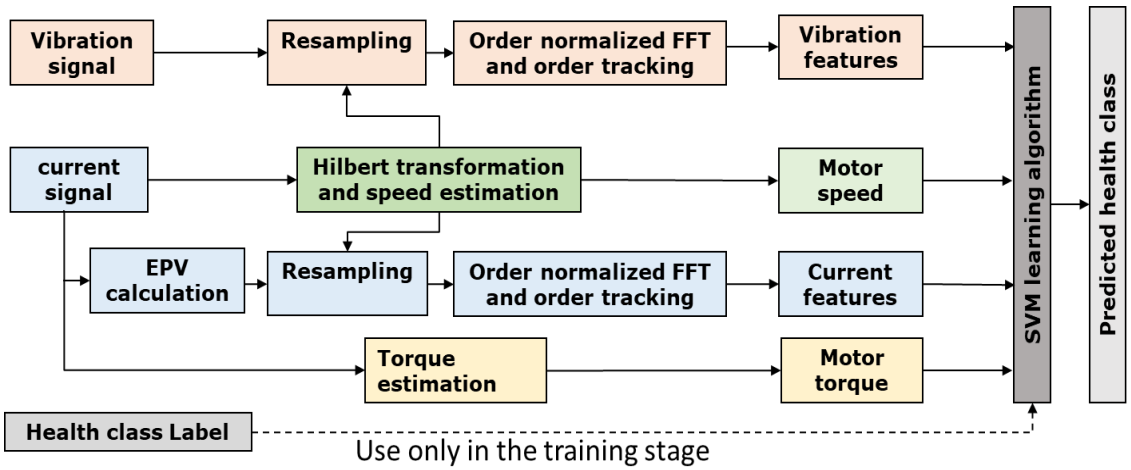

Figure B.1: The block diagram of proposed fault diagnosis and classification algorithm.

Several features based on vibration and current signals are calculated from the order normalized spectrogram. The faults related orders of the vibration spectrum are tracked. Furthermore, additional features of speed and torque are produced based on measured currents and calculated rotational speed. In this study, a nonlinear SVM algorithm is used as the classifier. Gaussian radial basis function

(RBF) kernel is used in the SVM algorithm, which produces a better nonlinear classification in the feature space. This study focuses on 4 types of health classes based on the health status of stator winding and bearing on a PMSM. The first class is the healthy class where both stator winding and bearings are healthy. In health class 2, the stator has 10% inter-turn winding short-circuit fault, and bearing is healthy. In health class 3, the stator is healthy, and an outer-race defect occurs on the bearing. In health class 4, both the stator winding and bearing fault are defective. As shown in Figure B.2, the SVM algorithm is trained using labelled training data. After the training process, the algorithm can be employed for predicting the health statuses using new current and vibration signals.

B.2.1 Hilbert transformation and motor speed estimation

In a PMSM, the current signal is usually sinusoidal with varying frequency and amplitude. Therefore, the current signal can be considered as a mono-component signal and Hilbert transformation can be used to extract the instantaneous frequency, amplitude and the phase.

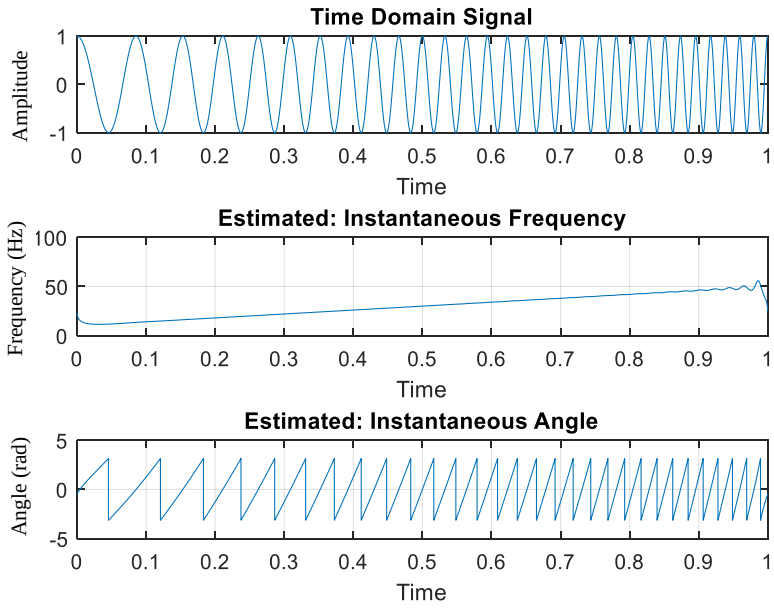

Figure B.2:Frequency and angle estimation of a mono-component signal: Hilbert transformation.

The instantaneous frequency and the angle estimation example of a mono-component signal using Hilbert transformation are given in Figure B.2. An analytic

signal of the original signal is required to extract the instantaneous frequency, amplitude and the phase of the original system. The analytic signal is a complex-valued function, which has no negative frequency values shown as follows [6].

The Fourier transform $S(f)$ of a time-domain signal $S(t)$ has a Hermitian symmetry at zero frequency axis, which is $S(-f) = S(f)^*$. where $S(f)^*$ is the complex conjugate of $S(f)$. The analytic function in the frequency domain is defined as:

$$\begin{aligned} S_a(f) &= \begin{cases} 2\,S(f), & if\ f > 0 \\ S(f), & if\ f = 0 \\ 0 & if\ f < 0 \end{cases} \\ &= 2u(f) \cdot S(f) \\ &= S(f) + sgn(f) \cdot S(f) \end{aligned} \tag{B.1}$$

where $u(f)$ is the unit step function and $sgn(f)$ is the sign function. The analytic function holds only non-negative frequency components of $S(f)$ and the operation is reversible due to the Hermitian symmetry of $S(f)$.

$$S(f) = \begin{cases} 0.5\,S_a(f), & if\ f > 0 \\ S_a(f), & if\ f = 0 \\ 0.5\,S_a(-f)^* & if\ f < 0 \end{cases} \tag{B.2}$$

The analytic signal of $S_a(t)$ can be drived using the inverse Fourier transform of $S_a(f)$:

$$\begin{aligned} S_a(t) &= F^{-1}[S_a(f)] \\ &= F^{-1}[S(f) + sgn(f) \cdot S(f)] \\ &= F^{-1}[S(f)] + F^{-1}[sgn(f)] * F^{-1}[S(f)] \\ &= S(t) + j\left[\frac{1}{\pi t} * S(t)\right] \\ &= S(t) + j\hat{S}(t) \\ &= S_m(t)e^{j\emptyset(t)} \end{aligned} \tag{B.3}$$

where $\hat{S}(t) = H[S(t)]$ is the Hilbert transformation, * is the convolution operator and j is the imaginary unit operator. $S_m(t) = |S_a(t)|$ is called the instantaneous amplitude or envelope, and $\emptyset(t) = arg\ [S_a(t)]$ is called the instantaneous phase.

The instantaneous angular frequency in hertz can be extracted by differentiating the unwrapped $\emptyset(t)$.

$$f(t) = \left(\frac{1}{2\pi}\right)\frac{d}{dx}\emptyset(t) \tag{B.4}$$

B.2.2 Resampling order normalized FFT and order tracking

In steady-state fault diagnoses, the frequencies are assumed as constants, and the constant time sampling rates can be used. Therefore, Fourier transform can be used for such a frequency domain analysis. However, in variable speed operations, the Fourier transform cannot be used because the analysis signals are not stationary or the frequencies change in time.

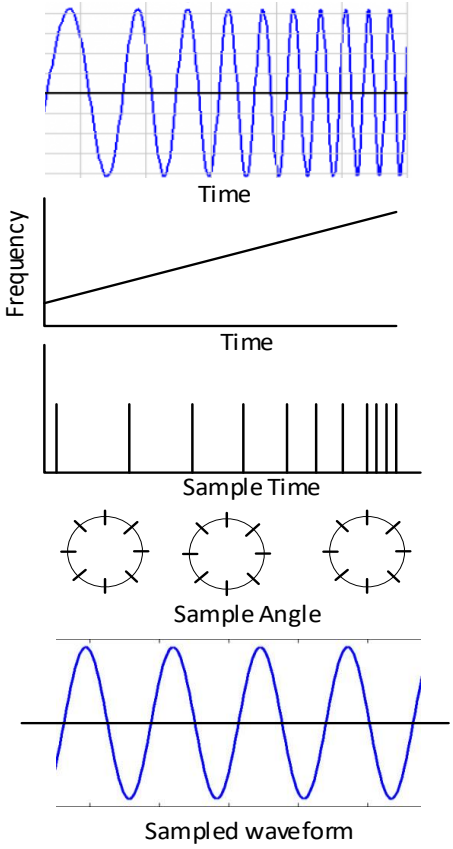

Figure B.3: Constant angle sampling of a variable speed signal.

To deal with nonstationary signals, short time Fourier transform (STFT) with constant time sampling may be used as it assumes that the frequency is constant

for a small-time period and Fourier transform is performed for those short time signal windows. However, using STFT requires a wise selection of window sizes in advance to archive the best resolution, which is not a solution to tackle the characteristic frequencies in variable speed operations as the characteristic frequency is changed according to the shaft speed. The solution is instead of using constant time sampling, using the constant angular sampling and order normalised FFT which is demonstrated in Figure B.3 for a simple frequency varying sine wave. The constant angle sampling method can be used to capture the underline constant-frequency sine wave from a varying frequency sine wave where the signal is resampled using the rotor position information, which is calculated in the previous section. More details on this method can be found in [7-8]. This method can be extended for complex vibration and current signals in variable speed operations.

B.2.3 Torque estimation

The voltage equations of a PMSM in $dq0$ transformation can be expressed as [9]:

$$\left.\begin{aligned} v_{sd} &= R_s i_{sd} + \frac{d\lambda_{sd}}{dt} + \omega_r \lambda_{sq} \\ v_{sq} &= R_s i_{sq} + \frac{d\lambda_{sq}}{dt} + \omega_r \lambda_{sd} \end{aligned}\right\} \quad \text{(B.5)}$$

where R_s is resistance of the stator windings. ω_r is the rotational speed of the motor. λ_{sd} and λ_{sq} are the flux linkages in the d and q axes, respectively.

$$\left.\begin{aligned} \lambda_{sd} &= L_s i_{sd} + \psi_{PM} \\ \lambda_{sq} &= L_s i_{sq} \end{aligned}\right\} \quad \text{(B.6)}$$

where L_s is the inductance of the stator windings. ψ_{PM} is the flux of rotor permanent magnets. The electromagnetic torque generated by a PMSM with n_p pole pairs and m_s phases can be expressed as:

$$T_e = \frac{m_s n_p}{2}\left(\lambda_{sq} i_{sd} - \lambda_{sd} i_{sq}\right) = -\frac{m_s n_p}{2}\psi_{PM} i_{sq} \quad \text{(B.7)}$$

Based on (B.7), the electromagnetic torque can be estimated and used as a feature for the classification algorithm.

B.2.4 Feature generation

Based on estimated rotor speed and measured vibration and current signals features are derived. As given in Table B.1, the devised features are used as inputs to the SVM algorithm. The motor speed is calculated by (B.4), and the motor torque is calculated by (B.7).

Table B.1: The features used in the SVM classification algorithm.

Signal Source	Feature name	Description
Current	Speed	Represent the speed
	Torque	Represent the torque
	$2f_s$	Characteristic frequency of Inter-turn winding fault from the Park's vector current i_p in (B.9)
	Torque Variance	Moving variance of 10 consecutive values of the torque signal
Vibration	3.05X order	Characteristic frequency of outer-race bearing fault
	1X	Motor rotating speed
	8X	Motor rotating speed *No of rotor pole pairs
	16X	Motor rotating speed *2nd harmonics of no of rotor pole pairs

An inter-turn stator winding fault can be analysed by calculating the extended Park's vector (EPV) of the motor current as below [10].

$$\left.\begin{aligned} i_d &= \sqrt{2/3}\, i_a - \sqrt{1/6}\, i_b - \sqrt{1/6}\, i_c \\ i_q &= \sqrt{1/2}\, i_b - \sqrt{1/2}\, i_c \end{aligned}\right\} \quad \text{(B.8)}$$

$$i_p = \left| i_d + j i_q \right| \quad \text{(B.9)}$$

where i_d and i_d are the direct and quadratic components of the Park's vector i_p. i_a, i_b and i_c are the stator currents in each phase. A stator winding fault can be detected by analysing the frequency spectrum $\mathrm{i_p}$ since the inter-turn fault results in an increase in $2f_s$ (two times of supply frequency) components of the i_p. Further, moving variance of 10 consecutive values of torque signal is also used as a feature, which represents any short-term variation of the torque profile. The vibration signals can be used to detect bearing faults. The characteristic bearing outer-race fault frequency is the ball pass frequency outer-race (BPFO), which can be calculated as [11]:

$$BPFO = \frac{N_b}{2} f_s(1 - \frac{D_b}{D_c} cos\theta) \tag{B.10}$$

where N_b is the number of rolling elements in the bearing, D_b represents the diameter of a rolling element, D_c denotes the pitch diameter, θ is the contact angle between the outer-race and rolling element, and f_s is the shaft speed. above BPFO frequency can be divided by the shaft rotational frequency, and a frequency order can be found which is a constant for any rotational speed. The related order of the bearing fault studied in this study is the 3.05 order (3.05X) of the shaft speed. In addition, the 1X, 8X and 16X frequency components are also used as the features for SVM classification algorithm.

B.2.5 SVM classification algorithm

SVM is a vector-space–based machine-learning method where the goal is to find a decision boundary between two or more classes that are maximally far from any point in the training data. The simplest SVM algorithm can be built to separate data linearly into two classes. This concept can be extended for multi-class cases and for nonlinear classification tasks [12-14]. In this study the fault, classification problem is solved as a nonlinear SVM classification problem. First, the linear case is studied.

Consider a set of training data points in Figure B.4 with inputs x_i and two output class labels $y_i \in \{\pm 1\}$; $i = 1, \ldots N$. A linear classifier can be defined as:

$$f_{w,b}(x) = sgn\,(w^T.x + b) \tag{B.11}$$

where the decision hyperplane is defined by an intercept term b and a decision hyperplane normal weight vector w, which is perpendicular to the hyperplane. A value of −1 specifies one class, and a value of +1 the other class. For a given data set and decision hyperplane, the functional margin of the i^{th} example x_i with respect to a hyperplane (w, b) can be measured by $y_i\,(w^T.x_i + b)$.

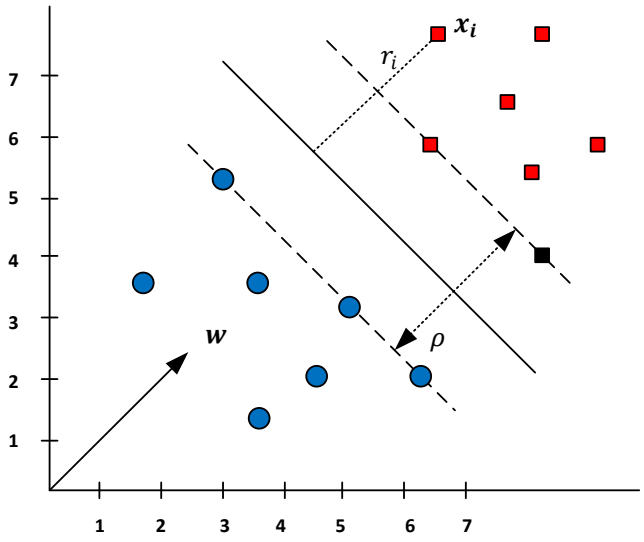

Figure B.4: Linear SVM classification.

The functional margin can be scaled to solve SVM problems, $|w|$ can be set to 1. The functional margin of all data points is at least 1 and there exist support vectors for which the inequality is equality.

$$y_i\,(w^T.x_i + b) \geq 1\,, i = 1,2,\ldots\ldots, N \tag{B.12}$$

For each sample, distance from the hyperplane is $r_i = \frac{y_i\,(w^T.x_i+b)}{|w|}$ and the geometric margin is $\rho = \frac{2}{|w|}$. The objective is to maximise the geometric margin. This means finding w and b such that $\rho = \frac{2}{|w|}$ maximising for all (x_i, y_i) and $y_i\,(w^T.x_i + b) \geq 1$. Maximising the $\rho = \frac{2}{|w|}$ is the same as minimizing $\frac{|w|}{2}$ and the final optimisation problem with a hard margin (without tolerating for wrong classification) is given in (B.13) and the solution is in (B.14).

$$Minimise \frac{1}{2} w^T w \text{ and for all } \{(x_i, y_i)\}, y_i (w^T . x_i + b) \geq 1 \quad \text{(B.13)}$$

$$f_{w,b}(x) = sgn (\sum_i \alpha_i y_i {x_i}^T x + b) \quad \text{(B.14)}$$

where most of α_i are zero and the each non-zero α_i represents that the corresponding x_i is a support vector. If a data set is not linearly separable, a soft margin can be assigned where wrong classifications are allowed when solving the optimisation problem. The new optimisation problem is:

$$Minimise \frac{1}{2} w^T w + C \sum_i \mathcal{E}_i \text{ and for all } \{(x_i, y_i)\}, y_i (w^T . x_i + b) \geq 1 - \mathcal{E}_i \quad \text{(B.15)}$$

where the parameter C is the regularisation term, $\mathcal{E}_i$ is the slack variable and non-zero $\mathcal{E}_i$ allows x_i to not meet the margin requirement at a cost proportional to value of $\mathcal{E}_i$. The linear SVM classifier solution in (B.14) depends on the dot product. By using a function $K(x_i, x_j) = {x_i}^T x_j$, the equation (B.14) can be modified as:

$$f_{w,b}(x) = sgn (\sum_i \alpha_i y_i K(x_i, x) + b) \quad \text{(B.16)}$$

The original data points can be mapped into a higher dimension space via some transformation $\Phi: x \rightarrow \phi(x)$. Then dot product become $\phi(x_i)^T \phi(x_j)$. Therefore, by using a proper transformations (kernels), the solution in (B.14) can be solved efficiently. With this kernel trick, the solution can be extended to nonlinear classification also. A kernel function *K* is such a function that related to a dot product in some extended feature space. The radial basic function (RBF) kernel [12-14] is used in this study. An RBF is equivalent to mapping the data into an infinite dimensional space, which is defined as

$$K(x, z) = e^{-(x-z)^2/(2\sigma^2)} \quad \text{(B.17)}$$

where σ is a constant and $(x - z)^2$ is the squared Euclidian distance between two feature vectors.

B.3 Experimental setup and results

B.3.1 The experimental setup

Experimental results are used to validate the proposed algorithm. Figure B.5 shows the experimental setup used to collect the data. There are two 400V, 2.5 kW, 375 rpm, 16 poles PMSMs which are directly coupled each other. One motor is used as the test motor, and another one is used as the load motor. The load motor is connected to a resistor bank. The vibration sensor is located on top of the bearing housing of test PMSM.

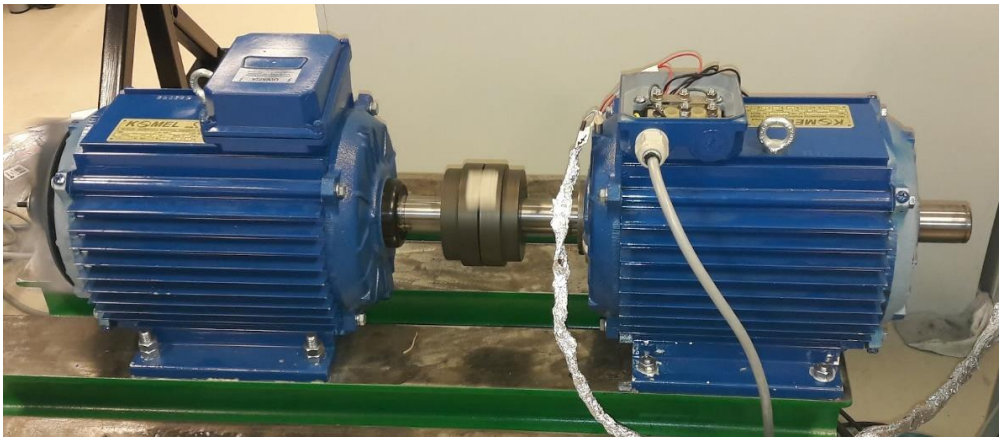

Figure B.5: The experimental setup.

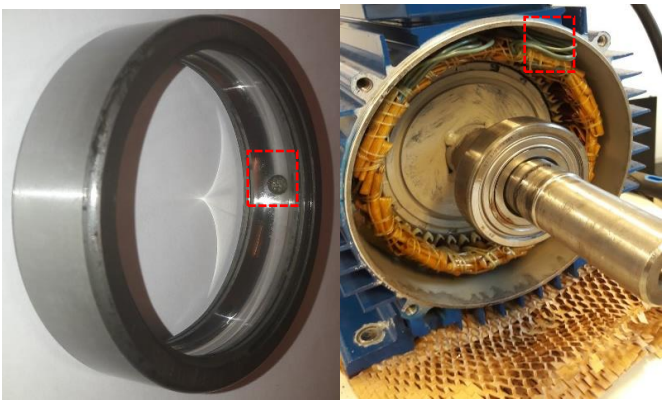

(a) (b)

Figure B.6:Faulty components (a) outer race bearing fault (b) stator winding fault.

Manually seeded faults are introduced for the bearing and the stator winding. The seeded faulty components of the PMSM are given in Figure B.6. The faults are tested at constant speeds (150, 250 and 350 rpm) and 2 types of variable speed profiles. A variable speed profile of 120 seconds used in the study is given in Figure B.7. Ten repeated testes have been conducted with this speed profile. Therefore, 50 samples of 2-minute data are recorded. Both vibration and current signals have been collected at the 20 kHz sampling rate. After making the order normalisation, the number of samples per 2-minute signal is approximately 360. This value is selected by balancing both order and time resolutions. Finally, a table of 18000 sample rows and 9 columns (8 features and the health class label) have been generated, and the proposed algorithm is used to generate features. Then 75% of available data in the table is used to train the SVM algorithm, and 25% data is used to validate the algorithm.

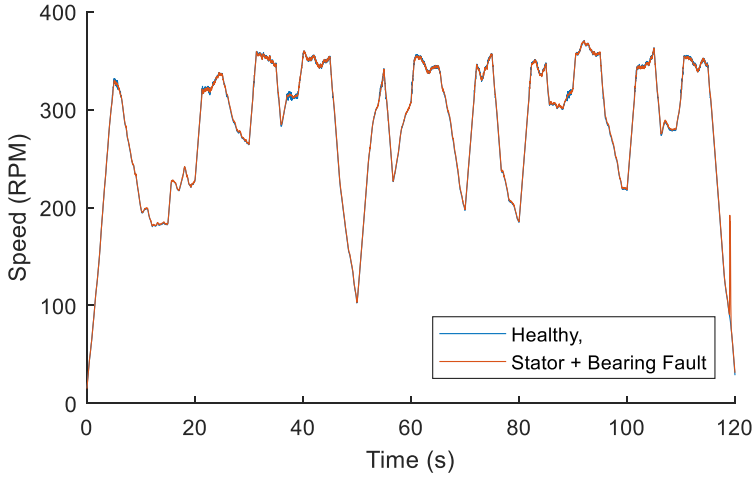

Figure B.7: The variable speed profile used in experiments.

B.3.2 Order normalized spectrum and order tracking for a bearing outer-race fault

The average i_p order spectrum is given in Figure B.8. There is no any significant difference of the i_p order spectrum in healthy and fault cases.

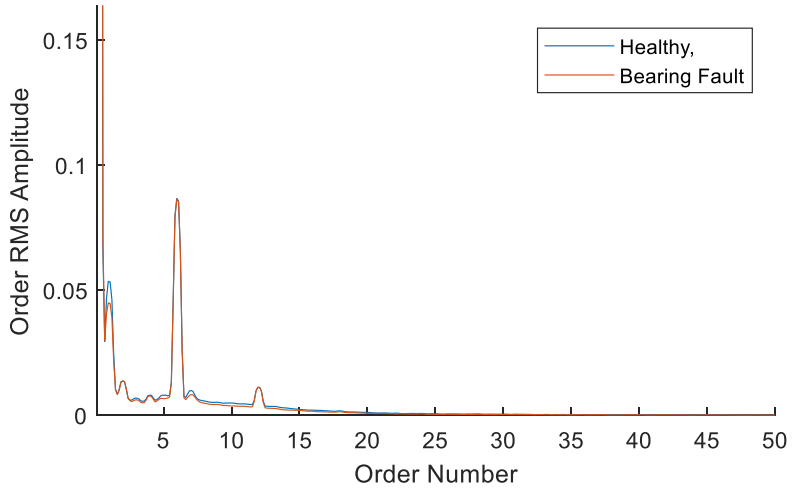

Figure B.8: Average i_p order spectrum

Figure B.9 shows the average order spectrum of the vibration signals in the healthy and faulty conditions, where 3.05X order and its 2nd harmonic (6.1X) has a significant increase when the outer-race bearing fault is present. The tracked 3.05X frequency component over time is given in Figure B.10 where the instantaneous amplitude is varying over time due to variable speed, load and noise conditions. Therefore, a simple decision based on threshold values will not work well and may produce many false or missing alarms. Therefore, a machine learning or statistical detection method is required and, in this work the SVM algorithm is trained to detect these variations.

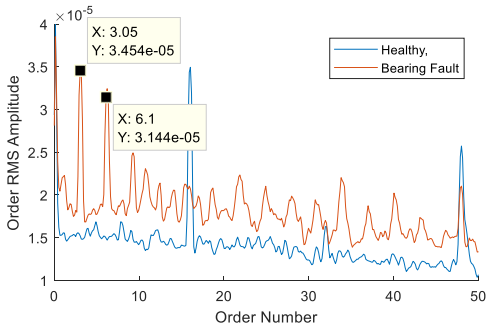

Figure B.9: Average vibration order spectrum.

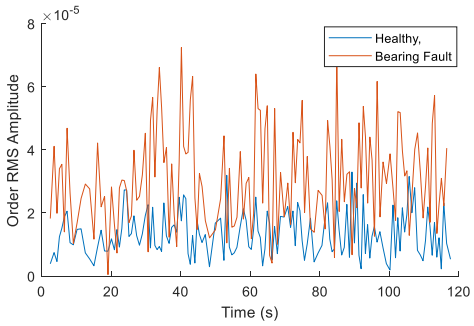

Figure B.10: Tracked 3.05X order.

B.3.3 Order normalized FFT and order tracking for stator winding fault

The average i_p order spectrum is given in Figure B.11, where there is a significant increase in the 2nd and 4th orders with a stator winding fault over healthy case. Figure B.12 shows the tracked 2nd order from the i_p spectrum over time, and which shows a clear variation for variable speed, load and noise over the healthy case. In the average vibration order spectrum given in Figure B.13, the 16th order shows a significant increase for stator winding fault. When this 16th order is tracked over time a significant increase of instantaneous amplitudes can be seen from Figure B.14. The 8th order has a similar behaviour. Therefore, both current and vibration information are useful for detecting stator winding faults.

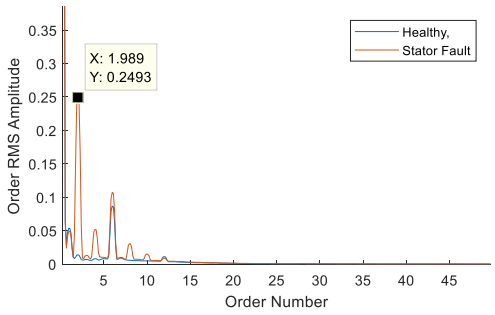

Figure B.11: Average i_p order spectrum.

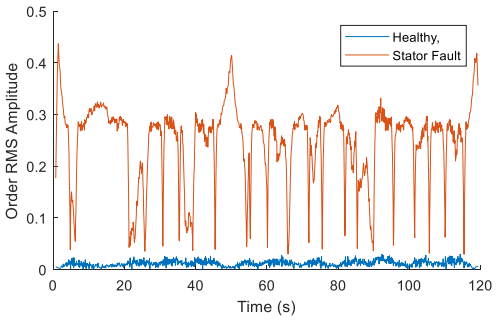

Figure B.12: Tracked 2nd order

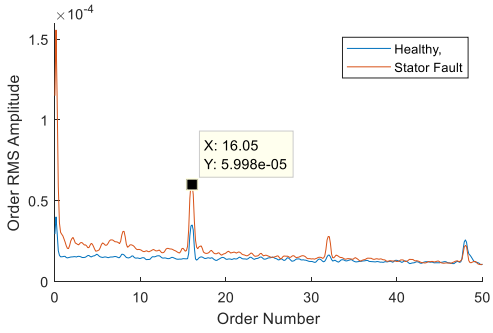

Figure B.13: Average vibration order spectrum.

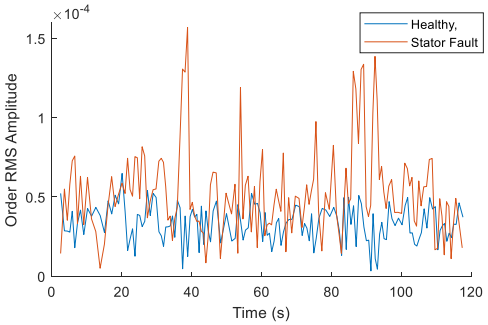

Figure B.14: Tracked 16.05 order.

B.3.4 Order normalized FFT and order tracking for stator winding and bearing outer-race fault

The analysis conducted in previous sections is focused on individual fault cases. In this section, the order spectrums are applied to multiple fault cases where both stator winding and bearing faults occur.

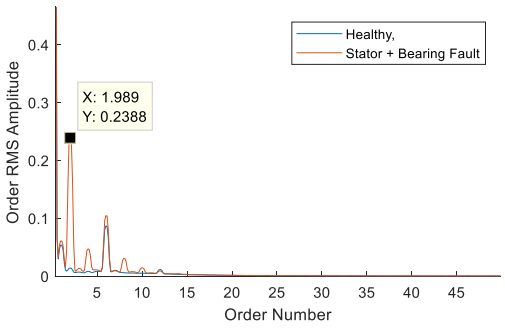

Figure B.15: Average i_p order spectrum.

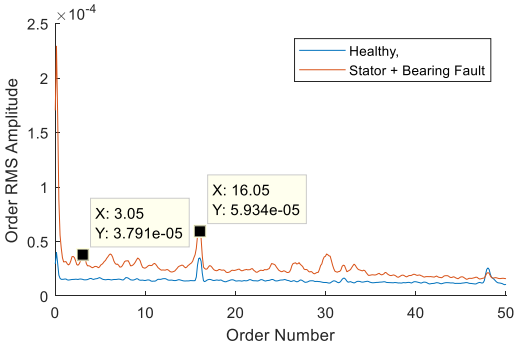

Figure B.16: Average vibration order spectrum.

The average i_p order spectrum is shown in Figure B.15 where only the 2nd and 4th orders of the supply frequency have significantly increased amplitudes when both faults exist. This is mostly like the individual stator winding fault since only the stator winding fault related information can be found. However, the average vibration spectrum in Figure B.16 shows both the bearing fault related characteristic order of 3.05X and the stator winding fault related order at 16X. These results show that it is possible to detect multiple faults and individual faults from the same order tracking method discussed in the previous Sections for individual faults.

B.3.5 Performance SVM classification algorithm

The confusion matrix for validating dataset is given in Figure B.17. Four fault classes are predicted by SVM namely HB (Stator winding healthy and bearing fault), HH (both stator winding and bearing are healthy), SB (both stator winding and bearing are defective) and SH (stator winding is faulty and bearing is healthy).

The overall accuracy of the SVM classifier is about 92.9%. For all the fault classes more than 90% classification accuracy is obtained and the highest classification accuracy is 94%. These results are highly acceptable, and the SVM can detect and classify considered two faults in variable speed and load conditions.

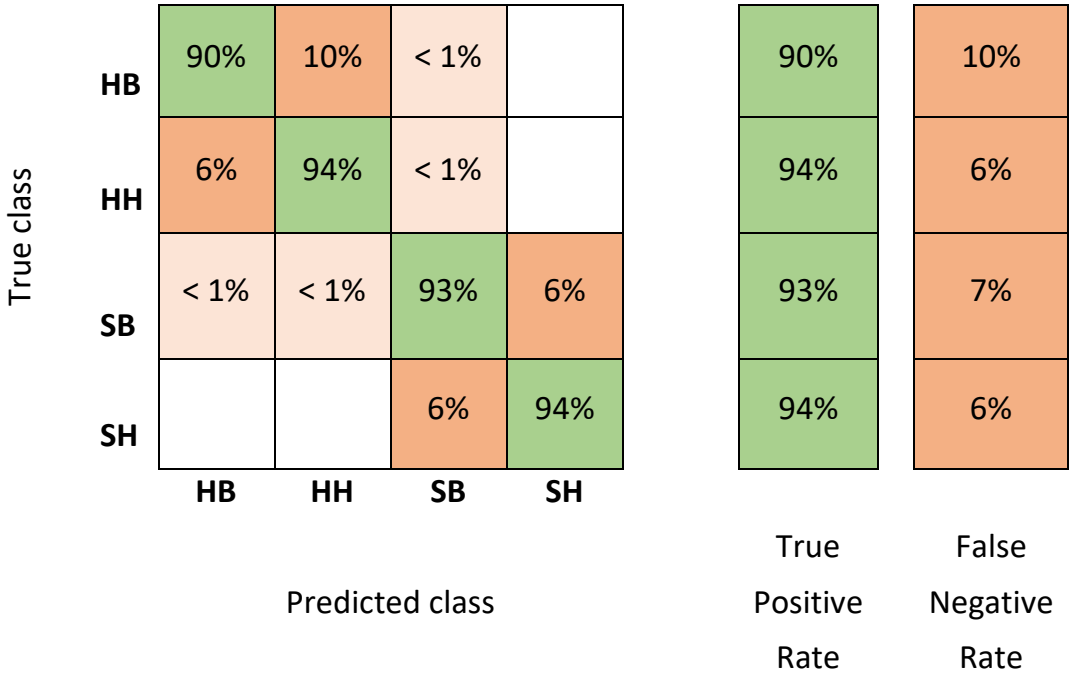

Figure B.17: The confusion matrix for the test dataset.

B.4 Conclusion

In this paper, a fault classifier is introduced for fault diagnosis of PMSMs in variable speed and load conditions. Features for the fault classification are produced based on the resampled vibration, current signals and estimated torque and speed. The fault detection and classification are implemented by a supervised machine learning algorithm, namely Support Vector Machine. The proposed method is validated by variable speed experimental data, and excellent performances have been obtained. Following contributions are provided in this study;

(1) The proposed method is based on estimated rotor speeds and separate speed sensor is not required. In PMSMs, the rotor speed can be accurately estimated using the measured current signals.

(2) In a real wind turbine, the generator is also vibrating on a flexible frame. This vibration can be very different depending on the operating conditions. However, in proposed method, only the fault related characteristic frequency bands of vibration signal are considered for fault diagnosis purpose and other parts of the signals are neglected. Also, current signal may not affect much by additional vibration and the feature level fusion method can give a robust result.

Therefore, the proposed method can be implemented in wind turbines and other similar industrial applications. In this study, only two types of individual faults and one multiple fault cases are considered. However, the proposed method can be extended to other types of faults in both motoring and generating operations.

References

[1] Norton M and Karczub D 2003 *Fundamentals of Noise and Vibration Analysis for Engineers* (Cambridge: Cambridge University Press)

[2] Nandi S, Toliyat H. A, and Li X 2005 Condition monitoring and fault diagnosis of electrical motors-a review *IEEE Trans. on Energy Conversion* **20** 719-29

[3] Senanayaka J S L et al 2017 Towards online bearing fault detection using envelope analysis of vibration signal and decision tree classification algorithm *2017 20th International Conference on Electrical Machines and Systems* (Sydney: NSW) pp. 1-6

[4] Senanayaka J S L et al 2015 Sliding-mode observer based sensorless control of a small wind energy conversion system *Recent Advances in Sliding Mode (RASM) 2015 Int. Workshop* (Istanbul: Turkey) pp 1-6

[5] Baccigalupi A and Annalisa A 2016 The Huang Hilbert Transform for evaluating the instantaneous frequency evolution of transient signals in non-linear systems *Measurement* **86** 1-13

[6] Justice J 1979 Analytic signal processing in music computation *IEEE Trans. on Acoustics Speech and Signal Processing* **27** 670-84

[7] Brandt A 2011 *Noise and Vibration Analysis: Signal Analysis and Experimental Procedures* (Chichester UK: John Wiley and Sons)

[8] Blough J 1998 *Improving the analysis of operating data on rotating*

automotive components PhD Thesis (USA: College of Engineering University of Cincinnati)

[9] Kinnunen J et al. 2006 Analysis of directly network connected non-salient pole permanent magnet synchronous machines *in Proc. Int. Symp. Ind. Elect.* (Montreal: Canada) pp 2217–2222

[10] Cardoso A M, Cruz S and Fonseca D 1999 Inter-turn stator winding fault diagnosis in three-phase induction motors by Park's vector approach *IEEE Trans. Energy Conversion* **14** 595-98

[11] Senanayaka J S L et al 2017 Early detection and classification of bearing faults using support vector machine algorithm *IEEE Workshop on Electrical Machines Design, Control and Diagnosis* (Nottingham,UK) pp 250-255

[12] Manning C D et al 2008 *Introduction to Information Retrieval* (Cambridge university press)

[13] Vapnik, V 1998 *The nature of Statistical Learning Theory* (New York: Wiley)

[14] Scholkopf B et al 1997 Comparing support vector machines with Gaussian kernels to radial basis function classifiers *IEEE Trans. on Signal Processing* **45** 2758-65

Paper C

Multiple Classifiers and Data Fusion for Robust Diagnosis of Gearbox Mixed Faults

Jagath Sri Lal Senanayaka, Huynh Van Khang, and Kjell G. Robbersmyr

This paper has been published as:

J. S. L. Senanayaka, H. Van Khang and K. G. Robbersmyr, "Multiple Classifiers and Data Fusion for Robust Diagnosis of Gearbox Mixed Faults," in *IEEE Transactions on Industrial Informatics*, vol. 15, no. 8, pp. 4569-4579, Aug. 2019. doi: 10.1109/TII.2018.2883357

Multiple Classifiers and Data Fusion for Robust Diagnosis of Gearbox Mixed Faults

Jagath Sri Lal Senanayaka, *Student Member, IEEE,* Huynh Van Khang, *Member, IEEE* and Kjell G. Robbersmyr, Senior *Member, IEEE*

Department of Engineering Sciences, University of Agder, 4879 Grimstad, Norway

E-mails: {jagaths; huynh.khang; kjell.g.robbersmyr }@uia.no

***Abstract*—Detection and isolation of single and mixed-faults in a gearbox are very important to enhance the system reliability, lifetime, and service availability. This paper proposes a hybrid learning algorithm, consisting of Multilayer Perceptron (MLP)- and Convolutional Neural Network (CNN)-based classifiers, for diagnosis of gearbox mixed faults. Domain knowledge features are required to train the MLP classifier, while the CNN classifier can learn features itself, allowing to reduce the required knowledge features for the counterpart. Vibration data from an experimental setup with gearbox mixed faults is used to validate the effectiveness of the algorithms and compare them with conventional methods. The comparative study shows that accuracies and robustness of the individual MLP- and CNN-algorithms are better than those of the compared methods and can be significantly improved using data fusion at the feature level. Furthermore, the robustness of the algorithm is secured under noises by combining the results of individual classifiers.**

***Index Terms*—** Convolutional neural network, data fusion, fault diagnosis, gearbox, mixed faults, multilayer perceptron.

C.1 Introduction

Fault detection for gearboxes has gained an increased attention in both research and industry since the gearboxes are among the most essential components in mechanical power transmission and industrial machineries [1-3]. A gearbox is a complex mechanical system, consisting of spur-, helical-, bevel- or worm gears, shafts, and bearings. A defect on a gear can produce a fluctuation in the gearbox bearing, resulting in a false alarm [4]. Once mixed faults occur in a gearbox, the fault diagnosis is very challenging, and the faulty parts can only be found offline by dissembling the gearbox.

A localized defect on a gearbox can be detected by current signature, lubrication oil or vibration analysis. The current signature can be used to detect certain faults in a gearbox when being connected to an electric drive [5-6]. The on-line or on-site lubrication oil analysis is relatively new and requires expensive equipment for monitoring, and testing, thus only economically viable in very critical machines. The off-line oil analysis is time-consuming as oil samples are collected and sent to separate laboratories for testing and reporting. This method can cause productivity loss due to longer monitoring cycles and slow analysis process [7]. The vibration analysis is more preferred than the lubricant oil analysis since it can be done without interrupting the system and collecting the analysis data is easier than the counterpart. The main challenge of the vibration analysis is that processing the collected data and understanding faulty features need a skilled manpower with an advanced knowledge of the gearbox fault. International Standard Organization (ISO) with ISO 18436-2:2014 specifies the necessities for the training, relevant experience, and examination of personnel performing condition monitoring and diagnostics of machines using vibration analysis [8].

An automatic fault detection and classification system based on vibration signals can reduce the manpower dependence and time consumption for condition monitoring of the gearboxes in industry. Increasing performance of the detection system might be more important than looking for a highly reliable feature since the machine cannot be completely healthy due to the absence of clear characteristic frequencies as argued in [9]. Table C.1 summarizes common faults on a gearbox and features captured by vibration analysis [10-11]. Gear defects result in an increased vibration energy at gear natural- and mesh frequencies, sidebands, and their higher harmonics. A localized fault on a bearing can be detected using

envelop detection [12], empirical mode decomposition and wavelet transformation [13] based on characteristic frequencies associated with the faults. Defining amplitude limits to distinguish healthy and faulty cases in the spectrum analysis is very difficult if the energy of the signals associated with a fault is very low or masked by random noises. Furthermore, the vital information on mixed faults are normally similar or overlapping in the spectra [9].

Table C.1: Common faults of a gearbox and features of vibration signals.

Component	Fault modes	Features
Gear	Crack in gear	Gear natural frequency, the sidebands around
	Cracked/broken tooth	Sidebands around gear mesh frequency
	Excessive wear / clearance	Sideband spacing
Bearing	Bearing inner race	Characteristics frequency
	Bearing outer race	Characteristics frequency
	Bearing rolling element	Characteristics frequency
	Excessive bearing clearance	Sub-synchronous whirl
Shaft	Rotor imbalance	1X shaft speed
	Shaft misalignment	2X shaft speed, high axial vibration
	Mechanical looseness	Higher harmonics of shaft speed

To reduce a false alarm in the spectrum analysis, an automatic fault diagnosis can be used. The automatic fault diagnosis can be developed via model-based, data-driven or hybrid algorithms [14-17]. The model-based diagnosis requires not only a detailed physical model of the system but also its accurate parameters, which are difficult to be obtained in case of gearboxes. Data-driven approach using statistical or machine learning algorithms does not need such a physical model [13], making it attractive for an automatic diagnosis system of a gearbox. A statistics method is usually based on the frequency spectrum to enhance the accuracy of fault detection techniques and reduce false and missing alarms [18]. However, mixed faults in a gearbox make the vibration spectrum very

complicated, causing the statistics-based fault classification costly, time-consuming and expertise-demanding. Alternatively, supervised machine learning methods, namely support vector machine (SVM) [19-20], decision tree (DT) [12], various neural network architectures [21-22] combined with advanced signal processing can be used to find the complex relations on the feature space by using predefined time-frequency features extracted by the domain knowledge [23]. Performance of the supervised machine learning highly depends on the feature selection. Irrelevant and redundant features will result in high-dimensional feature space, highly complex machine learning model, requiring more data for the training. Additional statistical and optimizations, e.g. principal component analysis, particle swarm optimization and independent component analysis, are thus required to find the best features for the classification algorithms [24-25].

To address challenges on feature selections and extra optimizations, a deep learning algorithm can be used to extract and transform features via nonlinear processing layers and learn itself the best features by detecting patterns from the training data of a signal or an image to differentiate faults. It therefore provides one advanced step towards online automatic fault detection systems. Deep learning methods are widely used in fault diagnosis due to their merit of analyzing complex or big data while the improved technologies of sensors, cost-effective powerful processors, graphics processing units (GPUs) and their parallel processing capabilities allow collecting and processing big data effectively [5], [26-31]. The algorithms are completely based on the information gathered from training data to identify patterns and relations within the data. In other words, the deep learning algorithms are advanced pattern recognizers without using domain knowledge. Consequently, the validity and accuracy of training dataset are the most important tasks in deep learning algorithms. To sum up, the most common analyses based on vibration signals for fault detection and classification are summarized in Table C.2. Root mean square (RMS) of the vibration signal can be used to detect single faults of a gearbox. Time domain analysis and time synchronous average (TSA) are simple tools for detecting gearbox faults, but the analysis requires a highly skilled manpower. Spectrum analyses are not applicable to an automatic diagnostic system for gearboxes due to the difficulty of fault classification and manpower demands. Machine- and deep learning algorithms are capable of highly-accurate fault classifications, providing a better solution to detect single or mixed faults in a gearbox effectively.

Table C.2: Different methods for fault diagnosis of Gearboxes.

Method	Advantages	Disadvantages
RMS, TSA and time domain analysis	Low computational cost, simple	Fault classification is difficult. Skilled manpower is required
Spectrum analysis and statistics.	Moderate cost, fault classification with skilled workers	Low-accurate fault classification required knowledge on advanced analysis
Machine learning + signal processing	Moderate cost, highly-accurate classification, improvable with data fusion	Accuracy of the fault classification depending on applications, difficult feature generation.
Deep learning + signal processing	Highly-accurate classification, improvable with data fusion, automatic feature detection, applicable to complex data.	Computational burden, classification based on pattern recognition, without using domain knowledge

This work first proposes a novel fault detection and classification scheme, taking both advantages of domain knowledge analysis in the machine learning and pattern recognition in the deep learning. The domain knowledge of gearbox is captured by measuring energies from several frequency bands in the vibration spectrum and applied to the MLP algorithm for classifying mixed faults in a gearbox. The CNN algorithm is trained to identify patterns in the spectrograms of vibration signals via Short-time Fourier transform (STFT) and Continuous Wavelet transform (CWT). Secondly, a data fusion algorithm is introduced to improve the robustness and accuracy of the learning algorithms so that the proposed diagnosis scheme can work effectively regardless of noises in the measured data. The data fusion is used at feature and decision levels in the fault diagnosis systems. The feature space dimension is enlarged at the feature level to identify complex relations in the feature space. Finally, Naïve Bayes combiner is selected to fuse results of the individual classifiers at decision level to enhance the reliability of the fault classification. Beside the Naïve Bayes combiner, weighted

majority and multinomial distribution are among the widely used ensemble learning methods [32]. This study focuses on developing a hybrid fault diagnosis system consisting of supervised - MLP and - CNN, and data fusion for a complex gearbox and enhancing its robustness, so selecting a best combiner or algorithm is out of scope of the work.

C.2 The proposed hybrid fault diagnosis scheme

A simplified diagram of the proposed hybrid fault classification is shown in Figure C.1. First, the individual classifiers based on MLP and CNN with feature-level fusion will be trained using the training dataset of vibration signals from 2 accelerometers and shaft speeds.

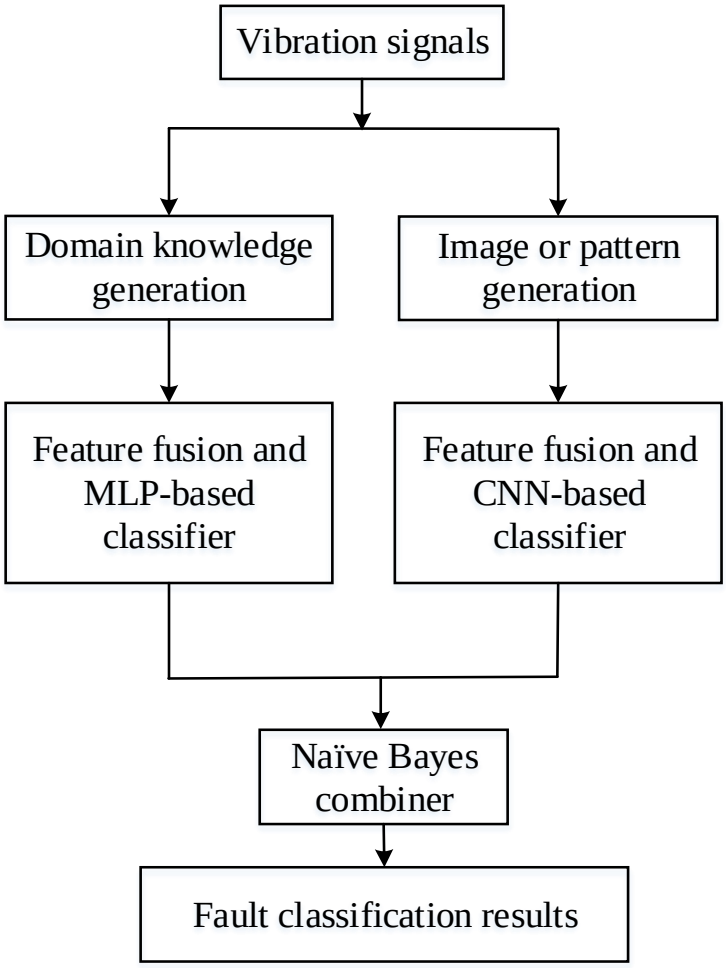

Figure C.1: Flowchart of the proposed hybrid fault diagnosis for gearbox.

Then the trained algorithms will be used to predict probabilities of the mixed health classes or individual decisions, and the individual decisions of the MLP and CNN - classifiers will be used to train the decision-level fusion algorithm or Naïve Bayes combiner for enhancing robustness of the proposed scheme. Finally, the trained combiner model will be used to predict multiple faults in the gearbox. The MLP classifier uses domain knowledge or physical-based knowledge to classify the faults while the CNN-based classifier is based on the image or pattern features. The MLP based classifier needs inputs of time and frequency domain features, characteristic frequencies calculated by bearing and gear parameters, filter designing and energy calculations at interested frequencies. The CNN based classifier needs a proper generation of spectrograms or images. This section describes the features used in each classifier and basic principles of the fault classification.

C.2.1 Domain knowledge and MLP-based classifier.

The MLP-based classifier requires the predefined features. As shown in Table C.1, the faults in a gearbox can be detected via features. In this work, both time- and frequency-domain features are selected for the domain-knowledge analysis [35]. The time-domain features are defined by RMS and crest factor of the vibration signal. Unlike the statistics approach using vibration spectra, the frequency-domain features for the MLP-based classifier are the energies at interested frequencies, which are extracted via bandpass filters as shown in Figure C.2. Bandpass filters are designed based on the fault-related characteristics frequencies [12].

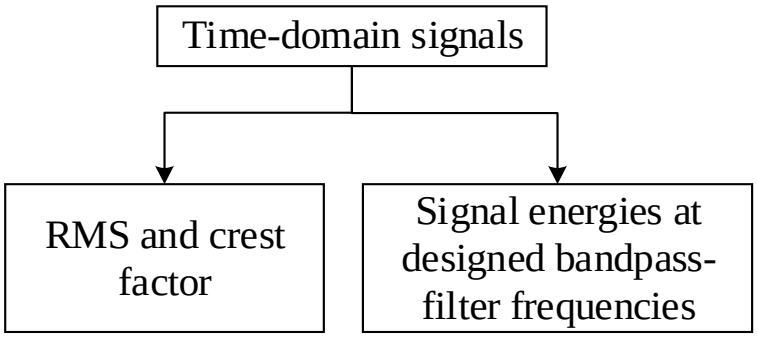

Figure C.2: Domain knowledge extraction for the MLP-based classifier.

Figure C.3 shows an exemplary vibration signal collected from a gearbox with mixed faults in the time- and frequency- domain. Various forcing frequencies are excited in different bands of the spectrum as indicated in Figure 3.C (b). As mentioned earlier, the vibration spectrum of multiple faults in a gearbox is very complicated, thus a statistics-based fault classification based on such a vibration spectrum alone is not feasible. The MLP-based classifier needs only the signal energies captured by the filters at different bands, in which the centre frequency of each filter is selected based on characteristic frequencies and the gearbox's specification.

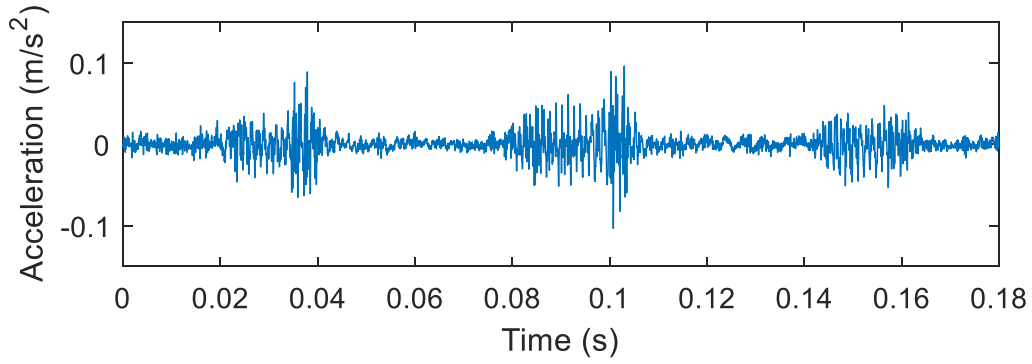

(a)

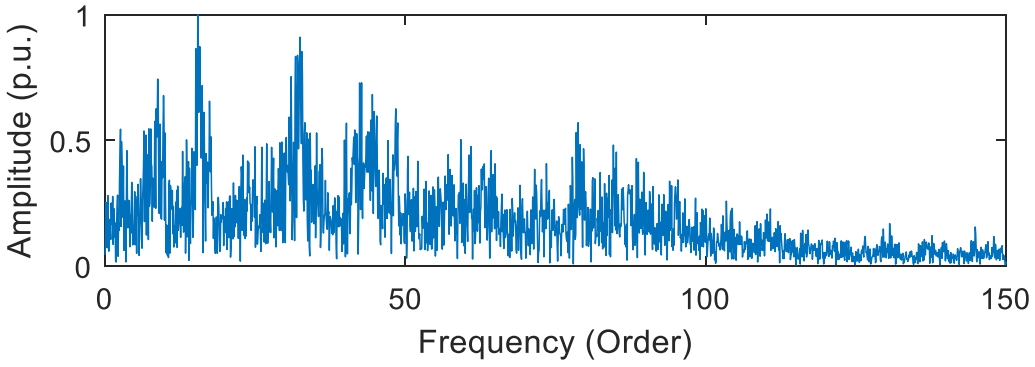

(b)

Figure C.3: Exemplary vibration signal of a gearbox with multiple faults in time- and frequency-domain: (a) time-domain (b) frequency-domain.

The MLP-based classifier can be trained from the features as shown in Figure C.2 and health classes, e.g. good or defective, of the subcomponents on a gearbox, namely bearings, gears, and shafts. Figure C.4 shows the MLP architecture for multiple-fault detection. Without a data fusion, the feature

dimension N is enlarged to $k \times N^2$ via k hidden layers. A small number of features renders a problem of identifying complex relations within the data and results in a low-accurate fault identification. Therefore, a data fusion among vibration sensors is implemented in this work to increase the feature number. If the number of vibration sensors is L and the number of input features is N, the number of features after k hidden layers is enlarged to $k \times (LN)^2$, enhancing effectiveness of learning a non-linear relationship within the data [36]. The output of the MLP-based classifier is the probability of each health class.

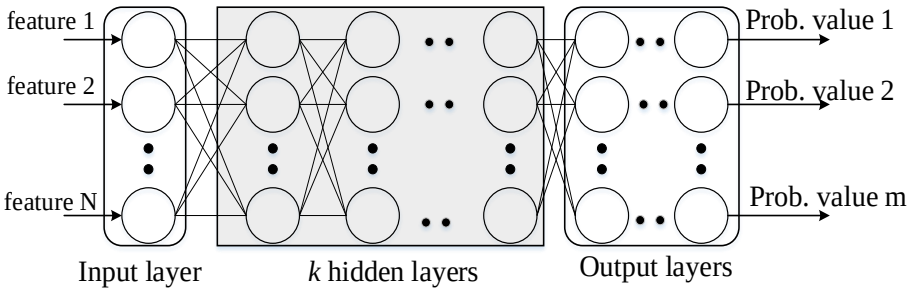

Figure C.4: The MLP architecture for gear-box fault detection.

C.2.2 Pattern Recognition and CNN-based classifier.

The domain knowledge or spectrum-based analysis is useful for explaining physical meanings of a gearbox defect. However, the MLP- based classifier may miss important features or capture false information since the mixed faults in a gearbox produce a complex vibration spectrum. In addition, the passband filters were designed based on single forcing frequencies, which are highly dependent on shaft speeds and contact angles between one faulty part to another.

To enhance the accuracy of mixed fault detection, the CNN is applied to reduce the dependence on domain knowledge or forcing frequencies. CNNs were highly successful in pattern recognition, and widely used in image classification. The CNN architecture for the gear-box fault classification in this study is shown in Figure C.5. If supplying the time-domain vibration signal directly to the classifier, the CNN pattern recognition is constrained by the 1-dimensional convolution [37]. For detecting signals associated with faults in both time and frequency domains, input data of the classifier are selected as 2-D images or spectrograms with 2-D convolution. The input spectrograms are used to train the

classifier via 3 layers: convolution, rectified linear unit, and pooling. After the training, probabilities of each fault class are calculated via flatten-, fully connected-, and SoftMax layers. Table C.3 describes layers and functionalities of each layer in the CNN-based classifier.

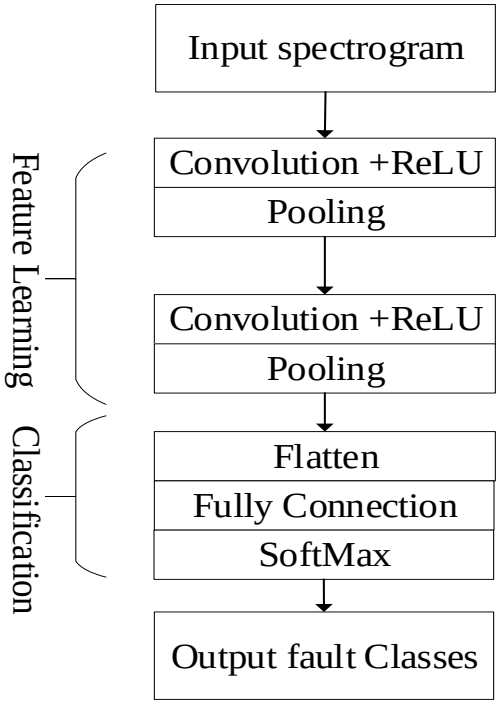

Figure C.5: The CNN architecture for gear-box fault detection.

Table C.3: Description of layers in the CNN.

Section	Layer	Functionalities
Feature learning	Convolution	Convolution operation with several kernels Reduce the dimensionality Learn local features
	REL (rectified linear unit)	Activate or deactivate some neurons based on their impact Introduce the non-linearity to the system
	Pooling	Reduce the dimensionality
Classification	Flatten	Convert 2D image to 1D array for classification
	Fully connected	Implement the classification task based on derived features in convolution and pooling operation
	SoftMax	Convert the classification probabilities to classes

STFT and CWT can be used to extract time-frequency features and show them as spectrogram images [38-40]. To study which transform or image generation can provide better features for the CNN-based classifier, both STFT and CWT are applied to analyze the vibration signals collected from a gearbox. Applications of the STFT and CWT to detect faults on a gearbox-based drivetrain via vibration signals are detailed in [41]. Figure C.6 shows an exemplary spectrogram generated by STFT of an accelerometer signal in the presence of multiple faults in the gearbox. The spectrogram generated by CWT on the same accelerometer is shown in Figure C.7.

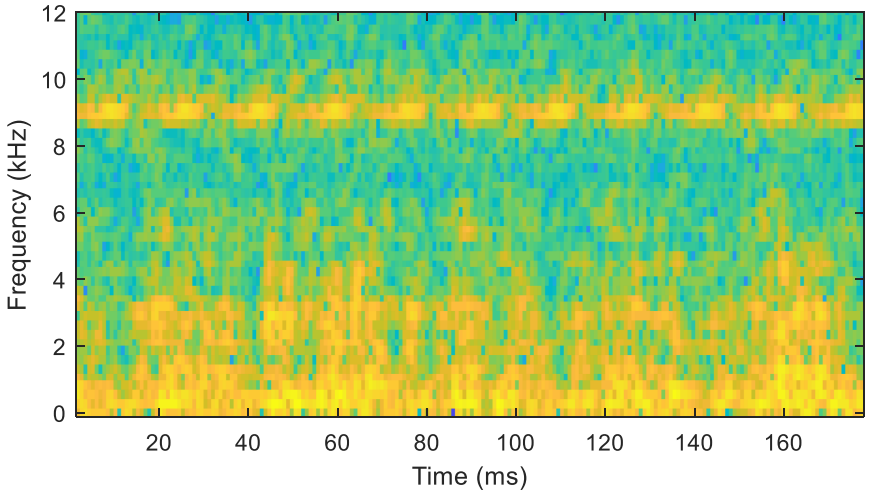

Figure C.6: The 2-D representation of 1-D non-stationary signals using STFT.

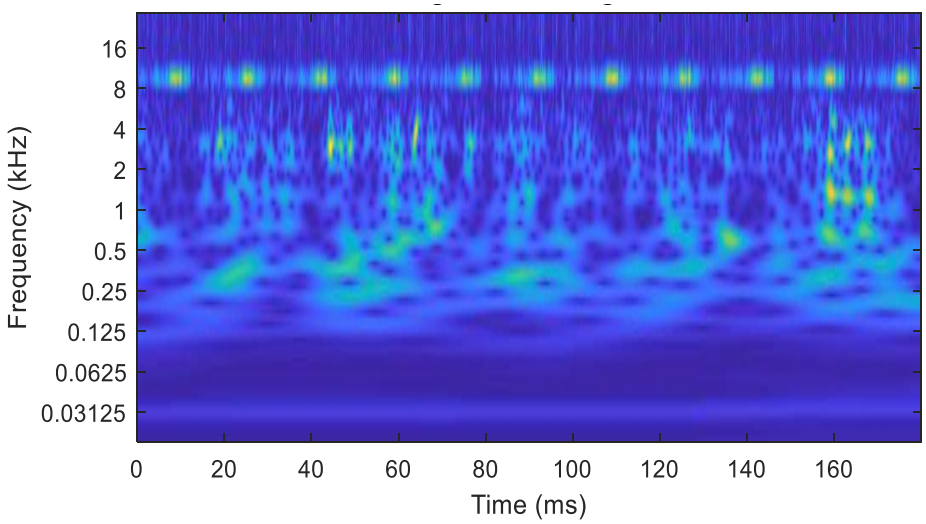

Figure C.7: The 2-D representation of the signal using wavelet transform.

Image classification using the CNN results in a highly computational burden as each pixel represents an input in the neural network. The 2-dimensional (2-D) convolution can be applied to an image with different sets of shared weights (or kernels) using a neuron map, in which the weights are optimized through a backward propagation algorithm. The convolution provides two advantages for a mixed-fault classification. First, local features of the input images can be well identified for the classification. Second, the convolution combined with pooling can reduce the dimensionality of mixed-fault classification problem, thus simplifying the structure of fully-connected neural networks for the classification. Details of CNN training and analysis can be found in [42], and are summarized here. The CNN is trained by using a backpropagation algorithm by minimizing the cost function with respect to an unknown weight.

$$\mathcal{L} = -\frac{1}{|X|}\sum_{i}^{|X|} \ln\left(p(y^i|X^i)\right) \tag{C.1}$$

where $|X|$ is the number of training images, X^i is the ith training image with the corresponding label y^i and $p(y^i|X^i)$ denotes the probability by which X^i is correctly classified.

If W_l^t denotes the weight of the lth convolutional layer at iteration t, and $\hat{\mathcal{L}}$ denotes the cost over a mini-batch size T, then the updated weight in the next iteration is computed as follows:

$$\begin{aligned} \gamma^t &= \gamma^{(tT/|X|)} \\ V_l^{t+1} &= \mu V_l^t - \gamma^t \alpha_l \frac{\partial \hat{\mathcal{L}}}{\partial W_l} \\ W_l^{t+1} &= W_l^t + V_l^{t+1} \end{aligned} \tag{C.2}$$

where α_l is the learning rate of the l^{th} layer, μ is the momentum to express the contribution of previous update, and γ is the scheduling rate, which reduces the learning rate at the end of each epoch.

C.2.3 Decision – level data fusion

The outputs of the MLP- and CNN- based classifiers are large datasets of probability values in the heath classes. A probability classifier is required to combine the results from the neural networks. In this work, a Naïve Bayes model is used to combine the classification results of each individual classifiers since it is simple to build and effective to big and complicated datasets. The Naïve Bayes combiner needs to be trained before applying it to classification [32]. The training steps are implemented as:

Step 1: Get an array $E_{(M,q)}$, which contains specific outputs of the *Q* classifiers for *M* entities in the training set. The true health class labels are extracted from the training set and included in $Z_{(M,1)}$ array.

Step 2: Obtain the numbers - $M_1, M_2, \ldots M_c$, which represent the number of entities in each health class within $Z_{(M,1)}$. Here the *c* represents the number of health classes.

Step 3: For each classifier D_i, i = 1, 2,.., *Q*, calculate a bespoke $c \times c$ confusion matrix C_i.

$$C_i(h_1, h_2) = \frac{K(h_1,h_2)+\frac{1}{c}}{M_{h1}+1} \tag{C.3}$$

where $K(h_1, h_2)$ is the number of entities in training set with true class label h_1, labelled by classifier D_i in class h_2. After the training process, the trained bespoke $c \times c$ confusion matrix C_i, can be used to fuse new results of individual classifiers. The calculation steps are as follows:

Step 1: For each new entity, find the class labels $s_1, s_2, \ldots s_L$ assigned by the *L* base classifiers.

Step 2: For each class ω_k, $k = 1, \ldots\ldots c$ find the probability $P(k)$ of each health class.

Set $P(k) = \frac{M_k}{M}$ (C.4)

Calculate $P(k) = P(k)C_i(k, s_i)$ for $i = 1, \ldots, L$ (C.5)

Step 3: Assign label k^* to the entity, where

$k^* = \arg max_{k=1}^{c} P(k)$ (C.6)

Step 4: Return the final label of the new entity.

C.3 Experimental data and pre-processing

C.3.1 The experimental setup and data

To validate the proposed algorithm, experimental data provided by PHM society data challenge in [43] is used. Figure C.8 shows the inside of the two-stage parallel shaft gearbox (with helical gears) used for collecting the vibration data

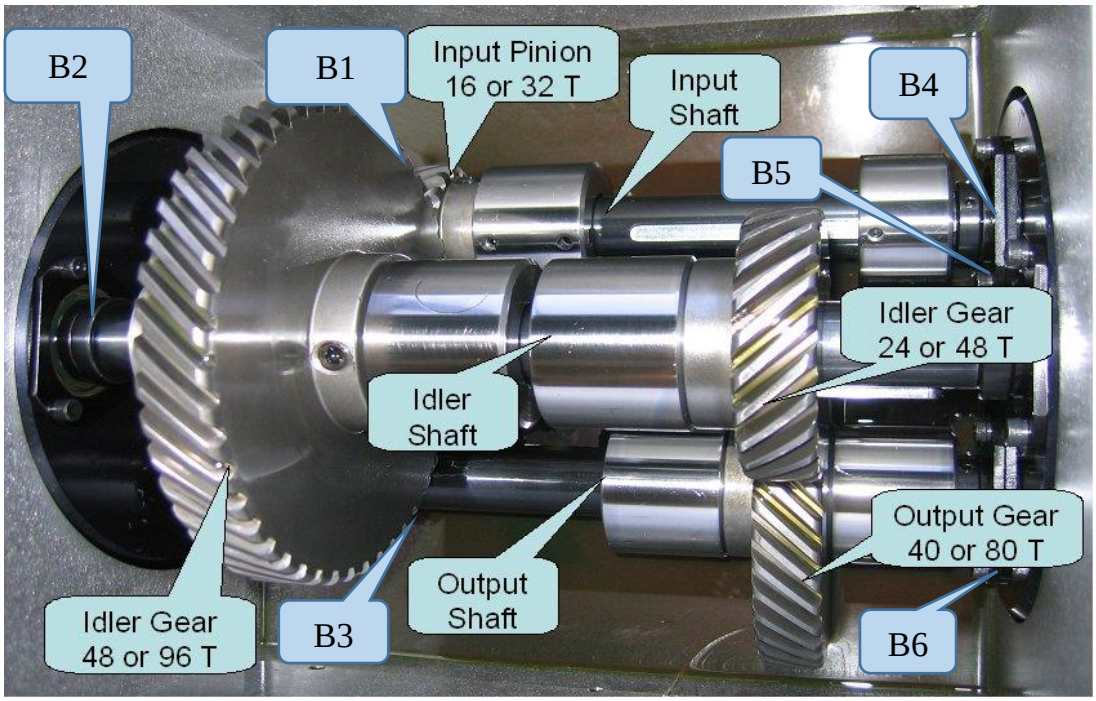

Figure C.8: The structure of the gearbox.

It consists of four gears, three shafts and six bearings. The gears are removable, and two types of gears, spur and helical, are used in this study. Eight fault cases of the spur gearbox and six fault cases for the helical gearbox have been tested. Each fault case includes multiple faults from gears, bearings or shafts. Two accelerometers and one tachometer are used to collect the vibration data and input-shaft speed. The accelerometers are placed on the input and output shafts of the gearbox. The data of each channel is sampled at 200 kHz. Each fault class was tested at five different speeds (30 Hz, 35 Hz, 40 Hz, 45 Hz, and 50 Hz) and two different load conditions (high and low), and repeated, thus 20 data files were collected. The bearing dimensions shown in Table C.4 are used to calculate the characteristic frequencies associated with bearing faults in Table C.5 [19].

Table C.4: Bearing dimensions.

Number of Elements	8
Roller Element Diameter	7.94 mm (or 0.3125 inch)
Pitch Diameter	33.5 mm (or 1.319 inch)
Contact Angle	0

Table C.5: Forcing frequencies of bearing faults.

Frequency component	Order
Fundamental train frequency (FTF)	0.38X
Shaft rotational frequency (1X)	1X
Ball/roller spinning frequency (BSF)	1.99X
Outer-race fault (BPFO)	3.05X
Rolling element fault (2*BSF)	3.98X
Inner-race fault (BPFI)	4.94X

In this work, 18 frequency-domain features described in [35] and 2 time-domain features are selected for the domain knowledge analysis based on MLP. Since the MLP-based classifier requires the energies at interested frequencies, the filter banks are applied at different bands of the spectrum to capture the energies of those bands. The central frequency of each filter is defined based on forcing frequencies and the specification of the gearbox as shown in Table C.6.

Table C.6: Description of the Filter bank.

Filter 01	Characteristic frequency of the input shaft unbalance
Filter 02	Characteristic frequency of the bent input shaft
Filter 03	Characteristic frequency of the outer-race defect of input-shaft bearing
Filter 04	Characteristic frequency of the ball defect of input-shaft bearing
Filter 05	Characteristic frequency of inner race defect of input-shaft bearing
Filter 06	Natural frequency of rotating element
Filter 07	Output-shaft helical 1X Gear Mesh Frequency (GMF)
Filter 08	Input-shaft helical 1X GMF, Output-shaft helical 2X GMF or output-shaft spur 1X GMF
Filter 09	Output-shaft helical 3X GMF
Filter 10	Input-shaft helical 2X GMF, output-shaft helical 4X GMF, Input-shaft spur 1X GMF or output-shaft spur 2X GMF
Filter 11	Output-shaft helical 5X GMF
Filter 12	Input-shaft helical 3X GMF, Output-shaft helical 6X GMF or Output-shaft spur 3X GMF
Filter 13	Output-shaft helical 7X GMF
Filter 14	Input-shaft helical 4X GMF, output-shaft helical 8X GMF, Input-shaft spur 2X GMF or output-shaft spur 4X GMF
Filter 15	Input-shaft helical 5X GMF or output-shaft spur 5X GMF
Filter 16	Input-shaft helical 6X GMF, Input-shaft spur 3X GMF or Output-shaft spur 6X GMF
Filter 17	Input-shaft helical 7X GMF or output-shaft spur 7X GMF
Filter 18	Input-shaft helical 8X GMF, input-shaft spur 4X GMF or output-shaft spur 8X GMF

Table C.7 shows fault classes of the spur and helical gearboxes under mixed defects in gears, bearings, and shafts. The fault classes Spur 3, Helical 2 and Helical 6 are single fault cases, which are useful to test whether the proposed algorithm is capable to detect single faults or not. In the study of gear faults, four health conditions, namely good, broken tooth, chipped tooth and eccentric gears,

are tested. In the case of the bearing, the health statuses of good, inner-race-, outer-race- and ball faults are examined. For the shafts, the statuses of good, imbalance-, bent- shaft and keyway sheared are tested.

Table C.7: Fault classes of the gearboxes.

	Gear				Bearing ID						Shaft	
Fault Class	32T	96T	48T	80T	B1	B2	B3	B4	B5	B6	Input	Output
Spur 1	Good	Good	Good	Good	Good	Good	Good	Good	Good	Good	Good	Good
Spur 2	Chipped	Good	Eccentric	Good	Good	Good	Good	Good	Good	Good	Good	Good
Spur 3	Good	Good	Eccentric	Good	Good	Good	Good	Good	Good	Good	Good	Good
Spur 4	Good	Good	Eccentric	Broken	Ball	Good	Good	Good	Good	Good	Good	Good
Spur 5	Chipped	Good	Eccentric	Broken	Inner	Ball	Outer	Good	Good	Good	Good	Good
Spur 6	Good	Good	Good	Broken	Inner	Ball	Outer	Good	Good	Good	Imbalance	Good
Spur 7	Good	Good	Good	Good	Inner	Good	Good	Good	Good	Good	Good	Keyw ay Sheared
Spur 8	Good	Good	Good	Good	Good	Ball	Outer	Good	Good	Good	Imbalance	Good
Fault Class	16T	48T	24T	40T	B1	B2	B3	B4	B5	B6	Input	Output
Helical 1	Good	Good	Good	Good	Good	Good	Good	Good	Good	Good	Good	Good
Helical 2	Good	Good	Chipped	Good	Good	Good	Good	Good	Good	Good	Good	Good
Helical 3	Good	Good	Broken	Good	Good	Good	Good	Combination	Inner	Good	Bent Shaft	Good
Helical 4	Good	Good	Good	Good	Good	Good	Good	Combination	ball	Good	Imbalnce	Good
Helical 5	Good	Good	Broken	Good	Good	Good	Good	Good	Inner	Good	Good	Good
Helical 6	Good	Good	Good	Good	Good	Good	Good	Good	Good	Good	Bent Shaft	Good

C.3.2 Data pre-processing

Accuracy and reliability of the MLP or CNN -algorithms are proportional to data samples for training. There are 280 files for 14 different fault classes, or 20 files for each class in the original dataset. Increasing data samples for training is to enhance the effectiveness of the proposed algorithm. A complete time-frequency representation of a vibration signal requires the data of one complete cycle of rotation. Based on this rule, one data file is subdivided into 20 samples, so 400 samples are created for each fault class. Therefore, 5600 samples for 14 fault classes are used for training and testing of the algorithm, in which 75% of the data is used for training the classifiers, and 25% of the data is used to validate the trained algorithms. To test the robustness of the proposed algorithms, two types of noises are added to the original signals. The first type or noise type-1 signal is generated by adding white Gaussian noise at the signal to noise ratio (SNR) of 14 dB, which means the actual signal power to noise power ratio (P_{sig}/P_{noise}) is approximately 25. Figure C.9. shows the original signal and the noise type-1 signal.

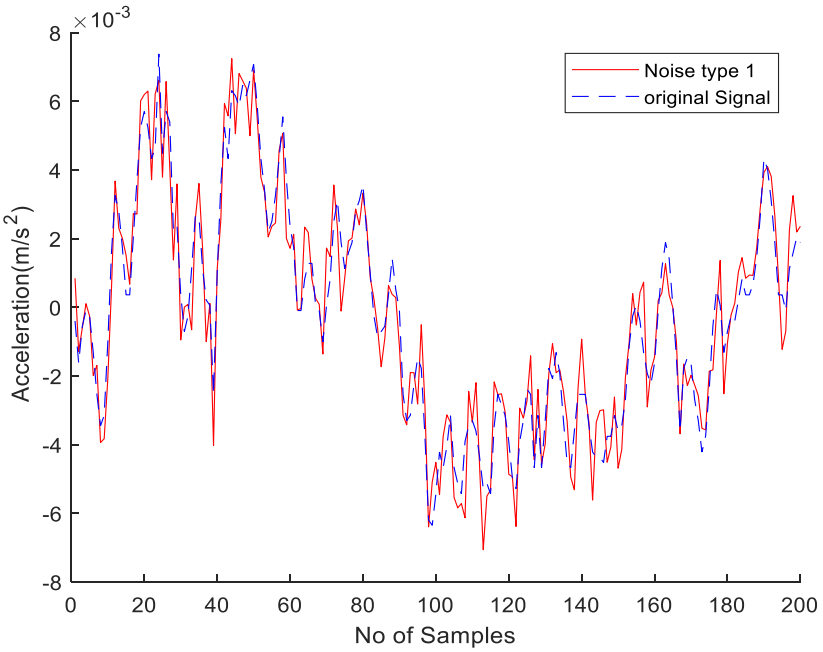

Figure C.9: The original signal and noise type 1 signal.

Noise type-2 signals are generated by mixing each signal to another signal. This scenario demonstrates a practical beating situation in a gearbox, where the original vibration signal (R_{su}) being measured is mixed with a fraction (f %) of another vibration source (R_e). The final signal is normalized using the weighted average of both signals. The signal mixing rule is defined in (A.7)

$$R_{snu} = \frac{(R_{su} + f * R_e)}{1+f} \tag{C.7}$$

where R_{snu} is the final noise type-2 signal of the uth fault class. u = 1, 2…, NG, in which NG = 8 for the spur gear and NG = 6 for the helical gear.

In the cases of helical gearbox, R_e is the helical fault class-2, which is selected as a noise to all other helical fault classes. The mixing weight (f %) is selected at 0.5. In spur gear faults, a similar rule is applied and the signal of the spur fault class-2 is used as a noise (R_e) for other spur fault classes. Figure C.10 shows the original and noise type-2 signal for the first 200 samples in the spur 1 fault class.

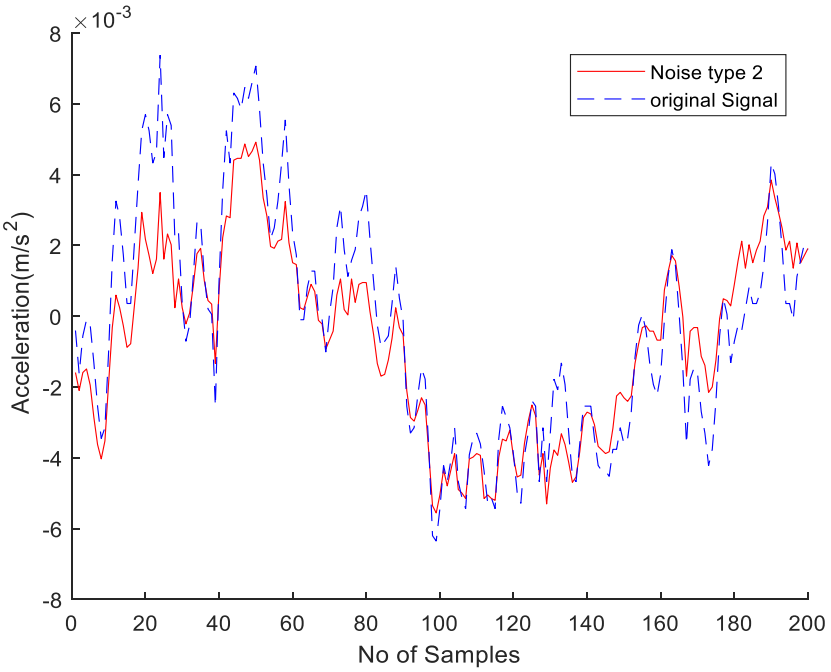

Figure C.10: The original signal and spur-gear type 2 signal.

C.4 Results and discussions

In this study, each algorithm, namely MLP and CNN, was first applied to the dataset with and without using data fusion at the feature level. The effect of feature extraction using STFT and CWT on the accuracy of the individual neural networks was also assessed on the individual algorithms. Finally, the effectiveness of the proposed hybrid approach and data fusion at the decision level was validated by the same dataset. The accuracy is selected as the performance metric of machine learning in this fault diagnosis problem, thus the assessment of the proposed algorithm is only based on the accuracy and improvement of accuracy.

C.4.1 Performance of the multiple-fault classification using MLP, CNN and feature level fusion

The MLP architecture of a multiple-fault classification shown in Figure C.4 is used. It includes 20 input nodes from 20 features and 10 hidden layers. 8 fault classes of the spur gearbox and 6 fault classes for helical gearbox are studied, so 8 nodes are used in the output layer of spur gearbox and 6 nodes for helical gearbox fault classification with SoftMax functions. The classification accuracy and the

difference of accuracy compared to respective decision fusion test case of each classifier with the test dataset is sumarized in Table C.8. The training process of neural networks holds a property of randomness. Therefore, 20 tests for each case are repetitively implemented to get the average accuracy values, minimizing the effect on randomness of the training process in this study.

Table C.8: Overall performances of individual MLP and CNN classifiers.

Test case	Algorithm	Signal	Spectrogram images	Feature fusion	Accuracy and difference compared to feature level fusion (%)			
					Spur		Helical	
1	MLP	input	-	No	94.1	- 4.2	81.8	- 16.2
2		output	-	No	97.0	- 1.3	86.2	- 11.8
3		**both**	**-**	**Yes**	**98.3**		**98.0**	
4	CNN	input	STFT	No	94.0	- 3.5	59.5	- 21.8
5		output	STFT	No	90.3	- 7.2	80.8	- 0.5
6		**both**	**STFT**	**Yes**	**97.5**		**81.3**	
7		input	CWT	No	92.0	- 6.0	87.8	- 8.4
8		output	CWT	No	90.6	- 7.4	90.8	- 5.4
9		**both**	**CWT**	**Yes**	**98.0**		**96.2**	

In the first case – test case 1, 20 features from the input-shaft vibration accelerometer alone are applied to the MLP algorithm to classify the multiple faults. The classification accuracies for the spur and helical gearboxes are 94.1% and 81.8%, respectively. In the second case - test case 2, the classification accuracies of those gearboxes are 97.0% and 86.2% when using 20 features from the output-shaft vibration accelerometer alone. In the test case 3, the data fusion of 40 features from the input- and output-shaft vibration accelerometers enhances the classification accuracies for the spur and helical gearboxes by 4.2% and 16.2%, respectively, compared to test case 1. In the test case 3, the feature level fusion improves the accuracy of classification for the spur gearbox only 1.3% as compared to test case 2. However, for the helical gearbox, it allows increasing the classification accuracy to 11.8%.

The CNN algorithm is applied to the image features extracted by STFT in the test cases: 4 (input-shaft signal), 5 (output-shaft signal) and 6 (fusion of the input- and output-shaft signals). The same procedure is implemented on the image features produced by CWT in the test cases from 7 to 9. The accuracy of the CNN algorithm on the fault classification of the spur gearbox is around 98% in case of using data- fusion on features extracted by either STFT or CWT, but the accuracy of the CNN algorithm reduces significantly to 81.3% if using data-fusion features extracted by STFT for the fault classification of the helical gearbox. Therefore, from the individual algorithm point of view, the MLP algorithm with feature-level fusion (case 3) and the CNN using CWT-base features with image fusion (case 9) are the best options for the multiple-fault classification for the gearbox in this study.

The accuracy of the test case 6 for the helical gearbox is only increased by 0.5 % as compared to the test case 5. However, for the spur gearbox the increase is 7.2% in the same test case. The classification accuracies for all test cases are improved from 0.5 % to 21.8%. From the type of gearbox point of view, the feature level fusion increases the accuracies for the spur-gearbox classification of about 5% (mean difference in 6 cases), and those of the helical gearbox classification of 10.7%, keeping consistent (less variant) for different test cases.

A graphical representation of the overall accuracy is shown in Figure C.11, in which the blue dotted-line -IP, green dashed-line -Op, and red solid-line -IP+OP fusion curves are referred to the signal sources from the input-, output-shaft accelerometers and fused signals, respectively. In the next section, further improvements on the best options (cases 3 and 9) will be presented with and without the presence of noises in the collected data.

Changing the time and frequency (scale in wavelets) resolution of the spectrograms has an impact on classification results. Low time-frequency resolution results in low classification accuracies due to low information contents. On the other hand, increasing the time-frequency resolution is effective up to some levels and after that more detailed information of the spectrogram will act as noises to the classifiers, reducing their accuracies. Increasing both time and frequency resolutions at same time is not feasible. For a given sampling rate, the frequency resolution is decreased, once time resolution is increased, and vice versa. Further, high time-frequency resolution and sampling rates require expensive data storage devices. Therefore, a balanced time and frequency (wavelet scale) resolution is experimentally selected as both are important for the classification, and high

classification accuracies are obtained in this study.

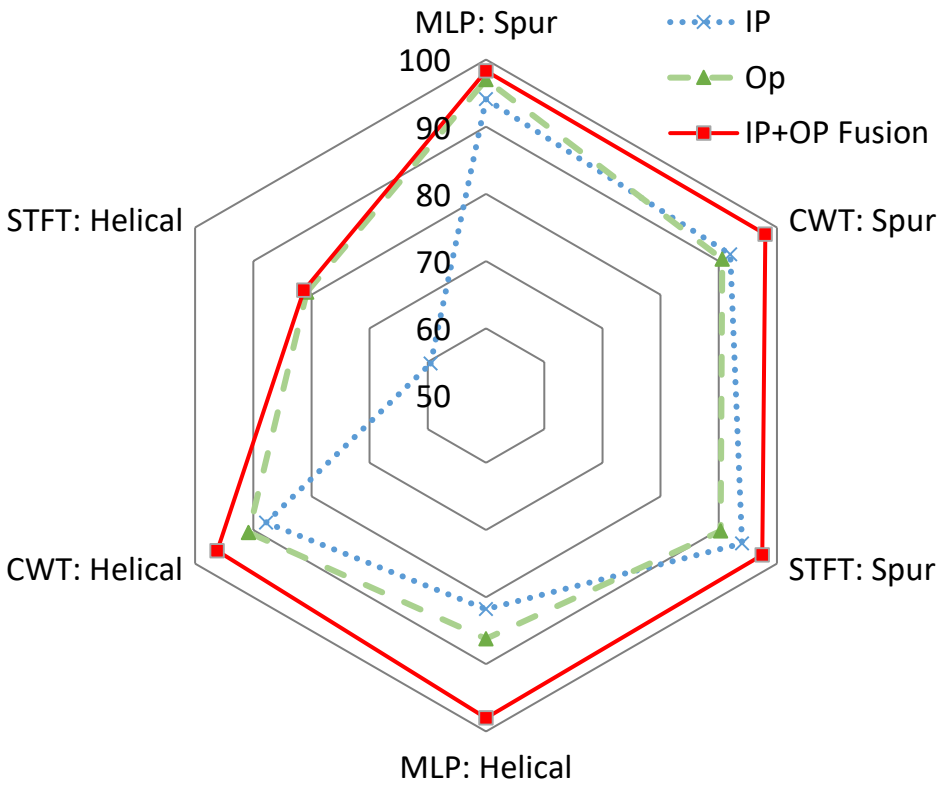

Figure C.11: Overall performances of individual MLP- and CNN- classifiers.

C.4.2 Accuracy and robustness comparison between the proposed method and other algorithms

In this section, the accuracies and robustness of the proposed algorithms are compared with those from other algorithms, which are commonly used in feature detection and classification. Figure C.12 shows the comparison results. Domain features (DF) generated from filter banks are supplied to the proposed MLP and support vector machine (SVM) classifiers in the first two studies, and their performances are shown as DF-MLP and DF-SVM in Figure C.12. The main objective of the SVM classification is to define a hyperplane in the feature space to differentiate each class with a maximum margin between classes [44-46]. In this study, the SVM algorithm is tested with different kernel functions (linear, quadratic and gaussian), and the highest accuracy SVM with the gaussian kernel is used for classification in Figure C.12.

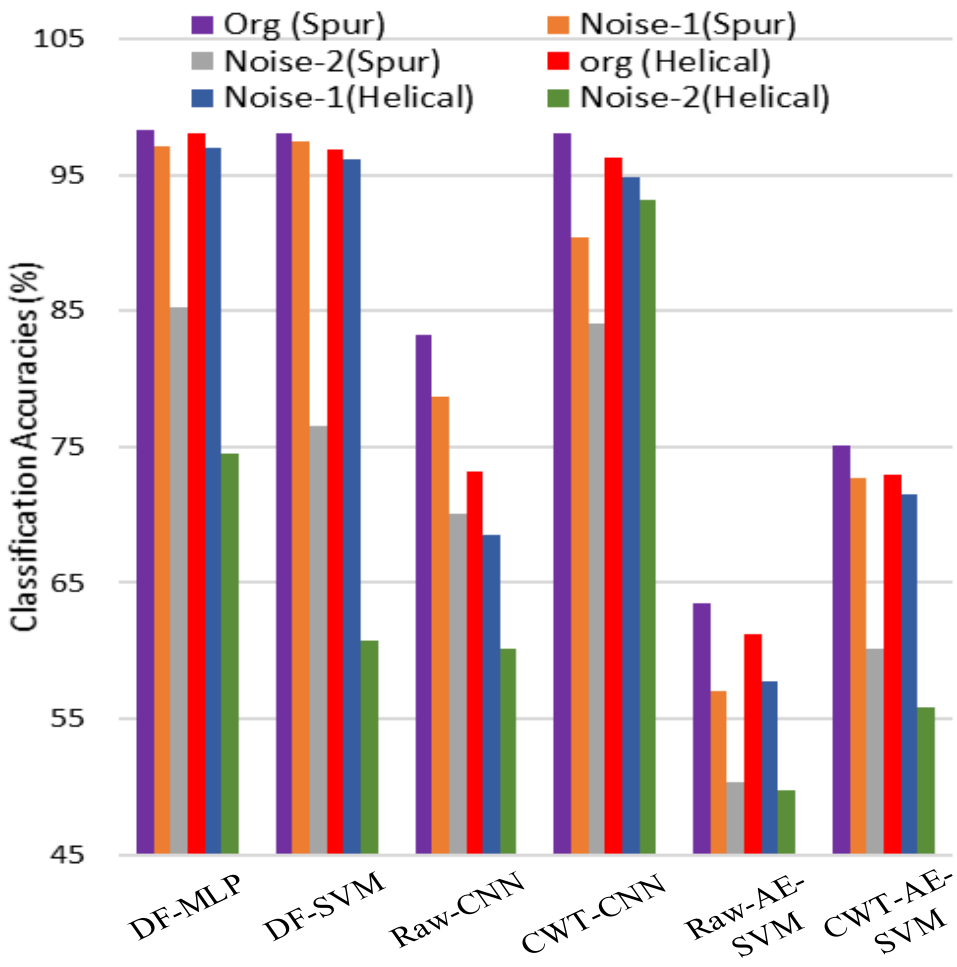

Figure C.12: Accuracy and robustness comparison of individual algorithms.

From the first two studies, the classification accuracies of the proposed MLP and SVM classifier are high when fed by original- and the noise-type-1 signals. However, under noise-2 signals the accuracy of the SVM classifier is considerably lower than the proposed MLP about 10% for the spur gearbox, and 9% for the helical gearbox. This verifies that the proposed MLP classifier is more robust and accurate than the SVM classifier.

The raw vibration signals (without any signal processing steps) are fed to the CNN in study 3 (Raw-CNN). In study 4 (CWT-CNN), first the raw vibration signals are converted to spectrograms by CWT, and then the supervised feature learning and classification are conducted using the proposed CNN. Using the raw vibration signal, the accuracy of the CNN classifier is significantly low as compared to the CNN using CWT spectrograms. These results confirm that using CWT spectrograms as inputs of the CNN classifier is better than using the raw signals.

To test the effectiveness of CNN feature learning, the raw vibration signals are used to derive pattern features in training a feed forward neural network, namely autoencoder (AE), and a SVM classifier is used in study 5 (Raw-AE-SVM). In the study, sparse autoencoders are implemented to learn the features from inputs in an unsupervised way. In this study, two stages sparse autoencoders are used to derive 100 features from each input data type [47-49]. The overall accuracy in study 5 is lower than that of the proposed CNN method (Raw-CNN). This confirms that the combined feature learning and classification in the CNN result in a higher accuracy as compared to the combination between an individual feature learning and a classification.

In study 6, the CWT spectrograms are used in training the autoencoders, and SVM is used as the classifier (CWT-AE-SVM). The classification accuracies in study 6 are lower than those in the proposed CNN method (study 4 or CWT-CNN), but greater than those in study 5 (Raw-AE-SVM). Using CWT spectrograms and the CNN is a better option to enhance classification accuracy as compared to using raw signals and individual feature learning and SVM classification.

The comparative study in this section confirms that the proposed domain features and MLP based algorithm and the CWT spectrogram-based CNN algorithm are the best individual algorithms in terms of average accuracies and robustness under noises.

C.4.3 Accuracy and robustness of the multiple-fault classification using the hybrid neutral networks and decision level fusion.

In the previous section, two best options of the multiple-fault classifications were identified: feature-level data-fusion based-MLP and feature-level data-fusion based CNN algorithm implemented on the CWT features. The next step is to enhance the accuracy and robustness of those best classifications by fusing the results of the two best individual classifiers at the decision level using the Naïve Bayes combiner. 9 different tests are conducted on the selected classifiers to verify the robustness of the proposed data fusion. Table C.9 summarizes the overall performance of the MLP and CNN classifiers with and without noises in the collected signals.

Table C.9: Overall performances of MLP and CNN classifiers with noise.

Test case	Algorithm	Noise Type	Decision level fusion	Accuracy and difference compared to decision level fusion (%)		
				Spur		Helical
1	MLP		No	98.3	- 0.1	98.0 - 0.2
2	CNN	-	No	98.0	- 0.4	96.2 - 2.0
3	**MLP + CNN**		**Yes**	**98.4**		**98.2**
4	MLP		No	97.1	- 0.4	97.0 - 0.7
5	CNN	Noise 1	No	90.4	- 7.1	94.8 - 2.9
6	**MLP + CNN**		**Yes**	**97.5**		**97.7**
7	MLP		No	85.3	- 5.8	74.5 - 19.0
8	CNN	Noise 2	No	84.1	- 7.0	93.2 - 0.3
9	**MLP + CNN**		**Yes**	**91.1**		**93.5**

Without noises in the first three test cases, the Naïve Bayes combiner allows maintaining the accuracy of the selected classifications at 98.4% in the spur gearbox and 98.2% in the helical gearbox. The effect of decision fusion on the accuracy improvement is small under this noise less case.

Under the effect of noise type 1, the accuracies of the individual MLP and CNN classifiers to the spur gearbox reduce by 1.2 % (test case 4 is compared to test case 1) and 7.6 % (test case 5 is compared to test case 2), and those to the helical gearbox drop by 1% and 1.4 %. The white Gaussian noises affect slightly on the accuracy of the MLP classifier, but significantly deteriorate the performance (7.6 % compared to spur gearbox test case 2) of the CNN classifier. The decision fusion of the MLP and CNN results keeps the accuracy of the multiple-fault classification for both the spur and helical gearbox close to 98%. This verifies that the proposed decision-level fusion algorithm is well robust against the white Gaussian noise at SNR of 14 dB.

When applying the type-2 noises to the signals collected from the spur gearbox, the accuracies of the MLP and CNN classification reduce by 13% (compared to the test case 1) and 13.9% (compared to the test case 2), respectively. The Naïve Bayes combiner enhances the accuracy of the overall classification by about 5.8% for MLP and 7.0% for CNN and keeps the final accuracy at 91.1% for spur-gearbox classification. For the helical gearbox dataset, the accuracy of the

MLP classifier drops significantly by 23.5% (compared to the test case 1) under the effect of the type-2 noise, but the accuracy of CNN classifier is only decreased by 3% (compared to the test case 2). The decision level fusion improves the classification accuracy by 19% for MLP and 0.3% for CNN and maintains 93.5% accuracy.

Figure C.13 shows the mean and standard deviations of accuracies of each algorithm for different test cases. The standard deviation of an algorithm is the square root of its accuracy variance, quantifying the variation of accuracies around its mean under different noise conditions. For example, the mean and deviation of MLP algorithm are 91.7% and 8.92% using the six classification accuracies (98.3%, 98.0%, 97.1%,97.0%, 85.3% and 74.5%) given in test cases 1,4 and 7 in Table C.9. This means that the MLP classifier has the mean accuracy of 91.7%, but it is not robust under noise conditions due to the big variation. As seen from Figure C.13, the mean accuracy is maximized, and the deviation is minimized if using decision fusion of the CNN and MLP results.

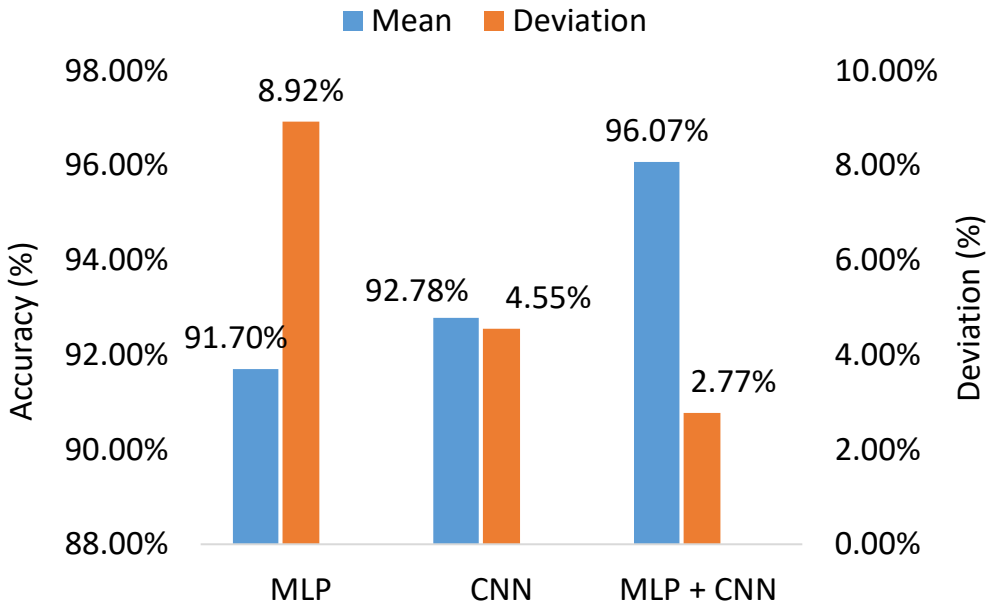

Figure C.13: Mean and deviation of algorithms in different test cases.

The importance of decision fusion is substantially highlighted since the individual MLP or CNN classifier alone is sensitive to the noise. Under the noise type 1 and 2 cases, the classification accuracies are dropped as the information

contents on the inputs (MLP features and spectrograms) are distorted. The accuracy of machine learning reduces further once the information distortion is increased from noise-less, noise type 1 to noise type 2. The proposed decision level fusion cannot prevent the dropping of accuracy, but it can minimize the accuracy reduction and standard deviation. It can be concluded that the individual algorithms are not robust against noise type-2 or external sources added to vibration signals, which are common in drivetrains of the wind turbines or heavy industry.

C.5 Conclusion

In this work, a hybrid neural network scheme, consisting of Multilayer Perceptron and Convolutional Neural Network, is proposed to detect mixed faults in a gearbox. Using the proposed MLP algorithm, CWT spectrograms as input data to CNN is recommended for the classification of gearbox mixed faults. The robustness and reliability of the proposed scheme are further improved by data fusion algorithms, and its accuracy is maintained at above 91% regardless of disturbances or noises in the collected data. The average accuracy of the proposed algorithm under different noise types is high as 96.07% with a standard deviation of 2.77%. This improvement is highly important since the main objective of multiple- fault classifications is to avoid the false and missing alarms. Other remarks are drawn from this work:

- Feature-level data fusion can significantly improve the accuracy of a fault diagnosis irrespective of the type of machine learning algorithm.
- Accuracy of the CNN-based classification depends on the quality of input data, image or patterns. Using the spectrograms as input data for CNN gives a higher classification accuracy than the raw vibration signals. In this application, the images extracted by continuous wavelet transform are more reliable than those from short-time Fourier transform or raw vibration signals.
- If an individual MLP- or CNN-based fault classifier is not robust under noises, using an additional classifier and decision fusion can enhance its robustness.

References

[1] S. H. Kia, H. Henao and G. A. Capolino, “Gear Tooth Surface Damage Fault Detection Using Induction Machine Stator Current Space Vector Analysis,” *IEEE Trans. on Ind. Electron.*, vol. 62, no. 3, pp. 1866-1878, 2015.

[2] H. Henao, S. H. Kia and G. A. Capolino, “Torsional-Vibration Assessment and Gear-Fault Diagnosis in Railway Traction System,” *IEEE Trans. Ind. Electron.*, vol. 58, no. 5, pp. 1707-1717, 2011.

[3] L. Hong and J. Dhupia, “A time domain approach to diagnose gearbox fault based on measured vibration signals,” *J. Sound Vib.*, vol. 333, no. 7, pp. 2164-2180, 2014.

[4] P. Girdhar and C. Scheffer, “Practical Machinery Vibration Analysis and Predictive Maintenance,” in *Machinery fault diagnosis using vibration analysis*, Oxford, Newnes, pp. 89-133, 2004.

[5] F. Cheng, J. Wang, L. Qu and W. Qiao, “Rotor Current-Based Fault Diagnosis for DFIG Wind Turbine Drivetrain Gearboxes Using Frequency Analysis and a Deep Classifier,” *IEEE Trans. on Ind. App.*, vol. 54, no. 2, pp. 1062-1071, March-April 2018.

[6] X. Gong and W. Qiao, “Bearing fault diagnosis for direct-drive wind turbines via current-demodulated signals,” *IEEE Trans. Ind. Electron.*, vol. 60, no. 8, pp. 3419-3428, 2013.

[7] P. Tchakoua et al, “Wind Turbine Condition Monitoring: State-of-the-Art Review, New Trends, and Future Challenges,” *Energies*, vol. 7, no. 4, pp. 2595-2630, 2014.

[8] --, "ISO 18436-2:2014, “International Organization for Standardization, 2014. [Online]. Available: https://www.iso.org/standard/50447.html. [Accessed December 2017].

[9] Z. Du, X. Chen, H. Zhang and R. Yan, “Sparse feature identification based on union of redundant dictionary for wind turbine gearbox fault diagnosis,” *IEEE Trans. Ind. Electron.*, vol. 62, no. 10, pp. 6594-6605, 2015.

[10] -- , “Domain fundamentals: PHM Data Challenge Competition 2009," Phm Society, 2009. [Online]. Available: https://www.phmsociety.org/competition/PHM/09/fundamentals. [Accessed December 2017].

[11] K. Mobley, “Vibration Fundamentals”, Elsevier, 2001.

[12] J. S. L. Senanayaka, H. V. Khang and K. G. Robbersmyr, "Towards online bearing fault detection using envelope analysis of vibration signal and decision tree classification algorithm," in *Proc. IEEE ICEMS,* Sydney, Australia, 2017.

[13] G. Niu, "Data-Driven Technology for Engineering Systems Health Management: Design Approach, Feature Construction, Fault Diagnosis, Prognosis, Fusion and Decision," *Springer*, 2016.

[14] D. Jung and C. Sundström, "A Combined Data-Driven and Model-Based Residual Selection Algorithm for Fault Detection and Isolation," *IEEE Trans. on Control Sys. Tech. (Early Access)*, pp. 1-15, 2017.

[15] X. Dai and Z. Gao, "From model, signal to knowledge: A data-driven perspective of fault detection and diagnosis," *IEEE Trans. Ind. Informat.*, vol. 9, no. 4, pp. 2226-2238, 2013.

[16] Z. Gao, C. Cecati and S. X. Ding, "A Survey of Fault Diagnosis and Fault-Tolerant Techniques-Part II: Fault Diagnosis with Knowledge-Based and Hybrid/Active Approaches," *IEEE Trans. Ind. Electron.*, vol. 62, no. 6, pp. 3768-3774, 2015.

[17] Z. Gao, C. Cecati and S. X. Ding, "A Survey of Fault Diagnosis and Fault-Tolerant Techniques—Part I: Fault Diagnosis with Model-Based and Signal-Based Approaches," *IEEE Trans. Ind. Electron.*, vol. 62, no. 6, pp. 3757-3767, 2015.

[18] N. Baydar, Q. Chen, A. Ball and U. Kruger, "Detection of incipient tooth defect in helical gears using multivariate statistics," *Mechanical Sys. and Sig. Proc.*, vol. 15, no. 2, pp. 303-321, 2001.

[19] J. S. L. Senanayaka, S. T. Kandukuri, H. V. Khang and K. G. Robbersmyr, "Early detection and classification of bearing faults using support vector machine algorithm," in *Proc. IEEE WEMDCD*, Nottingham, UK, 2017.

[20] P. Konar and P. Chattopadhyay, "Bearing fault detection of induction motor using wavelet and support vector machines (SVMs)," *Appl. Soft Comput.*, vol. 11, no. 6, p. 4203–4211, 2011.

[21] L. Wu, B. Yao, Z. Peng and Y. Guan, "Fault Diagnosis of roller bearings based on a wavelet neural network and manifold learning," *Appl. Sci.*, vol. 7, no. 158, p. 1–10, 2017.

[22] R. Zhang, H. Tao, L. Wu and Y. Guan, "Transfer Learning with Neural Networks for Bearing Fault Diagnosis in Changing Working Conditions," *IEEE Access*, vol. 5, pp. 14347-14357, 2017.

[23] G. Susto, A. Schirru, S. Pampuri, S. McLoone and A. Beghi, "Machine learning for predictive maintenance: A multiple classifier approach," *IEEE Trans. Ind. Informat.,* vol. 11, no. 3, pp. 812-820, 2015.

[24] M. Van and H. Kang, "Bearing defect classification based on individual wavelet local fisher discriminant analysis with particle swarm optimization," *IEEE Trans. Ind. Informat.,* vol. 12, no. 1, pp. 124-135, 2016.

[25] B. Xue, M. Zhang, W. N. Browne and X. Yao, "A Survey on Evolutionary Computation Approaches to Feature Selection," *IEEE Trans. Evol. Comput.,* vol. 20, no. 4, pp. 606-626, Aug. 2016.

[26] C. Sun, M. Ma, Z. Zhao and X. Chen, "Sparse Deep Stacking Network for Fault Diagnosis of Motor," *IEEE Trans. Ind. Informat.,* vol. 14, no. 7, pp. 3261-3270, July 2018.

[27] H. Hu, B. Tang, X. Gong, W. Wei and H. Wang, "Intelligent Fault Diagnosis of the High-Speed Train With Big Data Based on Deep Neural Networks," *IEEE Trans. Ind. Informat.,* vol. 13, no. 4, pp. 2106-2116, Aug. 2017.

[28] W. Sun, R. Zhao, R. Yan, S. Shao and X. Chen, "Convolutional Discriminative Feature Learning for Induction Motor Fault Diagnosis," *IEEE Trans. Ind. Informat.,* vol. 13, no. 3, pp. 1350-1359, June 2017.

[29] R. Liu, G. Meng, B. Yang, C. Sun and X. Chen, "Dislocated Time Series Convolutional Neural Architecture: An Intelligent Fault Diagnosis Approach for Electric Machine," *IEEE Trans. Ind. Informat.,* vol. 13, no. 3, pp. 1310-1320, June 2017.

[30] M. He and D. He, "Deep Learning Based Approach for Bearing Fault Diagnosis," *IEEE Trans. Ind. Appl.,* vol. 53, no. 3, pp. 3057-3065, 2017.

[31] F. Lv, C. Wen, Z. Bao and M. Liu, "Fault diagnosis based on deep learning," in *Proc. IEEE ACC*, Boston, USA, 2016.

[32] L. I. Kuncheva, "Combining Pattern Classifiers: Methods and Algorithms," *New Jersey*, John Wiley & Sons, 2014.

[33] M. Norton and D. Karczub, "Fundamentals of Noise and Vibration Analysis for Engineers," *Cambridge University Press,* 2003.

[34] H. V. Khang, R. Puche-Panadero, J. S. L. Senanayaka and K. G. Robbersmyr, "Bearing fault detection of gear-box drive train using active filters," in *Proc. IEEE ICEMS*, Chiba, Japan, 2016.

[35] F. Wu and J. Lee, "Information Reconstruction Method for Improved Clustering and Diagnosis of Generic Gearbox Signals," Int. Jour. of the Prog. and Health Manage. Society, vol. 2, no. 1, p. 9, 2011.

[36] -- , “Multi-Layer Neural Network,” *Stanford University*, [Online]. Available: http://ufldl.stanford.edu/tutorial/supervised/MultiLayerNeuralNetworks/.[Accessed November 2017].

[37] F. Jia, Y. Lei, N. Lu, and S. Xing, “Deep normalized convolutional neural network for imbalanced fault classification of machinery and its understanding via visualization,” Mechanical Sys. and Sig. Proc., vol. 110, pp. 349-367, 2018.

[38] S. Nawab, T. Quatieri and J. Lim, “Signal reconstruction from short-time Fourier transform magnitude,” *IEEE Trans. on Acoustics, Speech, and Sig. Proc.*, vol. 31, no. 4, pp. 986-998, 1983.

[39] R. Kronland-Martinet, J. Morlet and A. Grossmann, “Analysis of sound patterns through wavelet transforms,” *Int. J. Pattern Recogn. Artificial Intel.*, vol. 1, no. 2, pp. 273-302, 1987.

[40] O. Rioul and P. Duhamel, “Fast algorithms for discrete and continuous wavelet transforms,” *IEEE Trans. Inf. Theory*, vol. 38, no. 2, pp. 569-586, 1992.

[41] A. Jacop, H. Khang, K. G. Robbersmyr and A. J. M. Cardoso, “Bearing Fault Detection for Wind-turbine Systems using Adaptive Filter based Wavelet Transform,” in *Proc. IEEE ICEMS*, Sydney, Australia, 2017.

[42] N. Tajbakhsh, J. Y. Shin, S. R. Gurudu, R. T. Hurst, C. B. Kendall, M. B. Gotway and J. Liang, “Convolutional Neural Networks for Medical Image Analysis: Full Training or Fine Tuning?,” *IEEE Trans. Med. Imag.*, vol. 35, no. 5, pp. 1299-1312, 2016.

[43] -- , “PHM Challenge Competition Data Set,” Phm society, 2009. [Online]. Available: https://www.phmsociety.org/references/datasets. [Accessed August 2017].

[44] V. Vapnik, “The Nature of Statistical Learning Theory”, *Springer*, 2000

[45] C. Manning, P. Raghavan, H. Schütze, “Introduction to Information Retrieval”, *Cambridge University Press*, 2008.

[46] B. Scholkopf et al., “Comparing support vector machines with Gaussian kernels to radial basis function classifiers”, *IEEE Trans. Signal Process.*, vol. 45, no. 11, pp. 2758-2765, Nov. 1997.

[47] P. Vincent et al., “Extracting and composing robust features with denoising autoencoders,” in *Proc. 2th Int. Conf. Mach. Learn.*, Helsinki: Finland, 2008, pp. 1096-1103.

[48] E. Hosseini-Asl, J. M. Zurada and O. Nasraoui, “Deep Learning of Part-Based Representation of Data Using Sparse Autoencoders With Nonnegativity Constraints,” *IEEE Trans. Neural Netw. Learn. Syst.*, vol. 27, no. 12, pp. 2486-2498, Dec. 2016.

[49] J.S.L. Senanayaka et al., “A robust method for detection and classification of permanent magnet synchronous motor faults: Deep autoencoders and data fusion approach,” *J. Phys.: Conf. Ser.*, vol. 1037, no.3, 2018.

Paper D

Multiple Fault Diagnosis of Electric Powertrains under Variable Speeds using Convolutional Neural Networks

Jagath Sri Lal Senanayaka, Huynh Van Khang, Kjell G. Robbersmyr

This paper has been published as:

J. S. Lal Senanayaka, H. V. Khang and K. G. Robbersmyr, "Multiple Fault Diagnosis of Electric Powertrains Under Variable Speeds Using Convolutional Neural Networks," *2018 XXIII International Conference on Electrical Machines (ICEM)*, Alexandroupoli, pp. 1900-1905, 2018.
doi: 10.1109/ICELMACH.2018.8507096

Multiple Fault Diagnosis of Electric Powertrains under Variable Speeds using Convolutional Neural Networks

Jagath Sri Lal Senanayaka, Huynh Van Khang, Kjell G. Robbersmyr, *Senior Member IEEE*

Department of Engineering Sciences, University of Agder, 4879 Grimstad, Norway

E-mails: {jagaths; huynh.khang; kjell.g.robbersmyr }@uia.no

***Abstract* – Electric powertrains are widely used in automotive and renewable energy industries. Reliable diagnosis for defects in the critical components such as bearings, gears and stator windings, is important to prevent failures and enhance the system reliability and power availability. Most of existing fault diagnosis methods are based on specific characteristic frequencies to single faults at constant speed operations. Once multiple faults occur in the system, such a method may not detect the faults effectively and may give false alarms. Furthermore, variable speed operations render a challenge of analysing nonstationary signals. In this work, a deep learning-based fault diagnosis method is proposed to detect common faults in the electric powertrains. The proposed method is based on pattern recognition using convolutional neural network to detect effectively not only single faults at constant speed but also multiple faults in variable speed operations. The effectiveness of the proposed method is validated via an in-house experimental setup.**

***Index Terms* –** Fault diagnosis, convolutional neural networks, electrical fault detection, induction motors, electromechanical systems, gears, bearings.

D.1 Introduction

Electric powertrains are one of the most demanding components in modern engineering systems. Electric drives, gearboxes and various types of loads, e.g. pumps, fans, mixers, conveyor systems, are the workhorses of manufacturing and food processing industries. According to a recent survey in Germany, electric drives consume more than 70% of electric energy in industries [1]. Furthermore, in modern automobiles there is an increased trend to replace combustion-engine powertrains by hybrid or electric powertrains due to the merits of efficiency, controllability and maintenance [2]. Electric powertrains together with the electricity generated from renewable sources can reduce the environmental impacts of human activities.

Condition monitoring systems are necessary to prevent catastrophic failures in critical industrial machines via predictive maintenance. However, most of the condition monitoring techniques used for electric powertrains and other rotating machines are still based on manual or semi-automated techniques, which are costly and time-consuming. Manual condition monitoring methods are based on analysing the data collected from vibration, current, oil samples and acoustic sensors [3-4], which require maintenance teams with skilled human resources and proper training to deal with various signal processing and statistical analyses using time and frequency domain signals [5].

To address challenges associated with the conventional condition monitoring methods, online condition monitoring and fault diagnosis methods can be used to increase the monitoring reliability. However, implementing a full online condition monitoring and fault diagnosis systems is a challenging task, requiring expertise of analysing complex relations from many data sources and making combined or fused decisions. Modern machine learning, deep learning algorithms and cloud computing methods are among the best options for implementing an automatic fault diagnosis system [6-7]. In this work, a deep learning-based fault diagnosis method is proposed for electric powertrains. The proposed algorithm is based on convolutional neural network (CNN). The CNN algorithms are originally developed for image classification applications. The main advantages of using CNN for image classification is that it does not require any domain knowledge about images, and CNN can learn features from the training data. In fault classification applications, signal processing techniques are necessary to extract

the hidden fault signatures from the signals and later the processed signals can be used to generate spectrograms. Further, CNN can learn complex spatial relationships from the spectrograms of fault signals to compensate noises and other disturbances.

Machine-learning and deep-learning algorithms have been widely used in fault classification, but most of them have been focused or limited to fault detection and classification under constant speed conditions for individual faults [8]. However, electric powertrains in automotive applications normally work in variable speeds and loads according to driver's demands, and multiple faults may occur in such a condition. These situations render challenges for the existing techniques, i.e. nonstationary signals, or may cause false alarms. This work focuses on detecting multiple faults in variable speeds. Within the framework, individual CNN-based classifiers are trained to detect single faults, but the validation for the classification is done for both single and multiple faults. This suggested procedure of training and validation matches with practical implementation cases, where the classifiers can be easily trained for single fault cases, but there can be several combinations in multiple fault cases. By eliminating the training for multiple fault cases, the proposed method allows to reduce the training time and computational burden of the classifiers. This rest of paper is organised as follows: in Section D.2, the proposed fault diagnosis system is presented in detail. The experimental results are discussed in Section D.3. In Section D.4 the conclusion of the work is provided.

D.2 Proposed fault diagnosis system

A block diagram of the proposed fault diagnosis system for electric powertrains is shown in Figure D.1. A typical electric powertrain includes the electric power source, controller, electric motor, gearbox, mechanical power transmission components and load as described on the top of Figure D.1. This fault diagnosis system focuses on the most common faults in critical components. To identify the critical components, the important functionalities and component failure probabilities can be taken into consideration. For example, in electric motors, most of the faults occur in bearings and stator windings, which provide important functionalities [9]. Therefore, the diagnosis system has to detect common faults on bearing and stator winding. Within this study, multiple faults in electric motors, namely inter-turn fault on the stator and bearing outer-race fault, and a damaged

gear on the gearbox are selected as studied fault cases. For each fault, an individual classifier is designed to detect the fault.

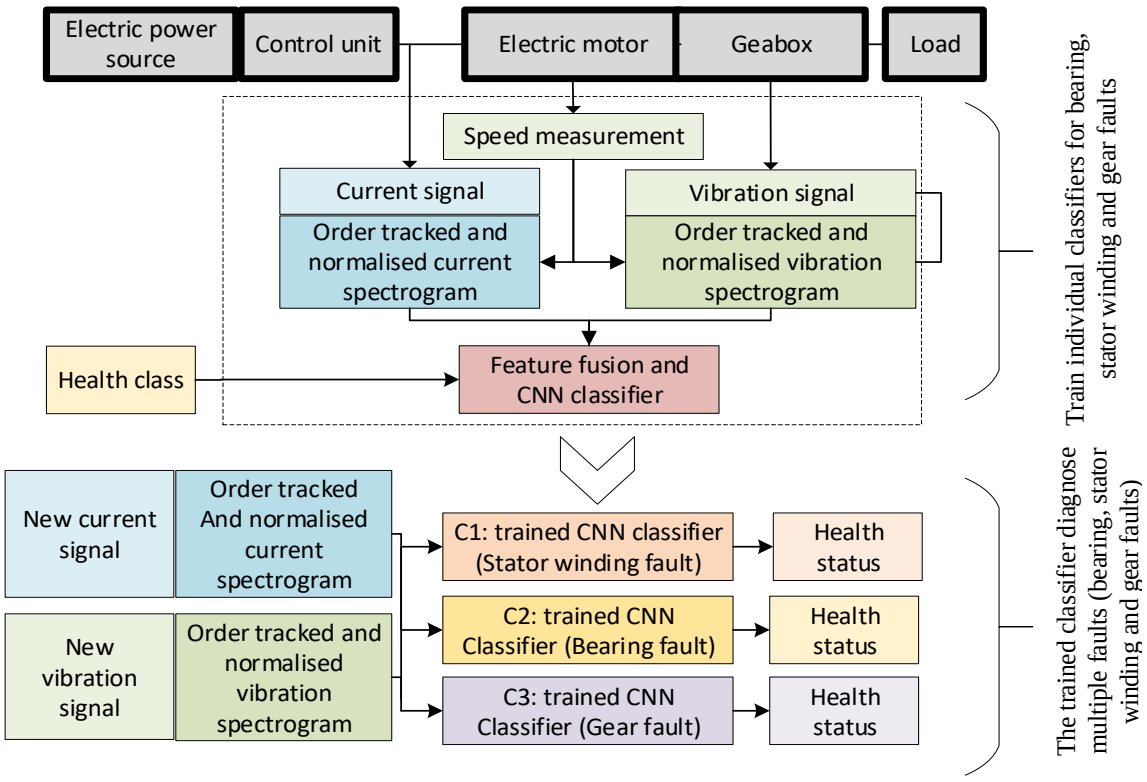

Figure D.1: A block diagram of the proposed fault diagnosis system.

Motor currents and the vibration sensors are used to diagnose faults in this work. Since the motor operates in variable speed conditions, the collected currents and vibration signals are order tracked and normalized to consider the variable speed operation. More details of this method are presented in Section D.2.2. Then spectrograms of both currents and vibration signals are generated and combined into large images. This combination provides an enlargement in the feature space. Based on the generated spectrograms, CNN can fuse the current and vibration spectrograms and implement a fault classification.

Although CNN are widely used in many applications of image classification, a CNN based fault diagnosis needs to be carefully implemented on spectrograms. The information of faults is hidden in the collected signals, thus proper signal processing methods are required to extract the hidden information from the signals and convert into spectrograms. For this purpose, the order normalization for vibration signals and the Park's vector of currents are used

together with CNN. In the training phase, three classifiers, namely C1, C2 and C3 as shown in Figure D.1, are individually trained to detect stator winding faults, bearing faults, and gear faults, respectively. After the training process, the trained classifiers are employed to detect multiple fault cases.

D.2.1 Fault diagnosis in constant speed operations

In a fault diagnosis of rotating machines, faults are detected by tracking the characteristic frequencies associated with the faults. For example, the characteristic frequency associated with an outer-race bearing fault (ball pass frequency outer-race (BPFO)) is calculated in (D.1) [10]. Such a characteristic frequency can be observed in analysed vibration signals when there is a defect on the bearing outer race.

$$BPFO = \frac{N_b}{2} f_s\left(1 - \frac{D_b}{D_c} cos\theta\right) \tag{D.1}$$

where N_b is the number of rolling elements in the bearing, D_b denotes the diameter of a rolling element, D_c represents the pitch diameter, θ is the contact angle between the outer-race and rolling element, and f_s is the shaft rotational frequency. The BPFO frequency divided by the shaft rotational frequency is equal to a frequency order, which is a constant for any rotational speed. Based on the bearing dimensions, the order of the bearing fault in this study is defined at 3.6 order (3.6X) of the shaft rotational frequency. An inter-turn stator winding fault can be detected using Park's vector (PV) analysis of motor currents [11].

$$\begin{aligned} i_d &= \sqrt{2/3}\, i_a - \sqrt{1/6}\, i_b - \sqrt{1/6}\, i_c \\ i_q &= \sqrt{1/2}\, i_b - \sqrt{1/2}\, i_c \\ i_p &= \left| i_d + j i_q \right| \end{aligned} \tag{D.2}$$

where i_d and i_q are the direct and quadratic components of the Park's vector i_p. i_a, i_b and i_c are the phase currents. A stator winding fault results in an unbalanced

winding, which produces a frequency of two times of the fundamental frequency in spectrum of i_p [11]. This means the second order of supply frequency ($2f_s$).

Similarly, a damaged gear fault results in an increase of vibration in the first order (1X) of the gear rotating frequency, gear natural resonance frequency and gear mesh frequencies and its 1X sidebands [12]. By tracking the mentioned frequency orders, the gear faults can be detected.

D.2.2 Fault diagnosis in variable speed operations using order tracking

In the fault diagnosis in constant speed operations, the sampling rate of signals is kept as a constant, and Fourier transform can be used to analyse the collected signals in such a steady-state operation. In variable speed operations, the Fourier transform cannot be applied because the analysed signals are not stationary or the frequency changes in time. Short-time Fourier transform (STFT) can be an alternative option as it assumes that the frequency is constant in small-time windows, thus Fourier transform is performed for those short-time signal windows. However, parameters of STFT need to be correctly selected in advance to compromise time and frequency resolution in spectrograms, thus it might not be a good solution to observe the characteristic frequencies in wide-range variable speeds. To address this challenge, instead of using a constant time sampling, the constant angular sampling is used for extracting the hidden stationary signal.

As shown in Figure D.2, the constant angle sampling method can be used to extract the underlined constant-frequency sine wave from a varying frequency sine wave. Details on this method can be found in [13-14]. Since the angle/phase information is required for this process. The rotational speed is measured from the test bench.

Figure D.3. shows how the constant angle sampling and order tracking are used in this study to detect a stator winding fault. The variable speed profile used in this study is given Figure D.3 (a). Figure D.3 (b) shows the STFT of the Park's vector i_p of the current signals, in which the $2f_s$ is clearly visible in the spectrum of i_p. After using the order tracking based on constant angle sampling, a constant 2X order is presented in the spectrogram for the variable speed operation as shown in Figure D.3 (c).

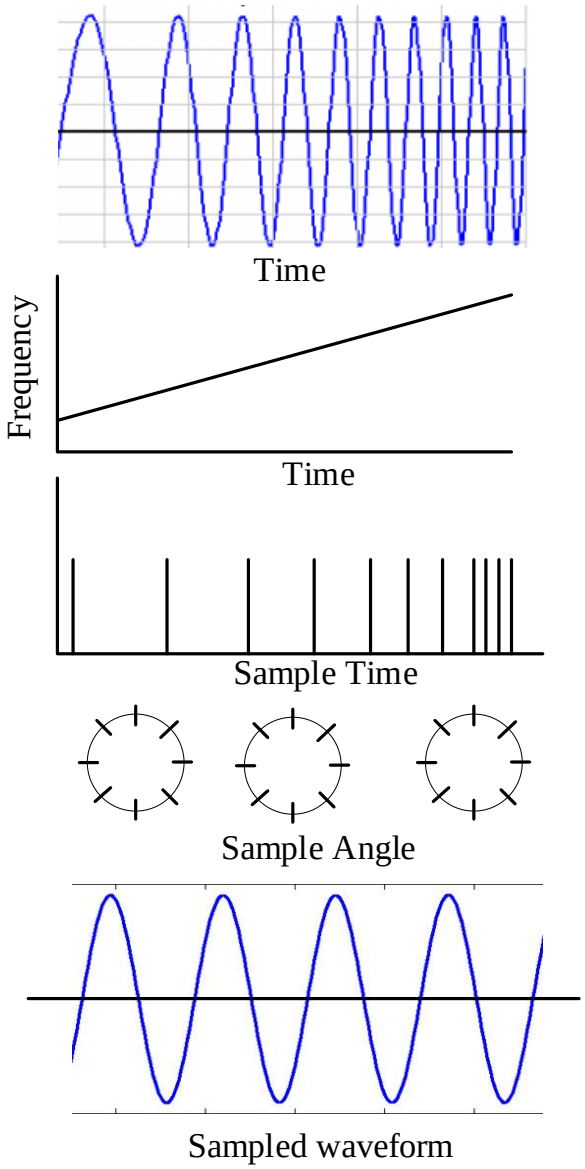

Figure D.2: Constant angle sampling of a variable frequency signal.

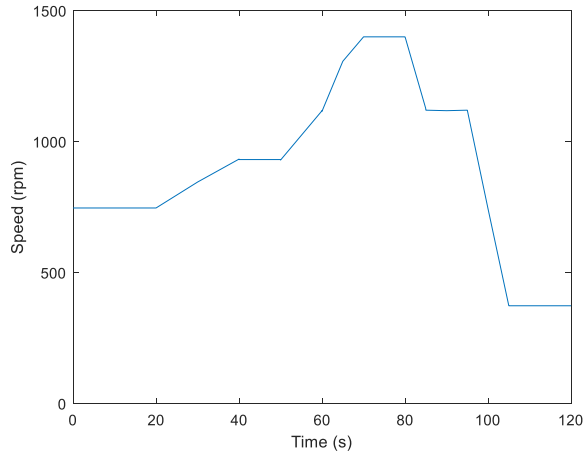

(a)

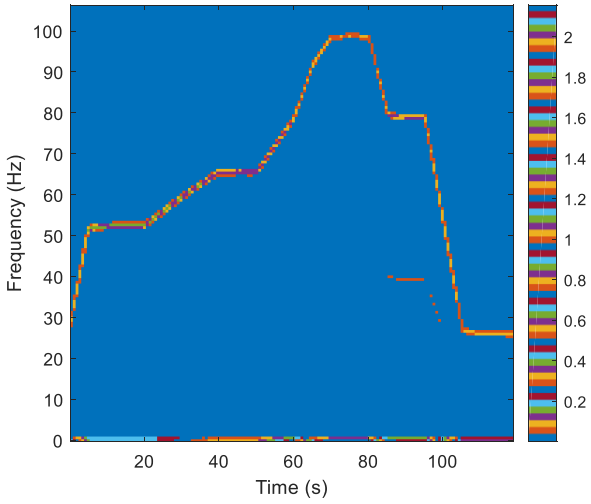

(b)

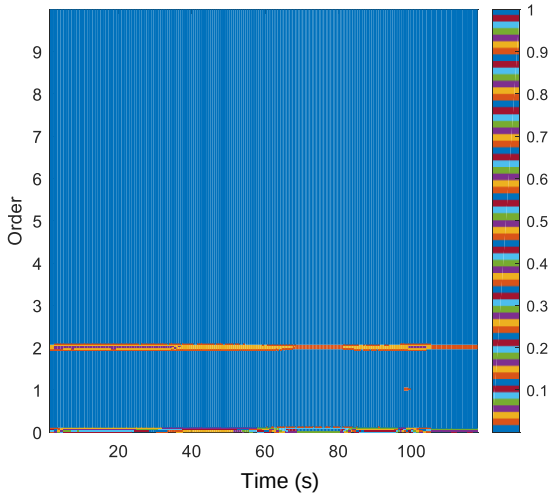

(c)

Figure D.3: Variable speed operation and order tracking of EPV signal for stator winding fault.

(a) variable speed profile (b) the spectrogram of the extended Park's vector (c) the spectrogram after order tracking and normalisation.

Figure.D.4. shows the order tracking spectrogram of vibration signals for the outer-race bearing fault and the 3.6X characteristics order is visible in the spectrogram. Similarly, for a damaged gear fault, the order tracking spectrograms can be generated.

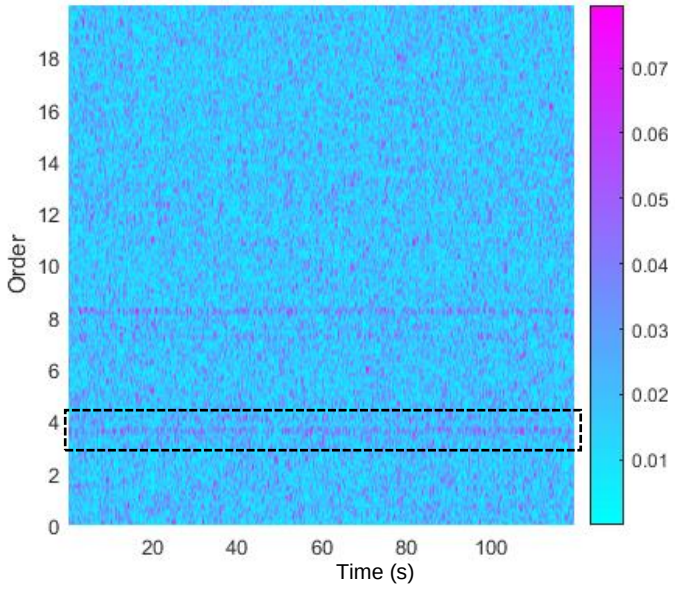

Figure D.4: Order tracked and normalised spectrogram for the bearing fault.

D.2.3 Convolutional neural network

A simplified block diagram of a CNN architecture is presented in Figure D.5. There are two main subsections of the network: feature learning and classification. Image classification using the CNN is a high computational intensive task as each pixel represents an input in the neural network. The 2-dimensional (2-D) convolution can be applied to an image with different sets of shared weights (or kernels) using a neuron map, in which the weights are optimised by a backward propagation algorithm. With convolution operation, local features of the input images can be identified for the classification. The convolution combined with pooling can reduce the dimensionality, allowing to simplify the structure of a fully-connected neural network for the classification. The rectified linear unit (ReLU) introduces the non-linearity to the system. Details of CNN training and analysis can be found in [15].

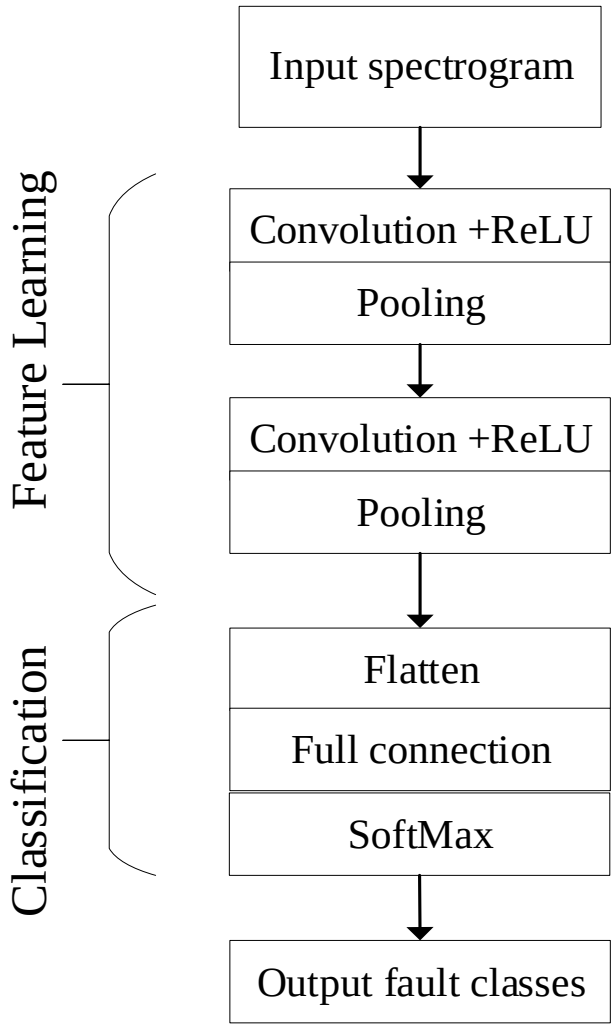

Figure D.5: A block diagram of a CNN architecture.

In the classification section, the learned features are utilised in a fully connected neural network architecture for classification. The Flatten operation is required to convert a 2-D image to the 1-D array for the classification. Based on derived features in the convolution and pooling operation, the classification task is done by the fully connected network, which finds the complex relations in the feature space. The SoftMax function converts the outputs of the fully connected network to probabilities of health classes. The highest probability value represents the output fault class of the network.

D.3 Experimental results and discussion

D.3.1 Experimental setup

The experimental test setup used in this study is shown in Figure D.6. The powertrain on the left side includes a 1.1 kW, 1450 rpm induction motor (IM) coupled to the 2-stages parallel shaft gearbox (GB) with 8.01 gear reduction. The internal components of the complete powertrain are disassembled and shown in Figure D.7. They include 8 bearings, 4 gears and 3 shafts. The gearbox is coupled to a permanent magnet synchronous generator (PMSG), and the generator output is connected to a fixed resistive load. Therefore, the powertrain load is proportional quadratically to the rotational speed. The output currents of the PMSG are measured and used to estimate the rotational speed of the electric powertrain. However, in real applications, an encoder is required to measure the speed.

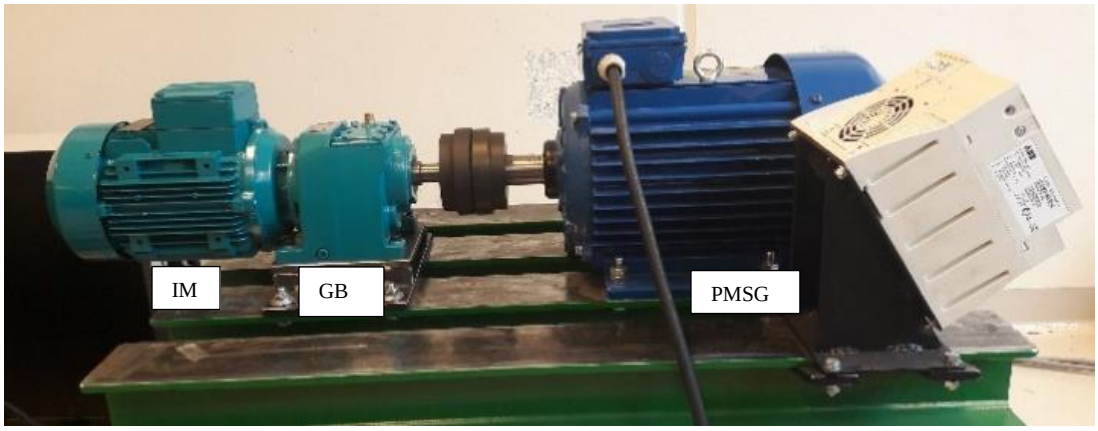

Figure D.6: The experimental setup.

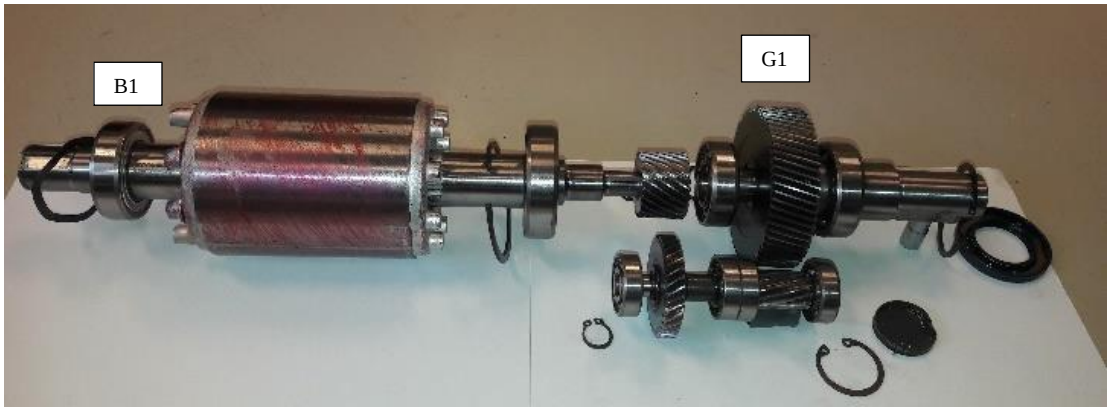

Figure D.7: The internal components of the electric powertrain.

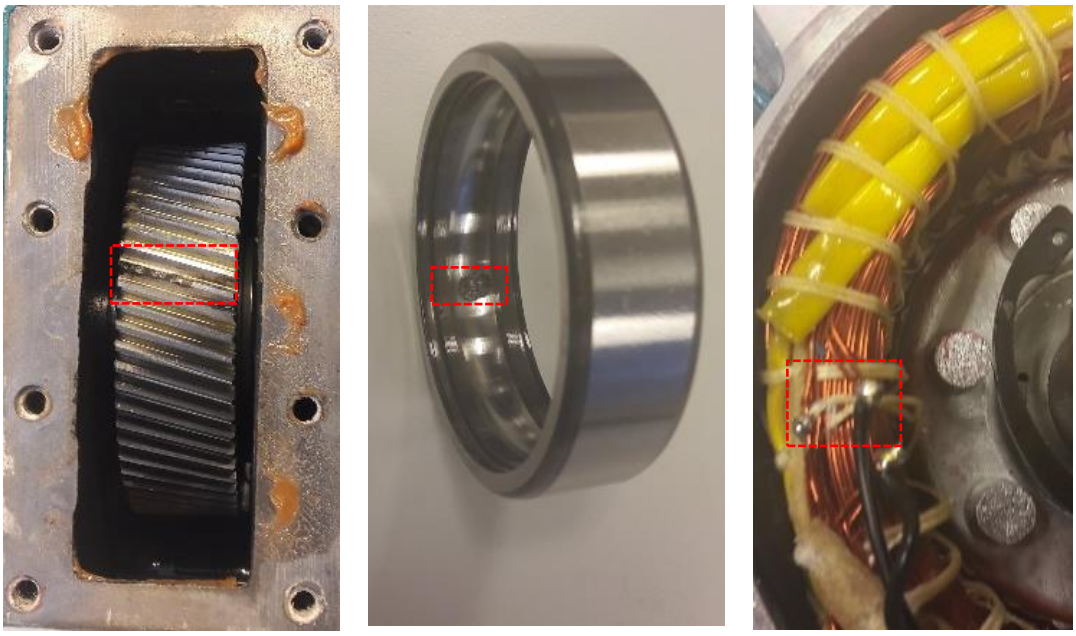

(a) (b) (c)

Figure D.8: The faulty components of electric powertrain. (a) damaged gear (b) outer-race damaged bearing (c) 10% inter-turn short circuit fault in the stator.

As shown in Figure D.8 (a), a small-scale damage is artificially produced in the large gear using an electric discharge machining. An outer-race defect on the induction motor bearing is made as shown in Figure D.8 (b). For stator winding faults, 10% inter-turn short circuit is seeded to one phase of the stator winding as shown in Figure D.8 (c). Eight fault cases with individual and multiple faults are conducted as shown in Tables D.1 and D.2.

For each fault case, the induction motor operates at constant speeds of 500, 1000, 1400 rpm and two variable speed profiles in Figure D.3 (a) the constant- and ramp speed and in Figure D.9 with the random speed. An acceleration sensor is placed on top of the gearbox, and the accelerometer data together with motor input currents are collected. The output currents and speed of the PMSG are also measured. With this test arrangement, data of 50 repeated runs for each fault class is collected, and each file contains 120-seconds data at the sampling rate of 20 kHz. Each file is subdivided into 20 pieces, producing 1000 samples for each fault class or 8000 samples for training and validation of all fault cases. Data of single fault cases, from Case 1 to Case 4 as shown in Table I, are used to train individual classifiers, where 75% of samples are used to train, and 25% of the data is used to validate. Data of multiple-fault cases, from Case 5 to Case 8 in Table II, are not used for any training task, and 25% of those data is used for validation.

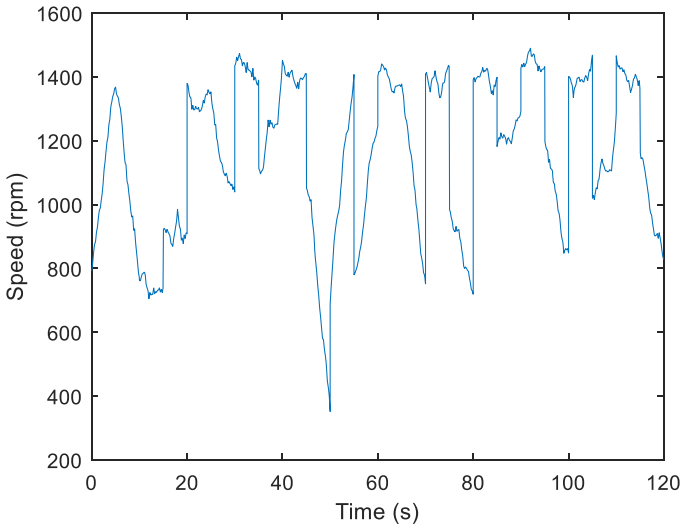

Figure D.9: A random-variable speed profile used in the experiments.

D.3.2 The experimental results

The confusion matrixes for individual classifiers are shown in Figure D.10 and the classification accuracies are summarized in Table I. The C1 classifier is trained to detect stator winding faults, and it gives an accuracy of 100 %. The classification accuracy of C2 - bearing outer-race fault classifier is 98.8 %, and the classification accuracy of C3 - gear fault classifier is 99.8%. In other words, all three classifiers work very effectively for detecting single faults.

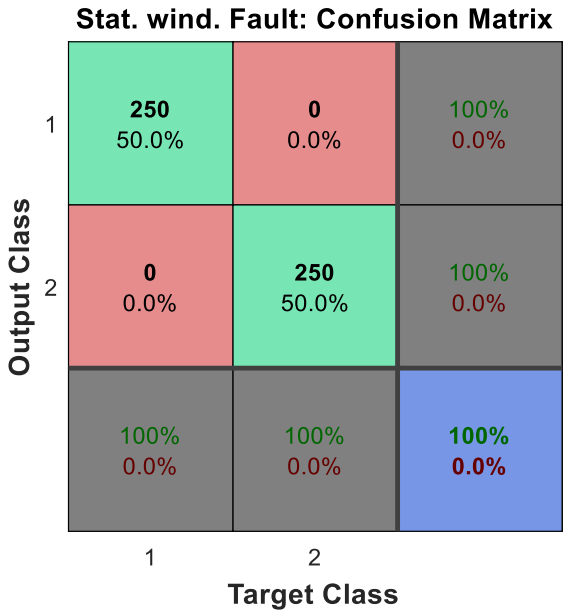

(a)

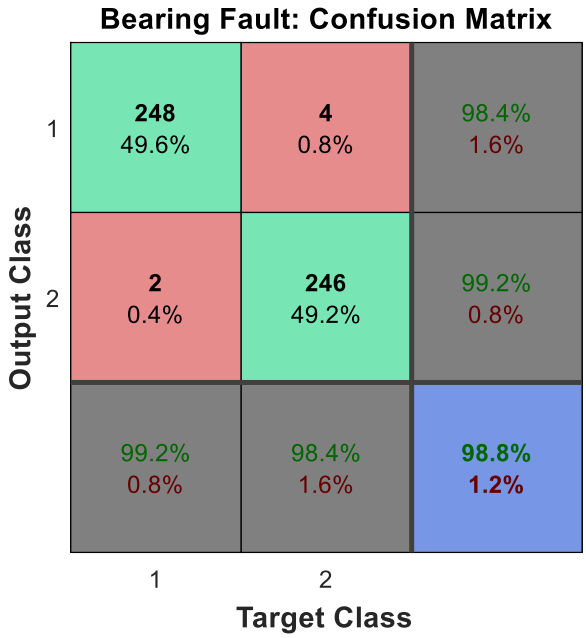

(b)

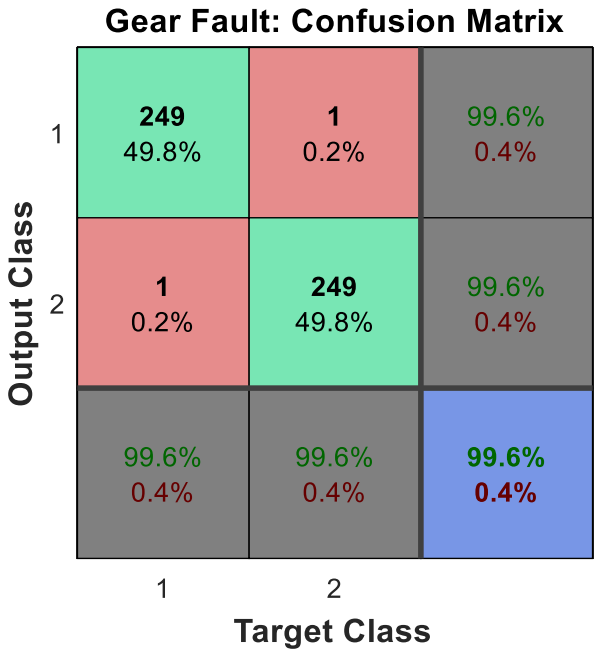

(c)

Figure D.10: The confusion matrixes of individual classifiers. (a) C1 classifier (b) C2 classifier (c) C3 classifier

The classification accuracies for multiple fault cases are summarized in Table II. The C1 classifier works well for detecting stator winding faults at any multiple fault cases considered in the study and classification accuracies are greater than 98.8 % in all the cases. The C3 classifier also effectively detects the

damaged teeth gear fault in multiple fault conditions with a minimum accuracy of 87.8 %. The weakest classifier in this study is the C2 classifier, which perform well in some multiple faults (Case 5 and Case 8), but not well for the outer-race bearing faults in Case 6 and Case 7, with the accuracies of 76.2 % and 71.5 %, respectively.

Table D.1: Performance summary: individual classifiers.

Case ID	Classifier ID	Component			Fault class	Test (%)	Accuracy
		Sw	B1	G1			
1	-	H	H	H	HHH	-	
2	C1	F	H	H	SHH	100	
3	C2	H	F	H	HBH	98.8	
4	C3	H	H	F	HHG	99.6	

Sw: stator winding, B1: bearing 1, G1: gear 1, .H: healthy, F: faulty.

Table D.2: Performance summary: multiple Faults.

Case ID	Component				Fault class	Test Accuracy (%)		
	Sw	B1	G1			C1	C2	C3
5	F	F	H	SBH		**100**	**86.8**	**87.8**
6	H	F	F	HBG		**99.8**	76.2	**98.6**
7	F	H	F	SHG		**100**	71.5	**100**
8	F	F	F	SBG		**98.4**	**90.2**	**99.4**

SBH: faulty stator, faulty bearing, and healthy gear.
HBG: healthy stator, faulty bearing and faulty gear.
SHG: faulty stator, healthy bearing and faulty gear.
SBG: faulty stator, faulty bearing and faulty gear.

D.4 Conclusion

In this study, a fault diagnosis system is proposed to detect faults in an electric powertrain in variable speeds and multiple fault conditions. The classifiers for the stator and gear fault diagnosis have given an excellence performance for fault classification under individual and multiple fault conditions. The experimental results confirm that the proposed can detect single and multiple faults under variable speed conditions Although the classifier for the bearing fault detection works well for single fault conditions, it has a limited capacity for classifying some multiple fault conditions.

Three types of localized faults in the stator winding, bearing and gearbox have been studied in this work, but the concept can be extended to other types of faults such as shaft unbalance, shaft misalignments, bearing inner race faults, gear misalignments, broken gear tooth etc. Furthermore, following improvements are suggested for future works:

1. Identify problems in the bearing fault classifier and improve its performance.
2. In this study, 10% inter-turn short circuit fault is considered, and the accuracy of the stator winding fault classifier for lesser faults (severities less than 10%) was not tested. Furthermore, one level of fault severity is studied for bearing and gear fault. Thus, testing accuracies of the classifiers for different fault severities is a possible extension of study.

References

[1] T. Javied et al., “A Study on Electric Energy Consumption of Manufacturing Companies in the German Industry with the Focus on Electric Drives,” *Procedia CIRP*, vol. 41, pp. 318-322, 2016

[2] National Research Council, “Cost, Effectiveness, and Deployment of Fuel Economy Technologies for Light-Duty Vehicles,” *Washington DC: The National Academies Press*, 2015.

[3] P. J. Tavner, “Review of Condition Monitoring of Rotating Electrical Machines,” IET *Elec. Power App.*, vol. 2, no. 4, pp. 215-247, July 2008.

[4] G.K Singh, S.A.A.S Saleh Al Kazzaz, "Induction Machine Drive Condition Monitoring and Diagnostic Research - a Survey", *Electric Power Systems Research*, vol. 64, pp. 145-158, February 2003.

[5] --, "ISO 18436-2:2014," International Organization for Standardization, 2014. [Online]. Available: https://www.iso.org/standard/50447.html. [Accessed December 2017].

[6] Z. Gao, C. Cecati and S. X. Ding, "A Survey of Fault Diagnosis and Fault-Tolerant Techniques—Part I: Fault Diagnosis with Model-Based and Signal-Based Approaches," *IEEE Trans. Ind. Electron.*, vol. 62, no. 6, pp. 3757-3767, 2015.

[7] Z. Gao, C. Cecati and S. X. Ding, "A Survey of Fault Diagnosis and Fault-Tolerant Techniques-Part II: Fault Diagnosis with Knowledge Based and Hybrid/Active Approaches," *IEEE Trans. Ind. Electron.*, vol. 62, no. 6, pp. 3768-3774, 2015.

[8] M. He and D. He, "Deep Learning Based Approach for Bearing Fault Diagnosis," *IEEE Trans. Ind. Appl.*, vol. 53, no. 3, pp. 3057-3065, 2017.

[9] F. Allbrecht, J.C. Appiarius, R.M. McCoy, E.L. Owen, D.K. Sharma, "Assessment of the reliability of motors in utility applications", *IEEE Trans. Energy Convers.* EC-1 (1) (1986) 39 /46.

[10] J. S. L. Senanayaka, S. T. Kandukuri, H.V. Khang and K. G. Robbersmyr, "Early Detection and Classification of Bearing Faults Using Support Vector Machine Algorithm," *IEEE Workshop on Electrical Machines Design, Control and Diagnosis (WEMDCD),* Nottingham, pp. 250-255, 2017.

[11] A. Marques Cardoso, S. Cruz, D. Fonseca, "Inter-Turn Stator Winding Fault Diagnosis in Three-Phase Induction Motors by Park's Vector Approach," *IEEE Trans. Energy Convers*, vol. 14, no. 3, pp. 595-98, 1999.

[12] --, "Vibration Analysis Definitions: Gearbox: Cracked or Broken Tooth," Mobius Institute, [Online]. http://www.mobiusinstitute.com/site2/item.asp?LinkID=8061&iVibe=1&sTitle=Gearbox, [Accessed June 2018].

[13] A. Brandt, "Noise and Vibration Analysis: Signal Analysis and Experimental Procedures," *Chichester, UK: John Wiley and Sons,* 2011.

[14] J. Blough, "Improving the Analysis of Operating Data on Rotating Automotive Components," *PhD Thesis University of Cincinnati*, College of Engineering, 1998

[15] N. Tajbakhsh, J. Y. Shin, S. R. Gurudu, R. T. Hurst, C. B. Kendall, M. B. Gotway and J. Liang, “Convolutional Neural Networks for Medical Image Analysis: Full Training or Fine Tuning?,” *IEEE Trans. Med. Imag.*, vol. 35, no. 5, pp. 1299-1312, 2016.

Paper E

Online Fault Diagnosis System for Electric Powertrains using Advanced Signal Processing and Machine Learning

Jagath Sri Lal Senanayaka, Huynh Van Khang, Kjell G. Robbersmyr

This paper has been published as:

J. S. Lal Senanayaka, H. Van Khang and K. G. Robbersmyr, “Online Fault Diagnosis System for Electric Powertrains Using Advanced Signal Processing and Machine Learning,” *2018 XXIII International Conference on Electrical Machines (ICEM)*, Alexandroupoli, pp. 1932-1938, 2018.
doi: 10.1109/ICELMACH.2018.8507171

Online Fault Diagnosis System for Electric Powertrains using Advanced Signal Processing and Machine Learning

Jagath Sri Lal Senanayaka, Huynh Van Khang, Kjell G. Robbersmyr

Department of Engineering Sciences, University of Agder Grimstad (4879), Norway
E-mails: {jagaths; huynh.khang; kjell.g.robbersmyr }@uia.no

***Abstract* – Online condition monitoring and fault diagnosis systems are necessary to prevent unexpected downtimes in critical electric powertrains. The machine learning algorithms provide a better way to diagnose faults in complex cases, such as mixed faults and/or in variable speed conditions. Most of studies focus on training phases of the machine learning algorithms, but the development of the trained machine learning algorithms for an online diagnosis system is not detailed. In this study, a complete procedure of training and implementation of an online fault diagnosis system is presented and discussed. Aspects of the development of an online fault diagnosis based on machine learning algorithms are introduced. A developed fault diagnosis system based on the presented procedure is implemented on an in-house test setup and the reliably detected results suggest that such a system can be widely used to predict multiple faults in the power drivetrains under variable speeds online.**

***Index Terms* —** online fault diagnosis, convolutional neural network, electrical fault detection, induction motors, electromechanical systems, gears, bearings.

E.1 Introduction

Electric powertrains are one of critical building blocks in automotive and manufacturing industries. Proper condition monitoring and fault diagnosis methods are essential to enhance their reliability and availability. Online fault diagnosis systems are useful to monitor the health status of critical machines, detecting the faults and planning maintenance schedules accordingly. However, a procedure to develop these online systems is not well detailed in literature.

Three main approaches, namely model-based-, signal-based- and knowledge-based, are widely used to implement fault diagnosis systems [1-3]. Furthermore, a hybrid approach is also a promising option by combining the mentioned methods in various ways [4]. In the model-based approach, the dynamic model of a system is developed using first-principle physics. The developed model should be sufficiently sensitive to represent different fault situations. The model parameters should be tuned properly to match real-plant behaviours. Then the responses of the model are compared with those of the real system via measured system parameters. A threshold is applied to the residual signal of the comparison to diagnose the faults [1-3]. This diagnosis method is reliable if the system model and its parameters are well identified in advance. However, identifying a detailed mathematical model to represent various machine health statuses is very difficult and time consuming. To address such a challenge, system identification, parameter estimation and observers are used to improve performance of the model-based approach [2].

In the signal-based approach, various signal processing methods, e.g. wavelet-, fast Fourier-, short-time Fourier transforms can be used to find fault characteristic frequencies for the fault diagnosis [5-6]. This approach requires expertise on signal processing and fault knowledge. However, missing harmonics of the characteristic frequencies associated with faults in the spectrum cannot guarantee that the system is healthy [7]. The knowledge-based approach combines the advantages of signal processing and modern artificial intelligent methods for a better fault diagnosis [1-3]. In this approach, a data-driven model can be developed from a large amount of measured data in various system conditions. Statistical and machine learning techniques can be used to develop such a data-driven model. If the data is sufficiently available, data-driven models can capture the health statuses of a system [8-9]. A predictive model based on data-driven models can detect the

faults without generation and analysis of the residual signals. Further details of data-driven models are discussed in section E.2.

In complex fault scenarios, e.g. multiple faults occur in a system in variable speed conditions, defining a clear rule to detect and classify faults is difficult or a given rule can be complicated. In addition, the data collected via sensors can be noisy or interfered by other sources. For example, vibration signals can be mixed of internal machine- and external vibrations. Furthermore, the data can be affected by electromagnetic interference (EMI) in the motor drive system. Therefore, by considering all above factors, a hybrid approach based on an advanced signal processing and machine learning is selected in this work regardless of some challenges when building a data-driven model based on machine learning-algorithm. The model accuracy, robustness, generalizability, complexity and computational speed are among important performance indicators, which should be addressed in designing an online fault diagnosis system [8]. In this study, a complete procedure to develop an online fault diagnosis system for an electric powertrain is presented and discussed. Further details of a fault diagnosis algorithm based on this procedure can be found in [9].

This paper is organised as follows: in Section E.2, the development procedure of an online fault diagnosis system is presented and discussed. In Section E.3, the development stages of integrating a predictive model into the online diagnosis system are described in detail. The experimental test setup, data and results are discussed in section E.4. The conclusion of the study is presented in section E.5.

E.2 Development procedure of the online fault diagnosis system

Figure E.1 shows a procedure for implementing an online fault diagnosis system. The system can be developed in three steps, namely development of a data-driven model, integration of the trained predictive model into the online diagnosis system, and development of an embedded system. In this study, the first two steps are presented and discussed. In many applications, the first two steps are sufficient for an online fault diagnosis. However, in more critical machines, the fault diagnosis system can be implemented as an embedded system or integrated into the existing control system, being placed closer to the machine for monitoring the health status. The algorithm development is an iterative process, which is to find the best

machine learning model [8]. In this iterative process, the important steps are:

- Analysis of the system requirements
- Sensor selection and raw data analysis
- Signal processing, feature extraction and dimension reduction in the feature space
- Integration of suitable data fusion methods
- Analyzing the model performance, parameter optimization and selection of the best learning algorithm

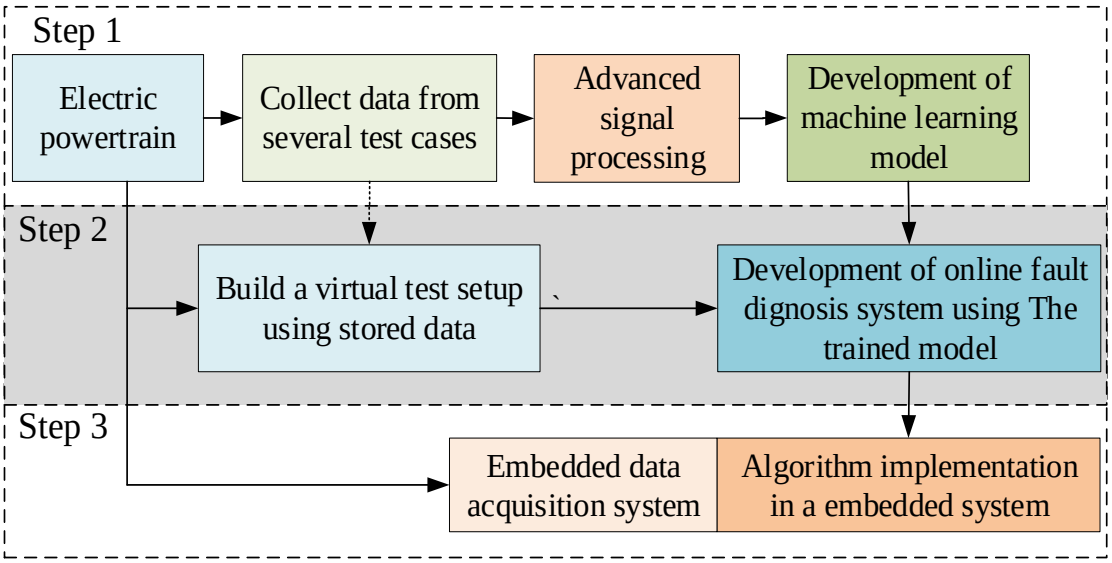

Figure E.1: The development procedure of the online fault diagnosis system.

E.2.1 System requirements

In this study, the requirements of a fully operational online fault diagnosis system are suggested. A block diagram of the developed fault diagnosis system is shown later in Figure E.2. The suggested system requirements are based on domain knowledge, critical components and failure rate analysis.

- The diagnosis system shall be able to detect and classify multiple faults in variable speed conditions reliably.
- The diagnosis system shall use a reasonably small number of sensors.
- The algorithm shall use a minimum training data for multiple fault cases.
- Fault types shall be detected: inter-turn fault in a stator winding, bearing and gear faults.

- The system shall be robust against sensor signal noises and interferences.

E.2.2 Sensor selection and raw data analysis

Current and vibration signals are selected as the inputs of the fault diagnosis system. Thus, a right selection of vibration and current transducers is important since each sensor is designed to work within certain operating ranges and sensitive levels, which should be matched with the fault diagnosis system requirements. Shielded cables must be used in the data acquisition system to reduce the external interference. The location of vibration sensors is very important to collect properly vibration information. The vibration sensors shall be tightly fixed to the machine to obtain sufficiently required information.

After the sensor selection and installation, the data must be collected in different health statuses and operating conditions of the electric powertrain. Then the collected raw data shall be analysed to find the statistical distribution of the signals, and the analysed data shall be normalised via a suitable normalization method. After the normalization, the signals shall be further processed using advanced signal processing methods discussed in Section E.2.3.

E.2.3 Advanced signal processing, feature extraction and dimension reduction

Once having the normalization on the collected data, the next step is to process the data and extract the important features from the signals for detecting faults. The domain knowledge-based features are the most reliable among features extracted by domain knowledge-, statistical- and deep learning algorithms since they are based the physical phenomena of the powertrain. The features based on statistical- and deep learning algorithm or using pattern recognition do not represent a direct physical meaning.

Domain knowledge-based features can be extracted by investigating the forcing frequencies associated with faults and powertrain parameters. If the fault severity and rotational speed are low, or signals are noisy, advanced signal processing methods are required to extract the hidden information associated with the faults in the collected signals. Various signal processing techniques used to extract the domain knowledge-based features can be found in literature [5], [10-14], and key techniques are summarized in Table E.1.

Table E.1: Signal processing techniques for fault diagnosis applications.

Signal processing objectives	Techniques
Noise and signal separation [5], [10-11]	Digital filters Time synchronous analysis Order tracking and normalizing Wavelet denoising Denoising autoencoders Adaptive noise cancellation Discrete/random separation (DRS) Cyclostationary analysis and spectral correlation
Time domain analysis [5]	Root mean square and autocorrelation
Frequency domain analysis [5], [12]	Fast Fourier transformation (FFT) Spectrum averaging
Time-frequency analysis [5], [13]	Short time Fourier transformation (STFT) and Wavelet transform (WT)
Instantaneous frequency and phase analysis [5], [14]	Hilbert transform Envelop analysis
Signals and system behavior [5]	Convolution
Analysis of the impulsivity [5]	Spectral kurtosis and the kurtogram

Statistical features can be generated without any prior knowledge of faults. The statistical features can capture patterns in the signals in various working conditions, which can be used in the fault classification based on machine learning algorithms. Some commonly used statistical features from time and frequency domain signals are the signal mean, standard deviation, minimum, maximum, skewness, kurtosis, crest factor, etc. [15].

Dimension reduction in the feature space is the next step after the feature extraction process. This step is to simplify the model and reduce the curse of dimensionality and training time. Further, it's useful to avoid the model overfitting, recognising noises as a concept in the training phase. To reduce the dimensions, new features are created by combining existing features based on the dimensional methods such as principle component analysis, factor analysis, and complex nonlinear techniques [16]. Alternatively, the best features are selected by the filtering strategy (e.g using information gain), wrapper strategy (e.g. accuracy-

guided search) and embedded strategy [17]. After reducing the feature space, those features can be fed to the supervised machine learning algorithms with the health class labels.

Feature generation based on deep learning is an alternative way to extract features. The original concept of using deep learning algorithms, e.g. Convolutional neural network (CNN), is to combine feature extraction, dimension reduction and classification in one algorithm. The CNN algorithm combines those tasks in image classification applications [18]. Using sparse autoencoders, features can be also generated in an unsupervised way and then the generated features can be used in a supervised classification algorithm [19]. However, an automatic feature extraction from raw data is not feasible in most of fault diagnosis applications. The extraction process should be always combined with advanced signal processing methods. In other words, using CNNs alone, a feature extraction is partly automatic in fault diagnosis applications.

E.2.4 Integration of data fusion methods

To reduce the noise effect and increase the accuracy and robustness of machine learning based classifications, data fusion methods should be applied on collected data and extracted features. The fusion methods can be applied at sensor, feature or decision level. In the feature level fusion, the features from multiple signals are combined to increase the feature space. In the decision level fusion, the fault classification can be done based on individual signals and the output of each classifier can be fused to get the final decision. One of the widely used decision level methods is ensemble learners, namely probabilistic approach, majority voting, weighted majority vote and Naïve Bayes combiner, in which the outputs of several classifiers are combined to create a more accurate classifier [20].

E.2.5 Analysing the model performance, parameter optimization and selection of the best learning algorithm

To assess the performance of a data-driven model, the generalizability, accuracy, robustness, complexity and computational speed are selected as the main performance indicators. Based on these indicators and system constraints, the best algorithm among trained models is identified and the test data set is then used to

validate the final model. The most commonly used machine learning algorithms for fault diagnosis applications are given in Table E.2 [8], [21].

Table E.2: Machine learning techniques for fault diagnosis applications.

Algorithms	Remarks
Support vector machine (supervised classification)	Linear SVM: fast training and prediction speed with less memory usage, used only for linear decision boundary cases. Nonlinear SVM: slow in both training and prediction, and requiring considerable memory, good performance for nonlinear cases.
Multi-layer perceptron (supervised classification)	Slow in training but moderate speed for prediction, requiring many training cases and large memory.
Decision tree (supervised classification)	Fast in both training and predations cases, requiring less training cases, possible model overfitting.
Convolutional neural networks (supervised deep learning)	large training samples and training time, but moderate prediction time, capturing complex spatial relationships from the spectrograms.
Sparse-autoencoders (unsupervised deep learning)	Applicable to feature extraction and feature dimension reduction, slow training process, requiring individual classifiers.

The generalisability is an important indicator because the algorithm should be able to detect and classify faults other than training and test datasets. Otherwise, there is no use of the trained algorithm. Overfitting is one of the most critical issues of any machine learning algorithm and may result in a reduction of the generalisability since the random noises is defined as a concept in the model. If the model is not properly trained, the model will only try to mimic the input data, thus it cannot be used in generalized fault diagnosis applications [22]. To address the overfitting problem, the data should be sufficiently enhanced to train the model. Adding a regularisation term into the cost function of the model is an alternative solution in many neural network models. Using the dropout is another technique for reducing the model overfitting, where some of the neurons are randomly disabled in the training process. Furthermore, to avoid the overfitting, the data can be subdivided into three subsets, namely training-, validation- and test set. The

training set is used to train the model, and the model performance is evaluated using the separate data set for validation.

The accuracy of fault classifications is also an important performance measure of a machine learning model. Further, the algorithm should be able to give a consistent accuracy when the input data is noisy or distorted. If the model accuracy is not good, the model parameters can be optimized and retrained until obtaining a good model. Machine learning algorithms require hyperparameters, which should be properly set according to the intended application. Optimization methods can be applied for tuning the hyperparameters of machine learning algorithms, e.g Bayesian optimization and grid search. Further, complexity and computational burden of algorithms need to be carefully evaluated to reduce the cost and increase the implementation speed.

E.3 Description of the development stages for an online fault diagnosis system

The development procedure detailed in the section E.2 is used to develop an algorithm to detect multiple faults in electric powertrain under variable speeds. In this section, the development stages of a machine learning algorithm for online fault diagnosis system are presented, but the development of an embedded system is not considered.

E.3.1 Stage-1: Advanced signal processing and development of machine learning algorithms

According to the system requirements or objectives (in Section E.2. 1) of detecting multiple faults, namely inter turn in the stator winding, bearing and gear faults based on machine learning algorithms, a CNN based binary classifier bank is selected for the fault diagnosis application in this work. Park's vector for the phase currents, order tracking and normalisation for vibration and current signals, short-time Fourier transform (STFT) for generating patterns or spectrograms are tools to process the collected signals. The rationales of using the mentioned methods can be found in literature and summarized in the Table E.3.

Table E.3: Selection of signal processing and machine learning methods.

Objectives	Selected methods	refs.
Inter-turn faults in stator winding, bearing and gear faults	Park's vector for the phase currents, short-time Fourier transform (STFT),	[23-25]
Variable speeds	Order tracking and order normalisation	[10-11]
Multiple fault detection and classification	CNN for the semi-automated feature extraction and classification under noises, variable speed and load conditions.	[18]

A block diagram of the developed algorithm detailed in [9] is given in Figure E.2. First the current, vibration and the rotational speed signals of the electric powertrain are collected. Then the order tracking algorithm [10-11] is used to normalize the speed variation of the vibration and current signals. The shaft speed and angular sampling are used in the order tracking and normalisation algorithm.

Next the processed signals are converted into spectrograms using STFT. Both vibration and current signal-based spectrograms are combined to create an extended spectrogram, which is fed into the CNN-based classifier. Based on the time-frequency features in the spectrograms, the CNN algorithm finds patterns or images to classify different health classes, e.g. good or defective, of the components.

The individual classifiers of C1 – stator winding fault classifier, C2 – bearing fault classifier and C3 – gear fault classifier, are first trained using the known health classes. Since the binary classifiers are used for each fault type, 4 health classes, namely healthy, stator winding fault, bearing fault and gear fault are sufficient for the training. However, the algorithm can classify 8 health classes, which include the trained single health classes and untrained multiple fault health classes. After that, the trained model is used to predict health classes (healthy or faulty) from new signals.

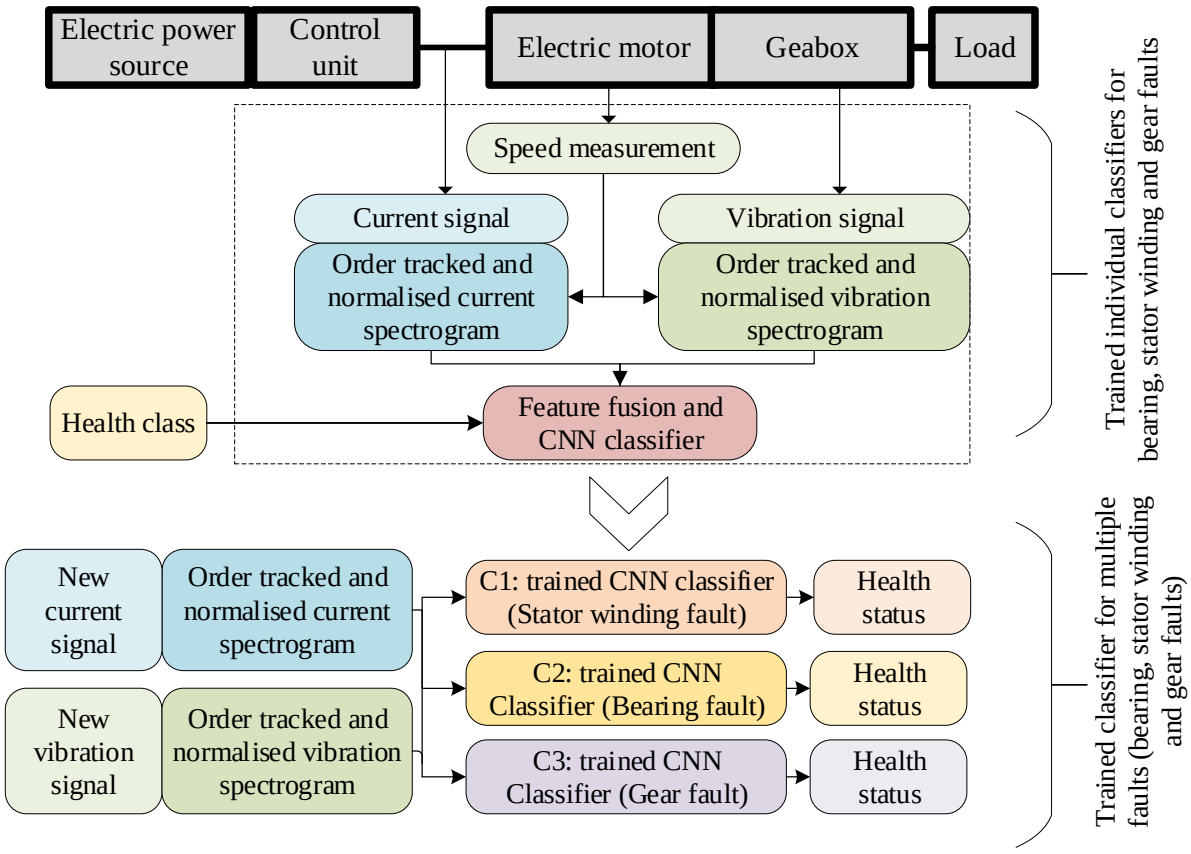

Figure E.2: A block diagram of training and testing of fault diagnosis system in the step-1 of the development process.

E.3.2 Stage-2: Development of online fault diagnosis system

Figure E.3 shows a block diagram of the developed online fault diagnosis system. There are two subunits: health class predictor and decision maker. In the first subunit, the health class of the collected signal is predicted. Next, several consecutive results are collected and analyzed in the second subunit for the final decision.

E.3.3 Data acquisition and processing buffer

For an online operation of the algorithm, two nested buffers have been used. In the data acquisition buffer, the data inflow is controlled. A large data processing buffer is used in case the length of the dataset is not sufficient for data processing. Further, this data set is sent for data preprocessing and feature generation, where the

extracted features via spectrograms are order-normalized. The trained CNN classifier bank is applied on these processed spectrograms to classify the faults.

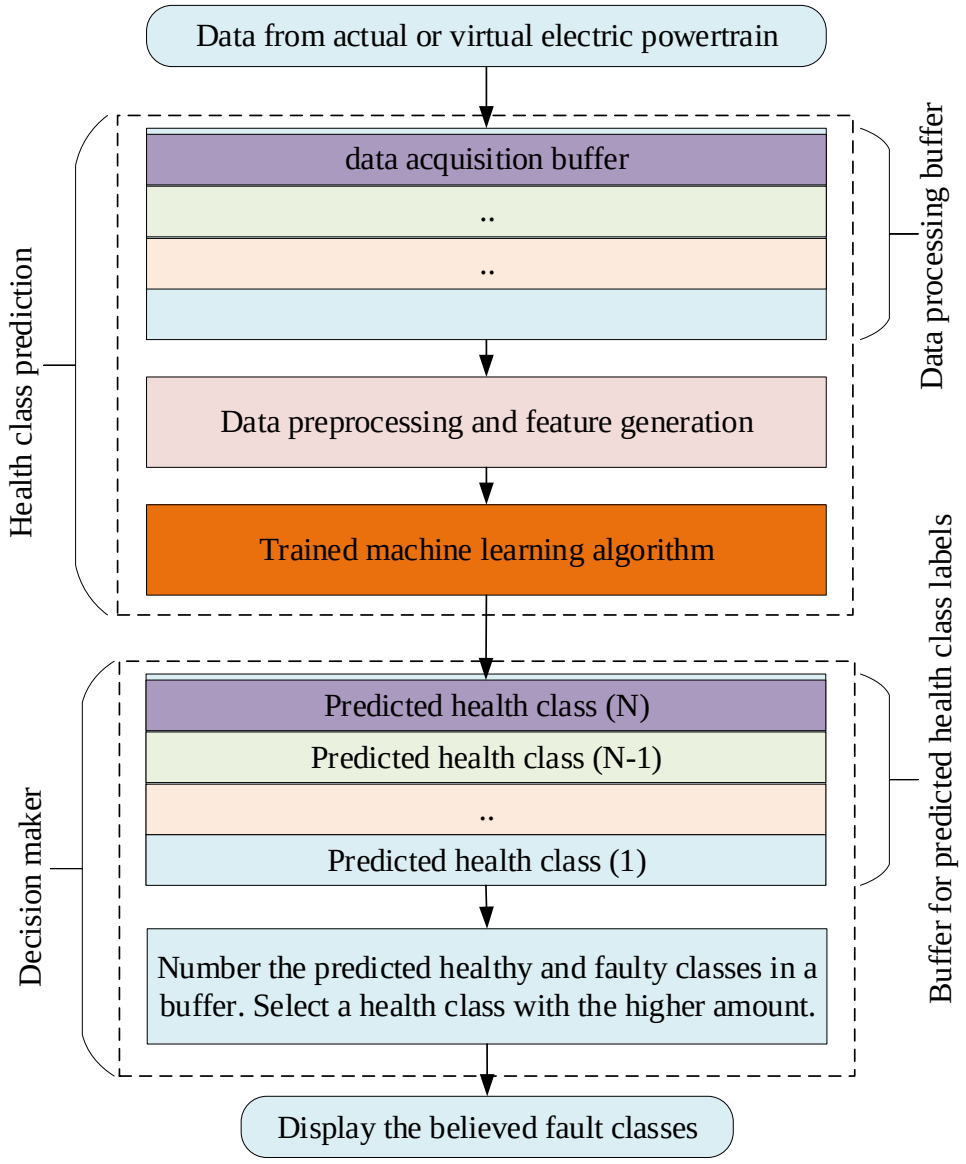

Figure E.3: The algorithm used in the online fault diagnosis system in the step 2.

E.3.4 Decision criterion of the online diagnosis algorithm

Confusion matrixes and Receiver Operating Characteristic (ROC) are commonly used to analyse the performance of the trained machine learning model. In online fault diagnosis applications, these measures cannot be obtained because the prior information of the faults is unknown. Therefore, a new decision criterion is

proposed in this study. Each classifier has three parallel buffers to store the predictions. In each buffer, the health class label with the maximum count is selected as the final decision. This method can compensate for false predictions from unexpected noises or interferences.

E.4 Experimental tests and results

An electric powertrain shown in Figure E.4 is used to collect data for training, validation and implementation of the developed online fault diagnosis algorithm. The internal components of the electric powertrain are shown in the Figure E.5. As shown in Figure E.6, seeded faults are introduced to the selected gear, bearing and stator winding. Then the data is collected from 8 different single and multiple fault conditions in various speed profiles.

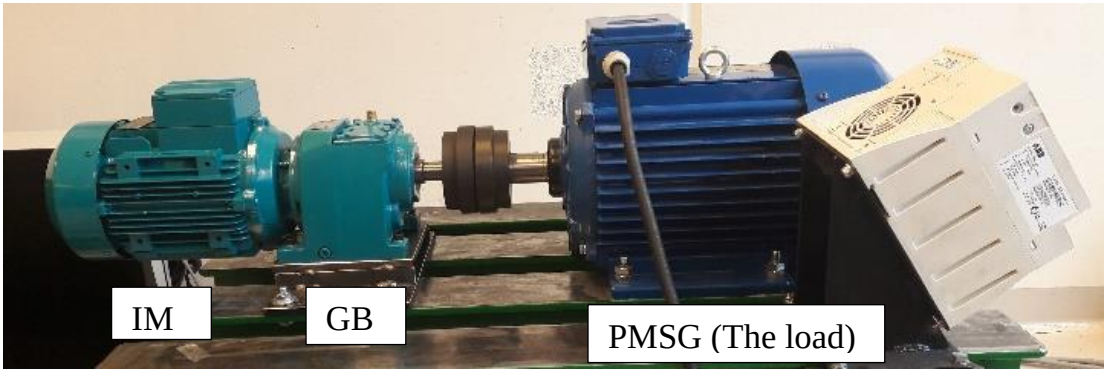

Figure E.4: The experimental setup (IM: Induction motor, GB: Gearbox, PMSG: Permanent magnet synchronous generator).

Figure E.5: The internal components of the electric powertrain.

The speed profiles include constant speeds and variable speeds as described in [9]. Based on the collected data, 50% of the data is used to train the model. 15% of the data is used for the validation and another 15% of the data is used to test the algorithm. The remaining 20% of the data is used for testing the online fault diagnosis system performance.

Three binary classifiers work in parallel, and each of them focuses on one type of fault. First, the individual CNN classifiers are implemented and trained using the training data. Then the parameters of the algorithm are optimized using Bayesian optimisation algorithm [26] until getting good performances for the validation dataset. Finally, the optimized algorithm is tested using the test dataset. Further, the online fault diagnosis system is implemented as discussed in section E.3. The interface of the implemented online fault diagnosis system is shown in Figure E.7, where the powertrain is in healthy condition. The measured vibration, currents and estimated rotor speed are shown using three graphs. The displayed signals are online analysed by the proposed algorithm and the results are displayed in the pie charts.

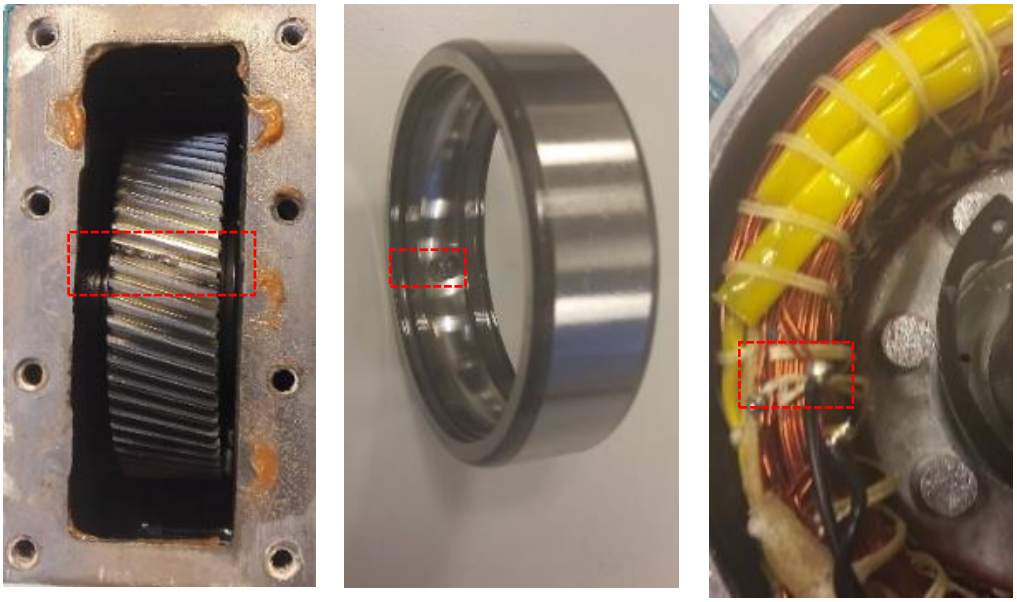

(a) (b) (c)

Figure E.6: The faulty components of the powertrain. (a) damaged gear (b) outer-race damaged bearing (c) 10% inter-turn short circuit fault in the stator.

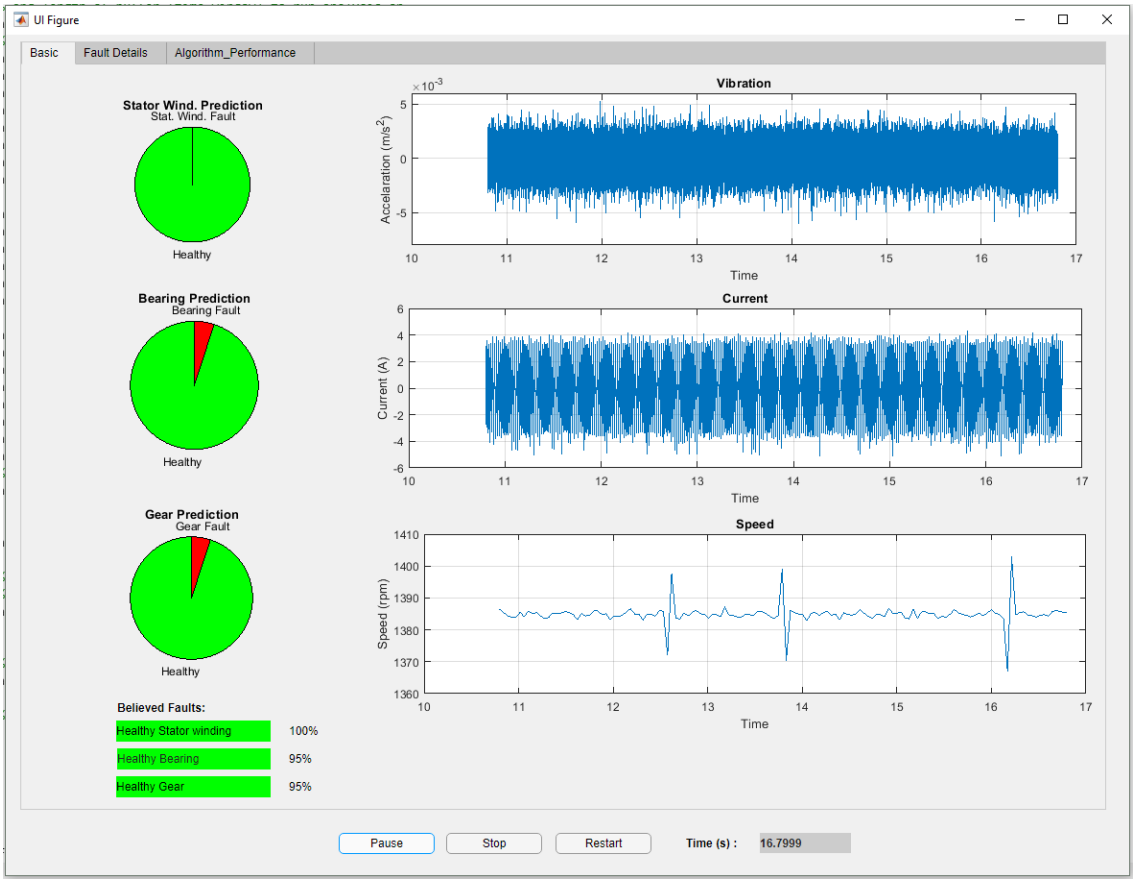

Figure E.7: The interface of the developed online fault diagnosis system for the electric powertrain.

E.4.1 Stage-1: The machine learning model performances

The classification accuracies of the trained binary classifiers with the test dataset are shown in Table E.4. For all the test cases, high classification accuracies have been obtained. The classification accuracies for each classifier with mixed fault cases are given in Table E.5. The C1 and C3 classifiers perform well for multiple fault cases. However, the classification accuracy of the C2 is low in multiple fault cases.

Table E.4: Performance summary: individual classifiers.

Case ID	Classifier ID	Component			Fault class	Test (%)	Accuracy
		Sw	B1	G1			
1	-	H	H	H	HHH	-	
2	C1	F	H	H	SHH	100	
3	C2	H	F	H	HBH	98.8	
4	C3	H	H	F	HHG	99.6	

Sw: stator winding, B1: bearing 1, G1: gear 1, H: healthy, F: faulty.

Table E.5: Performance summary: multiple faults

Case ID	Component			Fault class	Test Accuracy (%)		
	Sw	B1	G1		C1	C2	C3
5	F	F	H	SBH	**100**	**86.8**	**87.8**
6	H	F	F	HBG	**99.8**	76.2	**98.6**
7	F	H	F	SHG	**100**	71.5	**100**
8	F	F	F	SBG	**98.4**	**90.2**	**99.4**

SBH: faulty stator, faulty bearing, and healthy gear.
HBG: healthy stator, faulty bearing and faulty gear.
SHG: faulty stator, faulty bearing and faulty gear.
SBG: faulty stator, faulty bearing and faulty gear.

E.4.2 Stage-2: Performances of the online fault diagnosis system

The performance of the online fault diagnosis system for three fault cases is given in Figure E.8. Each pie chart shows the percentage of the predicted class labels in each classifier for 20 consecutive predictions. The prediction label with the highest count is selected as the believed fault type.

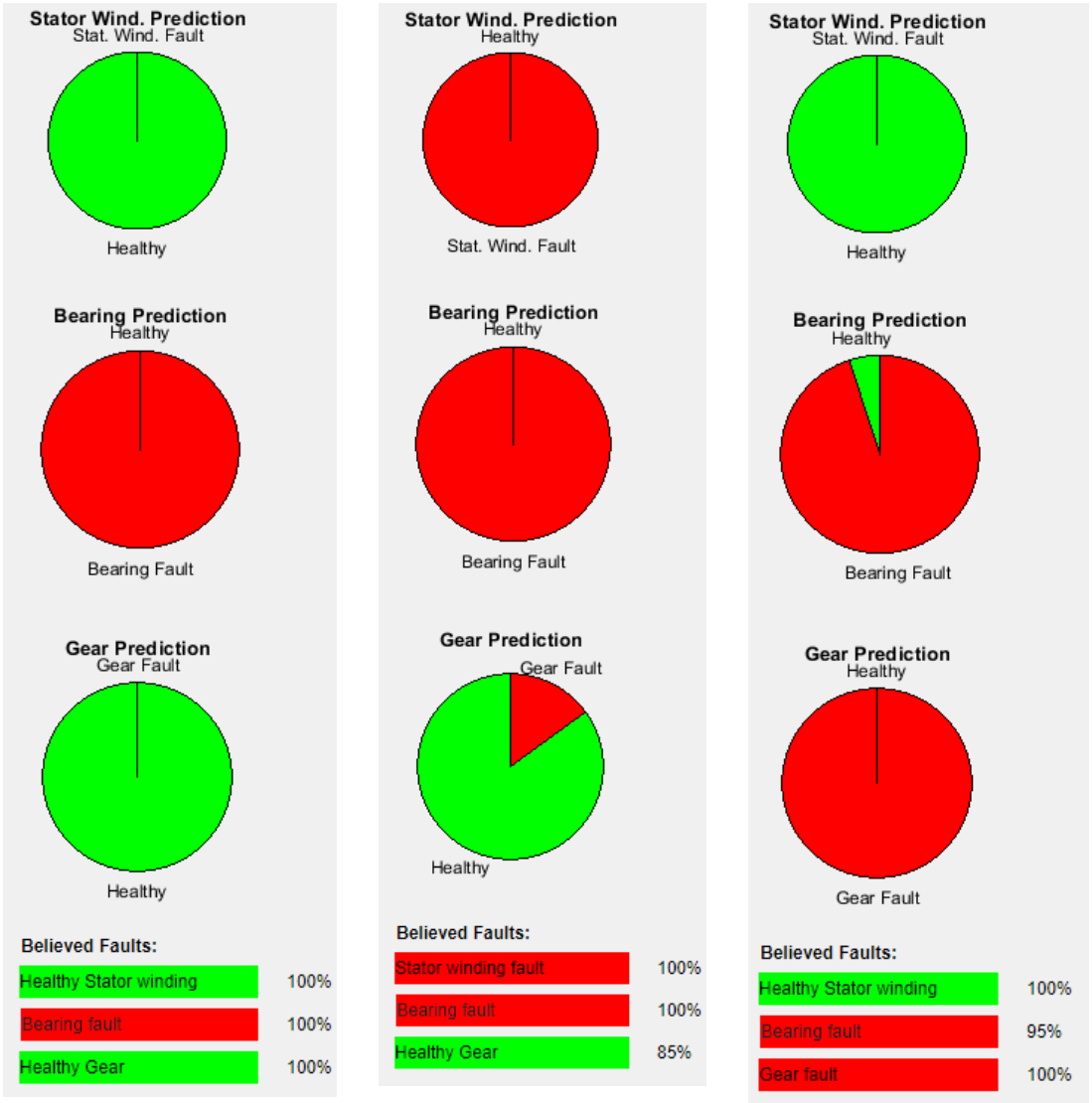

(a) (b) (c)

Figure E.8: A snap shot of online fault diagnosis system performance (a) bearing fault (b) stator winding and bearing faults (c) bearing and gear faults.

E.5 Conclusion

In this study, a complete procedure of developing an online fault diagnosis system is presented. The developed fault diagnosis system based on this suggested procedure is tested with the experimental data and implemented online on an in-house setup. The fault diagnosis system shows good performance in training cases, and the online fault diagnosis algorithm can predict multiple faults in the electric powertrain under variable speeds reliably. The developed fault diagnosis system can be used for online monitoring and detecting multiple faults in electric powertrains.

References

[1] X. Dai and Z. Gao, "From Model, Signal to Knowledge: a Data-Driven Perspective of Fault Detection And Diagnosis," *IEEE Trans. Ind. Informat.*, vol. 9, no. 4, pp. 2226-2238, 2013.

[2] Z. Gao, C. Cecati and S. X. Ding, "A Survey of Fault Diagnosis and Fault-Tolerant Techniques - Part I: Fault Diagnosis with Model-Based and Signal-Based Approaches," *IEEE Trans. Ind. Electron.*, vol. 62, no. 6, pp. 3757-3767, 2015.

[3] Z. Gao, C. Cecati and S. X. Ding, "A Survey of Fault Diagnosis and Fault-Tolerant Techniques - Part II: Fault Diagnosis with Knowledge-Based and Hybrid/Active Approaches," *IEEE Trans. Ind. Electron.*, vol. 62, no. 6, pp. 3768-3774, 2015.

[4] D. Jung and C. Sundström, "A Combined Data-Driven and Model-Based Residual Selection Algorithm for Fault Detection and Isolation," *IEEE Trans. on Control Sys. Tech.*, vol. PP, no. 99, pp. 1-15, 2017.

[5] R. B. Randall, "Vibration-based Condition Monitoring: Industrial, Aerospace and Automotive Applications", *Wiley*, Hoboken. Available from: ProQuest Ebook Central. [25 March 2018].

[6] S.T. Kandukuri, J.S.L. Senanayaka, H.V. Khang, H.R. Karimi, and K. G. Robbersmyr, "Current Signature-Based Fault Diagnosis of Field-Oriented and Direct Torque-controlled Induction Motor Drives," *Proceedings of the Institution of Mechanical Engineers, Part I: Journal of Systems and Control Engineering*, vol 231, no. 10, pp. 849-866,2017

[7] P. Nectoux, R. Gouriveau, K. Medjaher, E. Ramasso, B. Morello, N. Zerhouni and C. Varnier , "PRONOSTIA: an Experimental Platform for Bearings Accelerated Life Test," *IEEE International Conference on Prognostics and Health Management*, Denver, CO, USA, 2012.

[8] --, "Mastering Machine Learning: A Step-by-Step Guide with MATLAB", MathWorks Inc, [Online] https://se.mathworks.com/content/dam/mathworks/tag-team/Objects/m/machine-learning-workflow-ebook.pdf, [Accessed March 2018].

[9] J. S. L. Senanayaka, H.V. Khang and K. G. Robbersmyr, "Multiple Fault Diagnosis of Electric Powertrains under Variable Speeds using Convolutional Neural Networks," The XXIII International Conference on Electrical Machines - ICEM 2018, pp. 1-6, 2018 (accepted).

[10] A. Brandt, "Noise and Vibration Analysis: Signal Analysis and Experimental Procedures," *Chichester, UK: John Wiley and Sons*, 2011.

[11] J. Blough, "Improving the Analysis of Operating Data on Rotating Automotive Components," *PhD Thesis University of Cincinnati*, College of Engineering, 1998.

[12] J.W. Cooley, and J.W. Tukey, "An Algorithm for the Machine Calculation of Complex Fourier Series, " *Mathematics of Computation*, vol. 19, no 90 pp., 297–301, 1965

[13] A. Bouzida, O. Touhami, R. Ibtiouen, A. Belouchrani, M. Fadel, and A. Rezzoug, "Fault Diagnosis in Industrial Induction Machines through Discrete Wavelet Transform," *IEEE Trans. Ind. Electron.*, vol. 58, no. 9, pp. 4385–4395, Sep. 2011.

[14] A. Baccigalupi and A. Annalisa, "The Huang Hilbert Transform for evaluating the instantaneous frequency evolution of transient signals in non-linear systems," *Measurement,* vol. 86, pp 1-13, 2016

[15] M. D. Prieto, G. Cirrincione, A. G. Espinosa, J. A. Ortega and H. Henao, "Bearing Fault Detection by a Novel Condition-Monitoring Scheme Based on Statistical-Time Features and Neural Networks," *IEEE Trans. Ind. Electron.*, vol. 60, no. 8, pp. 3398-3407.

[16] L. V. D. Maaten E. Postma and J. V. D. Herik, "Dimensionality Reduction: A Comparative Review", *Tilburg centre for Creative Computing*, Tilburg University, The Netherlands, 2009.

[17] G. Chandrashekar, F. Sahin, "A Survey on Feature Selection Methods," *Computers & Electrical Engineering*, vol. 40, no. 1, pp 16-28, 2014.

[18] N. Tajbakhsh, J. Y. Shin, S. R. Gurudu, R. T. Hurst, C. B. Kendall, M. B. Gotway and J. Liang, "Convolutional Neural Networks for Medical Image Analysis: Full Training or Fine Tuning?," *IEEE Trans. Med. Imag.*, vol. 35, no. 5, pp. 1299-1312, 2016.

[19] E. Hosseini et al., "Deep Learning of Part-Based Representation of Data Using Sparse Autoencoders With Nonnegativity Constraints", *IEEE Trans. Neural Netw. Learn. Syst.*, vol. 27, no. 12 pp. 2486-98, 2016.

[20] L. I. Kuncheva, "Combining Pattern Classifiers: Methods and Algorithms," *New Jersey*, John Wiley & Sons, 2014.

[21] Z. Ge, Z. Song, S. X. Ding and B. Huang, "Data Mining and Analytics in the Process Industry: The Role of Machine Learning," in *IEEE Access*, vol. 5, pp. 20590-20616, 2017.

[22] K. P. Burnham, D. R. Anderson, "Model Selection and Multimodel Inference (2nd ed.)" *Springer-Verlag*, 2002

[23] J. S. L. Senanayaka, S. T. Kandukuri, H.V. Khang and K. G. Robbersmyr, "Early detection and classification of bearing faults using support vector machine algorithm," *IEEE Workshop on Electrical Machines Design, Control and Diagnosis (WEMDCD)*, Nottingham, pp. 250-255, 2017.

[24] A. Marques Cardoso, S. Cruz, D. Fonseca, "Inter-turn Stator Winding Fault Diagnosis in Three-Phase Induction Motors by Park's Vector Approach," *IEEE Trans. Energy Convers*, vol. 14, no. 3, pp. 595-98, 1999.

[25] --, "Vibration Analysis Definitions: Gearbox: Cracked or broken tooth," Mobius Institute, [Online]. http://www.mobiusinstitute.com/site2/item.asp?LinkID=8061&iVibe=1&sTitle=Gearbox, [Accessed March 2018].

[26] J. Snoek, J, H. Larochelle, R.P. Adams, "Practical Bayesian Optimization of Machine Learning Algorithms," http://arxiv.org/abs/1206.2944, 2012.

Paper F

Towards Self-Supervised Feature Learning for Online Diagnosis of Multiple Faults in Electric Powertrains

Jagath Sri Lal Senanayaka, Huynh Van Khang, Kjell G. Robbersmyr

This paper has been submitted as:

J. S. L. Senanayaka, H. V. Khang and K. G. Robbersmyr "Towards Self-Supervised Feature Learning for Online Diagnosis of Multiple Faults in Electric Powertrains", *Submitted to IEEE Transactions on Industrial Informatics (*Under review*).*

Towards Self-Supervised Feature Learning for Online Diagnosis of Electric Powertrain Faults

Jagath Sri Lal Senanayaka, Huynh Van Khang, Kjell G. Robbersmyr

***Abstract*— This paper proposes a novel online fault diagnosis scheme for industrial powertrains without using historical faulty or labelled training data. The proposed method combines one-class support vector machine (SVM) anomaly detection and supervised convolutional neural network (CNN) algorithm to online detect multiple faults and fault severities under variable loads and speeds. The one-class SVM algorithm is to derive a score for defining faults or health classes in the first stage, and the resulting health classes are used as the training data for the CNN -based classifier in the second stage. Within the framework, the self-supervised learning of the proposed CNN algorithm allows the online diagnosis scheme to learn the features based on latest data. The effectiveness of the proposed scheme is validated via a comparative study using experimental data from an in-house test setup. Finally, the online implementation of the proposed algorithm on the test setup is briefly introduced in this work.**

***Index Terms*—** One-class support vector machine, convolutional neural network, fault diagnosis, electric powertrains, self-supervised learning

F.1 Introduction

Reliable operation is the most important in industrial machines or electric powertrains, including electric motors [1], gearboxes and loads such as fans, pumps, conveyor belts, robotic arms, etc. Electrical and mechanical faults, namely inter-turn, bearing and gear faults, are common in interconnected complex systems. Condition monitoring (CM) and fault detection and diagnosis (FDD) techniques are therefore required to monitor the health status of industrial machines and ensure their safe and reliable operation. To achieve this, analysis methods of various sensor data, such as vibration, acoustic emission, motor current, temperature, lubricant oil, have been intensively developed for CM and FDD, mainly focusing on stationary quantities. Complexity of machines, variable loads and speeds renders challenges due to nonstationary signals, requiring lot of research in industrial and academic communities in recent years [2,3].

A summary of the most recent research on CM and FDD is presented in Table F.1, showing different condition monitoring and fault diagnosis approaches and their suitability for a powertrain consisted of electric motors, gearboxes and loads. The FDD methods can be broadly classified into model-based, data-driven or hybrid algorithms [2-5]. The model-based fault diagnosis requires precise physical models and parameters of the implemented system, which is difficult to obtain in reality. A data-driven method using statistical or machine learning algorithms does not need such physical models, making it attractive for an automatic diagnosis system. Various combinations among signal processing, statistics and machine learning methods have been intensively proposed in data-driven approaches for CM and FDD. Signal processing and statistical methods [6,7] need an identification of the fault-related characteristic frequencies or statistical features from the data being used for FDD with fixed or statistical thresholds. These methods are simple but are only applicable to single fault diagnosis. Multiple faults in a complex system require more advanced solutions. For example, mixed faults in a gearbox can be detected by a combination of traditional machine learning methods and data fusion [8]. However, expert knowledge to derive features manually for the algorithm, resulting in a time-consuming work, is the main disadvantage of using conventional machine learning methods.

Table F.1: Different methods for fault diagnosis of electric motors and gearboxes.

FDD approach	Key features and example methods	Advantages	Disadvantages.	Refs.
Model-based fault diagnosis	• Based on a precise mathematical model • The model output variables and actual output variables are compared, and residual of the comparison is used for FDD.	• Deterministic and more reliable diagnostic results	• The precise mathematical model is difficult to build and requires accurate parameters.	[2-5]
Signal processing and statistical methods	• **Feature generation:** the system vibration, acoustic emission or motor current is measured, and the signals are analyzed for finding fault-related features. (e.g. time-domain RMS, frequency domain analysis and amplitude of characteristics frequencies, filters and RMS of filtered signals, statistical features such as mean, variance, kurtosis in time and frequency domains, DWT, WPT) • **FDD:** Fixed or statistical thresholds are used (e.g. ISO vibration thresholds, statistical thresholds)	• Suitable for single fault diagnosis if fault-related characteristic frequencies appear or detectable statistical features exists	• Expert knowledge is required for finding the characteristic frequencies • Multiple faults diagnosis is difficult	[6, 7]
Signal processing, statistics and machine learning	• **Feature generation:** signal processing and mentioned statistical methods are used to manually collect designed features • In supervised **FDD:** case machine learning is used to classification of faults using the features. (e.g: MLP, k-NN, DT)	• In some cases, multiple faults can be detected.	• Expert knowledge is required for finding the characteristics frequencies. • Labelled training data is required, being impossible in reality	[20-24]
Deep learning-based methods	• **Feature generation:** automatic and supervised CNN, or unsupervised methods (e.g. AEs) • **FDD:** In supervised case, the fault diagnosis problem is solving as a pattern recognition problem using automatically detected features (e.g. CNN)	• Expert knowledge is not required as characteristic frequencies are not considered separately. • Multiple FDD	• Relatively costly to implement • Labelled training data is required for supervised FDD algorithms	[10, 11, 25-28]
Unsupervised / semi-supervised learning methods	• **Feature generation:** autoencoders, transfer learning (require few labelled training data) • **Fault detection:** fixed or statistical thresholds, one-class SVM	• Limited labelled training data or labelled training data is not required	• Autoencoders: even though labels are not required. the healthy and fault data is required for feature learning. • For transfer learning labelled training data is required for fine-tuning	[9, 12]
Hybrid systems	• Combination of data-driven and model-based diagnosis.	• Robust FDD results due to combination of both methods	• Complexity of implementation	[3, 5]

RMS: root mean square, DWT: discrete wavelet transformation, WPT: wavelet packet transformation, MLP: multi-layer perceptron, k-NN: k nearest neighbour, DT: decision three

Supervised deep learning methods were suggested to address the difficulty of feature generation [8-11], but the supervised deep learning methods for CM and FDD applications require a lot of historical faulty data for training. Unsupervised feature learning methods such as autoencoders (AEs) [9] require unlabeled data for healthy and faulty conditions, but historical data for faults may not exist for new machines, and autoencoder feature learning becomes irrelevant for such cases. On the other hand, transfer learning [12] is suggested to reuse the learned feature from one application to another, but these methods must use labelled training data for fine-tuning. An online fault diagnosis algorithm for an electric powertrain, based on supervised learning is proposed in [13,14], and a lot of training data is required to train the algorithm, which is restricted in practice. To avoid labelled data demanding in an online diagnosis system, self-supervised learning can be a promising solution. The self-supervised learning is a relatively new concept, and their existing applications are mainly focus on image classification, pattern recognition and robotics [15-17]. The advantage of self-supervised learning is that it does not require prior labels and can learn features online. No previously published work has tackled the labelled data problem for an online diagnosis of electric powertrains.

To address limitations of the existing data-driven fault diagnosis methods shown in Table F.1, namely limited faulty data, computation burden, offline implementation, expertise demand, this work proposes an online fault diagnosis algorithm including two stages. The first stage based on one-class SVM is to online detect multiple faults of an electric powertrain under variable speed and load conditions in an unsupervised way as a component risk analysis, and automatically store healthy and faulty data for the second stage. In the first stage, any deviation from healthy status is defined as an anomaly or fault, but the location of the fault is unknown. The one-class SVM algorithm [18, 19] calculates a distance or hyper-length between data points in the feature space to define whether the machine is healthy or faulty based on healthy machine data alone. The trained SVM algorithm separates the healthy data from faulty one. In the second stage, the stored data from the first stage is fed in a supervised fault classifier using convolutional neural network (CNN) to make a self-supervised feature learning and accurately isolate multiple faults online (or fault classifications). Within this framework, a novel decision criterion based on classification scores is proposed for the multiple fault diagnosis. Further, a comparative study is presented to highlight the effectiveness

of the proposed method. Finally, an online implementation of the proposed scheme is validated on an in-house test setup.

The rest of this paper is organized below. Section F.2 presents details of the proposed fault diagnosis scheme. The experimental details and results are discussed in Section F.3. The conclusion of this research study and future research directions are given in Section F.4.

F.2 Proposed fault diagnosis scheme.

A block diagram of proposed fault diagnosis scheme is given in Figure F.1, where the vibration, speed and current signals are collected from the gearbox, and motor. The collected vibration and current signals are order-normalised to remove the speed variation, and spectrograms are derived from the order normalised ones using short-time Fourier transform (SFFT) [14, 29-31]. These vibration and motor current spectrograms are combined as one spectrogram for each sample and stored in the cloud data storage.

The proposed online diagnosis scheme consists of two main stages, namely

1. Stage 1 - Unsupervised fault detection algorithm is to define the machine is healthy or faulty, but local faults or detailed locations of the faults are unknown.
2. Stage 2 – online multiple fault classification and decision making based on self-supervised feature learning, feature-level data fusion, supervised CNN fault classification.

This study focuses on multiple faults on gear, bearing and stator winding under variable speeds and loads. However, the concept can be extended to other faults and working conditions. The details of each stage are given in the following sections.

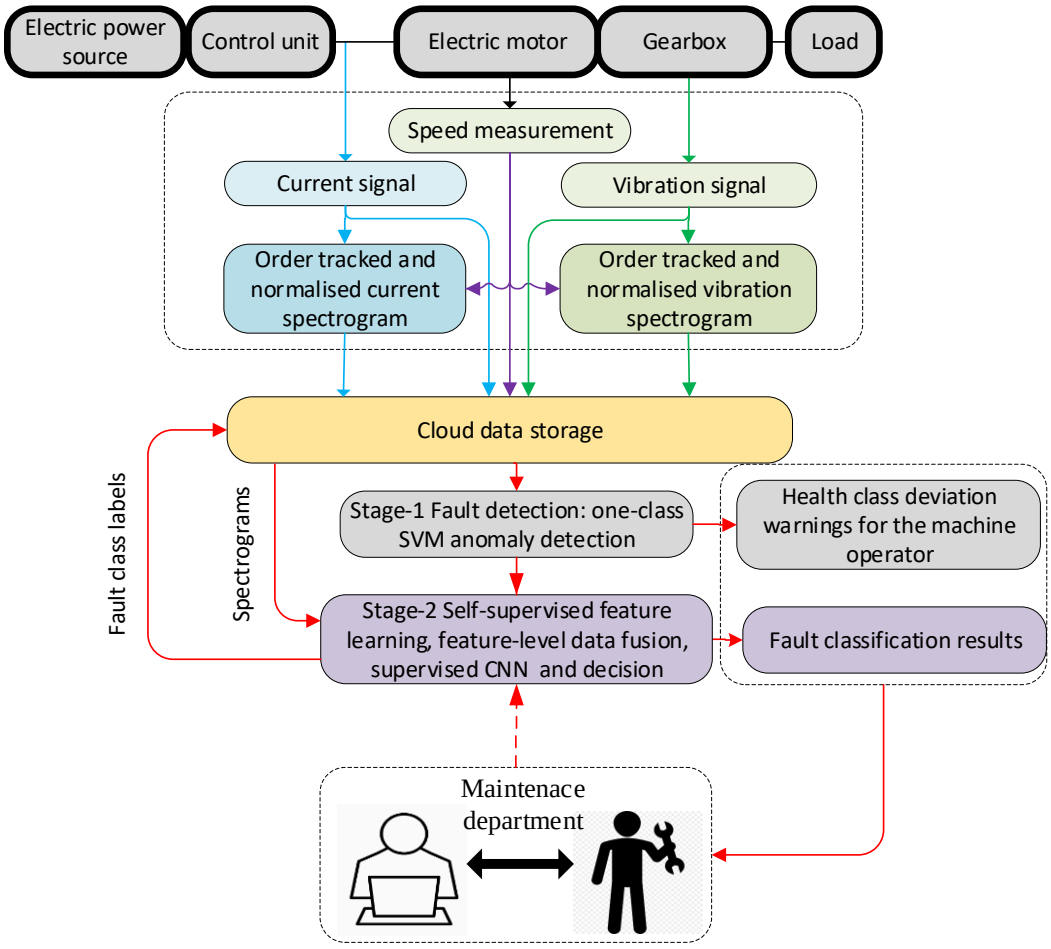

Figure F.1: A block diagram of the proposed fault diagnosis scheme for Electric Powertrain.

F.2.1 Stage 1: unsupervised fault detection

In industrial applications, data of healthy machines can be easily obtained, but data for faulty ones is restricted or unavailable. Training a data-driven model using healthy data alone is practically of importance in CM. In this study one-class SVM is used to identify the healthy cases using available healthy data, and then any data point different from healthy cases is considered as an anomaly. The aim of this anomaly detection (also referred as outlier detection) is to determine all such occurrences in a data-driven algorithm. In the one-class SVM, the input data is mapped into a high dimensional feature space using a kernel function to find the maximum margin hyperplane or the best separation of the training data from the origin [18, 19, 32]. Figure F.2 shows the one-class SVM concept.

The hyperplane defines the classification rule.

$$f(\mathbf{x}) = < \mathbf{w}, \mathbf{x} > + b \tag{F.1}$$

where **w** is the normal vector, and b is the bias term.

Consider a test example **x**. If $f(\mathbf{x}) < 0$ then **x** is an anomaly, otherwise **x** is normal.

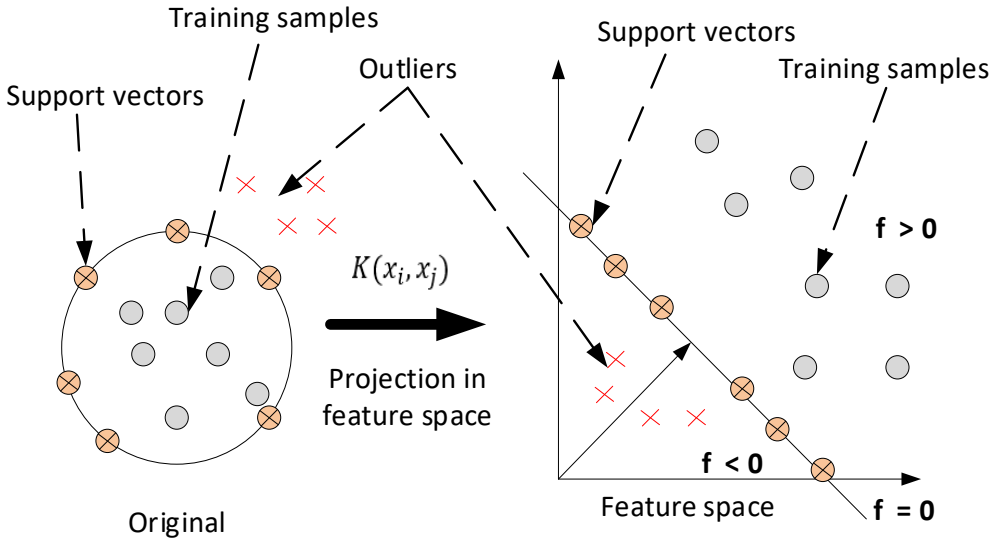

Figure F.2: A classification based on one-class SVM with two features.

To get the above decision rule, solving the one-class SVM optimization problem (using kernel function), is equivalent to solving the following dual quadratic programming problem:

$$\min_{\alpha} \frac{1}{2} \sum_{i,j} \alpha_i \alpha_j K(x_i, x_j) \tag{F.2}$$

Subject to the constraints

$$0 \leq \alpha_i \leq \frac{1}{vl} \quad \text{and} \quad \sum_i \alpha_i = 1 \tag{F.3}$$

where α_i is the Lagrange multiplier, and is the "weight" on example i such that vectors associated with non-zero weights represent "support vectors" and uniquely determine the optimal hyperplane. v is a parameter to control the trade-off between the maximum distance of the hyperplane from the origin and the number of data points contained by the hyperplane, l is the number of points in the training dataset, and $K(x_i, x_j)$ is the kernel function [18, 19, 32]. This study uses Gaussian kernel given in (4).

$$K(x_i, x_j) = e^{-\frac{\|x_i - x_j\|^2}{2\sigma^2}} \quad \text{(F.4)}$$

where σ^2 is the variance.

Three main steps in stage 1 of the proposed unsupervised fault detection algorithm are as follows

1) Train the boundaries for healthy class using features (RMS of vibration signal, RMS of motor current signal and motor speed) and one-class SVM.
2) Calculate the score from the trained one-class SVM for coming data in dynamic manner and take the average of latest samples. In this study, 20 latest samples are selected for the average score calculation. Depending on application, better averaging criteria can be revised.
3) Compare the average scores to define machine status. If the score is greater than zero, the machine is healthy, and otherwise, machine is faulty.

F.2.2 Stage 2: online multiple fault classification

The detailed flowchart of the operation of the proposed fault diagnostic scheme is given in Figure F.3, where the green colour boxes and lines represent the stage-1 algorithm, and the remaining boxes and lines represent the stage 2 algorithm. Once a fault is detected in stage 1, a temporary class label (e.g. Fault type 1 (FT-1)) is assigned. In the stage 2, the supervised CNN algorithm is trained using healthy data and the FT-1 data. In this self-supervised feature learning method, the algorithm can learn features related to multiple faults (FT-1, 2, …). The algorithm keeps a bank of feature types learned from the cloud data storage. For new data, the learned feature set is applied to generate a score, which represents the similarity

of new data respective to the corresponding feature type. The final decision is taken based on the decision defined in the Table F.2. When the powertrain is repaired, the actual label is available, and maintenance department can update the FT-1 with a correct label.

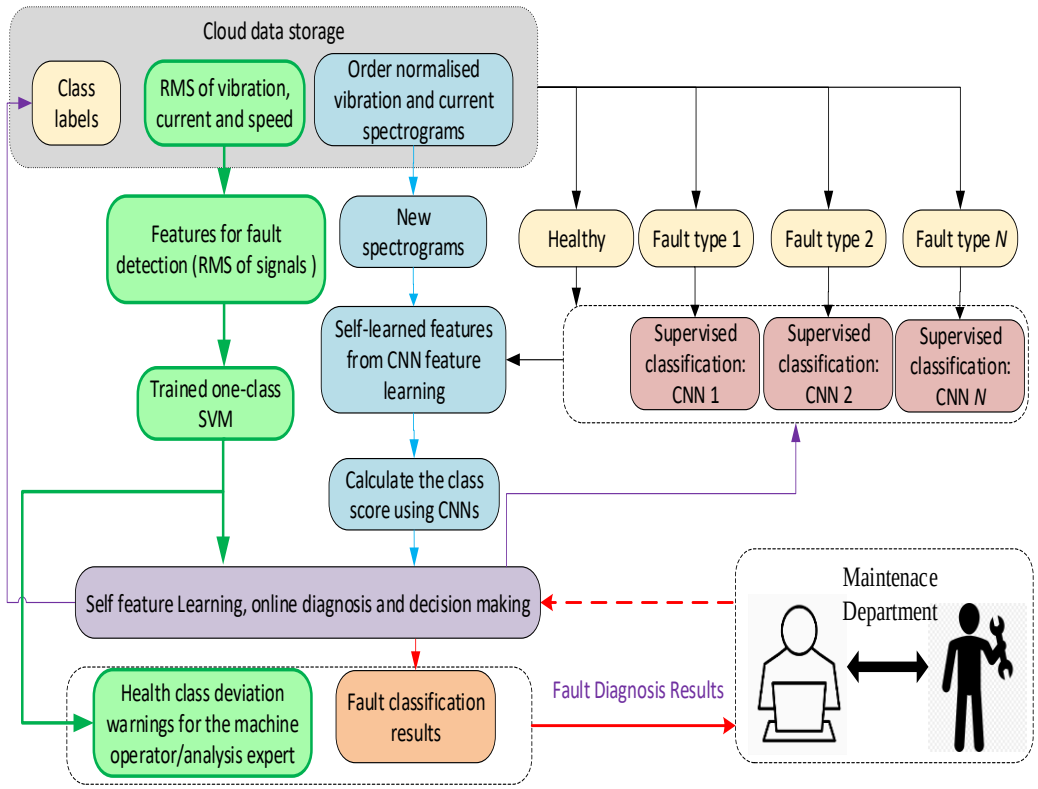

Note: The green color boxes and lines represent the stage-1 algorithm and the remaining boxes and lines represent the stage 2 algorithm

Figure F.3: Detailed flowchart of stage-1 and -2 of the proposed fault diagnosis scheme.

In most existing CNN based fault diagnosis methods, pre-labeled training data is required. In this work, the proposed self-supervised feature learning based on CNN in stage 2 does not require any pre-labeled training data. It uses only the temporary labels after stage 1 in self-supervised feature learning. A simplified block diagram of the CNN architecture is presented in Figure F.4. The algorithm consists of two main subsections: feature learning and classification. The 2-dimensional (2-D) convolution can be applied to an image with different sets of kernels (or shared weights) using a neuron map, in which the weights are optimized

by using a backward propagation algorithm. The convolution operation used to identify the local features of the input images. The convolution combined with pooling is to reduce the dimensionality, allowing for simplifying the structure of a fully connected neural network for the classification. The rectified linear unit (ReLU) introduces the non-linearity to the system. Details of the CNN training and analysis can be found in [33].

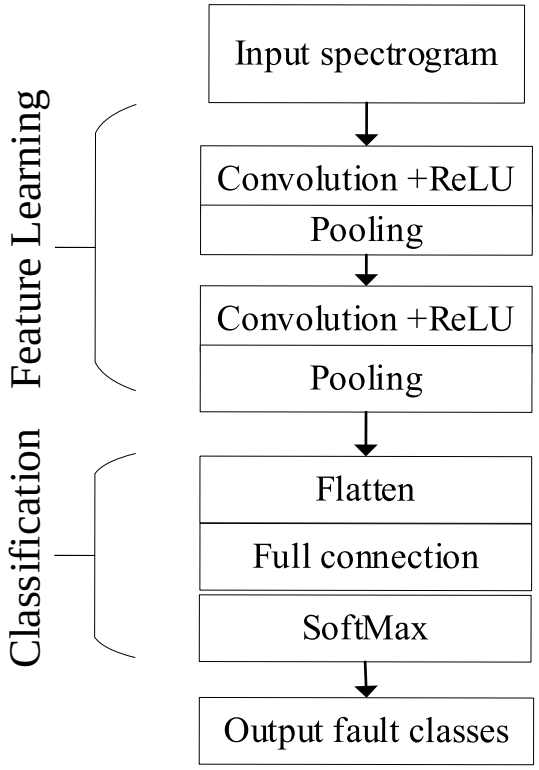

Figure F.4: A block diagram of a CNN architecture.

The learned complex relations in the feature space are utilised in a fully connected neural network for the fault classification. The Flatten operation is essential for converting a 2-D image to the 1-D array. Based on derived features in the convolution and pooling operation, the classification task is done by the fully connected network and Softmax function. The Softmax function converts the outputs of the fully connected network to probabilities of health classes. The highest probability value represents the output fault class of the network. Once trained, the output of the Softmax layer is used to produce a score to define the similarity of given input images respective to the learned feature map.

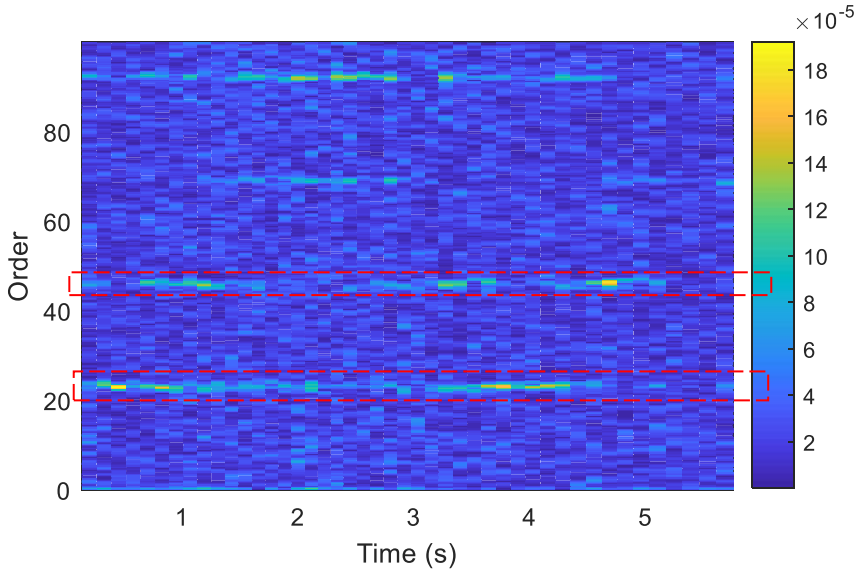

Figure F.5: Order normalized vibration spectrogram with a gear fault.

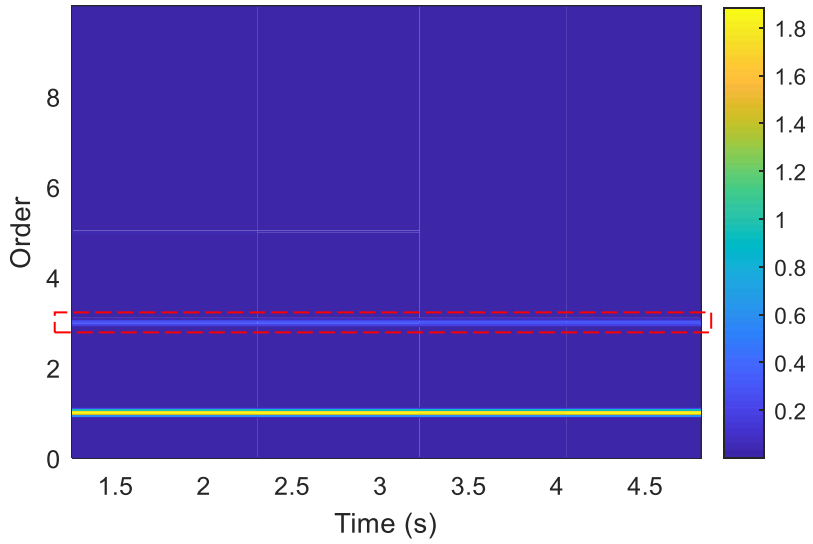

Figure F.6: Order normalized current spectrogram with a stator winding fault.

CNN is well known as a pattern recognition algorithm, which can detect the patterns within data. Figure F.5 shows a sample of an order normalized vibration spectrogram of a gear tooth damage fault, where the amplitudes of gear meshing frequencies and its harmonics are clearly visible (within red dotted lines), being detected by a CNN classifier. Compared to healthy spectrograms, any visible changes are not observed in the current spectrum for gear faults. However, in the case of stator winding fault, 3-times supply frequency components appear in the

current signal spectrum as shown in Figure F.6. Since vibration and current spectrograms are combined as one image and fed to CNN, the feature level fusion is applied, allowing the CNN to learn from both vibration and current spectrograms. The trained CNN is used to generate a label for new data (spectrograms). As shown in Figure F.4, the Softmax layer output is a score, representing the similarity of new data with respect to a trained fault type. A bank of CNN-based classifiers are to generate scores for new data of multiple fault types. The generated scores are used for a final decision. An outline for a preliminary decision criterion is shown in Table F.2.

Table F.2: Decision criteria for the final decision.

Decision type	Main criteria	Sub criteria	Decision	Confidence
DT1	score < 0.25 for each feature type	-	Healthy	HC
DT2	0.25 < Score < 0.5 for each feature type	-	Healthy	MC
DT3	0.5 < score < 0.75 for only one feature type (e.g FT1)	score < 0.25 for remaining feature types	FT1	MC
DT4		0.25 < score < 0.5 for least one remaining feature type	FT1	LC
DT5	0.75 < score < 0.9 for only one feature type (e.g FT1)	score < 0.25 for remaining feature types	FT1	HC
DT6		0.25 < score < 0.5 for least one remaining feature type	FT1	MC
DT7	0.9 < score for only one feature type (e.g FT1)	score < 0.25 for remaining feature types	FT1	HC
DT8		0.25 < score < 0.5 for least one remaining feature type	FT1	MC
DT9	0.5 < score for more than one feature type	-	Multiple faults	-

HC: High confidence, MC: Medium confidence, LC: Low confidence

The proposed decision criteria in Table F.2 are suggested criteria, which have not been optimized and can be improved further in future work since no standard was defined or available in literature. The multiple fault decision criterion is simplified in this work.

F.3 The Experimental data and results

F.3.1 Experimental setup and data

The in-house experimental setup shown in Figure F.7 is used to collect data and validate the proposed fault diagnosis scheme. The powertrain includes a 1.1 kW, 1450 rpm induction motor (IM) coupled to the 2-stages parallel shaft gearbox (GB) with 8.01 gear reduction. The gearbox is coupled to a permanent magnet synchronous generator (PMSG), and the generator output is connected to a resistive load. The powertrain load is proportional quadratically to the rotational speed. The output currents of the PMSG are measured and used to estimate the rotational speed of the electric powertrain. However, in real applications, an encoder can be required for speed measurements. The internal components of the complete powertrain are disassembled as shown in Figure 8, including 8 bearings, 4 gears and 3 shafts.

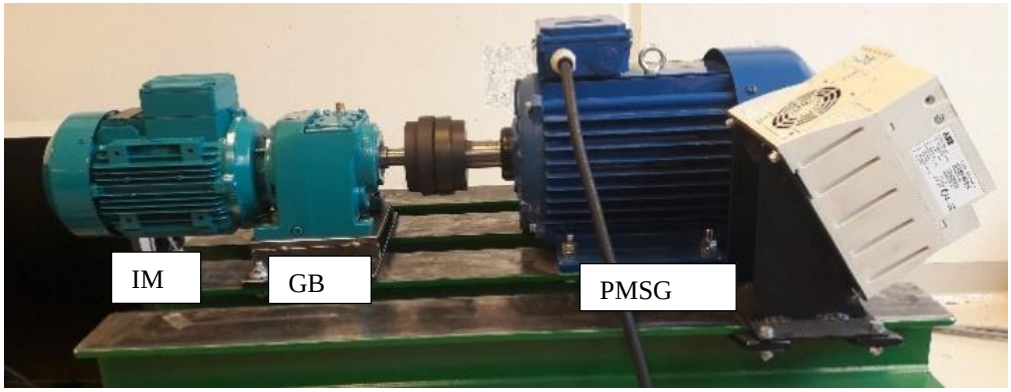

Figure F.7: The experimental setup.

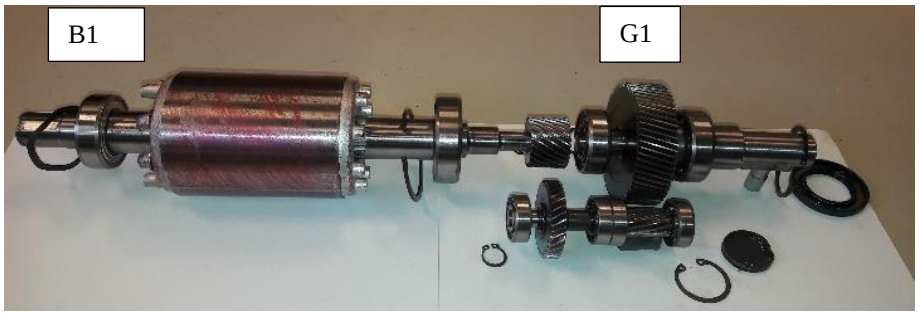

Figure F.8: The internal components of the electric powertrain.

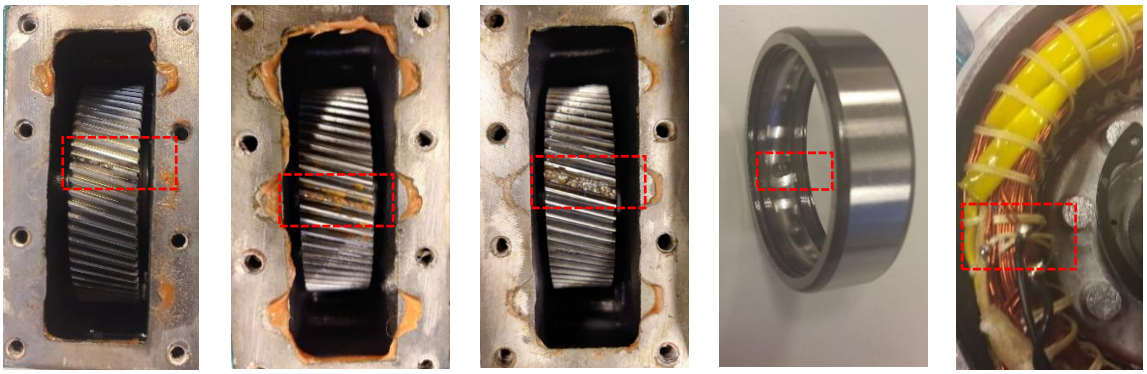

Figure F.9: The faulty gears of electric powertrain.
(a) small gear tooth damage (GF1), (b) moderate gear tooth damage (GF2), (c) broken gear tooth (GF3), (d) Outer-race damaged bearing (BF2), (e) 10% inter-turn short circuit fault in the stator (SF2).

The G1 gear in the powertrain, Figure F.8 has three fault severities: a small-scale gear tooth damage (GF1), a medium-scale tooth damage (GF2), and a broken tooth damage (GF3) as shown in Figures. F.9 (a), (b) and (c), respectively. Outer-race defects on the bearing B1 of the induction motor (IM) are made by using an electric discharge machining, and three bearing severities BF1, BF2 and BF3 are produced with 1, 2 and 3mm radius surface damages. The bearing shown in Figure F.9 (d) represents an outer race damage with 2 mm radius (BF2). Further, stator winding faults in the induction motor of 6% (SF1) and 10% (SF2) inter-turn short circuit faults are introduced in one phase as shown in Figure F.9 (e).

Eleven fault classes with individual and multiple faults are tested, and the details of fault classes are given in subsections F.2.2 and F.3.3. As specified in

Figure F.10, the induction motor operates at one constant speed of 1450 rpm and two variable speed profiles for each fault class. Two load levels of 55% and 100% the rated motor torque are applied to the constant speed profile. In the variable speed operation, the load also dynamically varies. A vibration sensor is used to collect vibration data, and a current sensor is used to collect IM current. The rotor speed is estimated using the PMSG current signal.

The sampling rate of the data acquisition system was 20 kHz. The data samples (120 seconds duration) are collected, and for each fault class, 5 repeated tests were conducted. Each 120-seconds file has 24×10^5 data points, and 191 samples are derived from each file with a section window (120000 data points representing 6 second of data), shifting the window by 12000 data points. Therefore, each fault class has 3820 samples. As described in Figure F.3, RMS of vibration and current, and the speed are recorded for stage 1 - unsupervised fault detection algorithm. Stage 2 - CNN algorithm uses order-normalized spectrograms generated from each signal. The first 100 orders are clipped in the vibration spectrograms, while in the current spectrograms, the first 10 orders are clipped. The dimension of each signal is 113×226. The spectrograms from each vibration and current samples are combined to produce images of 226×226 dimension, being fed to CNN-based multiple fault classifiers. In the next subsections, performances of stages 1 and 2 are individually evaluated before combining them in the proposed online scheme as shown in Figure F.3.

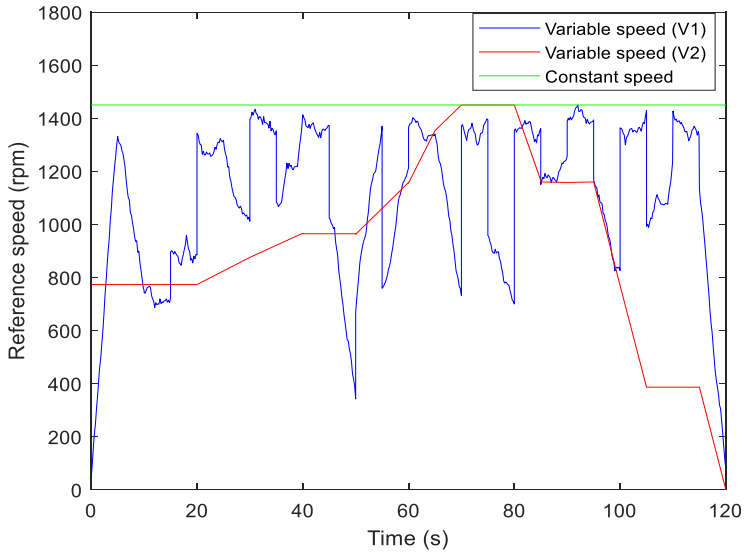

Figure F.10: Constant and variable speeds of each fault class.

F.3.2 Performance of Stage 1 - unsupervised fault detection

The proposed anomaly detection algorithm based on one-class SVM is implemented as discussed in section F.2.1, detecting whether machine status is deviated from its healthy status or not. Figure F.11. illustrates the vibration RMS of four gear fault classes in the G1 gear. Using the RMS of vibration signal alone is not able to detect a gear fault in variable loads and speeds as the RMS of vibration depends on load and speed variations.

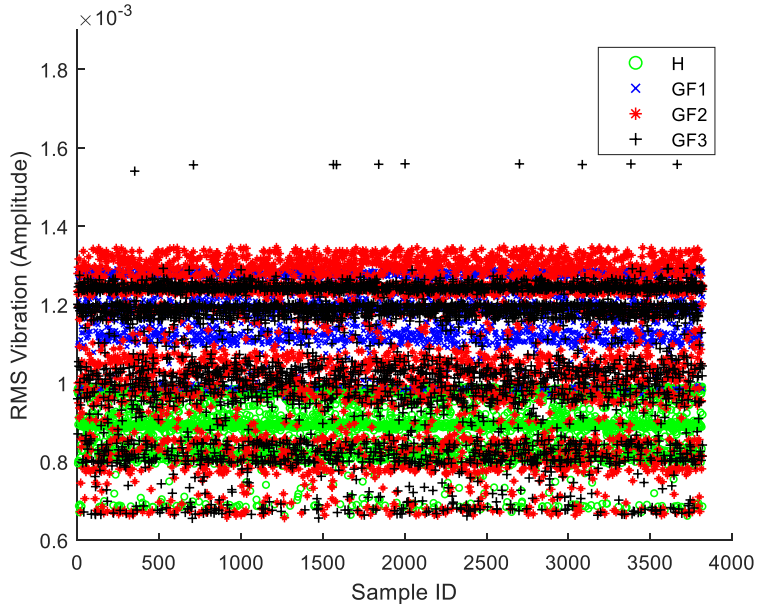

Figure F.11: RMS vibration for fault classes in G1 gear.

Figure F.12 shows the RMS of current under different gear fault cases, showing that the RMS current is not a reliable indicator to detect a gear fault since the RMS differences among fault severities are unclear. It is difficult to define a fixed threshold to detect a fault in both signals, thus a new health indicator is required for the fault detection in variable loads and speeds. In this work, a consistent health class indicator is produced by fusing the healthy classes based on RMS of vibration current signals, and rotor speed in the one-class SVM.

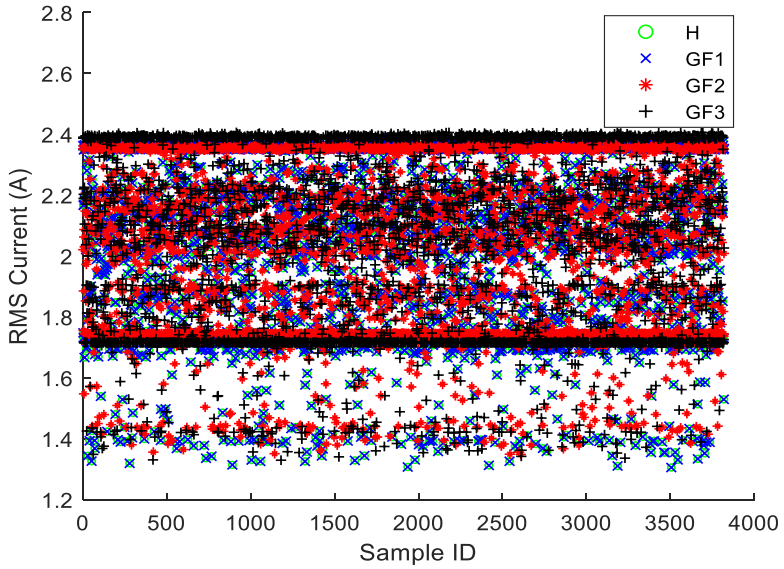

Figure F.12: RMS current for fault classes in G1 gear.

The trained one-class SVM algorithm is used to calculate scores for different fault classes. Figures. F.13, F.14 and F.15 show the scores of gear, bearing, and stator winding faults at different fault severities, in which a component is defined as a healthy one if the score is greater than 0 (healthy: score > 0), otherwise it is a faulty one (faulty: score < 0).

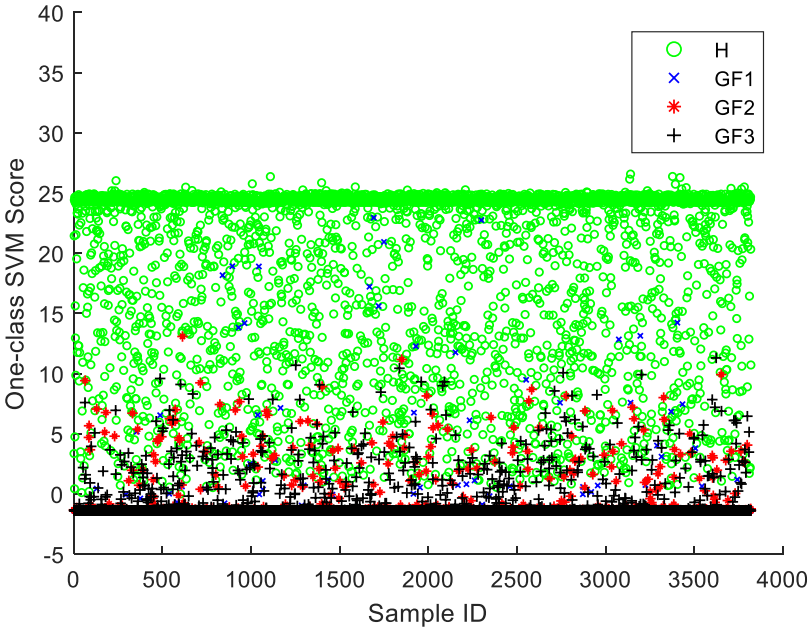

Figure F.13: One-class SVM score for gear faults.

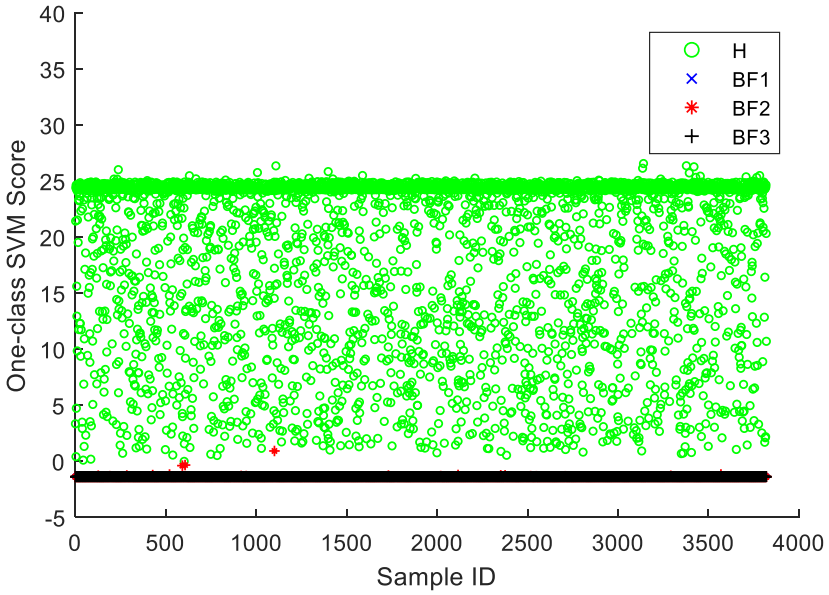

Figure F.14: One-class SVM score for bearing faults.

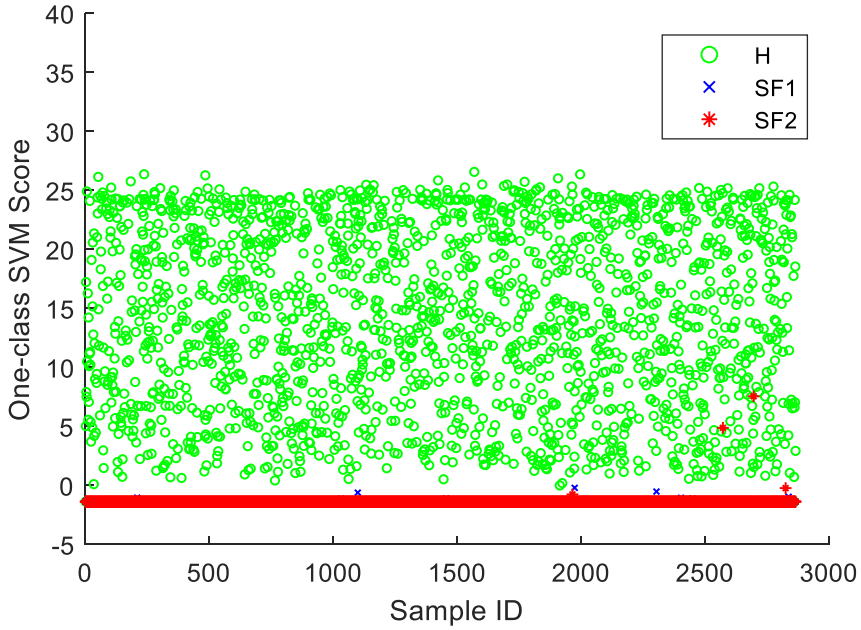

Figure F.15: One-class SVM score for stator winding faults.

The average accuracies of the stage 1 - one-class SVM algorithm are summarised in Table F.3. For the healthy class (H), the one-class SVM score is greater than 0 for 99.9% of the test samples. The scores become negative with the accuracies of 98.6%, 95.9% and 92.0% for the gear fault severities GF1, GF2 and GF3 classes, respectively. More than 99.9% detection accuracies can be observed for other fault

classes, namely bearing and stator winding fault severities, and the proposed fault detection algorithm works well for detecting the tested fault classes. It is worth mentioning that the state 1 is to identify whether a component is healthy or faulty, which is not able to know a fault type or severity. In an online diagnosis application, the fault classes are unknown, and fault isolation is not possible at stage 1.

Table F.3: One-class SVM performances for fault detection.

Fault class ID	Fault class	Detection score (%)	Detection criteria	Powertrain Status
1	H	99.9	Score > 0	Healthy
2	GF1	98.6	Score < 0	Faulty
3	GF2	95.9	Score < 0	Faulty
4	GF3	92.0	Score < 0	Faulty
5	BF1	100.0	Score < 0	Faulty
6	BF2	99.9	Score < 0	Faulty
7	BF3	100.0	Score < 0	Faulty
8	SF1	100.0	Score < 0	Faulty
9	SF2	99.9	Score < 0	Faulty

Therefore, a self-supervised feature learning procedure is implemented at stage 2, where temporary labels are assigned to incoming data from the faulty component, being stored in the cloud data storage. In the stage 2, the spectrograms from healthy powertrain and faulty components (with temporary fault class labels) will be used to train a CNN for detecting the features of temporary fault class. The decision criteria explained in Table F.2 will be used for isolating the single and multiple faults.

F.3.3 Performance of Stage 2 - supervised CNN fault diagnosis algorithm

Consider a practical gear fault scenario, where a small fault originates, and the severity gradually increases over time. Hence, the lowest severity data is first available. Once a faulty case is detected as a gear fault 1 (GF1) using stage 1 -

one-class SVM algorithm, the supervised CNN algorithm for GF1 or GF1-CNN algorithm can be trained using data at healthy and at gear fault 1 (GF1) severity level,, which is a small gear tooth damage. Similar scenarios are trained for bearing and stator winding. The trained CNN algorithms of stage 2 have been tested with other fault classes, and classification accuracies are summarized in Table F.4.

Table F.4: Classification accuracies of CNN classifiers.

Fault Class ID	Fault Class	Accuracy (%)		
		GF1-CNN	BF1-CNN	SF1-CNN
1	H	98.6	99.6	99.8
2	GF1	94.1	99.6	100
3	GF2	98.6	99.5	100
4	GF3	99.1	99.6	100
5	BF1	94.9	90.0	100
6	BF2	96.2	99.0	100
7	BF3	82.5	99.0	100
8	SF1	80.1	99.0	99.7
9	SF2	82.7	99.0	99.7
10	GF2_BF2	93.4	67.4	99.6
11	GF2_BF2_SF1	97.1	72.1	98.1

The GF1-CNN classifier can detect healthy class with high accuracy of 98.6% as shown in the first row of Table F.4. Further, it can effectively detect other gear fault severities of GF1, GF2 and GF3 at accuracies of more than 94.1%. Moreover, the GF1 classifier classifies bearing fault severities (BF1, BF2 and BF3) as ‘healthy’ respective to the learned gear faults features with a minimum accuracy of 82.5%. Correspondingly, it classifies stator winding faults (SF1 or SF2), as the ‘healthy’ respective to the gear fault features with a minimum accuracy of 80.1%. When a gear fault occurs with other faults, the GF1-CNN classifier can detect it correctly with accuracies of over 93.4% (93.4% for the fault class 10, and 97.1% for the fault class 11 in Table F.4). Similarly, single fault diagnosis with accuracies of over 90.0% and 99.7% can be obtained with BF1-CNN and SF1-CNN classifiers, respectively. However, the BF1-CNN classifier is able to detect

multiple faults at the moderate accuracy of 67.4% and 72.1%. In future studies, the reasons for low accuracies will be investigated.

F.3.4 Comparison with other fault diagnosis algorithms

A comparative study is used to highlight the performance of the proposed CNN fault diagnosis algorithm. Classifiers (GF1-MLP, BF1-MLP, and SF1-MLP) based on domain features (DF) and multi-layer perceptron (MLP) algorithms are used in as the first baseline algorithms in the comparison. The MLP consists of two layers. The average order spectrums of time-domain signals are derived, and the amplitude of fault-related characteristic frequency orders are extracted as features. The fault-related characteristic frequency orders used for feature generation are summarized in Table F.5 with 9 features.

Table F.5: Characteristics frequency orders for Domain features.

Feature	**Signal**	**Order**
1X IM rotational order	Vibration	1X
2X IM order	Vibration	2X
3.6X IM rotational order	Vibration	3.6X
Input shaft 1X gear mesh frequency (GMF)	Vibration	23X
Input shaft 2X GMF	Vibration	46X
Output shaft 1X	Vibration	0.12X
Output Shaft 1X GMF	Vibration	8.1X
Output Shaft 2X GMF	Vibration	16.25X
3X (three-time current frequency)	Phase current	3X

Domain feature generation is a time-consuming task, requiring the details of gearbox components (e.g: number of teeth in gears, number of balls in bearings etc.), signal processing and fault diagnosis expertise. However, the proposed CNN pattern recognition algorithm does not require the details of gearbox components and signal processing to calculate characteristic frequency features. The CNN algorithm can learn the fault-related time-frequency patterns from data. The second baseline classifiers (GF1-SVM, BF1-SVM, and SF1-SVM) consist of DF

with a binary SVM algorithm using Gaussian kernel Therefore, three types of classification methods for each fault type result in nine classifiers in Table F.6. showing the classification accuracies at different fault types and severities.

Table F.6: The classification accuracies of different classifiers.

		Classification accuracies (%)								
Fault Class ID	Fault Class	GF1-SVM	GF1-MLP	GF1-CNN	BF1-SVM	BF1-MLP	BF1-CNN	SF1-SVM	SF1-MLP	SF1-CNN
1	H	97.1	97.8	98.6	94.8	93.7	99.6	100.0	100.0	99.8
2	GF1	97.4	97.6	94.2	67.5	65.1	99.6	95.4	97.0	100.0
3	GF2	68.4	91.6	98.6	55.0	67.0	99.5	43.4	98.0	100.0
4	GF3	71.4	81.3	99.1	53.0	57.1	99.6	60.0	100.0	100.0
5	BF1	81.1	75.3	94.9	94.7	94.0	90.0	99.0	100.0	100.0
6	BF2	54.1	82.7	96.2	79.0	80.5	99.0	90.0	100.0	100.0
7	BF3	51.0	77.0	82.5	99.0	99.0	99.0	63.0	100.0	100.0
8	SF1	76.0	94.0	80.1	60.0	99.0	99.0	100.0	100.0	99.7
9	SF2	71.0	95.0	82.7	61.0	98.0	99.0	100.0	100.0	99.7
10	GF2_BF2	88.0	80.0	93.4	86.0	89.0	67.4	60.0	100.0	99.6
11	GF2_BF2_SF1	97.0	84.0	97.1	96.0	70.0	72.1	98.0	75.0	98.1
	Average	77.5	86.9	92.5	76.9	82.9	93.1	82.6	97.3	99.7
	Minimum	51.0	75.3	80.1	53.0	57.1	67.4	43.4	75.0	98.1
	Maximum	97.4	97.8	99.1	99.0	99.0	99.6	100.0	100.0	100.0

All gear fault algorithms (GF1-SVM, GF1-MLP and GF1-CNN) classifies the healthy class with accuracies over 97.1%. The GF1-SVM has the lowest performance with minimum and average accuracies of 51.0% and 77.5%, respectively while those minimum and average accuracies of the GF1-MLP are 75.3% and 86.9%. The proposed GF1-CNN classifier has the best performance with the minimum and average accuracies of 80.1% and 92.5%, respectively. The GF1-SVM classifier has the lowest average performances, but still the classification accuracy of its original trained class (GF1) is 97.4% while having moderate accuracies for other fault classifications. Domain feature-based classifiers (binary SVM and MLP) have some lower accuracies due to the limitations of DF, and the amplitudes of characteristics frequency bands are calculated from average order spectrum, which contains approximations for the

dynamic load and speed operations. However, the CNN feature learning covers the local regions in the spectrograms for dynamic operations, resulting in a better feature learning. The CNN-based classifier can compensate for spatial deviation of fault-related frequency bands in the spectrograms produced in order normalization algorithm during sudden speed changes. This cannot be achieved in DF-SVM and DF-MLP. Therefore, the performances of CNN classifiers are better than the other two methods.

F.3.5 Classification score and decision criteria

In the proposed algorithm, the score generated by Softmax layer of CNN is used for final decision. The reason is that the score gives more information than using final labels like existing studies [8, 27]. The scores of CNN-based classifiers for all data samples are calculated, and the average scores of all fault classes are summarized in Table F.7. The decision criteria explained in Table F.2 are used for final decisions. The score of the GF1-CNN classifier for healthy data is 0. However, the scores for GF1, GF2 and GF3 are high and more than 0.95. Therefore, the GF1-CNN classifier can isolate gear faults at GF1, GF2 and GF3 severities with high confidences. In the best case, the score of the GF1-CNN classifier is closer to zero except gear faults. When data of bearing faults - BF1, BF2 and BF3 is fed to the GF1-CNN classifier, the average scores are 0.01, 0.05 and 0.37, respectively. This proves that the GF1-CNN classifier (gear fault classifier) classifies the first bearing fault severities BF1 and BF2 into being not a gear fault with high confidence at while the bearing fault severity is classified into a similar one at a medium confidence. Figure F.16 illustrates the average scores of each classifier for single fault classes. Each classifier can independently isolate faults for respective trained fault classes with minimum missing and false alarms for data samples of other fault classes.

When multiple faults occur in the studied powertrain (fault classes 10 and 11), the GF1-CNN can isolate gear faults (0.76 and 0.96 scores). The SF1-CNN classifier also performs well for single and multiple faults. The performance of the BF1-CNN classifier is good for all single bearing fault detections, but moderate (0.71 for class 10 and 0.74 for class 11) for multiple fault detection.

Table F.7: CNN scores for various fault classes

Fault class ID	Fault class Name	Score			Final Decision	Decision type
		GF1-CNN	BF1-CNN	SF1-CNN		
1	H	0.00	0.00	0.00	healthy	DT1
2	GF1	0.96	0.00	0.00	GF	DT7
3	GF2	0.95	0.06	0.00	GF	DT7
4	GF3	0.98	0.02	0.00	GF	DT7
5	BF1	0.01	0.90	0.00	BF	DT7
6	BF2	0.05	0.95	0.00	BF	DT7
7	BF3	0.37	0.93	0.00	BF	DT8
8	SF1	0.33	0.00	0.99	SF	DT8
9	SF2	0.33	0.00	1.00	SF	DT8
10	GF2_BF2	0.76	0.71	0.00	Multiple	DT9
11	GF2_BF2_SF1	0.96	0.74	1.00	Multiple	DT9

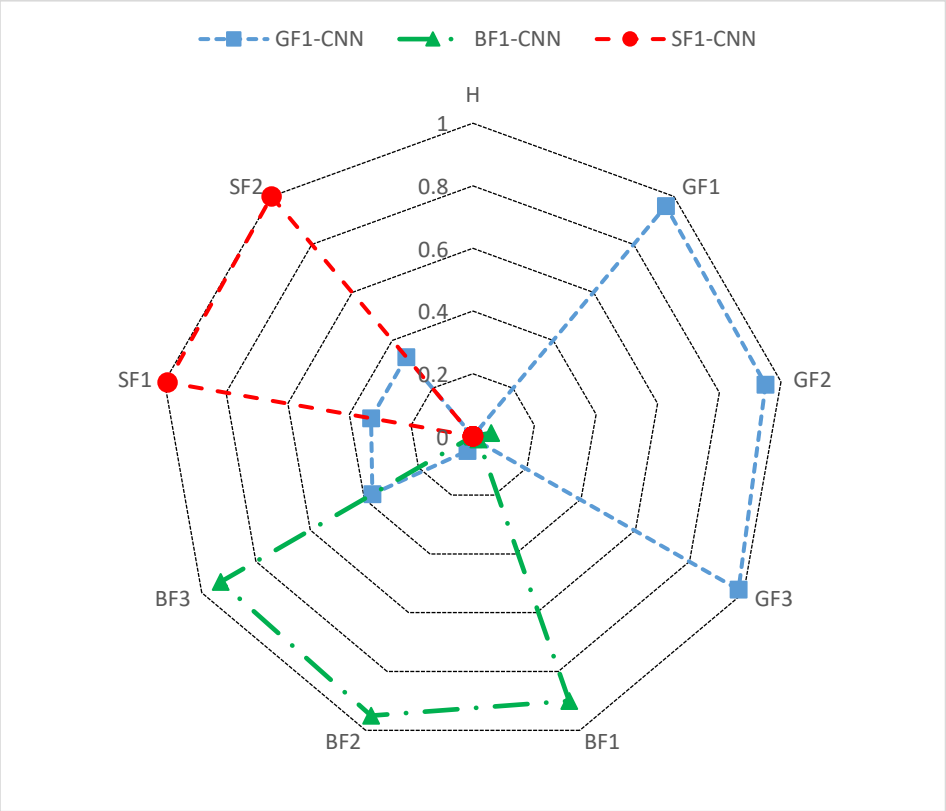

Figure F.16: Average scores of each CNN classifier for single fault classes.

F.3.6 Online implementation of the proposed algorithm

The online implementation of the proposed diagnosis scheme is briefly discussed in this section. The first interface is for data acquisition, where the vibration and current spectrograms are displayed to the machine operator together with the rotational speed. The one-class SVM was trained using data in the healthy powertrain under variable loads and speed conditions. The trained algorithm is used for calculating the score for online fault detection, and the scores for latest 800 samples are displayed in Figure F.17. The interface shown in Figure F.17 is a situation when the healthy machine operates at variable speed conditions, thus the health status indicator shows the green color (red for faults). After detecting a fault, a temporary label is assigned to new data (e.g. FT1), and a CNN-based classifier is trained using healthy and the fault data (FT1). The learned CNN feature set are used for generating a score (from 0 to 1) to define the similarity level of the new spectrogram data with respect to the learned fault types or severities. Multiple CNN classifiers are trained for detecting other fault types so that they calculate scores for new spectrogram data as shown in Figure F.3.

Figure F.17: One-class SVM fault detection interface.

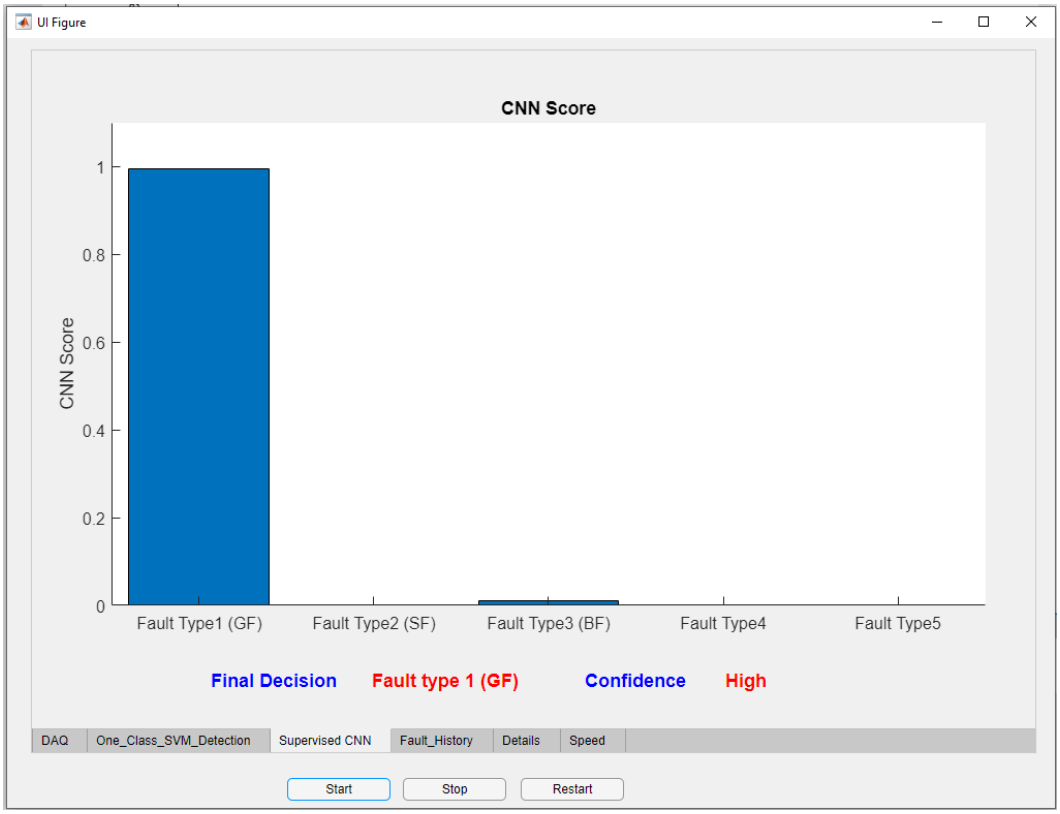

Figure F.18: CNN fault score and decision-making interface.

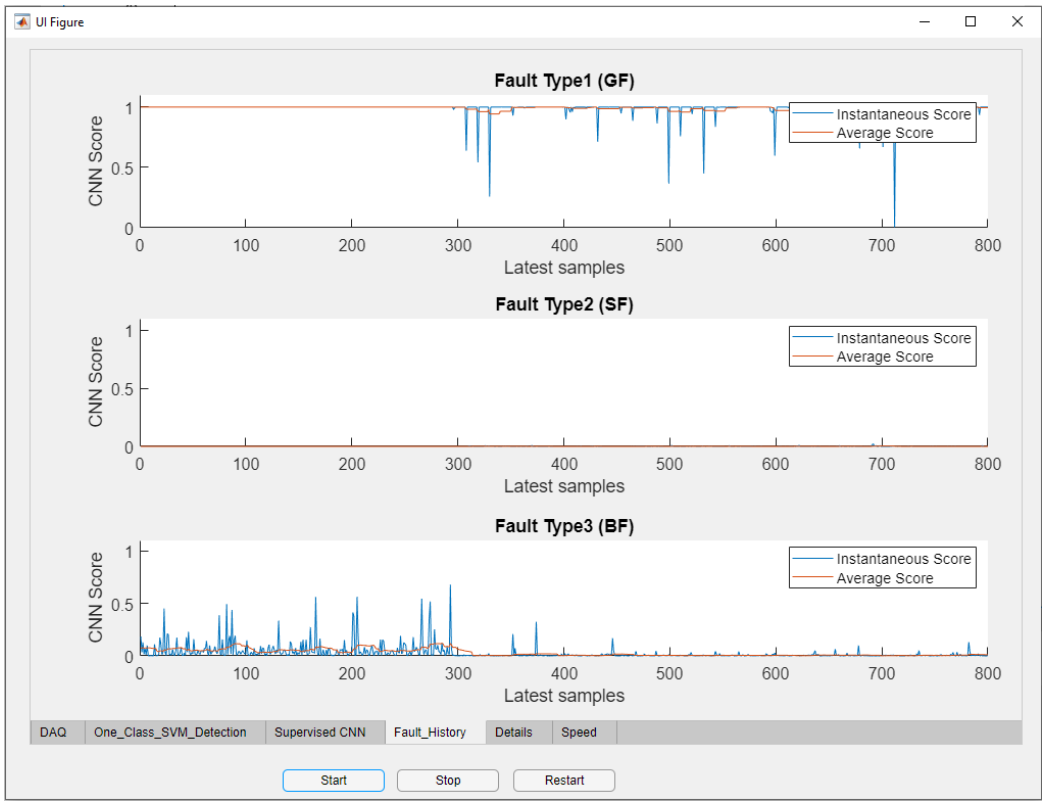

Figure F.19: CNN fault score history interface.

The decision criteria defined in Table F.2 are used for the final decision or classification. The scores for 3 CNN classifiers for GF2 data are shown in Figure F.18, where the score for fault type 1 (GF1-CNN) is closer to 1, and the scores for others are closer to zero. The CNN based classifiers for fault types 4 and -5 are not trained yet, being open for training next faults. The historical CNN scores are also displayed, being useful for a machine operator to define a machine condition. The historical scores of the CNN classifiers for the first 3 classifiers are shown in Figure F.19, in which some sudden score changes depend on the dynamic operation conditions, but the average scores are always consistent over time.

F.4 Conclusion

This paper proposes an online fault diagnosis scheme, aiming to use data in healthy condition alone by learning the features for fault diagnosis in a self-supervised manner. The powertrain health status or health class is defined in the first stage by using a one-class SVM. The resulting health classes are used to train the CNN -based classifiers. The comparative study shows that the proposed method performs better than those using domain feature extraction and existing algorithms, namely binary SVM or MLP. The order normalization process and CNN feature learning allow the proposed fault diagnosis scheme to perform well in dynamic operating conditions. The effectiveness of the proposed fault diagnosis scheme is validated using experimental data from an in-house test setup. In the proposed scheme, data of the lowest fault severity is used for training the CNN classifiers, but the trained algorithm can detect faults at higher severities, proving the generalization ability of CNN feature learning. The proposed scheme can be improved by testing the robustness under noises, revising decision criteria, self-supervised image learning, wireless sensors, and online diagnosis.

References

[1] F. Allbrecht, J. C. Appiarius, R. M. McCoy, E. L. Owen, and D. K. Sharma, “Assessment of the reliability of motors in utility applications,” *IEEE Trans. Energy Convers.*, vol. EC-1, no. 1, pp. 39-46, 1986.

[2] Z. Gao, C. Cecati, and S. Ding, "A Survey of Fault Diagnosis and Fault-Tolerant Techniques—Part I: Fault Diagnosis with Model-Based and Signal-Based Approaches," *IEEE Trans. Ind. Electron.*, vol. 62, no. 6, pp. 3757-3767, 2015.

[3] Z. Gao, C. Cecati, and S. Ding, "A Survey of Fault Diagnosis and Fault-Tolerant Techniques-Part II: Fault Diagnosis with Knowledge-Based and Hybrid/Active Approaches," *IEEE Trans. Ind. Electron.*, vol. 62, no. 6, pp. 3768-3774, 2015.

[4] X. Dai and Z. Gao, "From Model, Signal to Knowledge: A Data-driven Perspective of Fault Detection and Diagnosis," *IEEE Trans. Ind. Informat.*, vol. 9, no. 4, pp. 2226-2238, 2013.

[5] D. Jung and C. Sundström, "A Combined Data-Driven and Model-Based Residual Selection Algorithm for Fault Detection and Isolation," *IEEE Trans. on Cont. Sys. Tech.*, vol. 27, no. 2, pp. 616-630, 2019.

[6] M. Norton and D. Karczub, *Fundamentals of Noise and Vibration Analysis for Engineers*. Cambridge University Press, 2003.

[7] P. Girdhar and C. Scheffer, "Practical Machinery Vibration Analysis and Predictive Maintenance," in *Machinery fault diagnosis using vibration analysis*: Oxford, Newnes, 2004.

[8] J. S. L. Senanayaka, H. Van Khang, and K. G. Robbersmyr, "Multiple Classifiers and Data Fusion for Robust Diagnosis of Gearbox Mixed Faults," *IEEE Trans. Ind. Informat.,*, vol. 15, no. 8, pp. 4569-4579, 2019.

[9] M. Ma, C. Sun, and X. Chen, "Deep Coupling Autoencoder for Fault Diagnosis with Multimodal Sensory Data," *IEEE Trans. on Ind. Informat.*, vol. 14, no. 3, pp. 1137-1145, 2018.

[10] R. Liu, G. Meng, B. Yang, C. Sun, and X. Chen, "Dislocated Time Series Convolutional Neural Architecture: An Intelligent Fault Diagnosis Approach for Electric Machine," *IEEE Trans. Ind. Informat.*, vol. 13, no. 3, pp. 1310-1320, 2017.

[11] M. He and D. He, "Deep Learning Based Approach for Bearing Fault Diagnosis," *IEEE Trans. Ind. Appl.*, vol. 53, no. 3, pp. 3057-3065, 2017.

[12] C. Sun, M. Ma, Z. Zhao, S. Tian, R. Yan, and X. Chen, "Deep Transfer Learning Based on Sparse Autoencoder for Remaining Useful Life Prediction of Tool in Manufacturing," *IEEE Trans. on Ind. Informat.*, vol. 15, no. 4, pp. 2416-2425, 2019.

[13] J. S. Lal Senanayaka, H. V. Khang, and K. G. Robbersmyr, "Online Fault Diagnosis System for Electric Powertrains using Advanced Signal Processing and Machine Learning," in *XIII International Conference on Electrical Machines (ICEM)*, Alexandroupoli, 2018.

[14] J. S. L. Senanayaka, H. V. Khang, and K. G. Robbersmyr, "Multiple Fault Diagnosis of Electric Powertrains under Variable Speeds using Convolutional Neural Networks," in *XIII International Conference on Electrical Machines (ICEM)*, Alexandroupoli, 2018.

[15] S. Jenni and P. Favaro, "Self-Supervised Feature Learning by Learning to Spot Artifacts," *The IEEE Conference on Computer Vision and Pattern Recognition (CVPR)*, 2018.

[16] A. Kolesnikov, X. Zhai, and L. Beyer, "Revisiting self-supervised visual representation learning," *Comp. Vision and Pattern Recog.*, 2019.

[17] L. Jing and Y. Tian, "Self-supervised visual feature learning with deep neural networks: A survey," *arXiv preprint arXiv:1902.06162*, 2019.

[18] Y. Guerbai, Y. Chibani, and B. Hadjadji, "The effective use of the one-class SVM classifier for handwritten signature verification based on writer-independent parameters," *Pattern Recog.*, vol. 48, no. 1, pp. 103-113, 2015.

[19] K. Heller, K. Svore, A. Keromytis and S. Stolfo, "One class support vector machines for detecting anomalous windows registry accesses," *The Workshop on Data Mining for Computer Security*, 2003.

[20] P. Konar and P. Chattopadhyay, "Bearing fault detection of induction motor using wavelet and support vector machines (SVMs)," *Appl. Soft Comput.*, vol. 11, no. 6, pp. 4203–4211, 2011.

[21] G. Susto, A. Schirru, S. Pampuri, S. McLoone, and A. Beghi, "Machine learning for predictive maintenance: A multiple classifier approach," *IEEE Trans. Ind. Informat.*, vol. 11, no. 3, pp. 812-820, 2015.

[22] J. S. L. Senanayaka, S. T. Kandukuri, H. V. Khang, and K. G. Robbersmyr, "Early Detection and Classification of Bearing Faults using Support Vector Machine Algorithm," in *IEEE Workshop on Electrical Machines Design, Control and Diagnosis (WEMDCD)*, Nottingham, pp. 250-255, 2017.

[23] L. Wu, B. Yao, Z. Peng, and Y. Guan, "Fault Diagnosis of roller bearings based on a wavelet neural network and manifold learning," *Appl. Sci.*, vol. 7, no. 158, pp. 1–10, 2017.

[24] J. S. L. Senanayaka, H. V. Khang, and K. G. Robbersmyr, "Towards online bearing fault detection using envelope analysis of vibration signal and

decision tree classification algorithm," in *20th International Conference on Electrical Machines and Systems (ICEMS)*, Sydney, NSW, 2017.

[25] F. Lv, C. Wen, Z. Bao, and M. Liu, "Fault diagnosis based on deep learning," in *American Control Conference*, Boston, pp. 6851-6856, 2016.

[26] H. Hu, B. Tang, X. Gong, W. Wei, and H. Wang, "Intelligent Fault Diagnosis of the High-Speed Train With Big Data Based on Deep Neural Networks," *IEEE Trans. Ind. Informat.*, vol. 13, no. 4, pp. 2106-2116, 2017.

[27] W. Sun, R. Zhao, R. Yan, S. Shao, and X. Chen, "Convolutional Discriminative Feature Learning for Induction Motor Fault Diagnosis," *IEEE Trans. Ind. Informat.*, vol. 13, no. 3, pp. 1350-1359, 2017.

[28] C. Sun, M. Ma, Z. Zhao, and X. Chen, "Sparse Deep Stacking Network for Fault Diagnosis of Motor," *IEEE Trans. Ind. Informat.*, vol. 14, no. 7, pp. 3261-3270, 2018.

[29] J. Blough, "Improving the Analysis of Operating Data on Rotating Automotive Components," PhD Thesis College of Engineering, University of Cincinnati, USA, 1998.

[30] A. Brand, *Noise and Vibration Analysis: Signal Analysis and Experimental Procedures*. Chichester, UK: John Wiley and Sons, 2011.

[31] Order Analysis of a Vibration Signal MATLAB Examples, Available: https://se.mathworks.com/help/signal/examples/order-analysis-of-a-vibration-signal.html, Accessed: August 2019.

[32] B. Scholkopf, J. Platt, J. Shawe-Taylor, A. Smola and R. Williamson, "Estimating the support of a high dimensional distribution" *Neural Comput.*, vol. 13, no. 7, pp. 1443– 1472, 2001.

[33] N. Tajbakhsh *et al.*, "Convolutional Neural Networks for Medical Image Analysis: Full Training or Fine Tuning?," *IEEE Trans. Med. Imag.*, vol. 35, no. 5, pp. 1299-1312, 2016.